Characterization of novel virulence factors of *Shigella flexneri* and development of *Caenorhabditis elegans* as an animal model for *Shigella* infection

Divya George

A thesis submitted for the degree of Doctor of Philosophy of The Australian National University

January 2014

Declaration

I declare that this thesis is an original work and is an account of the research carried out by myself while enrolled as a PhD candidate at The Australian National University between 2011-2014. To the best of my knowledge, this thesis does not contain material that has been accepted for the award of any other degree or diploma in any University.

.....

Divya George

Acknowledgements

Over the past few years I have had the privilege of meeting and working with an incredible group of people. I'd like to take this opportunity to thank the people who have played an instrumental role in the completion of my PhD.

I would firstly like to thank my supervisor Naresh Verma, for his constant support and guidance throughout the course of my PhD. Thanks Naresh for allowing me to do my PhD in your lab and for putting up with me for all these years. Next I would like to thank the members of my academic panel, Carol, Uli, David Tscharke and Gwen Alison, for their suggestions and encouragement with this project.

I would like to especially thank Melanie Rug, Nav and Jo at the Center for advanced microscopy, ANU, for all their help with fixing and sectioning nematodes. Special thanks must also go to Professor David Hall and Ken Nguyen, at the Albert Einstein College of Medicine, for their hospitality and guidance with *C. elegans* electron microscopy in New York. Sincere thanks must also go to David Stephenson, Richa, Aruna, Miyung, Tony, Zarshis, Anesh, Farah, Angeline and all other past members of the Verma lab for their friendship and support over the years.

On the personal front I'd like to thank Mat, Jen, Iman, Pammy, Li Fan, Tim, Sharon, Seb, Luke, Megan, Laurence, Kate, Ranate, Simone and all the incredible friends I have been blessed with. Thank you for the many coffees, dinners and drinks, that have help maintain my sanity when experiments have been challenging. Next I'd like to thank my family back in India for their perpetual encouragement and love. Finally I'd like to thanks my fiancé, Ben for being so patient and supportive throughout this entire journey.

Abstract

Shigella flexneri strains are most frequently linked with endemic outbreaks of shigellosis (bacillary dysentery). *S. flexneri* invades the colonic and rectal epithelium of humans and non-human primates and causes severe tissue damage which manifests in a spectrum of clinical symptoms ranging from watery diarrhoea to severe dysentery. The overall aim of this study is to further our understanding of *S. flexneri* pathogenesis by characterizing novel virulence factors and to characterize a new animal model of shigellosis.

The first aim of this study is to further our understanding of the complex *S. flexneri* infection process by characterizing the contribution of L-asparaginase (AnsB) and γ-glutamyltranspeptidase (GGT), to bacterial pathogenesis. These proteins are of particular interest as they are characterized virulence factors in a number of other enteropathogenic bacterial species including *Helicobacter pylori* and *Escherichia coli*. Both AnsB and GGT of *S. flexneri* are immunogenic and have not been previously characterized for *S. flexneri*. Using a reverse genetic approach we show that both AnsB and Ggt are required for bacterial adherence to host epithelial cells. *In vivo* studies in both the *Caenorhabditis elegans* and the murine pulmonary model of shigellosis revealed that these genes contribute to *S. flexneri* virulence. Differential in-gel electrophoresis showed that *ansB* and *ggt* mutations exert pleiotropic effects on the expression of a number of *S. flexneri* genes, including prominent bacterial outer membrane proteins, OmpA and YaeT. This is the first report in *S. flexneri* where the functions of AnsB and GGT have been found to extend beyond their canonical metabolic roles. The requirement of AnsB and GGT for the virulence of *S. flexneri* makes these genes attractive candidates for designing new therapeutic measures and preventive approaches to curb the spread of shigellosis.

The second aim of this study is to identify bacteriophage genes that contribute to the virulence of *S. flexneri*. *S. flexneri* strains are susceptible to infection by several temperate lambdoid bacteriophages. To date in *S. flexneri*, the O-antigen modifying genes - the glucosyltransferase (*gtr*) cluster is the only set of bacteriophage genes that have been linked to bacterial pathogenesis. Studies in both Gram-positive and Gram-negative pathogens have identified bacteriophage genes that play a role in different stages of bacterial pathogenesis; these findings warrant the need to study *S. flexneri* phages further. In this study the *S. flexneri* phage SfII was isolated from a highly prevalent *S. flexneri* serotype 2a strain and completely sequenced to identify novel bacteriophage-encoded genes. The complete SfII genome sequences were analysed and compared to published bacteriophage genomes. Although sequence analysis of the SfII genome found similarities with *S. flexneri* bacteriophages, SfI, SfIV and SfV, the host ranges of all four phages were found to differ significantly. Homology searches of the predicted open reading frames of SfII using BlastX searches, identified, 41 had assigned functions and 17 as hypothetical proteins. Further studies designed to investigate the functions of these hypothetical proteins will broaden our understanding of the molecular biology of *S. flexneri* phages and potentially shed light on why *S. flexneri* serotype 2a strains are highly prevalent.

While bacteriophage SfII was being sequenced, uncharacterized genes in the sequenced *S. flexneri* serotype-converting phage, SfV were studied to identify potential phage-encoded genes that play a role in the virulence of *S. flexneri*. Reverse transcription PCR was used to determine the expression of 15 uncharacterized, bacteriophage-encoded genes in an SfV lysogenic strain grown at 37°C (*S. flexneri* virulence genes are expressed at this temperature). Using this approach, 12 uncharacterized, SfV-encoded genes were identified as expressed in lysogenic strain, making them potential virulence factors. A mutant lysogenic strain lacking 5

of these expressed phage genes, *orf28-32,* was generated and the effect of this mutation on the virulence of the host strain was assessed. *In vitro* and *in vivo* virulence studies indicate that genes within the SfV *orf28-32* five-gene cassette play a role in the virulence of the host strain. This is the first reported study to identify bacteriophage-encoded genes outside of the O-antigen modifying cluster that may enhance the virulence of *S. flexneri* strains.

The third aim of this study is to characterize *C. elegans* as a new small animal model of shigellosis. *S. flexneri* strictly infects human and non-human primate hosts consequently there is no simple intestinal animal model available. The lack of a relevant animal model of shigellosis has been one of the major impairments to vaccine development. In recent years the use of *C. elegans* as an animal model for several microbial diseases has been gaining momentum as these nematodes are extremely convenient animal models, as they are self-fertilizing hermaphrodites with a rapid generation time. Here we have shown that virulent strains of *S. flexneri* are ingested by the nematode *C. elegans* and that *S. flexneri* cells invade the nematode intestinal cells. In order to further characterize *S. flexneri* infection in *C. elegans* we used 2-dimensional gel electrophoresis to compare the proteomes of nematodes infected with *S. flexneri* and avirulent *E. coli* strains and successfully identified several differential expressed nematode proteins in response to *S. flexneri* infection. To further our understanding of the interactions between *S. flexneri* and *C. elegans* we used transmission electron microscopy (TEM) and proved for the first time that *S. flexneri* cells invade nematode intestinal cells. These findings are extremely significant as they provide further evidence supporting the use of *C. elegans* as a viable model to study shigellosis.

Publications

D.T.George, Stephenson D., Tran E, Morona R. and N.K. Verma. 2013. 'Complete Genome Sequence of SfII, a Serotype-Converting Bacteriophage of the Highly Prevalent *Shigella flexneri* Serotype 2a'. *GenomeA,* September/October 2013;1:doi:10.1128/genomeA.00626-13.

Publications under review

D.T.George, Mathesius U., Behm C.A. and N.K. Verma, 2013 'The periplasmic enzyme, AnsB, of *Shigella flexneri* modulates bacterial adherence to host epithelial cells by regulating the expression of outer membrane protein A', Submitted to PlosOne.

D.T.George, Behm C.A, Hall D.A., Mathesius U., Rug M., Nguyen K.C.Q. and N.K. Verma, 2013, *'Shigella flexneri* infection in *Caenorhabditis elegans*: Cytopathological Examination and Identification of Host Responses' Submitted to PlosOne.

Publication in preparation

D.T.George, Mathesius U., Behm C.A. and N.K. Verma, 2014 '*Shigella flexneri* γ-glutamyltranspeptidase (GGT) activity required for bacterial virulence', To be submitted to FEMS, Pathogen and Disease.

Abbreviations

2-DE	2-dimensional gel electrophoresis
aa	amino acid
AECOM	Albert Einstein College of Medicine
AGM	Advanced Microscopy Group
Amp	ampicillin
AnsB	L-asparaginase
ANOVA	Analysis Of Variance
ANU	Australian National University
bp	base pairs
BHK	Baby Hamster Kidney
BRF	Biomolecular Resource Facility
BSA	Bovine Serum Albumin
CAM	Centre for Advanced Microscopy
CASS	The CRISPR/Cas system
CDD	conserved domain
CDS	coding sequences
CFU	Colony Forming Units

CGC	Caenorhabditis Genetics Center
CIAP	Calf-Intestinal Alkaline Phosphatase
Cm	chloramphenicol
CMI	cell mediated immunity
CRISPR	Clustered Regularly Interspaced Short Palindromic Repeats
CRP	cyclic AMP receptor protein
Ctx	cholera toxin
Dam	DNA adenine methyltransferase
DIGE	Differential In-Gel electrophoresis
DNA	deoxyribonucleic acid
DMF	Dimethylformamide
EOP	Efficiency of plaquing
EAEC	Enteroaggregative *Escherichia coli*
ECVAM	European Centre for the Validation of Alternative Methods
EIEC	Enteroinvasive *Escherichia coli*
EPEC	Enteropathogenic *Escherichia coli*
ETEC	Enterotoxigenic *Escherichia coli*
FAE	follicle-associated epithelium
FCS	Foetal calf serum

GDAR	Glutamate-Dependent Acid Resistance
GGT	gamma-glutamyltranspeptidase
gtr	glucosyltransferase
HRP	Horse radish peroxidase
HSV	Herpes simplex virus
IEF	Isoelectric focusing
IFN	interferon
IL	interleukin
int	integrase
Ipa	invasion protein antigens
IPTG	iso-propyl-β-DD-thiogalactopyranoside
IS	insertion element
Kb	kilobase
kDa	kilodalton
LB	Luria-Bertani medium
LC-MS	Liquid chromatography–mass spectrometry
LEE	locus of enterocyte effacement
LPS	lipopolysaccharide
M	molar

M cell	microfold cell
MAPK	mitogen activated protein kinases
MCS	multiple cloning site
MEM	minimal essential medium
mM	millimolar
MM	minimal essential salts media
Mwt	Moleculat weight
MYD88	myeloid differentiation primary-response protein 88
NGM	nematode growth medium
NK	natural killer
oac	*O*-acteyltrensferase
OD	optical density
OMV	Outer Membrane Vesicle
orf	open reading frame
nt	nucleotide
NLRs	nod-like receptors
NRT	no reverse transcriptase
NTC	no template control
PAGE	polyacrylamide gel electrophoresis

PAI	pathogenicity island
PAMPs	pathogen-associated molecular patterns
PBS	phosphate buffered saline
PCR	polymerase chain reaction
PDK-1	phosphoinositide-dependent kinase 1
PEG	polyethylene glycol
PFU	plaque forming units
PMK-1	p38 MAPK family member 1
PMN	polymorphonuclear cell
PRRs	pathogen recognition receptors
PVDF	polyvinylidene fluoride
qRT-PCR	quantitative real time reverse transcriptase polymerase chain reaction
RBS	ribosome binding site
RdRP	RNA-dependent RNA polymerase
REML	restricted maximum likelihood
RFX	regulatory factor X
RISC	RNA-induced silencing complex
RNA	ribonucleic acid
ROS	reactive oxygen species

RT-PCR	reverse transcriptase polymerase chain reaction
Rpm	revolutions per minute
SEK-1	SAPK/ERK kinase 1
SDS	sodium dodecyl sulphate
SGK-1	serum/glucocorticoid-regulated kinase 1
T3SS	type three secretion system
TBE	Tris-Borate-EDTA buffer
TCA	trichloroacetic acid
TCP	toxin-coregulated pilus
TD_{50}	the time taken to kill 50% of the initial population
TE	Tris-EDTA buffer
TLRs	toll-like receptors
UPR^{mt}	mitochondria-specific unfolded protein response
U.V.	Ultraviolet
V	volts
WHO	World Health Organization
WRAIR	Walter Reed Army Institute of Research
X-Gal	5-bromo-4-chloro-3-indolyl-β-D-galactopyranoside
xis	excisionase

Table of Contents

Chapter 1

Introduction

Chapter 1: Introduction

1.1 Shigellosis

Shigellosis, also known as bacillary dysentery, is a food-borne illness caused by the enteric bacterium *Shigella*. *Shigella* cells invade the colonic and rectal epithelium of humans and non-human primates and cause severe tissue damage which manifests in a spectrum of clinical symptoms ranging from watery diarrhoea to severe dysentery; characterized by fever, abdominal cramping and bloody, mucoid stool [1]. *Shigella* species are commonly found in water contaminated with human faeces and are transmitted via the faecal-oral route.

1.2 Epidemiology of *Shigella flexneri*

Shigella species belonging to the family *Enterobacteriaceae,* are Gram negative, non-spore forming, facultative anaerobes that are believed to have evolved from multiple *Escherichia coli* strains [2]. The genus is subdivided into four recognized species: *S. flexneri, S. dysenteriae*, *S. boydii,* and *S. sonnei* [3]. Each species is further divided into serotypes based on differences in the structural and functional properties of their O-antigen, a component of the bacterial lipopolysaccharide (LPS) [4].

The O-antigen backbone of all serotypes except serotype 6, is composed of repeating units of the rhamnose-rhamnose-rhamnose-*N*-acetylglucosamine tetrasaccharide. *S. flexneri* cells with this basic O-antigen structure are recognized as serotype Y. Differences between the serotypes are conferred by the addition of bacteriophage-encoded glucosyl and/or O-acetyl groups to different sugars within the basic tetrasaccharide repeat unit [5]. More recently,

phosphorylated variants of the O-antigens of serotypes 4a, X and Y called 4av, Xv and Yv have been reported [6, 7]. These variants carry a phosphoethanolamine (PEtN) group on rhamnose II or III [6, 7]. There are currently 19 recognized serotypes of *S. flexneri* (Figure 1.1) [7-14]. Sero-diversity has been one of the leading impediments to *Shigella* vaccine development as each serotype elicits a specific immune response.

The World Health Organization (WHO) estimated that 165 million people are infected with *Shigella* annually, with over 1 million deaths per annum [15]. *Shigella flexneri* strains are most frequently associated with endemic outbreaks of shigellosis in developing countries [16]. *S. flexneri* is highly contagious with only as few as 10-100 bacterial cells required for infection [17]. The increasing global burden of shigellosis due to the numerous mechanisms the bacterium has evolved to evade human defense responses and the rapid emergence of multi-drug resistant strains, has resulted in the World Health Organization prioritizing the need to develop an effective vaccine against *S. flexneri* [15].

1.3 Pathogenesis of *Shigella flexneri*

Shigella invades the colonic and rectal epithelia of human and non-human primates in a complex multi-step process. This results in an acute inflammatory response which culminates in severe epithelial tissue damage. Destruction of the epithelial layer leads to the clinical symptoms of abdominal cramping, diarrhoea, and bloody, mucoid stool typical of shigellosis [1]. The process of colonic invasion and destruction is outlined in Figure 1.2 and discussed stepwise in the following sections.

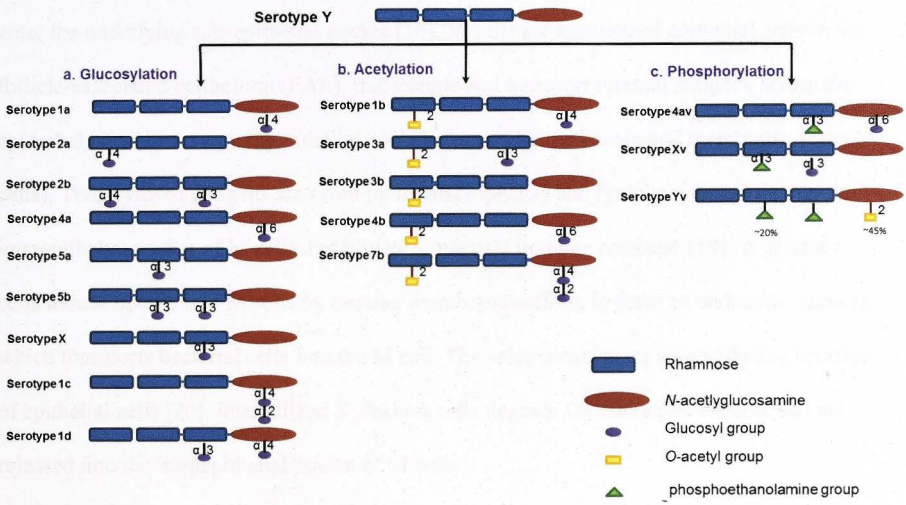

Figure 1.1: Serodiversity in *S. flexneri.* Diagrammatic representation of the chemical composition of the different serotypes of *S. flexneri.* The basic O-antigen (Serotype Y) consists of repeating units of the rhamnose-rhamnose-rhamnose-*N*-acetylglucosamine tetrasaccharide. Serotypes differ by the addition of either glucosyl (a), o-acetyl (b) or phosphoethanolamine (c) groups to different sugars within basic tetrasaccharide unit via linkages as indicated.

1.3.1 Crossing the epithelial barrier

The apical surfaces of host colonic epithelial cells are well protected by microvilli bearing filamentous brush border glycocalyx which prevents the entry of pathogens. To overcome this barrier, *S. flexneri* cells exploit the transcytotic properties of host microfold (M) cells to enter the underlying sub-epithelial pocket [18]. M cells are specialized epithelial cells in the follicle-associated epithelium (FAE), that sample and transport luminal antigens across the epithelial barrier into an intraepithelial pocket (formed by the basolateral membrane of the M cells). Transcytosed antigens are taken up by macrophages and lymphocytes occupying the intraepithelial pocket of M cells and initiate a mucosal immune response [19]. *S. flexneri* cells induce uptake into M cells by causing membrane ruffling to form an endocytic vacuole, which transports bacterial cells into the M cell. The same mechanism is used during invasion of epithelial cells [20]. Internalized *S. flexneri* cells degrade the endocytic vacuole and are released into the intraepithelial pocket of M cells.

There have been reports suggesting that *Shigella* cells may also manipulate tight-junction associated proteins between epithelial cells to gain access to the sub-epithelial space [21]. In the later stages of infection, *Shigella* exploit the host's inflammatory response to increase bacterial entry into the sub-epithelial space.

1.3.2 Macrophage apoptosis

Within the intraepithelial pocket of M cells, *Shigella* are engulfed by resident macrophages, however bacterial cells escape macrophage attack by triggering macrophage apoptosis. Apoptosis is induced by the virulence plasmid encoded invasion protein antigens (Ipa),

particularly IpaB [22]. Macrophage apoptosis releases *Shigella* cells into the sub-epithelial space.

Infected macrophages release pro-inflammatory cytokines IL-18 and IL-1β through the activation of *capsase*-1 [22]. The released IL-1β recruits polymorphonuclear (PMN) cells to the site of infection. PMN cells penetrate through the epithelial barrier to reach bacterial cells in the intestinal lumen and in the process destabilize the integrity of the epithelial barrier. This allows lumenal bacteria access to the sub-epithelial space. *Shigella* cells in the sub-epithelial space now have access to the less-protected, basolateral face of epithelial cells [23, 24].

1.3.3 Bacterial adherence and invasion of epithelial cells

Shigella cells released into the sub-epithelial space adhere to the basolateral surfaces of colonic epithelial cells which is followed by bacterial invasion, intra and intercellular spread. Adherence to host tissue is a prerequisite for bacterial infection. The molecular mechanisms that govern *Shigella* adherence to host tissues have not yet been fully characterized. Previous studies have reported that bacterial cells use the type three secretory (T3SS) apparatus, particularly the Ipa proteins to preferentially bind to host receptors expressed on the basolateral side of epithelial cells. These receptor proteins include α5β1 integrin, to which the secreted IpaB-C-D complex binds [25], and CD44, a major cell surface receptor of hyaluronic acid to which IpaB binds [26].

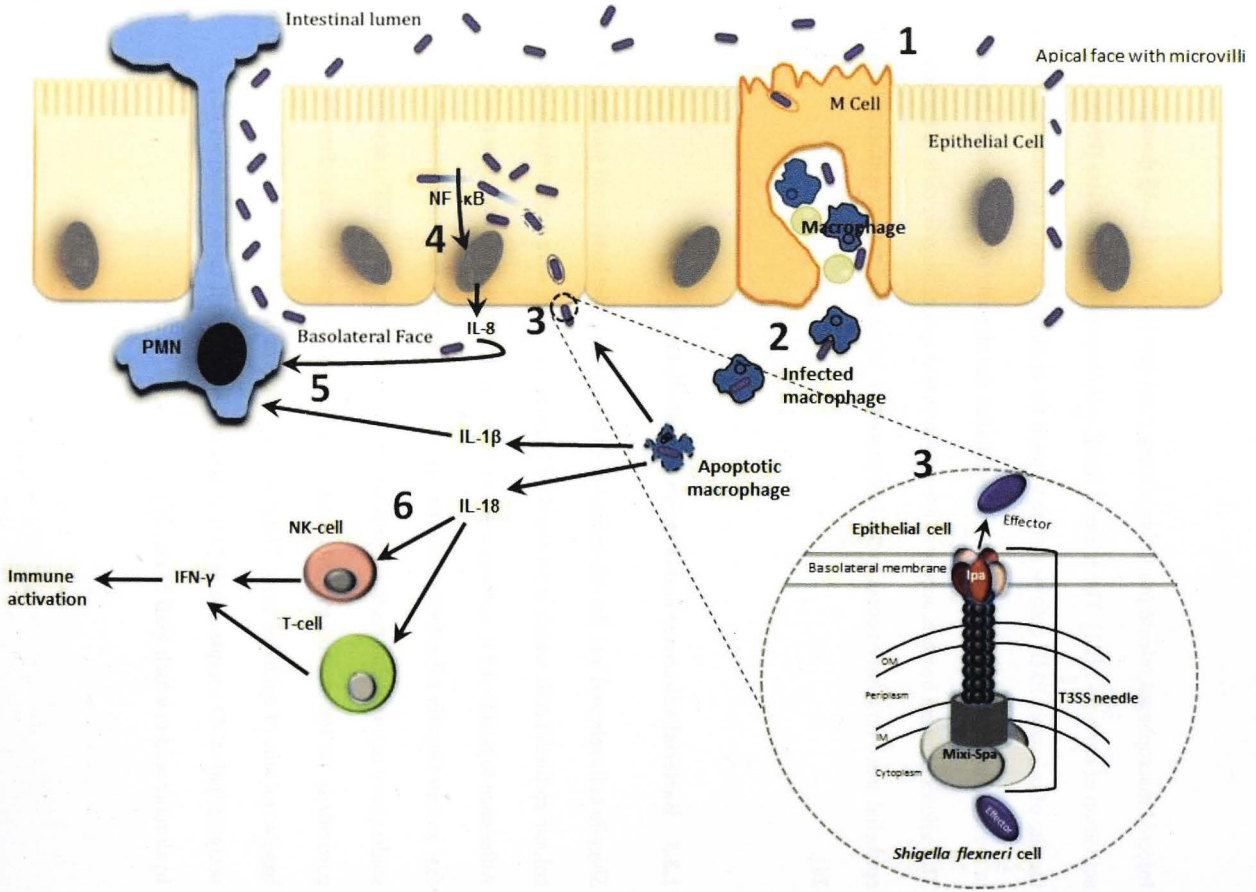
Intestinal lumen
1
Apical face with microvilli
M Cell
Epithelial Cell
Macrophage
NF-κB
4
IL-8
3
Basolateral Face
PMN
2
Infected macrophage
5
IL-1β
Apoptotic macrophage
6
IL-18
NK-cell
Immune activation
IFN-γ
T-cell
3
Epithelial cell
Effector
Basolateral membrane
Ipa
OM
Periplasm
IM
Cytoplasm
Mixi-Spa
T3SS needle
Effector
Shigella flexneri cell

Figure 1.2: Schematic representation of the main steps involved in *Shigella* pathogenesis.

(1) *Shigella* crosses the epithelial barrier by transcytosis through microfold (M) cells. The bacteria also manipulate tight junctions between epithelial cells to gain paracellular access to the sub-mucosa.

(2) *S. flexneri* cells in the sub-mucosa are engulfed by macrophages. *Shigella* evades macrophage attack by inducing macrophage apoptosis resulting in the secretion of proinflammatory cytokines, interleukin 1β (IL1β) and IL-18.

(3) Free *Shigella* cells invade the epithelial cells through their basolateral side by the secretion of effector proteins through the type-III secretion system (T3SS). Bacteria enter the epithelial cytoplasm and spread to adjacent cells by the active polymerization of actin.

(4) Invasion of epithelial cells triggers the NFκB-mediated up-regulation of interleukin-8 (IL8) production and secretion.

(5) Proinflammatory signals produced by apoptotic macrophages and infected epithelial cells attract polymorphonuclear neutrophil (PMN) cells to the site of infection. The influx of PMN disintegrates the epithelial lining, which initially exacerbates the infection and tissue destruction by facilitating the invasion of more bacteria.

(6) IL-18 produced by apoptotic macrophages activate natural killer (NK) cells and T cells to produce interferon γ (IFN-γ) which in turn activates a protective immune response involving macrophages and fibroblast cells.

After adhering to the basolateral membrane of epithelial cells, *Shigella* cells inject effector molecules into host cells through the T3SS. These effector molecules induce host cytoskeletal rearrangement to form macropinocytic pockets that engulf adherent bacterial cells into the host cell cytoplasm [27]. Skoudy and colleagues have identified the host Ezrin proteins belonging to the ERM family (ezrin-radixin-meosin) as important factors that are required for this cytoskeletal rearrangement [28]. Mammalian cells expressing a dominant negative form of Ezrin show reduced *S. flexneri* invasion [28]. As in the case of macrophages, IpaB facilitates the lysis of epithelial macropinocytic vacuoles resulting in the release of the pathogen into the epithelial cell cytoplasm.

In the cytoplasm, non-motile *Shigella* cells replicate and spread to adjacent cells by the active polymerization of actin via a polarly expressed IcsA protein [29]. In this manner *S. flexneri* is able to multiply and spread within the intestinal epithelial layer whilst avoiding exposure to the extracellular environment and it's circulating immune cells. Bacterial invasion and intracellular multiplication culminates in epithelial cell damage which generates the clinical symptoms of watery diarrhoea, severe abdominal pain and cramping and bloody mucoid stool characteristic of shigellosis.

1.4 Host immune responses to *S. flexneri*

1.4.1 Innate immune response

Colonic epithelial cells act as a primary line of defense by providing an impermeable physical barrier to invading pathogens. The renewal of host epithelial cells is an important innate defense response that prevents bacterial colonization. Iwai *et al.* indicate that the *Shigella* effector protein IpaB, when injected into epithelial cells, down-regulates host cell cycle

proteins which limit epithelial cell renewal [30].The IpaB-mediated cell cycle arrest contributes to the efficient colonization of host cells. This suggests that *Shigella* influences epithelial cell renewal in order to promote bacterial colonization of the intestinal epithelium.

Epithelial cells secrete antimicrobial peptides such as defensins (like HBD-1) and cathelicidins (like LL-37) in response to inflammation and infection at mucosal surfaces [31, 32]. Intestinal epithelial surfaces are thus covered with a mixture of antimicrobial peptides [33]. Islam *et al,* have shown that early in infection, *Shigella* cells down-regulate the expression of antimicrobial peptides HBD-1 and LL-37 to escape this innate immunes response [34]. They proposed that the down-regulation of these antimicrobial peptides promotes bacterial adherence and invasion.

Once *S. flexneri* cells cross the host epithelial barrier and invade the epithelial cells, their pathogen-associated molecular patterns (PAMPs) are recognized by various host pathogen recognition receptors (PRRs), including toll-like receptors (TLRs) and nod-like receptors (NLRs) [35-41]. Detection of PAMPs induces host innate signaling pathways, including those mediated by NF-κB and the mitogen activated protein kinases (MAPK) [42-45]. The activation of these pathways results in the secretion of pro-inflammatory cytokines, chemokines and antimicrobial peptides. The severe inflammation which is characteristic of shigellosis has been associated with the up-regulation of several cytokines including IL-1β, IL-6, IL-8, IL-18, TNF-α, TNF-β, TGF-β and IFN-γ [46]. More recently IL-22, IL-17A and IL-17G have been identified as first responders to *S. flexneri* infection [47]. IL-18 released by apoptotic macrophages activates NK cells and T cells to produce IFN-γ (Figure 1.2.6), a chemokine that plays an essential role in the early protection by activating macrophages and

fibroblast cells with increased bactericidal activity [48, 49]. *S. flexneri* virulence plasmid-encoded OspF, OspG and IpaH4.5 have been shown to suppress the production of cytokines by interfering with the activation of the NF-κB and MAPK signaling pathways [50-53]. Although the pro-inflammatory responses may be responsible for the increased entry of bacterial cells into the sub-epithelial space, they are also important for the control and containment of infection.

1.4.2 Humoral immune response

Several serological studies of humans and animal experiments following natural infection and vaccination have revealed that *Shigella*-specific immunity is characterized by the induction of a humoral response. This humoral response is the major component of protective immunity against shigellosis. Bacterial LPS is the key antigenic factor that activates both systemic and mucosal immune responses [54-56]. Protective immunity provided by the host antibody response to *Shigella* is serotype specific as previous infection or vaccination offers little or no protection against infection by heterologous serotypes [57-59]. This suggests that a large proportion of the humoral response is directed to the O-antigen, the serotype-specific determinant of the LPS. Antibodies against Ipa proteins are also produced after natural and experimental infection and are believed to contribute to protection [54, 60, 61]. Antibodies produced in response to *Shigella* infection have complement-mediated bactericidal activity [62] and promote opsonophagocytic killing by mononuclear cells [63].

Mucosal sIgA and serum IgG have been implicated in generating serotype-specific immunity against *Shigella* [64, 65]. The strong serotype-specific SIgA and serum IgG responses to

Shigella infection correlates with protection data from epidemiological and sero-epidemiological studies [66, 67]. It has long been debated whether protective immunity is predominantly due to mucosal sIgA anti-O-antigen antibodies, by serum IgG antibodies or by both. Strong mucosal sIgA anti-O-antigen antibody responses have been observed post wild type infection and experimental challenge [54, 68-73]. Other studies have identified serum IgG anti-O-antigen antibody response, as key elements of the protective immune response [74-76]. Additional research is needed to define the roles of intestinal sIgA and serum IgG antibodies in mediating protection against *Shigella.*

1.4.3 Cellular immune response

In comparison to other intracellular bacteria, very little is known about cell mediated immune (CMI) responses to *Shigella.* This is largely due to the absence of a natural mouse infection model for shigellosis. *In vitro* studies have shown that *Shigella* antigens can activate T cell responses [77-79]. *In vivo* studies using the murine pulmonary model of shigellosis have also shown that T and NK cells play a critical role in clearing *Shigella* [49]. Islam *et al.* have previously reported that *Shigella* induces the cellular activation of T and B cells in infected patients [80]. More recently Th17 has been identified to play a role in the adaptive response to *Shigella* infection [81]. In addition to these findings, the cytokines induced during *Shigella* infection, particularly IL-18 produced by apoptotic macrophages, are known to induce both Th1 and Th2 lymphocyte responses [82, 83]. The increased frequency and severity of shigellosis in AIDS patients (deficient in $CD4^+$ T cells) further suggest that a CMI response provides protection against shigellosis [84-86].

1.5 Virulence genes of *S. flexneri*

Several *S. flexneri* virulence genes that are required for bacterial invasion and colonization of intestinal cells have been identified in chromosomal pathogenicity islands (PAI) (Table 1.1) and on the large virulence plasmid of *S. flexneri* (Table 1.2). Given the *S. flexneri* genome is remarkably similar to *E. coli* (the sequence divergence between the two is only about 1.5% [87]), it is not unusual that the majority of *S. flexneri* virulence genes lie on the 220 kb virulence plasmid which is unique to *Shigella* and essential for pathogenesis [88].

The core region of the virulence plasmid, known as the entry region, is conserved between *S. flexneri* serotypes. This region covers 31 kb of the plasmid and carries 34 genes required for pathogenesis. The genes in the entry region are organized into two clusters that are transcribed in opposite directions. Based on their functions, genes in the entry region are further categorized into four groups; effector proteins secreted by the T3SS (Ipa proteins), proteins required for the assembly and secretion of T3SS effector proteins (Mxi/Spa proteins), chaperone proteins (Ipg proteins) and finally proteins required for the transcription of virulence plasmid genes (VirB and MxiE) [89]. The expression of genes in the entry region is under the tight control of a regulatory network, which responds to environmental changes encountered upon bacterial entry into hosts such as temperature shift to 37 °C, changes in pH, osmolality and iron levels [90-92].

Chromosomally-encoded factors, such as VirR and OmpR-EnvZ, are the initial elements of the regulatory cascade that sense and react to environmental changes. These proteins then induce the expression of virulence plasmid-encoded transcription activators, VirF, VirB and

MxiE. Gene expression from the virulence plasmid destabilizes the plasmid, resulting in high rates of plasmid loss. It is therefore critical to monitor strains for the maintenance of virulence plasmids. The common approach to monitor the presence of the virulence plasmid is to grow cells on Congo red agar plates, components of the virulence plasmid bind to Congo red and result in red pigmentation in the colonies [93]. A PCR based detection method is also used to confirm the presence of the virulence plasmid using primers designed to amplify distinct regions of the plasmid [94].

1.6 *Shigella* vaccine development

Advances in our understanding of the pathogenesis of *S. flexneri* and the identification of several virulence factors have led to the development of multiple vaccine candidates. However a commercially viable *Shigella* vaccine still eludes us. Several factors are responsible for the slow pace of *Shigella* vaccine development. The lack of a relevant small animal model of shigellosis and serotype-specific immune responses elicited by *Shigella* strains have been the leading impediments to vaccine development. Over the past five years, despite these obstacles, substantial progress has been made in *Shigella* vaccine development. The most recent *Shigella* vaccines can be broadly categorized into two groups; serotype-specific vaccines or conserved antigen vaccines. Recent advances in *Shigella* vaccine development over the past five years have been outlined in Table 1.3.

Table 1.1: Chromosomal virulence genes of *S. flexneri* adapted from [89]

PAI	Gene	Biochemical activity	Role in virulence	Reference
SHI-1	*sigA*	Immunoglobulin A-like cytopathic protease	Intestinal fluid accumulation, cytopathic toxin	[95, 96]
	picA	Serine protease, mucinase	Mucus permeabilization, serum resistance, Hemagglutination	[96, 97]
	set1A, set1B	Enterotoxin ShET1	Intestinal fluid accumulation, development of watery diarrhoea	[98, 99]
SHI-2	iucA to iucD, iutA	Siderophore (aerobactin) production and transport	Iron acquisition	[100-102]
SHI-O	*gtrA, gtrB, gtr$_{type}$*	Modification of O antigens, serotype conversion	Evasion of host immune response	[5]
SRL	*fecA to fecE, fecI, fecR*	Ferric dicitrate uptake	Iron acquisition	[103, 104]

Table 1.2: Virulence plasmid-encoded virulence genes of *S. flexneri*

Gene	Biochemical activity	Role in virulence	Reference
virA	Cysteine protease	Facilitates entry and intercellular spread by degrading microtubules	[105, 106]
virF	Positive regulation of *virB* and *virG*	Adherence, invasion and intracellular spread	[107, 108]
virB	Positive regulation of Ipa and *mxi-spa* locus	Adherence, invasion and intracellular spread	[109]
virG (*icsA*)	Active polymerization of actin	Inter and intracellular spread	[29]
icsB	-	Protects IcsA by preventing autophagic recognition	[110-112]
icsP	Serine protease	Cleavage of IcsA, modulation of actin-based motility	[113, 114]
mxi/spa locus	Encodes type 3 secretion system (T3SS)	Invasion	[115]
ipaA	Vinculin activation	Efficient invasion, actin cytoskeleton rearrangements, disassembly of cell-matrix adherence	[116]
ipaB	Membrane fusion	Control of type 3 secretion, translocon formation, phagosome escape, macrophage apoptosis	[117]
ipaC	Actin polymerization	Translocon formation, filopodium formation, phagosome escape, disruption of EC tight junctions	[118]
ipaD	Effector protein	Regulates secretion of Ipa proteins and insertion of IpaB and IpaC into host cells	[119]
ipaH	E3 Ubiquitin ligase	Assists in escape from macrophage vacuole. Host cell transcriptome modulation, reduction of inflammation	[120]

1.6.1 Serotype-specific *Shigella* vaccine candidates

Serotype-specific vaccines are designed to stimulate acquired immunity and serotype-specific protection. This category of vaccines include live attenuated strains, killed whole cell formulations, conjugate vaccines (composed of O-antigen molecules conjugated to a protein carrier) and genetically engineered O-antigen protein fusions. Live attenuated vaccine candidates are generated by mutating virulence and metabolic genes required for bacterial invasion and survival. These vaccines introduce a repertoire of *Shigella* antigens to the mucosal immune system and elicit a strong serotype-specific response. Live attenuated *Shigella* vaccine candidates have been shown to induce protective immunity against virulent challenge in volunteer studies [69, 121]. The main limitation of live attenuated vaccines has been achieving the right balance between safety and immunogenicity. A number of live attenuated *Shigella* vaccine strains have been engineered to carry mutations in critical metabolic genes required for bacterial survival within hosts, such as the *guaBA, iuc, msbB2* and *aroA-D* genes (Table 1.3). *Shigella* virulence and toxin genes including *virG, sen* and *stx,* have also been used as attenuation targets to design live vaccine candidates. The identification of new *Shigella* virulence factors will help us bridge the gap between the safety and immunogenicity of live attenuated vaccines.

1.6.2 Conserved antigen vaccine candidates

Conserved antigen vaccines are designed to provide heterologous protection against multiple serotypes of *Shigella.* These vaccines comprise of purified virulence factors expressed across multiple serotypes such as the Ipa proteins, outer membrane proteins-OmpA and IcsP (Table 1.3). The most promising conserved antigen vaccine has been the Invaplex vaccine developed at the Walter Reed Army Institute of Research. Invaplex is a complex of purified LPS and Ipa

Table 1.3: Recent advances in *Shigella* vaccine development: Vaccines candidates developed in the past five years

Vaccine Candidate	Description	Developmental stage	Route	Reference
Live attenuated vaccines				
S. dysenteriae 1 CVD 1256	Δ*guaBA,* Δ*sen,* Δ*stxA,* Δ*virG*	Preclinical	Oral	[122]
S. sonnei WRSs2, 3	Δ*virG,* Δ*senA,* Δ*senB,* Δ*msbB2*	Preclinical, non-human primate	Oral	[123-125]
S. flexneri 2a SC602	Δ*virG,* Δ*iuc*	Phase I–II	Oral	[126]
S. flexneri 2a WRSf2G11, 12, 15	Δ*virG,* Δ*senA,* Δ*senB,* Δ*msbB2*	Preclinical	Oral	[127, 128]
S. dysenteriae 1WRSd1	Δ*virG,* Δ*stxAB*	Phase I	Oral	[129]
S. enterica serovar Typhi strain Ty21a-Ss	*Salmonella* Ty21a strain stably expressing *S. sonnei* LPS	Preclinical, murine pulmonary model	Intraperitoneal	[130]
Conjugate vaccines				
GlycoVaxyn bioconjugate	*S. dysenteriae* 1 LPS-exoA	Phase I	Parenteral	[131]
Synthetic oligosaccharide O-antigen	mimic–tetanus toxoid	Preclinical	Parenteral	[132, 133]
Conserved antigen vaccines				
Purified Ipa proteins *S. flexneri* 2a	IpaB plus IpaD	Preclinical	Intranasal	[134, 135]
GMMA vesicles	Outer membrane and periplasmic proteins	Preclinical	Intranasal	[136]
Conserved proteins	IcsP, SigA Protein fragments	Preclinical	Mucosal	[137]
Invaplex	LPS plus IpaB, IpaC and IpaD	Phase II	Intranasal	[138, 139]
OMV	Purified non-capsulated and capsulated OMV	Preclinical, murine pulmonary model	Oral and Intranasal	[140-142]
OmpA	OmpA	Preclinical, murine pulmonary model	Intranasal	[143]

proteins (IpaB, IpaC and IpaD) which has been shown to be immunogenic after intranasal delivery in human volunteers [138, 139]. Although conserved antigen vaccines are safe and provide broad-spectrum protection, they suffer from lower immunogenicity and generally require adjuvants to boost the immune response.

1.7 Bacteriophages

The term bacteriophage has been derived from "bacteria" and the Greek *"phagein"* meaning to devour, as bacteriophages are the natural predators of bacteria. Bacteriophages are widely distributed in locations populated by bacterial hosts such as soil, sea water and the intestines of animals [144-146]. Bacteriophages are the most abundant organisms on the planet and are believed to outnumber bacteria by an estimated ten-fold [147]. Thus bacteria are faced with the constant threat of bacteriophage predation as a result of which bacterial host and bacteriophages are involved in cycles of constant co-evolution.

Bacteriophages have genetic material either in the form of DNA or RNA encapsulated in a protein coat, known as the capsid, which protect the genetic material and enables transfer between host cells. Bacteriophages possess the unique ability to laterally transfer genes between bacteria. This property plays a major role in bacterial evolution and increased pathogenicity [148-150]. A great majority of bacteriophages carry dsDNA and are responsible for the intraspecific genomic diversification in bacteria [151, 152]. This diversification is largely due to bacteriophage induced rearrangement of the host genome and the lateral transfer of bacterial genes.

1.7.1 Temperate phages

Based on their lifecycle, phages are divided into two basic classes: virulent and temperate phages. Virulent phages adopt a simple lifestyle known as the lytic cycle, that encompasses adsorption to host cells, penetration, phage multiplication and culminates in host cell rupture with the release of phage particles (Figure 1.3.A). Temperate phages adopt a more complex lifecycle with two reproductive options; the lytic and lysogenic cycles. Temperate phages can either reproduce lytically as virulent phages or they may remain as 'symbionts' within the host cells through the lysogenic pathway (Figure 1.3.B). Temperate bacteriophages achieve this by incorporating their DNA into the host genome to form prophages, as a consequence of which the phage genetic material is replicated by the host (now known as a lysogen), for several generations.

An important outcome of lysogeny is lysogenic conversion, where temperate bacteriophages induce changes in the phenotype of the host. Lysogenic conversion often involves alterations in the surface characteristics of the host to prevent further infection by other bacteriophages. Lysogenic conversion has also been found to provide selective advantages to prophages by increasing their virulence (discussed further in Section 1.8.3). When faced with unfavorable conditions such as ultraviolet (UV) radiations and chemical mutagens that damage DNA, prophages enter the lytic cycle and bacteriophage particles are released from lysogenized host cells.

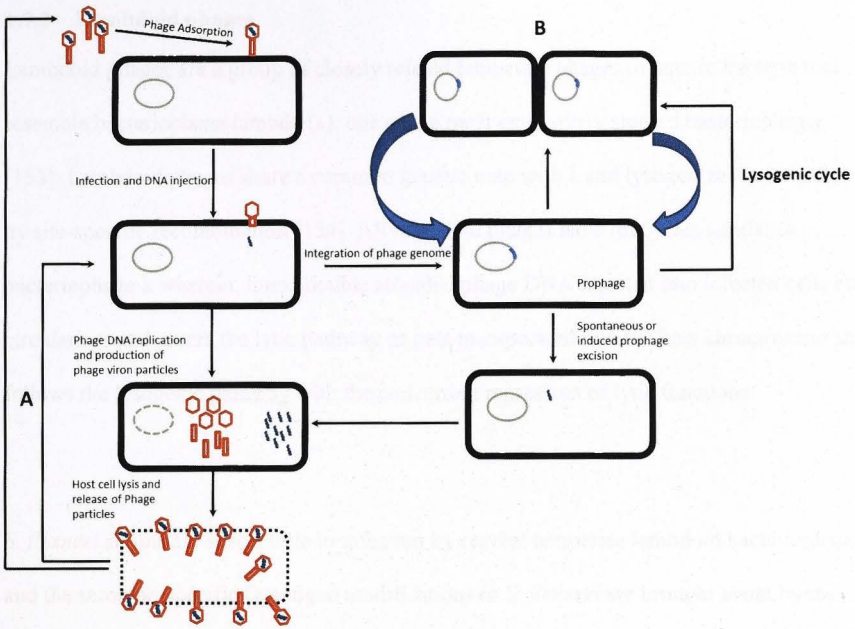

Figure 1.3: Lifecycle of temperate bacteriophages. The lifecycle of temperate bacteriophages is characterized by two cycles; the lytic (**A**) and lysogenic (**B**). Both cycles begin with phage absorption to its receptor on the bacterial cell wall, penetration of the cell wall and insertion of phage DNA into host cells. **A:** During the lytic cycle, injected phage DNA directs the host to produce multiple copies of phage protein and DNA. Empty phage heads are assembled and packed with DNA following which the collars, tail sheath and fibre proteins are assembled to produce mature phage particles. Bacterial cells are lysed and infectious phage particles are released. **B:** During the lysogenic cycle, injected phage DNA is incorporated by the activity of phage-encoded integrase protein into the bacterial chromosome becoming a prophage, phage DNA is replicated along with the host DNA producing daughter cells carrying the prophage. Replication of the prophage continues /indefinitely along with cell division. The prophage can be induced of spontaneously excised from the bacterial genome and proceed along the lytic pathway.

1.7.2 Lambdoid phages

Lambdoid phages are a group of closely related temperate phages of enteric bacteria that resemble bacteriophage lambda (λ), one of the most extensively studied bacteriophages [153]. Lambdoid phages share a common genetic map with λ and lysogenize bacterial hosts by site-specific recombination [154]. All lambdoid phages have lifecycles similar to bacteriophage λ wherein, linear double stranded phage DNA injected into infected cells either circularizes and enters the lytic pathway or gets incorporated into the host chromosome and follows the lysogenic pathway with the concurrent repression of lytic functions.

S. flexneri strains are susceptible to infection by several temperate lambdoid bacteriophages and the serotype-specific O-antigen modifications in *S. flexneri* are brought about by the temperate bacteriophage-encoded *glucosyltransferase* (*gtr*) gene cluster [5]. To date six serotype converting bacteriophages: SfI [155], SfII [156], SfIV [157], SfV [158], SfX [11, 159] and Sf6 [160] have been isolated and studied. Lysogenization of these phages has been shown to convert serotype Y strains to serotype 1a, 2a, 4a, 5a, X, and 3b, respectively. The genetic organization of these serotype converting phages is conserved and their genomes share high sequence similarity with bacteriophage λ in their head assembly and DNA packaging genes and their tail genes resemble a Mu-like Myovirus [5]. Apart from O-antigen modification, little is known about the molecular biology of these temperate serotype converting phages of *S. flexneri.*

1.7.3 Bacteriophages and bacterial pathogenesis

The notion that bacteriophages-encoded factors that enhance bacterial virulence has been around since 1927 when Forbisher and Brown discovered that non-toxin producing

Streptococci acquired the ability to produce the scarlatinal toxin on exposure to filtered supernatants of toxigenic strains [161]. We now know that the supernatants carried bacteriophages encoding the scarlatinal toxin gene and the investigators were in fact describing transduction; the process by which bacteriophages transfer genes between related bacterial species. This discovery has led to the widespread acceptance of the hypothesis that bacteria acquire virulence properties through lysogenic conversion. Advances in sequencing technologies have led to a massive increase in the number of sequenced bacterial genomes. Analysis of these genome sequences, particularly in pathogenic bacteria, has revealed that 10-20% of several bacterial genomes consist of prophage DNA [148, 162]. Over the years several bacteriophage-encoded virulence factors from a range of morphologically diverse bacteriophages, have been identified and implicated in all stages of bacterial pathogenesis including; adherence, colonization, resistance to host defense responses and the production of exotoxins (Table 1.4).

1.7.4 Bacteriophage-encoded virulence factors in prominent enteric pathogens

1.7.4.1 *Vibrio cholerae*

The cholera toxin (Ctx) is the only known toxin produced by *V. cholerae* and the production of this exotoxin is one of the main pathogenic mechanisms responsible for the severe watery diarrhoea following bacterial invasion of the small intestine. Cholera toxin up-regulates adenylate cyclase (an enzyme that catalyzes the conversion of ATP to cAMP) activity within human intestinal cells. The up-regulation of this enzyme results in profuse watery diarrhoea [163], which is widely assumed to contribute significantly to the fecal-oral transmission of *V. cholerae* [164]. Cholera toxin is encoded by the filamentous bacteriophage CTX-ϕ [165]. The delivery of the cholera toxin requires successful colonization of the small intestine by *V.*

Table 1.4: Bacteriophage-encoded bacterial virulence factors

Bacterial property altered	Proteins or phenotype	Bacteriophage	References
Exotoxin Production			
C. botulinum	Botulinum toxin	Phage C1	[166]
C. diphtheria	Diphtheria toxin	β-phage	[167, 168]
E. coli	The Shiga toxin	933, H-19B	[169, 170]
E. coli EPEC	cdt1 toxin	CDT-1ϕ	[171]
P. aeruginosa	Pseudomonas cytotoxins	CTXϕ	[172]
S. dysenteriae	Shiga toxins	933W, H-19A	[173]
S. aureus	Staphylococcal enterotoxins, exfoliative toxins and toxic shock syndrome toxins	ϕMu50A, ϕ13, ϕ315	[174-179]
V. cholerae	Cholera toxin	CTXϕ	[180]
Colonization/adhesion			
E. coli	The *lom* gene promote adhesion to buccal epithelial cells	λ	[181-183]
P. aeruginosa	Phage FIZ15 promotes adhesion to buccal epithelial cells	FIZ15	[184]
S. mitis	PblA and PblB, surface protein that promote adhesion to platelets	SM-1	[185, 186]
V. cholerae	TCP-pilus	VP1 Φ	[187]
Invasion			
E. coli EPEC	Type 3 secretion system effector proteins	Lambdoid prophages	[188-192]
S. enterica	Type 3 secretion system effector proteins	SOPϕ, Gifsy-1, Gifsy-2, Gifsy-3, ST64B	[193-196]
S. pyogenes	Hyaluronidase	H4489A	[197]
S. aureus	Fibrinolysin	Φ13	[176, 198]
Increased intracellular survival			
E. coli	The *bor* gene promotes survival in animal serum,	λ	[199]
S. enterica	SodC protein, a superoxide dismutase	Gifsy-2, Fles-1	[200-202]
	NanH, Neuraminidase	Fles-1	[203]
S. pyogenes	Lysogeny up-regulates antiphagocytic M protein	?	[152]
E. coli O157	SodC protein, a superoxide dismutase	Sp4, -10	
Altering antigenicity			
P. aeruginosa	O-antigen modifying enzymes	D3	[204]
S. enterica	O-antigen modifying enzymes	ε^{45}	[205, 206]
S. flexneri	O-antigen modifying enzymes	SfII, SfV, SfI, SfX, Sf6 and SfIV	[157]

cholerae, which is mediated by toxin-coregulated pilus (TCP) [207-209]. TCP, encoded by bacteriophage VP1ϕ [210], is another recognized virulence factor of *V. cholerae.* TCP mediates bacterium-bacterium interactions that promote microcolony formation. These interactions are required for bacterial attachment and colonization of host cells [201]. Therefore the acquisition of phage-encoded *ctx* and *tcp* genes are crucial events in the evolution of pathogenic *V. cholerae.*

1.7.4.2 Pathogenic *E. coli*

E. coli strains are widely distributed commensals that are known to colonize the human gut. Several *E. coli* strains such as Enterotoxigenic *E. coli* (ETEC), Enteropathogenic *E. coli* (EPEC), Enteroinvasive *E. coli* (EIEC) and Enteroaggregative *E. coli* (EAEC) have been identified to be pathogenic, causing a range of infections in humans and animals [211]. The versatility between *E. coli* strains is largely on account of genomic diversity between strains and bacteriophages are known to be one of the major sources of this diversity as they facilitate the acquisition of virulence genes by horizontal gene transfer [152]. Several prophage-encoded virulence factors from a range of temperate bacteriophages have been identified in pathogenic strains of *E. coli* including, the shiga-toxins Stx1and Stx2 (encoded by phages 933 and H19-B, respectively) [169, 212], the cdt1 toxin (encoded by the cdt1ϕ phage) [171], the *lom* and *bor* genes, from bacteriophage λ that are required for adherence and serum resistance [181-183, 199] and *sod*, encoding superoxide dismutase (encoded by phages Sp4, -10) required for survival within host cells. Furthermore, genes encoding effector proteins of EPEC including *tccP* [188], *nleA-F* [189], *nleH* [190], *espL2* [191] and *cif* [192] have also been identified to be encoded by lambdoid prophages. It has been suggested that the acquisition of these prophage-encoded virulence factors plays a critical role in the conversion of non-pathogenic *E. coli* strain to food-borne pathogenic strains [213].

1.7.4.3 *Salmonella spp.*

Virulence and host adaptation in *Salmonella* is influenced by a multitude of genes, many of which are encoded by bacteriophages. As in the case of *Shigella* spp, the invasive properties of *Salmonella enterica,* require the T3SS, which inject effector proteins directly into the cytoplasm of host cells [214]. SopE is one of these effector proteins which, on injection into host cells, activates human Rho GTPases and contributes to the invasion of *Salmonella* [194, 215]. GogB, SseI, SspH1 and SseK3 are other T3SS effector proteins that have been found to be involved in epithelial cell uptake [196, 202, 216, 217]. The genes encoding effector proteins SopE, GogB, SseI and SspH1 are all located on temperate *Salmonella* phages Sopϕ [218], Gifsy-1 [216], Gifsy-2 [217] and Gifsy-3 [202], respectively.

Following epithelial cell invasion, *Salmonella* preferentially localizes to Peyer's patches and the *gipA* gene (encoded by bacteriophage Gifsy-1) has been found to be required for the survival of *Salmonella* cells in this environment [195]. Lysogeny by temperate phages thus contributes to the virulence of *Salmonella* by promoting bacterial uptake in intestinal cells and survival within infected Peyer's patches.

Additional examples of bacteriophage-encoded virulence factors in *Salmonella* are the O-antigen modifying, *gtr* genes encoded by ε^{45} [206, 219], superoxide dismutase, SodC proteins (encoded by bacteriophages Gifsy-2 and Fels-1) that protect bacterial cells against stress [220, 221] and neuraminidase (NanH) encoded by bacteriophage Fels-1 [202].

1.7.4.4 *Shigella spp.*

Shiga toxins initially isolated from *S. dysenteriae* strains are encoded by the *stx-1* and *stx-2* genes. The *stx* genes in *S. dysenteriae* lie adjacent to lambdoid phage-like sequences interrupted by several insertion elements, suggesting that the toxin genes lie in a prophage [173]. The O-antigen modifying genes, *gtr* and *oac,* are the only phage-encoded genes that have been linked to the virulence of *S. flexneri* [5]. The identification of several phage-encoded virulence factors in other enteric pathogens, warrant the need to study *S. flexneri* phages further.

1.8 *In vitro* and *in vivo* models of shigellosis

Poorly differentiated or non-polarized cell lines such as HeLa, HEp-2 and BHK grown in culture flasks have been used extensively to study *S. flexneri*-epithelial cell interactions *in vitro*. More sophisticated systems have also been designed to study the intricate interactions between *S. flexneri* and host epithelia including human, Caco-2 or T84 intestinal cell lines grown on permeable filter supports with distinct upper (luminal) and lower (basal) chambers [222].

S. flexneri strictly infects humans and non-human primates as a result of which there is no convenient animal model available for studying *S. flexneri* infection. Non-human primates develop diarrhoea and dysentery after oral infection with a large inoculum of *Shigella,* and therefore is a useful animal model to evaluate the efficacy of vaccine candidates [223, 224]. However the routine use of this animal model poses large ethical and economic problems. The lack of a relevant small animal model of shigellosis has been one of the major limitations to *Shigella* vaccine development. A number of alternative animal models have been identified

which use mucosal surfaces other than the colon in mice, guinea pigs and rabbits (Table 1.5). However, the main drawback of these models is the lack of clinical relevance of infection site and symptoms produced. The murine pulmonary model of shigellosis is the most extensively used *in vivo* model of shigellosis. While adult mice infected with *S. flexneri* orally, fail to develop shigellosis, when inoculated with *S. flexneri* intranasally, mice develop pulmonary pneumonia as a result of *S. flexneri* invasion of the pulmonary epithelial lining of the trachea-bronchial tract [225]. Although this model of shigellosis is lacking in clinical relevance owing to the site of infection, it has been used extensively on account of lack of alternative animal models.

1.9 *Caenorhabditis elegans* as an *in vivo* model to study host-pathogen interactions

In the 1960's, Sydney Brenner established the use of *Caenorhabditis elegans* as a model organism for studying neurobiology, cell biology and genetics *in vivo* [226]. *C. elegans* is a free-living, soil-dwelling nematode (roundworm) that feeds on bacteria present in the soil. The small size (~1 mm), rapid generation time (3 days at 20 °C), their ability as self-fertilizing hermaphrodites to produce genetically identical progeny and simple anatomy are some of the features that make this nematode an attractive model for *in vivo* studies. In the laboratory, *C. elegans* are maintained on the non-pathogenic *E. coli* OP50 strain; bacterial infection of nematodes can thus be achieved by simply replacing the *E. coli* strain with pathogenic bacteria. These unique features of *C. elegans* have led to the use of this *in vivo* system to study host-pathogen interactions with an ever-growing list of bacterial pathogens that are known to infect *C. elegans* including: *Salmonella enterica, Pseudomonas aeruginosa* and *Serratia marcescens* [227-229].

Table 1.5: Animal models of shigellosis

Animal model	Description	Application	Limitations	Reference
Macaque monkey	Intragastric inoculation with a high dose of *Shigella* (~10^{10} CFU) develop shigellosis with symptoms similar to the human disease	Most relevant model of shigellosis	High infection dose required, high cost, ethically unsound	[230]
Murine pulmonary model	Intranasal inoculation with a high dose of *Shigella* in mice causes bacterial invasion of the pulmonary epithelial cells resulting in pulmonary pneumonia	Most commonly used *in vivo* model of shigellosis for vaccine research	Clinically irrelevant owing to the site of infection and symptoms produced	[231]
Newborn mice	Oral infection with a high dose of *Shigella* triggers an inflammatory respons that culminates in epithelial cell damage	Used to study early interactions between *Shigella* cells and the host mucosa	Newborn mice develop resistance to *Shigella* 4-5 days post birth.	[232]
Guinea pig, Sereny Test	*Shigella* inoculated into the keratoconjunctival sac invade the conjunctiva resulting in keratoconjunctivitis	The Sereny test is used extensively for comparing the virulence of *Shigella* strains	Clinically irrelevant owing to the site of infection and symptoms produced	[233]
Rabbit-ileal ligated assay	Ligated section of the rabbit ileum when inoculated with *Shigella*	Use to study interactions between *Shigella* cells and intestinal epithelial layer and innate responses to *Shigella* infection	The suitability for vaccine development has not been determined	[234]

1.9.1 *C. elegans* anatomy and lifecycle

The *C. elegans* lifecycle begins with an egg stage, followed by four successive larval stages (L1-L4) and an adult stage (Figure 1.4). Worms transitioning through each stage replace their old cuticle (exoskeleton) layer with a new cuticle layer. The entire lifecycle takes 3 days under optimum conditions (20 °C), however the lifecycle of these nematodes is temperature-dependent and the entire cycle can be fast-tracked by increasing the temperature to 22 °C; under these conditions the nematodes can complete their entire lifecycle in about 2 days [235]. The availability of food is another factor that influences the lifecycle of *C. elegans*. When food is scarce, worms progress from the L1 stage into the survival and dispersal stage called the dauer larva. Worms can remain in this stage for up to 4 months until conditions improve, at which point the worms molt and enter the L4 stage and complete their lifecycle.

Like other nematodes, the body of *C. elegans* is cylindrical and unsegmented with tapering ends. The body is comprised of two concentric cylindrical structures separated by a pseudocoelomic cavity. The outer cylinder forms the body wall and is comprised of an outer protective cuticle layer making up the exoskeleton, an underlying hypodermis which secretes the cuticle. The outer cylinder also carries the excretory system, muscles and neurons. The inner cylinder of the body consists of the pharynx, intestine, and gonads in adult worms (Figure 1.5.A). As most pathogenic bacterial infections in *C. elegans* predominantly affect the intestine, a detailed outline of this organ follows.

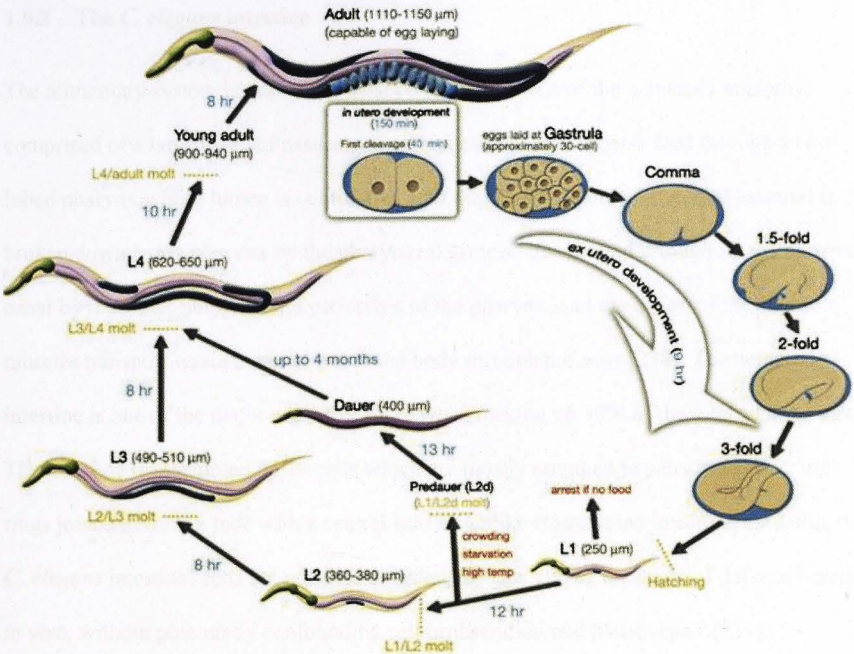

Figure 1.4: Lifecycle of *C. elegans* at 22 °C. Adults lay eggs that proceed through numerous stages of embryogenesis, indicated as *ex utero* development. Egg carrying fully developed embryos hatch to release the first larval stage (L1). Under optimal conditions L1 larvae transition through three more larval stages (L2-L4) and finally develop into adults. Under unfavorable conditions, such as a shortage of food, L1 larvae enter a survival stage known as the dauer larva and worms remain at this stage until conditions become favorable. Numbers in blue indicate the duration of each stage at 22 °C and numbers in brackets indicate the average size of worms. Figure from Altun and Hall 2005 [236].

1.9.2 The *C. elegans* intestine

The alimentary system is one of the most complex portions of the nematode anatomy; comprised of a large array of tissues and cell types [237]. *C. elegans* feed through a two-lobed pharynx whose lumen is continuous with the intestinal lumen. Ingested material is broken down in the pharynx by the pharyngeal grinder, transported throughout the alimentary canal by muscular pumping and peristalsis of the pharynx, and the action of the enteric muscles transport waste material out of the body through the anus [238]. The nematode intestine is one of the major organs of *C. elegans,* making up 30% of the total somatic mass. The intestine is assembled by 20 cells which are mostly arranged in pairs to form 9 "int" rings joined to form a tube with a central lumen. Unlike mammalian intestinal epithelia, the *C. elegans* intestinal cells are not shed or renewed. This allows the study of defense functions *in vivo,* without potentially confounding cell proliferation and tissue repair [239].

C. elegans intestinal cells, also known as enterocytes, show striking similarities to human intestinal epithelial cells, including their organization into apical and basolateral domains and presence of actin-rich microvilli throughout the apical domain (Figure 1.5.C). The apical brush border glycocalyx of the *C. elegans* enterocytes share the same morphology and function as the brush border in mammalian cells and acts as the first line of defense against invading pathogens. The microvilli are anchored into an actin-rich terminal web which spans the apical surface of the enterocyte. Like human enterocytes, the structural integrity of the *C. elegans* enterocytes is also maintained by ERM-1, a member of the ERM family of proteins located beneath the intestinal apical surface, that connect the actin cytoskeleton to the plasma membrane [240, 241]. Vesicular trafficking in *C. elegans* enterocytes resembles polarized trafficking in human epithelial cells, with distinct sorting to apical and basolateral sides.

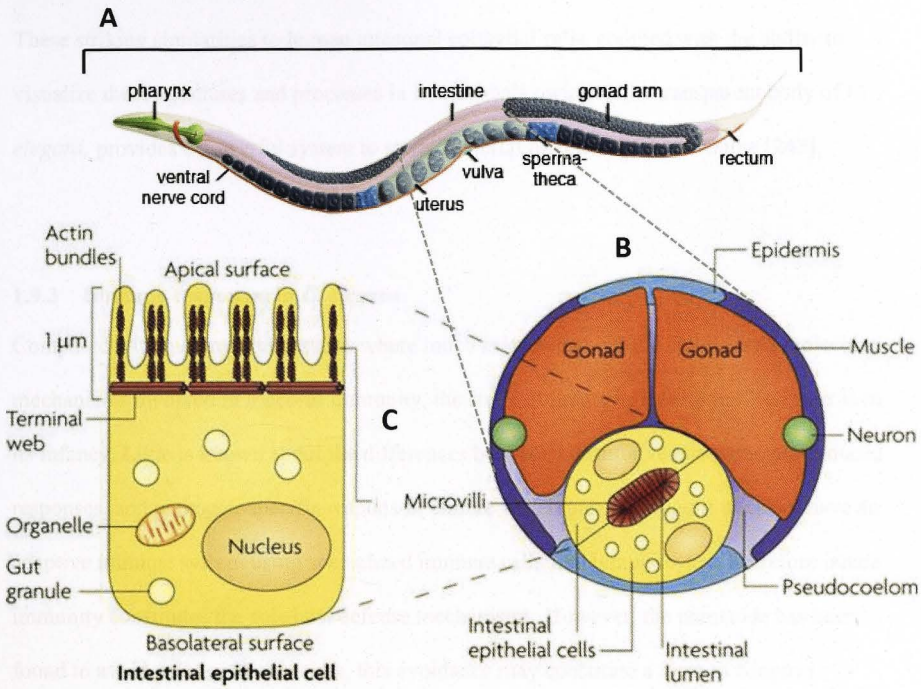

Figure 1.5: The intestine of an adult *C. elegans* hermaphrodite. A-Schematic representation of the anatomy of an adult *C. elegans* hermaphrodite showing the principal anatomical features with the anterior end of the body, the head, towards the left and the posterior tail end towards the right. The nematode intestine is composed of 20 intestinal epithelial cells organized in nine rings. **B:** Schematic representation of a transverse mid body section of a healthy nematode showing one of the nine intestinal rings composed of two intestinal cells (in yellow). **C:** Diagrammatic representation of a single nematode intestinal epithelial cell which shares similarities with human intestinal cells such as organization into apical and basolateral surfaces and the presence of an apical actin-rich microvilli brush border layer toward the intestinal lumen. Figure adapted from [242].

These striking similarities to human intestinal epithelial cells, coupled with the ability to visualize these structures and processes in live animals owing to the transparent body of *C. elegans,* provides a powerful system to study bacterial infection of the intestine [243].

1.9.3 Immune responses in *C. elegans*

Compared with mammalian systems where much is known about the cellular and molecular mechanisms involved in mucosal immunity, the study of innate immunity in *C. elegans* is in its infancy. Little is known about the differences between constitutive and pathogen-induced responses, and pathogen-specific responses. Unlike vertebrates, *C. elegans* does not have an adaptive immune system using specialized immune cells like lymphocytes. Therefore innate immunity constitutes the sole host defense mechanisms. However, the nematode has been found to avoid pathogens over time, this avoidance may constitute a form of adaptive immunity using behavioral changes instead of specialized cells [244].

1.9.3.1 The intestinal epithelial layer and pathogen resistance

As in humans, the *C. elegans* intestinal epithelial cells act as a physical barrier which provides protection from invading pathogens. This physical barrier is highly effective in protecting nematodes from bacterial invasion. Although several intracellular pathogens have been found to infect *C. elegans,* they fail to penetrate the epithelial barrier, with the exception of *P. aeruginosa* [242]. Mammalian intestinal cells produce antimicrobial peptides in response to inflammation and infection (Section 1.4.1). *C. elegans* also produces antimicrobial peptides in response to injury or infection [245, 246], thus it has been suggested that the most basic cellular and molecular mechanisms of inflammation, encompassing

cellular migration and rapid release of antimicrobial peptides to infected tissues, are present in the nematode [247].

1.9.3.2 Innate immunity in *C. elegans* is TLR-independent

Innate immunity relies on the recognition of microorganisms, achieved through a limited number of PRRs. A number of mammalian PRRs have been recognized, such as the toll-like receptors (TLRs) and Nod-like receptors (NLR) [248, 249]. As a primary response to bacterial infection, mammalian enterocyte TLRs recognize bacterial cells by interacting with structurally-conserved surface molecules, particularly bacterial LPS, which leads to the activation of NF-κB. NF-κB then translocates into the nucleus through signaling pathways involving myeloid differentiation primary-response protein 88 (MYD88) and drives the transcription of inflammatory response genes, including those encoding cytokines and chemokines [250, 251]. Although a TLR homologue (TOL-1) has been found in *C. elegans,* the nematode seems to detect and respond to infection in a TLR-independent manner [242].

The *C. elegans* genome lacks NF-κB and MYD88 homologues. Furthermore, nematodes fail to produce homologues of known mammalian cytokines. It is therefore surprising that *C. elegans* has the capacity to mount pathogen-specific innate immune signaling cascades. Nematodes utilize several evolutionarily conserved signaling pathways to produce effector molecules in response to infection [252]. The p38 MAPK pathway, and the insulin signaling pathway (DAF-2-DAF-16) are important mediators of innate immune responses in nematode intestines and have been shown to function in parallel [253].

1.9.3.3 The p38 mitogen-activated protein kinase pathway (MAPK)

The p38 MAPK signaling cascade is the main regulator of immune responses in *C. elegans* and was first identified in a forward genetic screen for mutant worms with enhanced susceptibility to infection with *P. aeruginosa* [254]. This pathway acts autonomously in the intestinal cells to coordinate defense responses against a wide array of ingested pathogens. Nematodes carrying mutations in this pathway show increased susceptibility to infection with both Gram-negative pathogens: *P. aeruginosa* [253, 254], *S. enterica* [255] and *Yersinia pestis* [256] and *S. marcescens* [257]; and the Gram-positive pathogens *Enterococcus feacalis* [257], and *S. aureus* [258].

The p38 MAPK signaling cascade involves the neuronal symmetry family member 1 (NSY-1), SAPK/ERK kinase 1 (SEK-1) and p38 MAPK family member 1 (PMK-1) (Figure 1.6.A). This pathway is orthologous to the ASK-1 MAPK pathway in mammals [252], which is involved in the mammalian cellular immune response [259]. In mammals, the MAPK cascade acts downstream of TLRs [260-263], however in *C. elegans* the activation of this pathway is TLR-independent and this pathway is required for nematode defense against every intestinal pathogen that has been tested to date [242].

1.9.3.4 The insulin signaling pathway

The DAF-2-DAF-16 (also known as FOXO) insulin-like signaling pathway in *C. elegans* is involved in metabolism, reproduction, development, lifespan and resistance to environmental stresses [264]. This pathway also plays an important role in innate immunity [265], but its precise role in innate immunity remains unclear. The insulin signaling pathway has been

identified in response to infection with *P. aeruginosa* [266], enteropathogenic *E. coli* [267] *S. aureus* and *E. faecalis* [265].

DAF-2 is an insulin receptor that is expressed on the surface of numerous *C. elegans* cells, including the intestinal epithelial cells. Insulin-like peptides (such as INS-7), up-regulated in response to bacterial infection [266, 268], interact with DAF-2, which subsequently inhibits the downstream transcription factor DAF-16 through a kinase cascade (Figure 1.6.B). Loss of function mutations in *daf-2* activate the constitutive expression of *daf-16,* which increases the expression of several DAF-16-dependent genes [269], many of which show homology to antimicrobial defense genes [270, 271]. *daf-2* mutant worms have prolonged lifespans and increased resistance to death caused by both Gram positive and Gram negative bacteria [265], which is most likely due to DAF-16-mediated up-regulation of antimicrobial peptides. Studies have shown that although the constitutive activation of DAF-16 enhances pathogen resistance, DAF-16 is not normally activated during pathogen infection [272-274], which implies that DAF-16 independent pathways may be involved in nematode responses to intestinal pathogens.

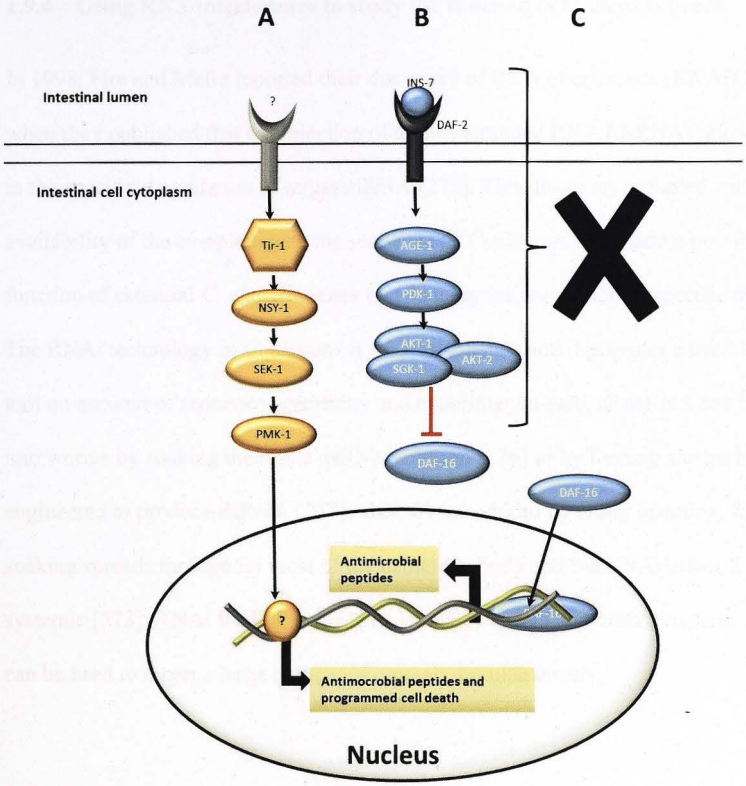

Figure 1.6: Parallel signaling pathways in *C. elegans* intestinal innate immune responses. A: p38 MAPK pathway. The NSY-1-SEK-1-PMK-1 cassette is pivotal to the regulation of *C. elegans* defense responses and is activated by the scaffolding protein TIR-1. **B:** The insulin signaling pathway (DAF-2-DAF-16). Insulin-like peptides, e.g. INS-7, bind to the DAF-2 receptor, which sequentially activates the phosphatidylinositol-3 OH kinase AGE-1, phosphoinositide-dependent kinase 1 (PDK-1), AKT-1, AKT-2 and serum/glucocorticoid-regulated kinase 1 (SGK-1) to phosphorylate, and thereby inhibit, the forkhead box O transcription factor DAF-16. **C:** DAF-2 mutant worms constitutively express DAF-16, which up-regulates the transcription of antimicrobial peptides.

1.9.4 Using RNA interference to study the function of *C. elegans* genes

In 1998, Fire and Mello reported their discovery of RNA interference (RNAi) in *C. elegans* when they published that the injection of double stranded RNA (dsRNA) into worms resulted in the specific degradation of target mRNA [275]. This discovery, coupled with the availability of the complete genome sequence of *C. elegans,* has made it possible to study the function of essential *C. elegans* genes by silencing the expression of specific target genes. The RNAi technology in *C. elegans* is well established and it provides a useful experimental tool on account of sequence specificity and experimental ease, as dsRNA can be introduced into worms by soaking them in a dsRNA solution [276] or by feeding worms bacteria engineered to produce dsRNA [277]. dsRNA introduced by either injection, feeding or soaking spreads throughout most of the nematode body and the RNAi effect is nearly systemic [278]. RNAi feeding is the least labour intensive and most inexpensive method that can be used to target a large number of animals simultaneously.

1.9.4.1 The mechanism of RNAi in *C. elegans*

dsRNA taken into *C. elegans* cells is cleaved into small interfering RNAs (siRNA) by the enzyme Dicer (Figure 1.7) [279]. Dicer forms a complex with RDE-4 (a dsRNA binding protein), RDE-1 (believed to interact with siRNA) and DRH-1 (a DexH box helicase) [280]. The Dicer-complex bound siRNAs then interact with MUT-7 and RDE-2/MUT-8, nematode proteins found to be essential for *C. elegans* RNAi [281]. siRNAs can also bind to ERI-1 which interferes with the RNAi pathway by targeting siRNAs for degradation [282]. siRNAs that escape degradation and are then incorporated into a RNA-induced silencing complex (RISC) which bind to endogenous messenger RNA (mRNA) with complementary sequence. The mRNA is then cleaved and degraded by the endonuclease activity of the RISC complex

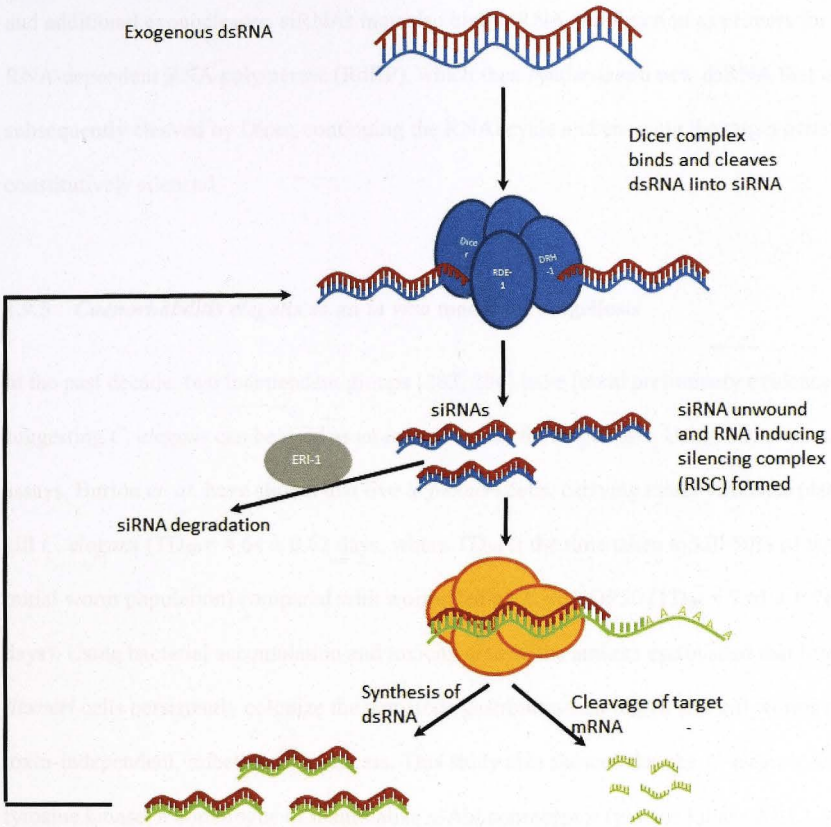

Figure 1.7: Schematic representation of the RNA interference pathway in *C. elegans*.

Exogenous dsRNA enters nematode cells and is cleaved into siRNAs by Dicer, which forms a complex that includes RDE-4, RDE-1 and DRH-1 (all enzymes represented by blue ovals). The siRNAs are either bound by ERI-1, which targets them for degradation, or by a complex that includes MUT-7, RDE-2 and CSR-1 which form the RISC complex (represented in orange), which directs them to bind to complementary, endogenous mRNA. RISC-bound siRNA/mRNA products are either targeted for degradation, leading to cleavage of the mRNA target or for the RNA-dependent RNA polymerase-mediated synthesis of new dsRNA. Newly synthesized dsRNA is bound and cleaved by the Dicer complex and the cycle continues, leading to the constitutive silencing of target mRNA.

and additional exonucleases. siRNAs may also bind mRNA and function as primers for RNA-dependent RNA polymerase (RdRP), which then synthesizes a new dsRNA that is subsequently cleaved by Dicer, continuing the RNAi cycle and ensuring the target gene is constitutively silenced.

1.9.5 *Caenorhabditis elegans* as an *in vivo* model for shigellosis

In the past decade, two independent groups [283, 284] have found preliminary evidence suggesting *C. elegans* can be used as an animal model for shigellosis. Using bacterial survival assays, Burton *et. al.* have shown that live *S. flexneri* cells, carrying intact virulence plasmids, kill *C. elegans* ($TD_{50} = 4.64 \pm 0.62$ days, where TD_{50} is the time taken to kill 50% of the initial worm population) compared with worms fed on *E. coli* OP50 ($TD_{50} = 7.61 \pm 0.76$ days). Using bacterial accumulation and toxicity assays, the authors established that live *S. flexneri* cells persistently colonize the nematode gastrointestinal lumen and kill worms in a toxin-independent, infection-like process. This study also showed that the *C. elegans* ABL-1 tyrosine kinase, a homologue of mammalian c-Abl nonreceptor tyrosine kinase ABL1, was required for *S. flexneri*-induced killing.

More recently, Kesika *et. al.*[284] developed a *C. elegans* survival assay in liquid cultures and have shown that the nematodes were more susceptible to *S. flexneri* infection in liquid culture, with $TD_{50} = 23 \pm 1$ hours while worms fed *E. coli* OP50 showed 100% survival for up to 55 hours. This group also showed that worms infected with *S. flexneri* laid significantly fewer eggs (26 ± 6 eggs per worm) compared with control worm (275 ± 15 eggs per worm). Using semi-quantitative real-time polymerase chain reactions, they found that *S. flexneri* infection resulted in the down-regulation of *C. elegans* antimicrobial genes *clec-60* and *clec-87*.

Data obtained from both these studies prove that *C. elegans* is susceptible to *S. flexneri* infection and *S. flexneri* suppresses nematode antimicrobial responses. The use of *C. elegans* to study shigellosis has several advantages: firstly, unlike the other animal models that have been used to study shigellosis, the site of bacterial infection in *C. elegans* is clinically relevant and the nematode enterocytes share similarities with human intestinal cells, as described in section 1.8.2. Secondly, this model has been used extensively to study host-pathogen interactions of a number of human pathogens, including *Pseudomonas aeruginosa* [285-290], Enteropathogenic *E. coli* [267, 291, 292] *Salmonella enterica* [255, 293-295] and *Serratia marcescens* [296, 297]. Next, *C. elegans* is an ethical alternative to using mice and primates that has been recommended by the European Centre for the Validation of Alternative Methods (ECVAM) [298]. And, finally, *C. elegans* has a small genome (97 Mb) that has been completely sequenced, making it possible to carry out both forward and reverse genetics.

Besides the two reports mentioned above, no studies have used *C. elegans* as a model to study *S. flexneri;* a more comprehensive understanding of the interactions between *S. flexneri* and *C. elegans* is warranted in order to establish *C. elegans* as a small animal model of shigellosis.

1.10 Objectives of thesis

S. flexneri strains are the leading cause of shigellosis in developing countries and despite over half a century of research, a safe and effective vaccine that offers substantial protection is yet to be designed. The vast antigenic diversity and lack of a relevant animal model of shigellosis

have been the main impediments to *S. flexneri* vaccine development. The broad aim of this thesis is to further our understanding of *S. flexneri* infection by identifying and characterizing novel virulence factors encoded by *S. flexneri.* This thesis also aims to characterize *C. elegans* as a new potential *in vivo* model of shigellosis.

The specific objectives of this study are:

1. To elucidate the role of periplasmic enzymes, L-asparaginase (AnsB) and γ-glutamyltranspeptidase (GGT) in the pathogenesis of *S. flexneri,* by constructing and analyzing gene disruption mutants for variations in physiological and virulence properties.
2. To identify pleiotropic effects caused by *ansB* and *ggt* mutations using differential in gel electrophoresis to compare the proteomes of mutant and wild type cells.
3. To isolate and completely sequence the genome of serotype converting bacteriophage SfII isolated from the highly prevalent *S. flexneri* serotype 2a and to compare the genome of bacteriophage SfII with SfI, SfIV, SfV, SfX and Sf6 to further our understanding of *S. flexneri* phages.
4. To identify novel phage-encoded virulence factors in *S. flexneri* by characterizing the functions of cryptic bacteriophage SfV genes in a *S. flexneri* serotype 5a lysogenic strain.
5. To characterize *C. elegans* as a new *in vivo* model of shigellosis by investigating the interactions between *S. flexneri* and the *C. elegans* intestine using transmission electron microscopy.
6. To identify nematode responses to *S. flexneri* infection using differential in gel electrophoresis to compare the proteomes of nematodes infected with virulent *S. flexneri* and control worms.

Chapter 2

Materials and methods

Chapter 2: Materials and methods

2.1 Bacterial culture conditions and media

Liquid overnight cultures of bacteria were grown routinely in Luria Bretani (LB) broth (Appendix A), containing antibiotics where required, in a shaking incubator (180-200 rpm). For maintaining overnight cultures for propagation of bacteriophages, bacterial strains were grown in NZCYM medium overnight (Appendix A). For maintenance of the virulence plasmid, *S. flexneri* cultures were grown at 30 °C whenever possible, as at 37 °C the plasmid-based virulence genes are expressed, making the virulence plasmid unstable and readily lost from bacterial cells. Bacteria were plated onto LB agar plates (Appendix A), containing antibiotics as required. For long-term storage, strains were inoculated into 50% LB: 50% glycerol and stored at -80 °C.

2.2 Bacterial strains and plasmid vectors

All *S. flexneri* and *E. coli* strains and plasmids used in this study have been described in Tables 2.1, 2.2 and 2.3, respectively. Cloning with pBC SK and pBS SK vectors (Figure 2.1) was performed in the *E. coli* JM109 strain.

Table 2.1: ***S. flexneri*** **strains used in this study**

Strain	Characteristics	Source
SFL1223	*S. flexneri* 2a 2457T, devoid of the virulence plasmid. Congo red negative and invasion negative	[88]
SFL1520	*S. flexneri 3b*, Congo red positive, virulent in Sereny test.	ICDDRB
SFL1871	*S. flexneri* 5a, SFL1 with SFV lysogen, *int-xis* disruption mutant, Congo red positive.	F. Robertson
SFL1339	*S. flexneri* Y, SFL1, Congo red positive	G. Allison
SFL2076	SFL1520 carrying the helper plasmid , pKM208	F. Thanweer
SFL2283	SFL1520 *ansB* disruption mutant, *kan* gene insertion	This study
SFL2285	SFL1520 *ggt* disruption mutant, *kan* gene insertion	This study
SFL2309	SFL2283 carrying pNV1372 to complement the *ansB* mutation	This study
SFL2310	SFL2285 carrying pNV1434 to complement the *ggt* mutation	This study
SFL2311	SFL1223 carrying pNV1908 expressing GFP^+	This study
SFL2312	SFL1520 carrying pNV1908 expressing GFP^+	This study
SFL2313	SFL2283 carrying pNV1908 expressing GFP^+	This study
SFL2314	SFL2285 carrying pNV1908 expressing GFP^+	This study
SFL2443	SFL1520 carrying pNV2052 expressing OmpA	This study
SFL2444	SFL2285 carrying pNV2054 expressing YaeT	This study
SFL2498	SFL1871 *gtrV* disruption mutant, *cat* insertion	This study
SFL2500	SFL1871 SFV*ORF28-32* disruption mutant, *cat* insertion	This study
SFL2503	SFL1339 carrying pNV1908 expressing GFP^+	This study
SFL2504	SFL1871 carrying pNV1908 expressing GFP^+	This study
SFL2505	SFL2500 carrying pNV1908 expressing GFP^+	This study
SFL2506	SFL2500 carrying pNV2062 expressing SFV ORF 28-32	This study

Table 2.2: *E. coli* strains used in this study

Strain	Characteristics	Source
JM109	*recA1 supE44 endA1 hsdR17 gyrA96 relA1 thi Δ (lac-proAB) F' [traD36 proAB + lacI^q lacZ ΔM15]*	[299]
B2298	OP50 *E.coli* (CGC)	[300]
B2286	JM109 carrying pNV1875	D.T. George*
B2287	JM109 carrying pNV1876	D.T. George*
B2290	JM109 carrying pNV1878	This study
B2291	JM109 carrying pNV1879	This study
B2363	E1315 carrying pNV1942	Elizabeth Tran
B2364	E1315 carrying pNV1943	Elizabeth Tran
B2366	E1315 carrying pNV1945	Elizabeth Tran
B2367	E1315 carrying pNV1946	Elizabeth Tran
B2368	E1315 carrying pNV1947	Elizabeth Tran
B2511	HT115 carrying the RNAi construct targeted to the *C. elegans aco-1* gene	Vidal library
B2512	HT115 carrying the RNAi construct targeted to the *C. elegans cct-2* gene	Vidal library
B2513	HT115 carrying the RNAi construct targeted to the *C. elegans eef-2* gene	Vidal library
B2514	HT115 carrying the RNAi construct targeted to the *C. elegans hsp-60* gene	Vidal library
B2515	B2298 carrying pNV1908 expressing GFP$^+$	This study
B2517	JM109 carrying pNV2060	This study
B2520	HT115 carrying the RNAi construct targeted to the *C. elegans daf-19* gene	Arhinger library
B2521	HT115 carrying the RNAi construct targeted to the Arabidopsis CB19 gene	Cab lab
B2522	JM109 carrying pNV2062	This study
B2523	JM109 carrying pNV2063	This study
B2502	JM109 carrying pNV2052, expressing OmpA	This study
B2504	JM109 carrying pNV2054, expressing YaeT	This study

*D. T. George- these strains have been created by me during my honours.

Table 2.3: Plasmids used in this study

Plasmid	Characteristics	Source
pBC SK	Cloning and expression vector, Cm^r	Stratagene
pBS II KS	Cloning and expression vector, Amp^r	Stratagene
pGEX-4T-1	IPTG inducible expression vector	Amersham Biosciences
pKD3	lambda red PCR KO system, *cat* cassette template	(95)
pKD46	lambda red PCR KO system, helper plasmid arabinose induced	(95)
pKM208	lambda red PCR KO system, helper plasmid IPTG induced	(96)
pNV1372	*ansB* gene cloned into pBS II KS	A.V. Jennison
pNV1434	*ggt* gene cloned into pGEX-4T-1	A.V. Jennison
pNV1875	*ansB* knockout template carrying the *cat* gene flanked by *ansB* and its flanking regions, cloned into pBS SK	D.T. George*
pNV1876	*ggt* knockout template carrying the *cat* gene flanked by *ggt* and its flanking regions cloned into pBS SK	D.T. George*
pNV1878	*ansB* knockout template carrying the *kan* gene flanked by *ansB* and its flanking regions, cloned into pBS SK	This study
pNV1879	*ggt* knockout template carrying the *kan* gene flanked by ggt and its flanking regions cloned into pBS SK	This study
pNV1908	gfp^+ gene cloned into pCR 2.1	This study
pNV1942	SfiI *PstI* fragment 1 cloned into pBS SK	Elizabeth Tran
pNV1943	SfiI *PstI* fragment 2 cloned into pBS SK	Elizabeth Tran
pNV1945	SfiI *PstI* fragment 5 cloned into pBS SK	Elizabeth Tran
pNV1946	SfiI *PstI* fragment 6 cloned into pBS SK	Elizabeth Tran
pNV1947	SfiI *PstI* fragment 7 cloned into pBS SK	Elizabeth Tran
pNV2052	*ompA* gene from SFL1520 cloned into pBS II KS	This study
pNV2054	*yaeT* gene from SFL1520 cloned into pBS II KS	This study
pNV2063	pNV2062 harbouring an internal deletion within ORF 28-32 + *cat* gene inserted into the site of deletion	This study
pNV2062	SFV ORF 28-32 cassete from SFL1871 cloned into pBS II KS	This study
pNV2060	pNV731 harbouring an internal deletion within the *gtrV* cassette+ *cat* gene inserted into the site of deletion	This study

*D. T. George- these strains have been created by me during my honours.

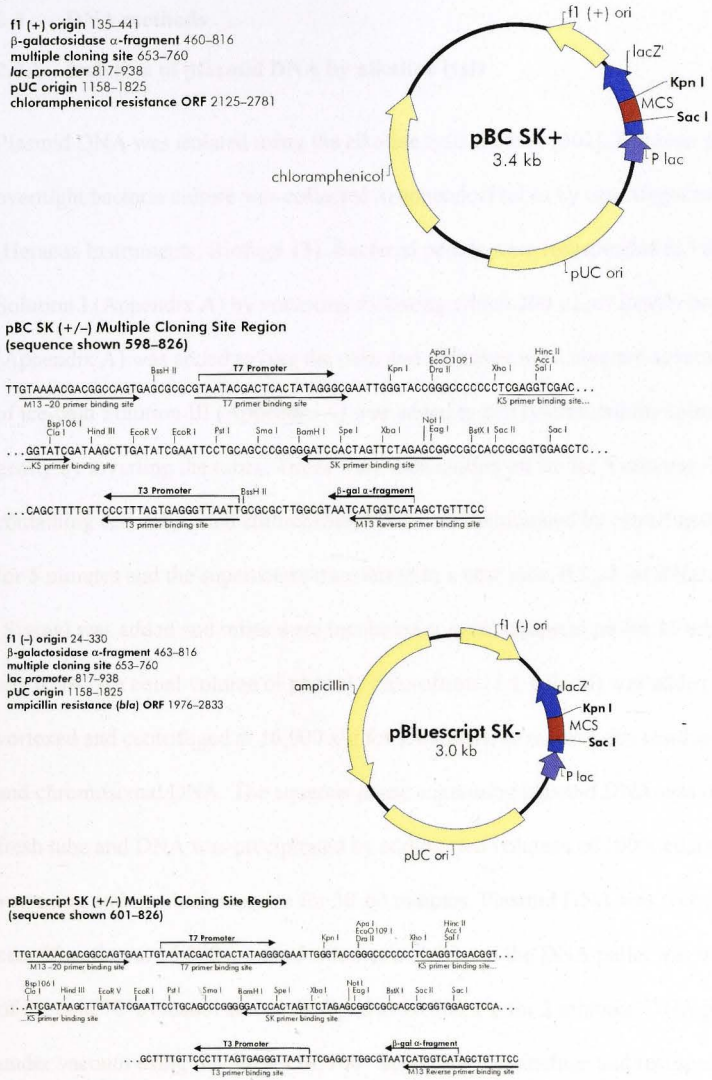

Figure 2.1: Plasmid maps of pBC SK and pBS SK, used as cloning vectors in this study. The Multiple cloning site (MCS) in both plasmids is located within the N-terminal region of the β-galactosidase gene fragment, allowing blue white screening of recombinant plasmids (Adapted from Stratagene).

2.3 DNA methods

2.3.1 Isolation of plasmid DNA by alkaline lysis

Plasmid DNA was isolated using the alkaline lysis method [301]. Between 1.5-3 mL of overnight bacteria culture was collected in eppendorf tubes by centrifugation at 16,000 x *g* (Heraeus Instruments, Biofuge 13). Bacterial pellets were resuspended in 100 µL of ice-cold Solution I (Appendix A) by vortexing following which 200 µL of freshly prepared Solution II (Appendix A) was added to lyse the cells and the tubes were inverted several times. 150 µL of ice-cold Solution III (Appendix A) was added to cell lysates and the solutions were mixed gently by inverting the tubes. Tubes were then chilled on ice for 5 minutes. The precipitate containing cell debris and chromosomal DNA was eliminated by centrifugation at 16,000 x *g* for 5 minutes and the supernatant transferred to a new tube. 0.5 µL of RNase (10 mg/mL) (Sigma) was added and tubes were incubated at room temperature for 15 minutes to degrade any RNA. An equal volume of phenol : chloroform (1:1 vol/vol) was added and tubes were vortexed and centrifuged at 16,000 x *g* for 2 minutes, to remove any residual RNA, protein and chromosomal DNA. The aqueous phase containing plasmid DNA was transferred into a fresh tube and DNA was precipitated by adding two volumes of 100% ethanol, followed by vortexing and incubation on ice for 30-60 minutes. Plasmid DNA was recovered by centrifugation at 16,000 x *g* for 5 minutes at 4 °C and the DNA pellet was washed with 1 mL of ice cold 70% ethanol and centrifuged at 16,000 x *g* for 2 minutes. DNA pellets were dried under vacuum using the Savant SC100 "Speed Vac" centrifuge and resuspended in 20-50 µL of Milli-Q water and stored at -20 °C.

2.3.2 Isolation of plasmid DNA using the Axygen miniprep Spin kit

Plasmid DNA was isolated form overnight bacterial cultures using the Axygen MiniPrep Kit according to the manufacturers' instructions. Briefly, 1.5 mL of overnight culture was centrifuged at max speed in a microcentrifuge for 1 minute (Heraeus Instruments, Biofuge 13). Collected bacterial pellets were resuspended in 250 µL of buffer S1 followed by the addition of 250 µL S2 buffer (provided in the kit). Tubes were inverted 5-10 times, until the solution became viscous. 350 µL of S3 buffer was added and the solution was mixed gently by inversion. Cell debris was collected by centrifugation at 12,000 x *g* for 10 minutes. The supernatant was transferred to into an Axyprep spin column. The spin column was centrifuged for 1 minute at 12,000 x *g*, the flow through discarded and 750 µL of W1 buffer added to wash the column. The column was centrifuged for 1 minute as above and washed with 500 µL of buffer W2 as above. Empty spin columns were centrifuged for an additional minute to ensure all W2 buffer had been removed from the column. The column was then placed in an empty eppendorf tube and the DNA eluted by the addition of 30-50 µL of Milli-Q water. After a minute incubation at room temperature, the plasmid DNA was collected by centrifugation at 12,000 x *g* for 1 minute. Plasmid DNA was stored at -20 °C.

2.3.3 Determination of DNA concentration

The quantity of DNA in suspension was measured using the NC-1000 spectrophotometer Nanodrop (BioScience). Absorbance at 260 nm was determined and the concentration of DNA in ng/µL calculated using the standard that A_{260} of 1 represents 50 µg/mL. A ratio of A_{260} nm/A_{280} nm was also used as an indicator of the purity of the DNA sample. A ratio of ~1.8 is generally accepted as pure for DNA.

2.3.4 DNA separation and purification by electrophoresis

2.3.4.1 Agarose gel electrophoresis

Agarose gels were prepared using 0.5%-2% agrose in 0.5 x TBE buffer (Appendix A). Ethidium bromide was added to the gel at a final concentration of 10 µg/mL. 0.5 x TBE buffer was used to conduct an electric current at 50-120 V. DNA samples were loaded into the wells of agarose gels with 1/10 the volume of blue loading dye (Appendix A). SPP-1 phage DNA/*Eco*RI (500 ng) was run as a molecular size marker (Figure 2.2). DNA was visualized under UV light using a Gel-Doc set-up, and photographs were taken using the NIH-Image program and printed on a thermal printer (Mitsubishi).

2.3.4.2 DNA purification form agarose gels

DNA bands of interest visualized under UV light, were cut out using a scalpel blade and placed in a pre-weighted eppendorf tube. The Wizard® SV Gel and PCR clean up kit (Promega), was used for purification of isolated DNA fragments from the agarose gel fragments according to manufacturer's specifications. Purified DNA was stored at -20 °C.

2.3.5 Sequencing and polymerase chain reaction (PCR)

2.3.5.1 Primer design

Primers were designed to have similar melting temperatures, a GC content similar to the gene of interest, little or no false priming, and little or no secondary structure. The primers used in this study are listed in Table 2.4. All primers used in this study were manufactured by SigmaAldrich

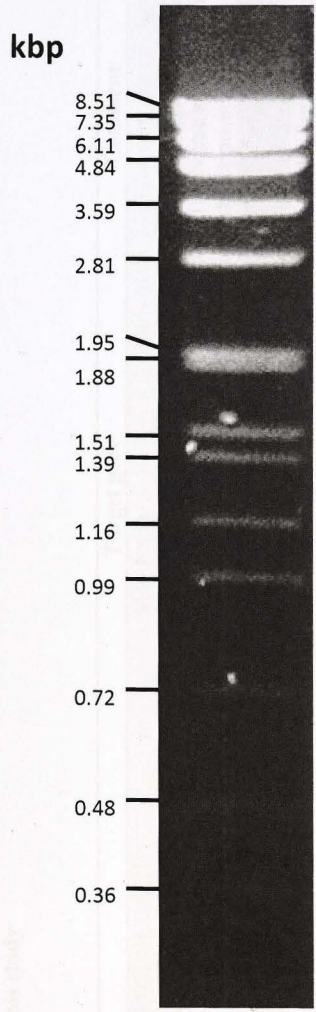

Figure 2.2: Size bands (kbp) in the SPP-1 phage DNA/*Eco*RI marker. All agarose gels displayed in this study use the SPP-1 marker (GibcoBRL)

Table 2.4.: Primers used in this study

Primer name	Sequence	Target gene	Comment
M13F	GTAAAACGACGGCCAGT	M13 F site	Binds to the M13 forward site on cloning vectors used in this study for primer walking
M13R	GGAAACAGCTATGACCATG	M13 R site	Binds to the M13 reverse site on cloning vectors used in this study for primer walking
AnsB-FP1	AGGCGCGAAAAGCCGCGT	*ansB* upstream element	Forward primer amplifying the 640 bp upstream element of the *ansB* gene
AnsB-RP6	TGGGTATTC AACGCAGATTCA	*ansB* downstream element	Reverse primer amplifying the 608 bp downstream element of the *ansB* gene
AnsB-KO F2	TGCGCAAAATGCTGCTGGC	*ansB* upstream element	Sequencing primer binding 872 bp upstream of the *ansB* start codon
AnsB-SacF	atctagagATGGAGTTTTTCAAAAAG	*ansB*	Forward primer amplifying the *ansB* gene.
AnsB-XbaR	cagagctcTTAGTACTGATTGAAAAT	*ansB*	Reverse primer amplifying the *ansB* gene
Ggt-FP1	GATTGACGTGATTGGTCCGA	*ggt* upstream element	Forward primer amplifying the 599 bp upstream element of the *ggt* gene
Ggt-RP6	TTGACTCGCATTTGAAAG	*ggt* downstream element	Reverse primer amplifying the 618 bp downstream element of the *ggt* gene
Ggt-KO F2	GGAACTGCCGCGTGGTTTA	*ggt* upstream element	Sequencing primer binding 812 bp upstream of the *ggt* start codon
Ggt-SacF	cggagctcATCACTCACTTCGCATCT	*ggt*	Forward primer that binds 427 bp away from the start of the *ggt* gene
Ggt-XbaR	gtctagaGTATTTCTCCGCTTCTGC	*ggt*	Reverse primer binds 995 bp away from the start of the *ggt* gene
Cat-FP1	CACGTCTTGAGCGATTGTGTAGG	*cat*	Forward primer amplifying the *cat* gene.
Cat-RP2	GACATGGGAATTAGCCATGGTCC	*cat*	Reverse primer amplifying the *cat* gene
CmF (NheI)	CTAGCTAGCCACGTCTTGAGCGATTGTGTAG	*cat*	Forward primer amplifying the *cat* gene with *NheI* flanking sites
CmR (NheI)	CTAGCTAGCGACATGGGAATTAGCCATGGTC	*cat*	Reverse primer amplifying the *cat* gene with *NheI*

			flanking sites
pACYC NheI F	ctagctagcGCCACGTTGTGTCTCAAAATC	*kan*	Forward primer amplifying the *kan* gene with *NheI* flanking sites
pACYC NheI R	ctagctagcCGGGAAGATGCGTGATCTG	*kan*	Reverse primer amplifying the *kan* gene with *NheI* flanking sites
KanXbaIF	GCtctagaGCCACGTTGTGTCTCAAAA	*kan*	Forward primer amplifying the *kan* gene with a *XbaI* flanking sites
KanXbaIR	GCtctagaCGGGAAGATGCGTGATCT	*kan*	Reverse primer amplifying the *kan* gene with A *XbaI* flanking sites
KO1	TTTAAAGAAGTTCCTATTCC	*cat*	Reverse primer that binds towards the start of the *cat* gene and reads out of the 5` end into flanking resgions
KO2	ACTTCGGAATAGGAACTAAG	*cat*	Forward primer that bind to the 3` end of the *cat* gene.
ORF28-32BamHIF	tcaGGATCCGCCAGCGCGTTAATAATT		Forward primer amplifying the SFV ORF 28-32 gene cassette
ORF28-32XhoIR	CCGCTCGAGCATAATGTACCCAAGAGA		Reverse primer amplifying the SFV ORF 28-32 gene cassette
GtrVF-sacI	GatgagctcTGAGAAACAAAAATGAAAAGCC	*gtrV*	Forward primer amplifying the GtrV gene with a 5` *sacI* site
GtrVR-XbaI	acgtctagaACCATTCAACATTAAGGC	*gtrV*	Reverse primer amplifying the GtrV gene with a 5` *XbaI* site
OmpAF(SacI)	CGgagctcGGAGATATTCATGGCGTATT	*ompA*	Forward primer amplifying the *ompA* gene with a 5` Sac*I* site
OmpAR(XbaI)	GCtctagaTTAAGCCTGCGGCTGAGT	*ompA*	Reverse primer amplifying the *ompA* gene with a 3` *XbaI* site
YaeTF(SacI)	CGgagctcGAGTTAGTTAGGAAGAAC	*yaeT*	Forward primer amplifying the *yaeT* gene with a 5` Sac*I* site
YaeTR(XbaI)	GCtctagaTTACCAGGTTTTACCGAT	*yaeT*	Reverse primer amplifying the *yaeT* gene with a 3` *XbaI* site
HisG-qRTF	GCGCTGTGGCATTAAAATCA	*hisG*	Forward quantitative real time PCR primer
HisG-qRTR	ATTACCAGACAGGGAATGTC	*hisG*	Reverse quantitative real time PCR primer

RplL(qRT-F)	CGGTTGAAGCTGCTGAAGAA	*rplL*	Forward quantitative real time PCR primer
RplL(qRT-R)	TGCAGATTCTACCAGGTCTT	*rplL*	Reverse quantitative real time PCR primer
Udp(qRT-F)	GCCGCATATTAATGTGGGTG	*udp*	Forward quantitative real time PCR primer
Udp (qRT-R)	AGCGCAGTCGTACATTCGAA	*udp*	Reverse quantitative real time PCR primer
mdh(qRT-F)	GCGGAACTGAAAGGCAAACA	*mdh*	Forward quantitative real time PCR primer
mdh(qRT-R)	CCTGCTCGGTAAAACTAACG	*mdh*	Reverse quantitative real time PCR primer
OmpA(qRT-F)	CCAATCACTGACGATCTGGA	*ompA*	Forward quantitative real time PCR primer
OmpA(qRT-R)	GCCAGTGTCGTGGTCTTTAA	*ompA*	Reverse quantitative real time PCR primer
GroEL(qRT-F)	GCTGATCATCGCTGAAGATG	*groEL*	Forward quantitative real time PCR primer
GroEL(qRT-R)	GCATAGCTTTACGACGATCG	*groEL*	Reverse quantitative real time PCR primer
DnaK(qRT-F)	GAACCGGTAACTGAAGCTGT	*dnaK*	Forward quantitative real time PCR primer
DnaK(qRT-R)	GGTCGGTTCGTTGATGATAC	*dnaK*	Reverse quantitative real time PCR primer
PpsA(qRT-F)	CCTCAACGTTCAGGGTTTTG	*ppsA*	Forward quantitative real time PCR primer
PpsA(qRT-R)	CTGGTGCACACGATAAGAGA	*ppsA*	Reverse quantitative real time PCR primer
gadB (qRT-F)	TATGGACCCGAAACGCATGA	*gadB*	Forward quantitative real time PCR primer
gadB(qRT-R)	TGCGGGAACTCATAGTTACC	*gadB*	Reverse quantitative real time PCR primer
tig(qRT-F)	CGCTATCAACCTGAAGAAAG	*tig*	Forward quantitative real time PCR primer
tig(qRT-R)	CAGACCTTCTACGGAACCAT	*tig*	Reverse quantitative real time PCR primer
FtsZ(qRT-F)	GCTGTCGTCACTAAGCCTTT	*ftsZ*	Forward quantitative real time PCR primer
FtsZ(qRT-R)	GTTTGTCGTTCGGGATAGTG	*ftsZ*	Reverse quantitative real time PCR primer
RpsA(qRT-F)	GGGTAGCTATCGCTAAACGT	*rpsA*	Forward quantitative real time PCR primer
RpsA(qRT-R)	GAAACGTGTACCAGACCTTC	*rpsA*	Reverse quantitative real time PCR primer
YaeT(qRT-F)	TGAACGTTGATGCGGGTAAC	*yaeT*	Forward quantitative real time PCR primer
YaeT (qRT-R)	ACCATGCACCTTCCATCTGA	*yaeT*	Reverse quantitative real time PCR primer
Hsp-6-RT-F	GGAGATAAGATCATCGCTGT	*hsp-6*	Forward quantitative real time PCR primer
Hsp-6-RT-R	TCGAAGACGCCCTTTTGGAT	*hsp-6*	Reverse quantitative real time PCR primer
Act-2-RTF	TCCAAGAGAGGTATCCTTAC	*act-2*	Forward quantitative real time PCR primer
Act-2-RTR	AGGTCTCGAACATGATTTGG	*act-2*	Reverse quantitative real time PCR primer
Aco-1-qRTF	TCGTTACAACGAGCTTCCAA	*aco-1*	Forward quantitative real time PCR primer

Aco-1-qRTR	CGGCTGGAACTCCAGTAAAA	*aco-1*	Reverse quantitative real time PCR primer
Cct-2-qRTF2	ATGGGAATCGACATCGAGAA	*cct-2*	Forward quantitative real time PCR primer
Cct-2-qRTR2	GGAAGAAACCATGCACAACT	*cct-2*	Reverse quantitative real time PCR primer
Hsp-60RTF	**ATCGAGCACATCACCGAT**	*hsp-60*	Forward quantitative real time PCR primer
Hsp-60qRTR	TGACACGGTCCTTCTTCTCT	*hsp-60*	Reverse quantitative real time PCR primer
Unc-41qRTF	TATCAGTATAAGGTTGAAATCG	*unc-41*	Forward quantitative real time PCR primer
Unc-41qRTR	CAATTCGGTAGCCTTGTTGA	*unc-41*	Reverse quantitative real time PCR primer
Unc-54qRTF	GCAGGTTTTGGAGGATCAAT	*unc-54*	Forward quantitative real time PCR primer
Unc-54qRTR	TTGAGGGTGACCTCATTTCC	*unc-54*	Reverse quantitative real time PCR primer
Daf-19qRTF2	CGCCGTACTATCAGTATTCAA	*daf-19*	Forward quantitative real time PCR primer
Daf-19qRTR2	GGAAGCTCGTTGATTGTTCG	*daf-19*	Reverse quantitative real time PCR primer
Eef-2qRTF	AACCTTCCAACGTATCGTTG	*eef-2*	Forward quantitative real time PCR primer
Eef-2qRTR	GAGCTTGTCAACTTGAACTC	*eef-2*	Reverse quantitative real time PCR primer

2.3.5.2 Sequencing reaction and purification

All clones and gene disruption mutants obtained in this study were confirmed by sequencing. Sequencing was performed using the BigDye Terminator method. Approximately 50-200 ng of DNA was added to 3.5 µL of 5 X BigDye reaction buffer, 1 µL BigDye Terminator and 0.125 µM of primer in a 20 µL reaction. The sequencing reaction was then subjected to thermal cycle sequencing using the following parameters:

Denaturation Step	96°C for 10 seconds, × 25
Primer Annealing Step	50°C for 5 seconds, × 25
Extension Step	60°C for 4 minutes, × 25

Purification of the products from the BigDye Terminator sequencing reaction was achieved by ethanol precipitation. The 20 µL reaction was transferred to an eppendorf tube containing 2 µL of 3 M NaOAc (pH 4.6), 2 µL of 125 mM EDTA and 50 µL of 100% ethanol. After a brief vortex, the tube was centrifuged at 16,000 x *g* (Heraeus Instruments, Biofuge 13) for 30 minutes at 4 °C. The ethanol was gently decanted and the DNA pellet washed thrice in 70% ethanol, with 2 minute spins between washes. The pellet was then dried for 10 minutes under vacuum using the SC100 "Speed Vac" centrifuge (Savant). The dried sample was sent for automated sequencing at the Biomolecular Research Facility (BRF) (JCSMR, ANU).

2.3.5.3 Sequence analysis

Sequences obtained from reactions sent to the BRF were stored and analysed using pDRAW32 (http://www.acaclone.com/), CLC Main Workbench version 6.5, Bioedit [302] and/or ClustalW2 (http://www.ebi.ac.uk/Tools/clustalw2/index.html).

2.3.6 PCR amplification of genes

PCR reactions were performed using either *iTaq* polymerase (Scientifics) or *Pfu* Ultra II polymerase (Stratagene). The high fidelity *Pfu* Ultra II polymerase was used for amplification of genes for cloning and sequencing, while *iTaq* polymerase was used for screening and colony PCR (Section 2.6.5). Generally, 20 µL PCR reactions were set up containing the following: 1× PCR buffer, 0.125 µM forward primer, 0.125 µM reverse primer, 0.2 mM dNTPs, 0.5 U of *iTaq* or 0.25 units of *Pfu* Ultra II, and template DNA. The amount of DNA template used varied based on the type of DNA template used, typically for plasmid DNA templates between 50–200 ng of DNA was used. The annealing temperature was determined from the primer composition using the equation: Tm = 2× [A+T] + 4× [G+C]. The following PCR parameters were used for all PCR reactions:

Initial Denaturation Step	95 °C for 2 minutes, × 1
Denaturation Step	95 °C for 30 seconds, × 35
Primer annealing Step	3-5 °C below lowest Tm of primer pair for 30 seconds, × 35
Extension Step	72 °C for 1 minutes/kb for *Taq* or 2 minutes/kb for *pfu* ultra II, × 35
Final Extension Step	72 °C for 7 minutes, × 1

PCR amplified fragments were visualized on agarose gels (Section 2.4.1).

2.3.6.1 Colony PCR

Colony PCR was used to screen for potential transformants, gene disruptions in *S. flexneri* strains, the presence of virulence plasmids, and for the isolation of chromosomal and virulence plasmid-encoded genes. Single colonies of the strain of interest or transformants were obtained by dilution streaking onto LB agar plates containing the appropriated

antibiotic. Individual colonies were suspended in 100 µL of Milli-Q water and boiled at 100 °C for 10 minutes to disrupt bacterial cells. 5 µL of this crude bacterial lysate was mixed with 0.125 µM of each primer, 0.2 mM of dNTPs, 1 × *iTaq* buffer, and 0.5 U of *iTaq* polymerase (Scientifics). This 20 µL PCR reaction mix then underwent the same PCR cycle parameters as described in Section 2.5.4 and amplified PCR fragments were visualized on agarose gels (Section 2.4.1).

2.4 Cloning techniques and DNA manipulations

2.4.1 Restriction enzyme digestion

Plasmid, chromosomal and PCR-amplified DNA samples were digested according to the manufacturer's instructions (New England BioLabs). In a standard digestion reaction containing about 1 µg DNA, 5-15 U of enzyme was used for cloning, and 2 U of enzymes for screening. Enzyme digestion reactions were arrested by either the addition of loading buffer, precipitation, or heat inactivation. In cases where DNA was digested with two different enzymes that failed to function in a single buffer, DNA was first digested with the enzyme requiring the lower-salt buffer, or alternatively, the enzyme that was more resistant to heat-inactivation. The first enzyme reaction was halted by precipitation before digestion with the second enzyme was performed.

2.4.2 Dephosphorylation of DNA 5'-termini

Plasmid DNA fragments linearized using single restriction endonucleases, were treated with calf intestinal alkaline phosphatase (CIAP, Fermentas) to cleave the 5' phosphate group. This was done to prevent plasmid re-ligation. For dephophorylation, linearized plasmids were

added to a reaction mixture with a final volume of 50 µL containing 1 x CIAP buffer and 0.25–1 U of CIAP followed by incubation at 37 °C for 30 minutes. The CIAP enzyme was heat inactivated at 85 °C for 5 minutes. Plasmid DNA was then separated using agarose gel electrophoresis and purified as described in Sections 2.4.1 and 2.4.2.

2.4.3 Ligation reactions

T4 DNA ligase (Promega) was used to ligate vector with insert DNA. Reactions containing vector to insert ratios of either, 1:3, 1:6, or 1:10, 1 x ligase buffer and 0.3–1.0 U of T4 DNA ligase in a final volume of 10 µL were incubated overnight at 15 °C. The ligated recombinant plasmids were then transformed into electrocompetent cells or stored at -20 °C.

2.4.4 Transformation of DNA into competent cells

2.4.4.1 Preparation of electrocompetent cells

Electrocompetent cells were used for all transformations as these cells show much higher transformation efficiencies compared to chemically competent cells. Overnight bacterial cultures were diluted 1:100 into 250 mL fresh LB (Appendix A), containing the appropriate antibiotics, and grown at 37 °C for *E. coli* strains and 30 °C for *S. flexneri* strains, for approximately 3 hours, until the cells reached mid log phase (OD_{600} = 0.6 - 0.8). Cells were harvested by centrifugation at 9,500 x *g*, 4 °C for 10 minutes (Sorvall RC 5C Plus Centrifuge with SLA3000 rotor). All subsequent steps including centrifugation were carried out at 4 °C. The supernatants were discarded and bacterial pellets were washed thrice in sterile ice-cold Milli-Q water, twice in 100 mL and the last time in 50 mL. Cells were collected by centrifugation at 9,500 x *g*, 4 °C for 10 minutes after each wash. The cell pellets were then

resuspended in 25 mL sterile ice-cold Milli-Q water and transferred into 50 mL centrifuge tubes and centrifuged at 13,000 x *g*, 4 °C for 10 minutes, using the SS-34 rotor. Pellets were then resuspended in 1 mL sterile cold 10% (v/v) glycerol, transferred into 2 mL eppendorf tubes and centrifuged at 16,000 x *g*, 4 °C for 5 minutes. Cell pellets were resuspended in 200-400 µL of sterile cold 10% (v/v) glycerol. Aliquots of 40–50 µL were made into pre-chilled eppendorf tubes and cells were stored at -80 °C.

2.4.4.2 Determining the efficiency of competent cells

In order to determine the efficiency of a batch of competent cells, 10 ng of plasmid, pBC SK DNA (Figure 2.1) was transformed into an aliquot of cells as described in Section 2.7.3. 100 fold dilutions of the recovered cell suspension were plated onto LB agar plates containing chloramphenicol (25 µg/mL) and incubated overnight at 37 °C. Resulting colonies were counted to determine the number of transformed cells in 1 mL of the original cell suspension. Efficiency was expressed as number of transformed cells per 1 µg of DNA. Therefore the figure determined from transforming cells with 10 ng of pBC SK was multiplied by 10^2. Efficiency varied depending on the type of cells but generally ranged from 10^6-10^9 transformed cells/µg of DNA for *E. coli* and 10^4-10^5 transformed cells/µg of DNA for *S. flexneri*.

2.4.4.3 Transformation of DNA into electrocompetent cells

Aliquots of electrocompetent cells were thawed on ice and between 2–4 µL of either plasmid DNA or ligation mixes were added. The DNA/cell mixtures were then transferred into pre-chilled electrocuvettes (Bio-Rad). Electroporation was carried out using the Genepulser (Bio-

Rad) set at 2.5 kV, 200 Ω and 25 μFD. Immediately following electroporation, 1 mL of LB was added to the cuvette. The solution was then transferred to a clean eppendorf tube and the cells were allowed to recover for 1 hour at 37 °C for *E. coli* strains and 30 °C for *S. flexneri* strains. Bacterial cells were collected by centrifugation at 16,000 x *g* for 2 minutes (Heraeus Instruments, Biofuge 13) and resuspended in 100 μL of LB before spreading on an LB agar plate containing the appropriate antibiotics. Plates were incubated overnight at 37 °C for *E. coli* strains and 30 °C for *S. flexneri* strains. The resulting colonies were then screened by colony PCR (Section 2.5.5) or restriction enzyme digestion of isolated plasmids (Section 2.6.1) to identify required clones.

2.5 Screening techniques for cloned plasmids and gene disruption mutant strains

2.5.1 Antibiotic selection

25 μg/mL of chloramphenicol (Appendix A) added to LB or LB agar was used to select for cells containing the plasmid pBC SK or derivatives of the same. Lambda-red mediated PCR knockout strains, containing an integrated chloramphenicol or kanamycin gene were selected on LB agar plates containing 35 μg/mL and 50 μg/mL (Appendix A) of chloramphenicol and kanamycin, respectively. 100 μg/mL of ampicillin (Appendix A) was used to select for cells containing plasmids pBS KS, pKM208, and pKD46 or their derivatives.

2.5.2 Blue-white screening

Plasmids pBC SK and pBS KS have their polylinker located within a *lacZ`* gene fragment (Figure 2.1), thereby facilitating blue-white screening. Cells transformed with recombinant plasmids derived from pBC SK and pBS KS were selected on plates containing the

appropriate antibiotics as described in section 2.8.1. The resulting colonies were then patched onto LB agar plates containing 20 μg/mL iso-propyl-β-DD-thiogalactopyranoside (IPTG), 20 μg/mL 5-Bromo-4-chloro-3-indolyl β-D-galactopyranoside (X-Gal) and the appropriate antibiotics. Plates were incubated at 37 °C for 12-16 hours. Any blue colonies were discarded as this suggests that they produced functional LacZ protein, indicating that the polylinker was not disrupted by the insert. White colonies were positively selected for further screening by colony PCR (Section 2.5.5) or plasmid MiniPrep and restriction enzyme analysis (Section 2.6.1) as these indicate that the *lacZ* gene has been disrupted. Positive clones were finally confirmed by sequencing.

2.6 PCR Lambda red recombinase gene disruption in *S. flexneri* strains

2.6.1 Generating knockout templates carrying antibiotic cassettes flanked by regions of homology to target genes of interest

Genes of interest were cloned into pBS KS as described in Figure 2.3. Ligation mixes were transformed into electrocompetent *E. coli* JM109 cells (Section 2.7.3) and transformants were screened by antibiotic selection and blue-white screening (Section 2.8.1 and 2.8.2). Primers flanked by restriction digest sites were designed to create deletion within the gene of interest and introduce restriction enzyme sites into the deleted region (Figure 2.3). The *cat* and *kan* genes encoding chloramphenicol and kanamycin resistance, respectively, were amplified from pKD3 and pACYC, respectively using primers flanked by the same restriction digest sites as above. Both PCR products were digested with the appropriate restriction enzymes and antibiotic cassettes were cloned into the deleted region of the gene of interest (Figure 2.3). Ligation mixes were transformed into electorcompetent *E. coli* JM109 cells and transformants were screened by antibiotic selection (Section 2.8.1). The antibiotic gene

flanked by 500 – 1000 bp regions of homology to the gene of interest, was isolated from the plasmid using PCR.

2.6.2 PCR transformation into red-recombinase induced strains

A *S. flexneri* strain of interest was transformed with either pKD46 or pKM208, helper plasmids (Table 2.3) carrying genes encoding enzyme required for λ red-mediated homologous recombination (Figure 2.4). Electrocompetent cells of the *S. flexneri* strains carrying the helper plasmid were freshly prepared. Briefly, 125 mL of SOB media (Appendix A), containing 100 μg/mL ampicillin, was inoculated with 2.5 mL overnight culture and incubated at 30 °C for 1.5 hours. Expression of the helper plasmid was induced by the addition of 1 mM IPTG (for pKM208) or 100 mM arabinose (for pKD46) followed by an incubation period of 2 hours at 30 °C, to ensure that the heat sensitive helper plasmid and bacterial virulence plasmids were not lost. Electrocompetent cells were prepared as described in section 2.7.1 and resuspended in 200 – 400 μL of 10% (v/v) glycerol. Aliquots of 40–50 μL were used and ~1 – 2 μg of the appropriate knockout template was used to transform the freshly prepared *S. flexneri* electrocompetent cells, expressing the helper plasmid encoded genes. Cells were recovered in SOC media (Appendix A), containing 1 mM IPTG (for pKM208) or 100 mM arabinose (for pKD46) and recovered for 3 – 4 hours at 30 °C. Recovered cells were plated on LB agar plates, containing the required antibiotic, and incubated at 30 °C for upto 3 days. Resulting colonies were routinely restreaked onto fresh LB plates containing the required antibiotics to eliminate contaminants and false positives. Colonies were screened for successful disruption by colony PCR (Section 2.5.5). Gene disruption mutants were sequenced to confirm the insertional inactivation of target genes.

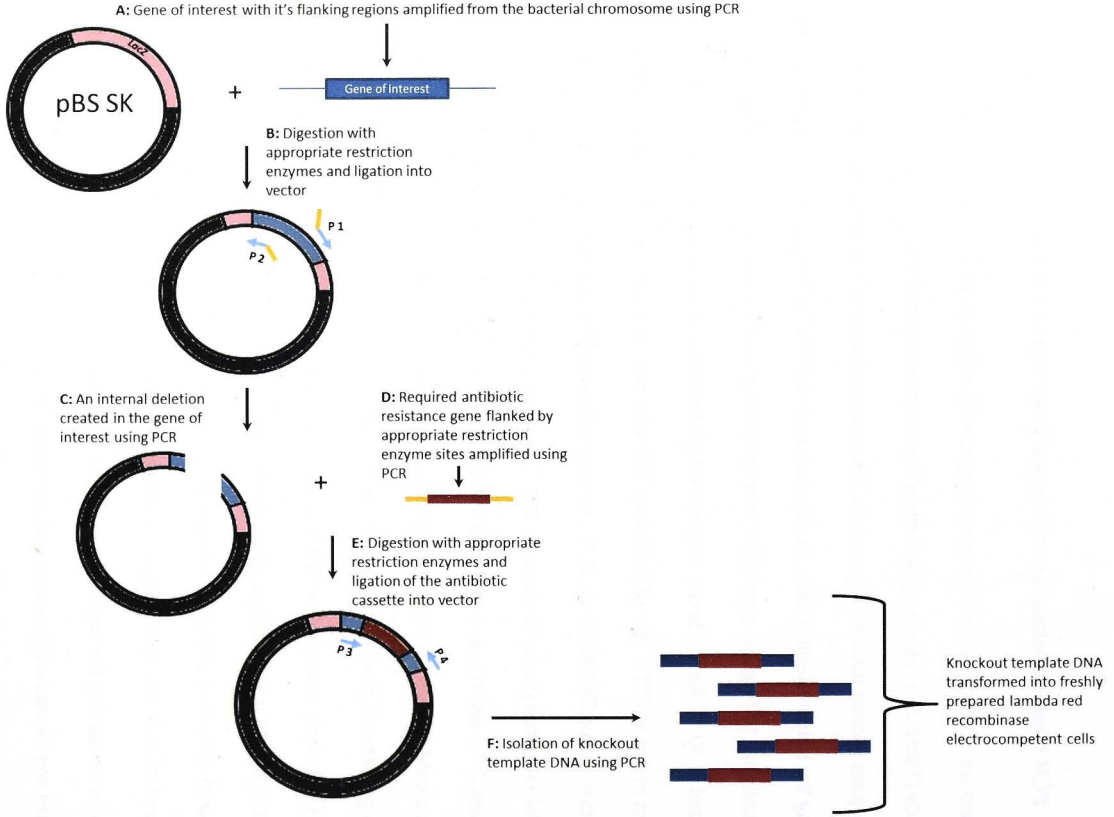
A: Gene of interest with it's flanking regions amplified from the bacterial chromosome using PCR
lacZ
pBS SK
+
Gene of interest
B: Digestion with appropriate restriction enzymes and ligation into vector
P 1
P 2
C: An internal deletion created in the gene of interest using PCR
D: Required antibiotic resistance gene flanked by appropriate restriction enzyme sites amplified using PCR
+
E: Digestion with appropriate restriction enzymes and ligation of the antibiotic cassette into vector
P 3
P 4
F: Isolation of knockout template DNA using PCR
Knockout template DNA transformed into freshly prepared lambda red recombinase electrocompetent cells

Figure 2.3: Schematic representation of the steps involved in the generation and isolation of a knockout template for the PCR-mediate targeted gene disruption. **A:** The gene of interest is first isolated from the bacterial chromosome using PCR and **(B)** cloned into an appropriate cloning vector (pBS KS is used in this study as this vector carries the ampicillin resistance gene thus allowing for antibiotic screening for insertion of the *cat* and kan^R genes). **C**: An internal deletion is created in the gene of interest using primers P1 and P2 carrying appropriate restriction enzyme sites. **D:** The required antibiotic resistance gene cassette (*cat* and kan^R genes were used in this study) is amplified using the same restriction enzyme sites cloned into the gene of interest. **E:** The vector (pBS KS + gene of interest with internal deletion) and insert (antibiotic cassette) are digested with the selected restriction enzyme and ligated together. Ligation mixes are transformed into appropriate *E. coli* strains and transformants are identified by antibiotic selection (positive clones are resistant to both chloramphenicol/kanamycin and ampicillin). **F:** PCR reactions using primes P3 and P4 were set up to isolate the knockout template.

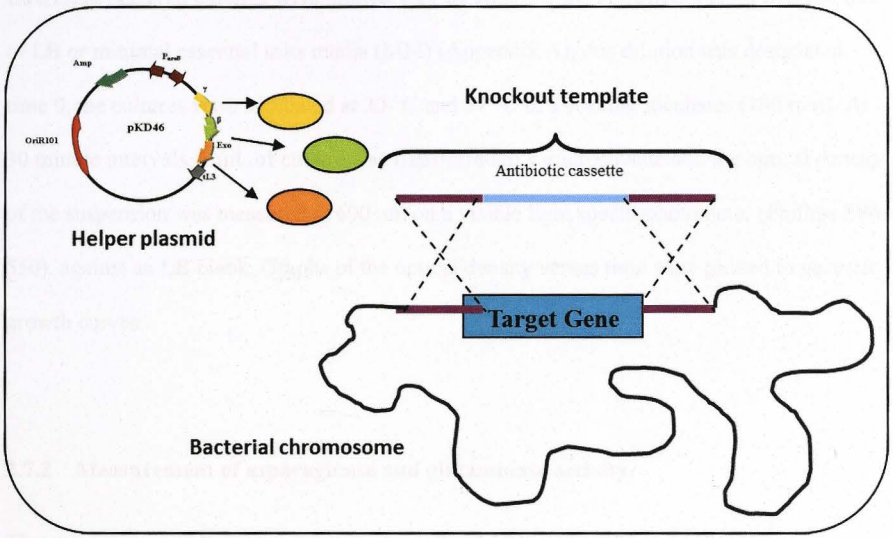

Figure 2.4: Schematic representation of the lambda red-mediated recombineering approach for gene disruption. In this technique a knockout template carrying an antibiotic cassette flanked by ~500-1000 bp regions of homology to regions flanking the target gene, is transformed into the strain of interest carrying a helper plasmid (pKD46 or pKM208) expressing the lambda phage genes γ, β, and *exo* whose products are required to prevent degradation of linear DNA and for homologous recombination. Introduction of the knockout template into *S. flexneri* strain carrying the helper plasmid, the large regions of homology facilitate homologous recombination producing a double cross-over reaction resulting in the replacement of the target gene with the antibiotic cassette.

2.7 Characterization of gene disruption mutants

2.7.1 Growth curves

Overnight bacterial cultures were diluted 1:20 by adding 5 µL of bacterial culture to 100 mL of LB or minimal essential salts media (MM) (Appendix A), this dilution was designated time 0, the cultures were incubated at 30 °C and 37 °C in a shaking incubator (180 rpm). At 30 minute intervals, 1 mL of culture was transferred to a microcuvette and the optical density of the suspension was measured at 600 nm on a visible light spectrophotometer (Phillips SP6-550), against an LB blank. Graphs of the optical density versus time were plotted to generate growth curves.

2.7.2 Measurement of asparaginase and glutaminase activity

The asparaginase and glutaminase activities of SFL1520, SFL2283 and SFL2285, were measured using the ammonia assay kit (Sigma) with log phase culture supernatants, according to the manufacturer's instructions. Briefly, fresh log phase cells were harvested and washed once in 1 x phosphate buffered saline (PBS), and 3 x 10^8 colony forming units (CFU) of bacteria was resuspended in 1 ml of 1 x PBS with 5 mM asparagine or glutamine. Aliquots were collected after 30, 60, 90 and 180 minutes of incubation at 37 °C and centrifuged to precipitate bacterial cells. The ammonia concentration in the cell-free supernatants was measured using the ammonia assay kit, according to the manufacturer's guidelines.

2.8 RNA methods

2.8.1 Isolation of total bacterial RNA

Overnight cultures of *S. flexneri* strains grown at 30 °C (to maintain virulence plasmids) were diluted 1:50 in LB or MM media and grown to mid log phase (OD_{600} = 0.7-0.8) at 37 °C. The volume of bacterial cultures corresponding to 1 x 10^9 CFU was estimated (Section 2.13.3) and bacterial cells were harvested by centrifugation. Bacterial pellets were treated with with 1 mL of TRIZOL reagent (Invitrogen) and tubes inverted 20 times followed by incubation at room temperature for 5 minutes. 200 µL of chloroform was added to cell suspensions and samples were agitated vigorously and incubated at room temperature for 15 minutes to precipitate proteins. Samples were centrifuged at 12,000 x *g* for 10 minutes at 4 °C following which the aqueous phase containing RNA and some contaminating DNA, was collected. The chloroform treatment was repeated to eliminate contaminating DNA. The aqueous phase collected after the second chloroform treatment was treated with 500 µl of ice-cold isopropanol and incubated at -20 °C overnight to precipitate bacterial RNA. RNA was collected by centrifugation at 12,000 x *g*, for 20 minutes at 4 °C. RNA pellets were washed using 1 mL of freshly prepared 75% ethanol. RNA pellets were air-dried and dissolved in 50 µl of nuclease-free water. The isolated RNA was cleaned up using the Qiagen RNeasy Kit, this step was performed to remove any residual DNA and organic salts. The amount of RNA isolated was quantified (Section 2.3.3). One microgram of isolated RNA was treated with 20 units of Turbo DNase (Ambion) to eliminate any contaminating genomic DNA.

2.8.2 Reverse transcription polymerase chain reaction

200 ng of DNase treated RNA was used to set up reverse transcription reactions using Superscript II (Invitrogen) and random hexamer primers according to the manufacturer's instructions. All reactions were set up with a negative control containing no reverse transcriptase (NRT) to ensure that the RNA preparations were free of genomic DNA. 1 µl of cDNA along with the NRT was used to set up PCR reactions (Section 2.5.4) using gene-specific primer to determine if the target genes were expressed under the conditions studied.

2.8.3 Quantitative real time reverse transcriptase PCR (qRT-PCR)

qRT-PCR was performed on the cDNA samples using the power SYBR Green RT-PCR kit (Applied Biosystems) according to the manufacturer's instructions except, primers were used at a final concentration of 0.4 µM and the final reaction volume was reduced to 10 µl from the recommended 20 µl. Expression of *hisG* was used as a control to normalize the expression of all bacterial genes as the expression of this housekeeping gene should remain constant in all bacterial strains used in this study. All qRT-PCR reactions were performed in triplicate with a NRT and NTC set up for each run. Reactions were run in a Rotor-Gene Q Real-Time cycler (Qiagen) with the following program;

Initial Denaturation Step	95 °C for 10 minutes, × 1
Denaturation Step	95 °C for 15 seconds, × 45
Primer annealing Step	55 °C 15 seconds, × 45
Hold step 1	40 °C for 5 minutes, × 45
Hold step 2	55 °C for 1 minute, × 1
Melt	55 °C to 99 °C, with 1 °C increase in every 10 seconds.

The Rotor-Gene Q series software package (Qiagen) was used to analyse the results of qRT-PCR runs and melt curves were also examined for each run to ensure that reactions were free of non-specific products and primer dimers.

2.9 Protein methods

2.9.1 1-D SDS PAGE and western blotting

2.9.1.1 Preparation of whole cell lysates

Log phase cultures of bacterial strains were obtained and the volume corresponding to 1 x 10^{10} CFU was determined (Section 2.13.3). Bacterial cells corresponding to 1 x 10^{10} CFU were harvested by centrifugation and the cell pellets were washed in 1 x PBS and resuspended in the appropriate amount of 2 x sample loading buffer (Appendix A). Samples were boiled for 10 minutes and loaded onto 12% SDS-PAGE gels.

2.9.1.2 Isolation of secretory proteins

Overnight cultures of the required *S. flexneri* strains were diluted 1:20 in LB broth and grown to late log phase (OD_{600} = 0.8 - 0.9) at 37 °C. The secretion of type 3 effector proteins was induced by adding Congo red (final concentration 10 mM) following which cells were incubated at 37 °C for 30 minutes. Bacterial cells were harvested by centrifugation and the supernatants were passed through 0.45 µM filters (Sartorius) to eliminate cellular debris. Secretory proteins were precipitated using 25 % trichloroacetic acid (TCA) in acetone and incubation on ice for 20 minutes. Protein precipitates were collected by centrifugation at 8,500 x *g*, for 10 minutes at 4 °C and washed twice using acetone. Mild sonication using a sonic water bath was used to suspend protein pellets in acetone. Washed protein pellets were

allowed to dry completely following which they were resuspended in solubilization buffer (Appendix A). Protein concentration was estimated using the BCA kit (Pierce) according to the manufacturer's instructions and 20 µg of supernatant protein samples were loaded onto 12 % (v/v) SDS-PAGE gels for Western blots.

2.9.1.3 1D SDS- PAGE gel preparation and electrophoresis

Mini SDS-PAGE gels were cast using the Mini-Protean electrophoresis apparatus (BioRad). 5 mL of 12% resolving gel mixture was prepared fresh and poured into the gel cast unit, 0.1% SDS was gently overlaid on top of the unploymerized gel to prevent drying, and the gel was allowed to polymerize at room temperature for 30 minutes. The SDS solution was then replaced with 2 mL of 5% stacking gel mixture and the required combs were inserted and the gel was allowed to polymerize for 45-60 minutes. After the gel set, the comb was removed, the wells rinsed out with 1 x SDS-PAGE running buffer (Appendix A) and the gel was placed in the electrophoresis tank. Both the inner and outer chambers of the tank were filled with running buffer, protein samples were loaded and allowed to separate at 100-150 V until the dye front reached the end of the gel. The Prestained Page-Ruler ladder (Fermentas) was used as a marked (Figure 2.5)

2.9.1.4 Coomassie staining of SDS-PAGE gels

The SDS-PAGE gels were soaked in Coomassie Brilliant Blue R250 dye (Appendix A) overnight to allow for visualization of protein bands. Excess stain was washed off and the gels were treated with destain solution (Appendix A) for 2-3 hours until the background stain faded and the protein bands were clearly visible.

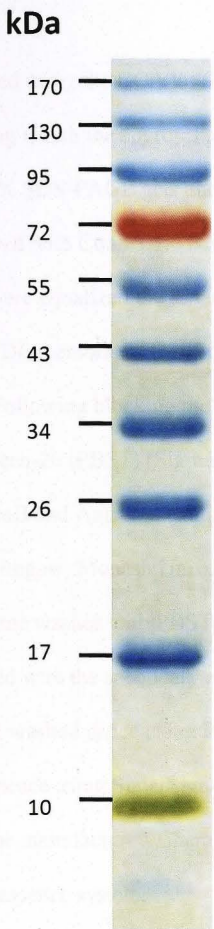

Figure 2.5: The PageRuler Prestained protein ladder (Fermentas) used in SDS-PAGE gels. Sizes indicated are only approximate, the lot-specific exact marker sizes are provided with each batch of marker. (Figure adapted from Frementas).

2.9.1.5 Western blotting

Protein concentrations were estimated using the BCA kit (Pierce) according to the manufacturer's instructions following which the appropriate amount of each protein preparation was loaded onto two 12% SDS-PAGE gels and allowed to separate (Section 2.12.1.3). One of the gels were stained with Coomassie Brilliant blue R250 to ensure equal loading of samples. Once samples were equalized the separated proteins on the second gel were transferred onto Hybond-P PVDF membranes (Millipore) and blocked in 5% skimmed milk in 1 x PBS at 4 °C overnight. Following blocking the membranes were washed thrice in 1 x PBS containing 0.05% (v/v) Tween-20 (PBST) (Sigma). Membranes were then incubated with the primary antibodies (Anti-IpaB and Anti-IpaD antisera generated in-house in mice or αHp-BamA obtained from Trevor Lithgow, Monash University) for 2 hours. Unbound antibodies were washed off using three washes with PBST as outlined above, following which the membranes were incubated with the secondary antibodies (Anti-mouse IgG; Sigma) for 1 hour. Membranes were washed thrice using PBST. The binding of antibodies was then detected by chemiluminescence using SuperSignal West Pico Chemiluminescent Substrate (Pierce) as described by the manufacturer. Chemiluminescence was then detected using the Fisher Biotec chemiluminescence system.

2.9.2 Differential in gel electrophoresis (DIGE) and liquid chromatography mass spectrometry (LCMS)

2.9.2.1 Isolation of total bacterial protein for differential in gel electrophoresis

Overnight cultures of SFL1520 (wild type parent), SFL2283 (Δ*ansB*) and SFL2285 (Δ*ggt*) grown at 30 °C, were diluted 1:100 in LB media and grown to log phase at 37 °C. Bacterial

cells were harvested by centrifugation and washed thrice using cell wash solution (Appendix A). Bacterial pellets were resuspended in 500 µl of cell lysis buffer (Appendix A) and incubated on ice for 10 minutes. Subsequently, the suspensions were sonicated 10 times for 15 s with 30 s intervals on ice. Cellular debris was sedimented by centrifugation at 14,000 x *g*, 4 °C for 10 minutes. Supernatants were treated with 10 volumes of ice-cold acetone and incubated at -20 °C overnight to precipitate proteins. The protein pellets were washed thrice using ice-cold acetone and air dried. Acetone-free proteins were solubilized in 200 µl of cell lysis buffer (Appendix A) and pH was adjusted to 8.5.

For DIGE, total protein from wild type and both mutant strains were isolated from four independent experiments. Protein concentration was determined using the BCA kit (Pierce) and Bradford method [303]. 500 µg of each protein sample was labeled with fluorescent dyes Cy3 or Cy5 (GE Healthcare), an internal standard, consisting of 250 µg of each sample, was labelled with Cy2. Samples were labeled with CyDye DIGE Fluors (minimal dyes) from the Ettan DIGE kit (GE Healthcare), according to the manufacturers' instructions with minor modifications as described by Mathesius *et al.* [304]. Briefly, 500 µg of each protein sample was labeled with 400 pmol amine reactive cyanine freshly dissolved in anhydrous dimethyl formamide (DMF). CyDye labeling was carried out on ice and in the dark for 30 minutes. Each reaction was terminated using 10 nmol lysine to eliminate any unbound dye. Labeled samples were treated with DTT (20 mg/ml) and Bio-ampholytes (50 µl/ml). To identify differences in the proteomes of wild type and mutant *S. flexneri* strains, 500 µg of total protein from the wild type parent (SFL1520) labeled with Cy3 or Cy5 was combined with 500 µg of oppositely labeled proteins from each mutant strain. Each wild type-mutant pair was then mixed with 500 µg of the combined protein preparations labeled with Cy2 as an internal control.

2.9.2.2 2-D electrophoresis

2-D electrophoresis was performed in darkness to maintain the stability of the Cy dyes. Immobiline pH 3-10 or 3-7 NL Drystrips (24 cm, GE Healthcare) were used for the first dimension isoelectric focusing (IEF). The strips were rehydrated overnight in rehydration solution (Appendix A). Wild type-mutant pairs with internal controls were loaded onto rehydrated Immobiline strips and IEF was carried out in a Multiphor II Electrophoresis System (GE Healthcare) at 20 °C for a total of 35,000 volt hours [304]. For separation of proteins across the second dimension, self-cast 12.5% SDS-PAGE gels were prepared using the EttanDaltsix system (GE Healthcare). The gels were cast using low fluorescent glass plates, which are compatible with the Ettan DIGE system. Focused first dimension strips were equilibrated as described by [304] and placed on the second dimension gels. SDS-PAGE was carried out at 10 °C in SDS running buffer (Appendix A) at 600 V, 10 mA, and 2.5 W per gel for the first hour; 600 V, 40 mA, and 13 W per gel until the bromophenol blue front reached the bottom of the gel.

2.9.2.3 Gel imaging and image analysis

After second dimension electrophoresis, DIGE-labeled proteins were visualized using a Typhoon Trio laser scanner (GE Healthcare). Gels were scanned with the specific excitation wavelengths of Cy3 (532-nm laser and a 580-nm band pass 30 emission filter), Cy5 (633-nm laser and a 670-nm band pass 30 emission filter) and Cy2 (488-nm laser and a 580-nm band pass 40 emission filter). Spot detection and analysis was carried out using the DeCyder Version 5 (GE Healthcare) software package followed by careful manual confirmation and rematching of matching errors. Statistics and identification of differentially expressed spots were carried out in the DeCyder DIA and BVA modules (one-way ANOVA).

2.9.2.4 In gel trypsin digestion of protein spots and LC-MS

After analysis of gel images identified spots of interest were excised from the 2D-DIGE gels using an Ettan spot picker (GE Healthcare). The spot picker was calibrated and tested several times prior to spot excision. In-gel trypsin digest was carried out as described by Mathesius *et al.* [304] with a few modifications. Briefly, excised protein spots were washed four times in acetonitrile: 50 mM ammonium bicarbonate (50:50, v/v). Spots were then dried in 100% acetonitrile for 30 minutes following which they were air dried to eliminate all acetonitrile. Gel pieces were rehydrated using a trypsin solution (20 units; Promega) and incubated for 2 hours at 4 °C (to allow the trypsin solution to diffuse through the gel) followed by overnight incubation at 37 °C. Peptides were then extracted from the gel pieces using an extraction buffer consisting of acetonitrile: water: trifluoroacetic acid (TFA) (50%:50%:1%, v/v) followed by gentle sonication in a sonic water bath for 40 minutes. This extraction step was performed twice using a reduced volume of extraction buffer and 20 minutes sonication the second time round. Peptides were collected and dried completely to remove all traces of TFA. Dried peptides were resuspended in 20 µl of acetonitrile: water: formic acid (10%:89.9%:0.1%, v/v). Digested, desalted peptides were identified by LC-MS/MS (at the Mass spectrometry facility, The Australian National University, ANU). Proteins were identified through MS/MS spectra using the MASCOT database (Matrix Science). One missed cleavage per peptide was allowed and a mass tolerance between 0.3 and 0.1 Da was used in most searches, unless otherwise specified. Carbamidomethylation was set as a fixed modification and oxidation (M) as a variable modification.

2.10 Cell culture

Baby hamster kidney (BHK) cells were routinely grown at 37 °C in Minimal essential medium (MEM) F15 (Invitrogen) supplemented with 10% (v/v) foetal calf serum (FCS) (GIBCO) in a 5% CO_2 humidified atmosphere. For adherence and invasion assays, cells were inoculated in 6-well tissue culture plates at 6 x 10^3 cells/well in 3 mL media and grown to 75-80% confluency. For the coverslip adherence assay, sterilized coversilps were placed into the wells of 6-well plates and BHK cells were grown over the coverslips.

2.10.1 Subculturing cells

The epithelial cell line, BHK was used in all tissue culture assays in this thesis. The cells were grown in 25 cm^2 or 75 cm^2 tissue culture flasks (Falcon, Becton Dickinson) to 70% confluency. MEM with 10% (v/v) FCS and 200 µg/mL of neomycin and streptomycin and 120 µg/mL of penicillin was prewarmed to 37 °C. The media in the flasks was poured off and 5 mL sterile 1 x PBS (Appendix A) was added to wash off any remaining media. This washing step was repeated and followed by the addition of 2 mL of 0.05% (w/v) Trypsin-0.20% (w/v) EDTA. The flask was incubated at 37 °C for approximately 5 minutes. The reaction was halted by the addition of 4 mL of MEM as soon as the cells began to lift off the floor of the flask. Trypsinized cells were resuspended in the media by gentle pipetting to obtain a uniform solution. 10 µL of this solution was treated with an equal volume of 0.4% (w/v) trypan blue and incubated at 37 °C for 5 minutes. 10 µL of this solution was loaded onto a haemocytometer to determine the number of viable cells per mL (Section 2.13.2). About 1.5 x 10^5 cells were used to seed a new 25 cm^2 flask containing 10 mL MEM/FCS and 1.7 x 10^6 cells were used to seed a 75 cm^2 flask containing 20 mL MEM/FCS. Flasks were

incubated at 37 °C, 5 % CO_2. Media was changed every 2 days until the next passage was required.

2.10.2 Counting cells with a haemocytometer

Cells were counted using the Improved Neubauer Haemocytometer from Baxter Scientific. The cell suspension was dropped onto the edge of the haemocytometer and the solution was pulled under the cover slip by capillary action. The slide was viewed using a light microscope under 100 X magnification and the number of dye excluding cells in each of the four corner squares and the centre square were counted. The number of cells in the squares was averaged and this number was multiplied by 10^4 to give the number of cells per mL.

2.10.3 Preparing bacterial inocula for *in vitro* cell culture assays

Overnight cultures of required bacterial strains were diluted 1:100 in LB containing the appropriate antibiotics and allowed to grow to log phase (OD_{600} = 0.6 – 0.8) at 37 °C. Bacterial cells were harvested from 50 mL of cultures by centrifugation and washed using ice cold 1 x PBS. Washed cells were resuspended in 1 mL of 1 x PBS and the number of cells in the suspension was calculated using an absorbance-based method. Briefly, bacterial pellets were resuspended in 750 µL of ice cold 1x PBS and transferred into pre-chilled eppendorf tubes. Cells were washed using 1 x PBS and resuspended in 200 µL of ice cold PBS by vigorous vortexing. 7, 8, 9, and 10 µL of resuspened cells were transferred to eppendorf tubes containing 1 mL 1 x PBS and the optical density of the cell suspensions was measured at 600 nm on a visible light spectrophotometer (Phillips SP6-550), against a PBS blank. The volume of cell suspension corresponding to $O.D._{600}$=1 was determined as the number of cells at this

OD is assumed to be around 2.5 x 10^8 CFU/mL, from previously generated growth curves. Using this information, the volume of cell suspensions corresponding to 2.0 x 10^8 CFU/mL was resuspended in cell culture media to obtain the bacterial inoculum for all cell culture assays. 100 µL of the inoculum was removed and used to make serial dilutions. The appropriate dilutions were plated in duplicate to obtain the bacterial count in the infecting inoculum. The remaining bacterial inoculum was supplemented with the appropriate antibiotic to maintain selection for any introduced plasmids. The tubes were kept on ice while the BHK cells were prepared for cell culture assays.

2.10.4 Preparing BHK monolayers for *in vitro* cell culture assays

The BHK monolayers grown to 70-80% confluency in 6-well plates were washed twice using 1 X PBS. 1 mL prewarmed, cell culture media containing no antibiotics or FCS was added to each well and monolayers were incubated at room tempreature for 10 minutes. The medium was removed and 2 mL of each bacterial inoculum (Section 2.13.3) was gently applied to duplicate wells. The plates were centrifuged at 2,400 x *g* for 10 minutes at room temperature (Beckman GS-6R Benchtop Centrifuge).

2.10.5 Invasion Assay

Two 6 well plates were seeded with BHK cells and grown to confluency over 3 days. Two 6-well plates were required for this assay; an intracellular bacterial plate and a total bacterial plate with 2 wells per sample on each plate to carry out the assay in duplicates. BHK monolayers infected as described in section 2.13.4 were incubated at 37 °C, 5% CO_2 for 2 hours to allow bacterial invasion of the epithelial layer. Monolayers were washed twice using

1 mL 1 x PBS to wash off any unbound bacteria. The wells on the intracellular bacterial plates were treated with 1 mL MEM +10% FCS +16 μg/mL gentamycin. Gentamycin cannot penetrate epithelial cells therefore this antibiotic kills bacterial cells on the surface of the monolayer and not intracellular bacteria. The wells on the total bacterial plates were treated with 1 mL MEM +10% FCS (so all attached extracellular bacterial + intracellular bacteria survive). Plates were incubated at 37 °C for 2 hours and washed thrice in 1 x PBS to remove any killed or unattached bacteria. 200 μL of 0.05% (v/v) Triton X-100 in 1 x PBS was added to each well and incubated at room temperature for 10 minutes to lyse the mammalian cells. 800 μL of LB was added to each well and agitated with a Pasteur pipette to obtain homogenous suspensions of bacterial cells. Solutions were transferred into eppendorf tubes and placed on ice. The bacterial cell suspensions obtained from each well were serially diluted in 1 x PBS and appropriate dilutions were plated on duplicate LB agar plates containing the appropriate antibiotics. Plates were incubated overnight at 37 °C and colonies obtained were counted and used to calculate the number of intracellular and total-associated bacteria for each strain.

$$\% \text{ Intracellular Bacteria} = \frac{\text{Average Number of Bacteria counted on Intracellular plate}}{\text{Number of Bacteria in Inoculum}} \times 100$$

$$\% \text{ Adherent Bacteria} = \frac{\text{Average Number of Bacteria counted on Total plates}}{\text{Number of Bacteria in Inoculum}} \times 100$$

$$\% \text{ Invasion} = \frac{\text{Average Number of Bacteria counted on Intracellular plates}}{\text{Average Number of Bacteria counted on Total plat}} \times 100$$

2.10.6 Bacterial adherence assay

BHK cells in 6-well plates were infected with 4 x 10^8 CFU of each strain. Bacterial cells were allowed to infect the monolayer for 90 minutes at 37 °C, 5% CO_2. Unbound bacterial cells were washed off the BHK monolayer using 1 x PBS after which the mammalian cells were lysed using 0.05% (v/v) Triton-X in 1 x PBS. Appropriate dilutions of the cell lysates were plated on LB agar plates carrying the appropriate antibiotics to determine the number of adherent and intracellular bacterial cells.

2.10.7 Coverslip adherence assay

The coverslip adherence assay was performed based on the protocol developed by Cravioto *et al,* [305]. Briefly, overnight cultures of all *S. flexneri* strains grow at 30 °C were diluted and grown to log phase at 37 °C (OD_{600} = 0.6-0.8). 4 x 10^8 CFU of each strain was used to infect a confluent layer of BHK cells grown on coversilps placed within wells of 6-well culture plates. The plates were incubated for 90 minutes at 37 °C to allow for infection. The coverslips were washed thrice in 1 x PBS to remove any unbound bacterial cells. Samples were fixed using fresh 70% (v/v) methanol following which they were stained with 10% Giemsa stain for 30 minutes. Excess stain was washed off. Coverslips were mounted on glass slides and examined using an oil immersion lens.

2.11 Mouse studies

All animal work was performed under the approval of the ANU Animal Experimentation Ethics Committee.

2.11.1 *In vivo* studies: mouse pulmonary model

6-8 week old female Balb/c mice weighing approximately 20-25 g (Animal Resource Centre,WA) were inoculated intranasally with a sub-lethal dose (2 x 10^7 CFU/ 10 µL) of the pathogenic wild type SFL1520 strain, SFL2283 (Δ*ansB*) or SFL2285 (Δ*ggt*). The mice were lightly anesthetized with isoflurane prior to inoculation. 20 mice were euthanized 24 and 48 hours post infection and their lungs were extracted and homogenized in PBS with 0.05% Triton-X. Appropriate dilutions of the homogenates were plated on LB agar with antibiotics, where appropriate, to obtain the live counts of intracellular bacteria per lung.

2.11.2 Monitoring infected mice

Infected mice were monitored for 48 hours post infection for the development of symptoms. Weights were recorded over this period and the degree of sickness was scored. Based on the symptoms of illness displayed, mice were scored as healthy, moderately healthy, mildly sick, medium sick, sick and severely sick as described below;

Symptom Score Key

1.	Healthy:	Smooth coat, groomed, active
2.	Moderately Healthy:	Showed slightly ruffled coats otherwise appeared healthy
3.	Mildly Sick:	Showed slightly ruffled coats, slight hunch and slight lethargy
4.	Medium Sick:	Showed ruffled coats, slight hunch and lethargy.
5.	Sick:	Showed ruffled coats, pronounced hunching and lethargy
6.	Severely Sick:	Showed a very ruffled coat, acutely hunched and immobile

2.12 Bacteriophage techniques

2.12.1 Propagation of bacteriophage

U.V. induction was used to induce bacteriophage SfII from the serotype 2a *S. flexneri* strain NCTC4 (SFL2345) [156]. An overnight culture of SFL2345 was diluted 1:10 in LB media and grown to log phase at 37 °C. Bacterial cells were harvested by centrifugation and resuspended in half the original volume of 10 mM $MgSO_4$. Half of the cell suspension was transferred into a petri dish and irradiated with U.V. light for 2 minutes using a U.V. lamp placed 10 cm above the culture plate. An equal volume of LB media was added to the irradiated cells and cultures were incubated overnight at 37 °C. The remaining bacterial suspension was also incubated overnight as a non-irradiated control. Bacteriophage SfV was isolated from overnight cultures of SFL1693, an SfV lysogenized SFL1. SfV is unstable in this strain therefore growing SFL1693 overnight at 37 °C leads to the spontaneous induction of SfV. The overnight cultures carrying induced bacteriophage were treated with chloroform and the bacteria/phage mix was incubated at 37 °C for 25 minutes. Unlysed bacterial cells and other cellular debris were collected by centrifugation and the supernatant containing bacteriophages was passed through a 0.45 µm filter to collect bacteriophage stocks. Bacteriophage stocks of SfII and SfV were collected and propagated on a serotype Y strain, SFL124 (SFL1353) [306]. For propagation, equal volumes of a log phase culture of SFL1353 in NZCYM medium (Appendix A) were added to phage stock incubated overnight at 37 °C with shaking.

2.12.2 Titration of phage

Phage numbers in stock solutions were titrated by measuring the efficiency of plaquing (EOP). Overnight bacterial cultures were diluted 1:20 in LB media and grown to log phase at 30 °C with shaking. 3 mL aliquots of soft agar (Appendix A) was prewarmed to 42 °C. Serial dilution (10^1-10^8) of phage stocks were made in SM buffer (Appendix A) and 100 µL aliquots of each dilution added to appropriately labeled eppendorf tubes. Equal volumes of log phase bacterial culture was added to each eppendorf tube and the phage/bacteria mix was incubated in a water bath at 37 °C for 20 minutes. The phage/bacteria mix was added to the prewarmed soft agar, mixed gently, poured onto a LB agar plate and allowed to set. Plates were incubated overnight at 37 °C and the number of plaques on each plate were counted and the number of plaque forming units per mL (PFU/mL) was calculated to determine the bacteriophage titer in the original stock.

2.12.3 Purification of bacteriophage

Purification of SfII and SfV phage preparations was performed as described for phage lambda [301]. An overnight culture of phage/bacteria mix treated with chloroform (Section 2.15.1) was transferred into centrifuge bottles and centrifuged at 8,250 x *g*, 4 °C for 10 minutes in a Sorvall RC 5C Plus centrifuge, using a SLA300 rotor. The supernatants were transferred into fresh centrifuge bottles and centrifuged again to remove any remaining bacterial cell debris. Supernatants were collected and treated with 1 µg/mL of both RNase and DNase (Sigma), and stirred at room temperature for 30 minutes. 5.84% (w/v) NaCl was added to each solution and stirred for 8 minutes, following which the mixtures were incubated on ice for 60 minutes. Solutions were centrifuged at 13,000 x *g*, , 4 °C for 20

minutes. Supernatant were transferred into sterile flasks and 10% (w/v) Polyethylene glycol (PEG) was added, following which solutions were stirred slowly at room temperature until all the PEG dissolved. This was followed by incubation on ice for 60 minutes and centrifugation at 16,000 x *g*, 4 °C for 20 minutes. The precipitated phage pellets were dried and resuspended in a minimal volume of gelatin-free SM Buffer (Appendix A). Any residual PEG was removed by chloroform extraction. The resulting phage suspension was purified by CsCl density gradient centrifugation (final density of solution=1.40-1.45 g/ml) at 110,000 x *g* for 24 h at 15 °C in a swinging bucket rotor. Resulting phage bands were aspirated and dialysed against 1 L of gelatin-free SM buffer containing 1 M NaCl at 4 °C overnight followed by two repeated dialysis in 1 L of SM buffer for 3 h at room temperature. Dialysed phage preparations were filter sterilized and stored at 4 °C.

2.12.4 Isolation of bacteriophage DNA

Purified bacteriophage preparations were extracted with chloroform thrice to remove any residual PEG and cellular debris. The aqueous phase collected from each chloroform extraction was treated with 150 µg of proteinase K (Roche) in 0.5% SDS, 20 mM EDTA, 10 mM Tris-HCl and incubated at 55 °C, for 30 minutes to disrupt bacteriophage particles and release phage DNA. DNA was extracted using an equal volume of phenol and the aqueous phase was collected and extracted with phenol thrice followed by a final extraction with 1:1 phenol:chloroform. The aqueous phase was collected and dialysed overnight at 4 °C with stirring and three changes of TE buffer (Appendix A) to remove all traces of phenol. Purified phage DNA was removed from the dialysis tubing and stored at 4 °C.

2.12.5 Determining bacteriophage host range

To determine the host range of bacteriophages SfII and SfV, 20-50 µl of purified phage preparations were streaked across LB agar plates. Once phage streaks were completely dry, overnight cultures of the required bacterial host strains were streaked across the bacteriophage streak. Plates were incubated overnight at 30 °C to allow bacteriophage particles to infect each host strain tested. After incubation, the appearance of lysis zones on the bacterial streaks across the bacteriophage streak was examined. Bacterial strains were categorized as susceptible to bacteriophage infection (S) if they showed zones of lysis and resistant to bacteriophage infection (R) if they failed to display zones of lysis.

2.13 *C. elegans* techniques

2.13.1 *C. elegans* strains and growth conditions

Unless otherwise stated all *C. elegans* strains were obtained from the Caenorhabditis Genetics Center (CGC, University of Minnesota, USA). The *C. elegans* wild type N2 strain [300] was routinely used in this study. A *hsp-6*::GFP transcriptional reporter strain-SJ4100 (provided by Carolyn Behm, ANU) was also used in this study to monitor the expression of HSP-6 in nematodes infected with various *S. flexneri* strains. Nematodes were maintained at 22 °C on modified nematode growth medium (NGM, 0.35% peptone) agar medium seeded with *E. coli* OP50 [226]. To prevent the formation of dauer worms were transferred onto fresh *E. coli* OP50 lawns.

2.13.2 *E. coli* strains

C. elegans were cultured with *E. coli* OP50, (CGC), an auxotrophic mutant deficient in uracil production, as a result of which it grows slower than the wild type strain [300]. For all RNAi feeding experiments the *E. coli* HT115 (DE3) was used, as this strain lacks RNAse III and expresses the T7 polymerase on exposure to IPTG [277].

2.13.3 Obtaining a synchronized population of young adult Nematodes

A mixed population of worms was chuncked onto *E. coli* OP50 lawns on 9 cm or 15 cm NGM plates. Worms were allowed to grow for 2-3 days at 22 °C until there were lots of eggs and gravid adults on the plates. Eggs and adult worms were then transferred into 15 or 50 mL falcon tubes using 2-5 mL of sterile S-basal (Appendix A) and allowed to sediment for 5-10 minutes at room temperature. The S-basal solution was removed and 500 µl of alkaline hypochlorite solution (Appendix A) was added to the tubes. Worm pellets were agitated by vigorous vortexing for 90 seconds at room temperature and tubes were filled with S-basal. Eggs were collected by centrifugation at 500 x *g* for 3 minutes. Eggs were washed with S-basal several times, to remove all the belach. 5 mL of S-basal was added to the tubes and eggs were allowed to hatch overnight at room temperature with shaking. L1's were then concentrated by centrifugation at 500 x *g* for 3 minutes, following which they were quantified and seeded onto *E. coli* OP50 lawns and allowed to grow to the L4 stage at 22 °C.

2.13.4 Liquid killing assays

Overnight cultures of *S. flexneri* strains maintained at 30 °C were diluted 1:50 in LB media and grown to log phase at 37 °C (OD_{600} = 0.6-0.8). A synchronized population of L4 stage *C.*

elegans worms collected off *E. coli* OP50 plates, was treated with 200 µg/mL of gentamycin for 3 hours and washed thoroughly with S-basal to remove any residual antibiotic. This antibiotic treatment was to remove any surface-bound *E. coli* OP50 cells. Approximately 20-50 washed L4's were transferred into each well of a 24-well plate containing 100 µL of the appropriate log-phase bacterial culture to be tested. The volume of solution in each well was adjusted to 500 µL with S-basal and plates were incubated at 22 °C for up to 48 hours. The number of live worms in each well was scored at 12 hour intervals and the percentage survival was calculated. Worms that showed no pharyngeal pumping and remained immobile on tapping the plate were considered dead. A minimum of three replicates for each test strain was set up per trial.

2.13.5 *C. elegans* bacterial accumulation assays

All bacterial strains used for the accumulation assay were grown overnight at 37 °C on modified NG agar medium to stimulate expression of virulence plasmid-encoded genes [283]. Plates were cooled to room temperature before they were inoculated with 50-100 synchronized young adult nematodes (L4's) that have been treated with gentamycin (Section 2.13.4). The worms were allowed to grow at 22 °C for 24 hours, after which 10-20 worms were picked off each bacterial lawn and washed thoroughly using sterile S-basal with 1 mM of sodium azide to anesthetize the animals. The worms were treated with 200 µg/mL of gentamycin for 3 hours after which they were washed thoroughly using S-basal with 1 mM of sodium azide to remove any residual antibiotic. Washed worms were suspended in S-basal + 0.1% Triton-X and lysed by mechanical disruption using glass beads [284]. Appropriate dilutions of the lysates were plated onto LB agar with the appropriate antibiotics, to obtain intraluminal bacterial counts. In order to visualize bacterial accumulation within nematode

intestinal lumens, worms were fed *S. flexneri* strains tagged with GFP^+. Following 24 hours of infection, bacterial fluorescence was observed using the EVOS digital inverted microscope (Advanced microscopy Group-AMG).

2.13.6 Isolation of Total Nematode RNA

Approximately 50,000 synchronized young adult worms were infected with either *E. coli* OP50 or *S. flexneri* serotype 3b for 24 h at 22 °C. Adult worms were separated from eggs and bacterial debris using sucrose floatation [307]. Infected adult worm pellets were snap frozen in liquid nitrogen. 700 µl of Trizol reagent (Invitrogen) was added to the frozen worm pellets followed by vigorous vortexing at room temperature until the pellets completely thawed. Samples were then subjected to three freeze-thaw cycles by snap freezing them in liquid nitrogen followed by rapid thawing at 37 °C. In order to completely homogenize the samples and denature proteins, samples were subjected to six cycles of vortexing at room temperature for 30 seconds followed by 30 seconds on ice. Samples were centrifuged at 14,000 x *g*, 4 °C for 10 minutes. The aqueous phase was transferred into a fresh eppendorf tube and 100 µl of chloroform was added. Samples were mixed thoroughly by vortexing followed by incubation at room temperature for 15 minutes. To separate DNA from RNA, tubes were centrifuged at 14,000 x *g*, 4 °C, 15 minutes. The aqueous phase was transferred into a fresh eppendorf tube and 500 µl of ice-cold isopropanol was added and tubes were vortexed and incubated at room temperature for 30-90 minutes to precipitate RNA. RNA was collected by centrifugation at 14,000 x *g*, 4 °C, 10 minutes. RNA pellets were washed with 1 mL of ice-cold 75% ethanol, air-dried for 15-30 minutes and resuspended in 35 µl of nuclease-free water. 5 µl aliquots of each RNA preparation was stored at -80 °C.

2.13.7 qRT-PCR of nematode mRNA

2.13.7.1 Primer design for qRT-PCR

Primer pairs were designed to amplify *aco-1, cct-2, eef-2, daf-19, hsp-60, unc-41, unc-54,* and *hsp-6* from mRNA isolated form adult *C. elegans* grown of either *E. coli* OP50 or wild type *S. flexneri* 3b (SFL1520) for 24 hours. The *C. elegans act-2* gene which encodes actin was used as a control gene to normalize all reactions, as the mRNA levels of *act-2* were expected to remain constant in the worms fed different dsRNA. Primers were designed to span exon-exon junctions conserved between the different isoforms of each target gene. BlastN searches were performed to ensure that primers did not bind to any other region in *C. elegans* genome. Primers were designed according to the instructions provided in the ABI power SYBR Green manual. Briefly, each primer was 20 bp long with a GC content in the 30-80% range and Tm between 58-60 °C, care was also taken to ensure that the 5 nucleotides in the 3' end contained no more than two G and/or C. The complete list of qRT-PCR primers can be found in Table 2.4.

cDNA was synthesized from 200 ng of total RNA isolated for worms fed either *E. coli* OP50 or wild type *Shigella flexneri* 3b (SFL1520) for 24 hours. Reverse transcription reactions were set up using Superscript II (Invitrogen) and random hexamer primers according to the manufacturer's instructions. qRT-PCR reactions were set up as described in Section 2.11.3.

2.13.8 Isolation of Total Nematode Protein

Approximately 500,000 young adult nematodes were infected with *E. coli* OP50 (control) and wild type *S. flexneri* 3b (SFL1520) for 24 hours at 22 °C. Post infection the nematodes were

washed thoroughly using sterile S-basal with 1 mM of sodium azide. Worms were treated with 200 µg/mL of gentamycin for 3 hours to reduce the presence of bacterial spots on the gels. Sucrose floatation was used to separate adult worms from eggs and any bacterial debris. Infected worms were snap-frozen in liquid nitrogen and the frozen pellets were ground to a fine powder using fine glass powder in an ice-cold mortar and pestle. The ground worms were resuspended in solubilisation buffer (Appendix A). The suspensions were homogenized and kept on ice, following which they were sonicated 5 times for 10 s with 30 s intervals on ice. Samples were centrifuged at 14,000 x *g*, 4 °C for 10 minutes to sediment cellular debris. ¼ th volume of 100% TCA was added and proteins were precipitated by incubation on ice for 15-30 minutes. Precipitated proteins were collected by centrifugation at 14,000 x *g*, 4 °C for 10 minutes. Pellets were washed using 200 µl of ice-cold acetone and incubated at -20 °C for 5-10 minutes. The acetone wash was repeated thrice following which the isolated proteins were air dried and resuspended in 20-30 µl of 0.2 M NaOH followed by 100-200 µl of solubilization buffer (Appendix A). Protein concentration was determined using the Bradford method [303] and 2 mg of each sample was labeled with fluorescent dyes Cy3 or Cy5 (GE Healthcare) an internal standard, consisting of 1 mg of each sample, was labeled with Cy2. Differential in gel electrophoresis was performed as described in Section 2.12.2.

2.13.9 RNAi Experiments

2.13.9.1 RNAi constructs

RNAi feeding strains consisted of *E. coli* HT115 transformed with an RNAi plasmid, pL4440 with a fragment of the target gene cloned into its multiple cloning site (MCS). The MCS of pL4440 is flanked by two T7 polymerase promoters in opposite orientations such that a gene cloned into the MCS is expressed as dsRNA when T7 polymerase in induced (Figure 2.6). *E.*

coli HT115 harboring genes-encoding double stranded RNA targeted towards, *aco-1* (ZK455.7), *cct-2* (T21B10.7) and *hsp-60* (Y22D7AL.5), were obtained from the Ahringer lab library (provided by Peter Boag, Monash University) and the *daf-19* (F33H1.1) RNAi construct was obtained from the ORF-RNAi Library v1.1 (Source Bioscience).

2.13.9.2 Feeding protocol for RNA interference (RNAi) in *C. elegans*

Glycerol stocks of *E. coli* HT115 strains carrying the required RNAi vector (expressing double-stranded RNA targeting the gene of interest) were grown overnight on LB agar containing 100 µg/mL ampicillin. Single colonies from the overnight cultures were then inoculated into LB broth containing 100 µg/mL ampicillin and allowed to grow overnight at 37 °C. Expression of specific dsRNA from each RNAi construct was induced at 37 °C using IPTG at a final concentration of 1 mM for 3 hours. After induction, bacterial cells were harvested by centrifugation and resuspended in a small volume of LB (0.5-1 mL). Induced cells were spread onto NGM plates containing Carbenicillin (final concentration 100 µg/mL) and IPTG (final concentration 1 mM). The plates were allowed to dry. Synchronized L1 larvae were seeded onto the RNAi lawns and allowed to grow to the L4 stage at 22 °C. During this period developing worms feed on the respective *E. coli* HT115 strains carrying the required RNAi vector and in the process the target gene is knocked down. RNAi silenced L4 worms were harvested and treated with gentamycin (at a final concentration of 200 µg/mL) for 3 hours. These worms were then used to set up bacterial accumulation assays (Section 2.13.5) and liquid killing assays (Section 2.13.4).

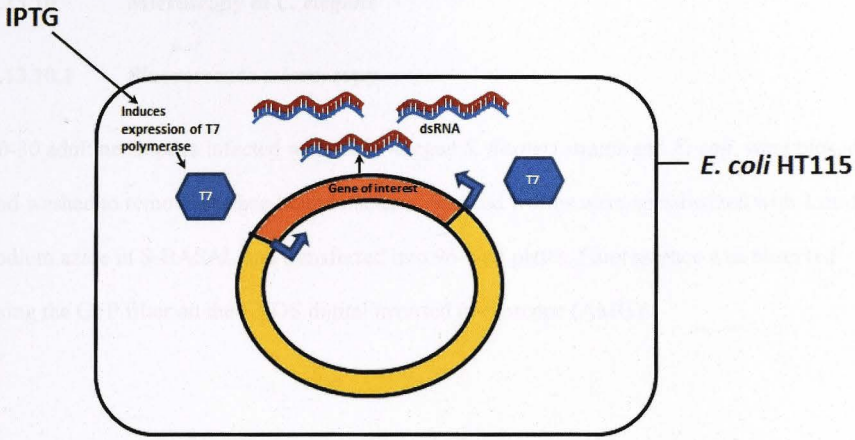

Figure 2.6: Schematic diagram of RNAi in *C. elegans* by the feeding method using pL4440 and *E. coli* HT115(D3). A gene of interest (or fragment of the gene of interest) is cloned into pL4440 between two T7 polymerase promoters in opposite orientations (blue arrows). IPTG induces the expression of T7 polymerase in the *E. coli* cells. T7 polymerase binds to the two T7 promoter regions in pL4440 and drives the expression of the cloned genes to produce dsRNA. *C. elegans* feeding on these *E. coli* strains take up dsRNA into their cells which results in the silencing of target genes.

2.13.10 Microscopy of *C. elegans*

2.13.10.1 Fluorescence microscopy

20-30 adult nematodes infected with GFP^+-tagged *S. flexneri* strains and *E. coli*, were picked and washed to remove surface-bound bacteria. Washed worms were anesthetized with 1 mM sodium azide in S-BASAL and transferred into 96-well plates. Fluorescence was observed using the GFP filter on the EVOS digital inverted microscope (AMG).

2.13.10.2 Electron Microscopy

50-100 adult worms were picked off from virulent and avirulent *S. flexneri* lawns 1 day, 4 days and 6 days post infection. For prolonged infection periods, worms were transferred onto fresh *S. flexneri* lawns each day. Worms were transferred into Beem capsules and washed thrice using S-basal. In order to penetrate the nematodes thick cuticle layer, live worms were fixed, rinsed and stained using the microwave-assisted irradiation protocol developed by Hall *et al.* [308]. A Pelco Biowave oven at the Centre of Advanced Microscopy (CAM, ANU), was used for the microwave assisted fixation of worms. To minimize excessive heating of samples during prolonged irradiation, animals were kept in Beem capsules containing liquid fixatives that were then placed on top of the Pelco Coldspot device inside the over chamber and a temperature probe was used to monitor temperature and the restriction temperature was set to 39 °C. Worms were treated with fixing solution 1 (Appendix A) and irradiated twice (5 min ON and 3 min OFF) followed by a 60 minute incubation at room temperature. Samples were then rinsed thrice in wash solution (Appendix A) each wash step was followed by a cycle of irradiation for 1 minute and incubation at room temperature for 10 minutes. Washed samples were treated with fixing solution 2 (Appendix A) and irradiated twice (5 min ON and

3 min OFF) followed by a 15 minute incubation at room temperature. Samples were rinsed thrice in wash solution as described above and incubated at room temperature for 7 minutes that was followed by three rinse cycles using 0.15 M sodium acetate buffer pH 5.2. Samples were stained using 0.5% uranyl acetate in 0.15 M cacodylate buffer pH 7.2 and two cycles of irradiation (5 min ON and 3 min OFF) followed by incubation at 4 °C overnight. Stained samples were rinsed thrice in 0.15 M sodium acetate buffer pH 5.2 followed by three washes using 0.15 M cacodylate buffer pH 7.2 and incubated at room temperature for 7 minutes. Samples were dehydrated at room temperature using the following dehydration cycles; 50% ethanol for 10 minutes, 70% ethanol for 10 minutes, 80% ethanol for 10 minutes, 90% ethanol for 10 minutes, three treatments with 100% ethanol for 10 minutes each. This was followed by infiltration of the sample at room temperature with the resin LR-White using the following infiltration regime; 2:1 100% ethanol: LR White 2 hours, 1:1 100% ethanol: LR White 2 hours, two treatment with 100% LR White for 2 hours each. LR White was cured at 65 °C under nitrogen gas overnight. Thin sections were obtained using a Power Tome XL ultramicrotome (RMC, Boekeler Instruments, Tucson, AZ at the Albert Einstein College of Medical (AECOM)). Sections were collected on copper slot grids and stained with 2% uranyl acetate in 50% ethanol for 10 minutes and with lead citrate (Reynolds's formulation) for 15 minutes. TEM micrographs were collected on a Phillips CM10 electron microscope at AECOM.

2.14 Statistical analysis

Statistical analysis was carried out in collaboration with Terry Neeman at the Statistical Counselling Unit, ANU. Data analysis was carried out using the PRISM (version 4.02) and GenStat software packages. Statistical difference between strains/groups were determined

using the t-test (when two sets of data were compared) and a One-way analysis of variance (ANOVA) followed by post hoc analysis using Dunnett's, Bonferroni Multiple Comparison and LSD tests (when more than two data sets were analyzed) . Survival curves were compared using the Kaplan-Meier analysis and Logrank tests were used to determine if survival curves were significantly different. When analysing data from un-balanced experiments (where the number of biological repeats varied between strains), linear mixed models were generated using restricted maximum likelihood (REML) to compare all data sets.

Chapter 3

Characterizing the role of L-asparaginase (AnsB) and γ-glutamyltranspeptidase (GGT) in the virulence of *Shigella flexneri*

Chapter 3: Characterizing the role of L-asparaginase (AnsB) and γ-glutamyltranspeptidase (GGT) in the virulence of *Shigella flexneri*

3.1 Introduction

A clear understanding of the bacterial genes expressed at various steps of host-pathogen interactions can facilitate the identification of potential attenuation targets and vaccine candidate antigens. To identify immunogenic proteins expressed during infection, Jennison and colleagues [309] used 2-dimensional gel electrophoresis (2DE) to separate the soluble and membrane-bound protein fractions of a *S. flexneri* serotype 2a strain, 2457T. Separated proteins were probed with sera from shigellosis patients, to identify immunogenic bacterial proteins. Using this approach, they identified two chromosomally encoded, periplasmic enzymes, L-asparaginase (AnsB) and γ-glutamyltranspeptidase (GGT) from the membrane fractions of *S. flexneri*. Interestingly AnsB and GGT have been shown to be antigenic in a number of other bacterial pathogens, including *E. coli, Salmonella* spp., *Campylobacter jejuni* and *Helicobacter pylori* [310-314], but have not been characterized in *S. flexneri,* thus making them potential candidates for vaccine studies.

The *E. coli* AnsB, which shares 99.1% amino acid (aa) identity with *S. flexneri* AnsB, is an enzyme that converts L-asparagine to L-aspartate and ammonia. AnsB has high affinity for L-asparagine. Expression of *ansB* is induced by anaerobiosis and positively regulated by the cyclic AMP receptor protein (CRP) and the *fnr* gene product [315]. The *E. coli* γ-glutamyltranspeptidase (GGT), which shares 99% aa identity with *S. flexneri* GGT, cleaves γ-

glutamyl linkages in compounds such as glutathione and transfers the γ-glutamyl group to other amino acids and peptides [316].

In this study, a reverse genetic approach was used to characterize the role of AnsB and GGT in the virulence of *S. flexneri* serotype 3b. Recombineering, a λ-red-mediated PCR-based approach [317], was used to knockout the *ansB* and *ggt* genes from the wild type serotype 3b strain of *S. flexneri* (SFL1520). SFL1520 was chosen because it was identified as a highly virulent strain, in the murine pulmonary model of shigellosis. The *ansB* and *ggt* genes were successfully disrupted by generating insertional mutations. The effects of each mutation on bacterial physiology and virulence was analyzed using *in vitro* growth studies, cell culture assays and two *in vivo* models of shigellosis, namely the murine pulmonary model and the *C. elegans* infection model, a new potential animal model of shigellosis (discussed in Chapter 5). Both AnsB and GGT were found to promote the adherence of *S. flexneri* to host cells.

To investigate how AnsB and GGT affect bacterial virulence, the proteomes of each mutant strain was compared to that of the wild type *S. flexneri* serotype 3b strain using differential in-gel electrophoresis (DIGE). This approach identified a prominent outer membrane protein, OmpA to be up-regulated in *ansB* mutants. DIGE analysis of the *ggt* mutant identified many differentially expressed proteins which constitute the σ^E regulon, expressed in response to environmental stresses. These findings highlight the importance of AnsB and GGT in the pathogenesis of *S. flexneri*, paving the way to designing new vaccine strategies.

3.2 Results

3.2.1 Insertional inactivation of *ansB* and *ggt* in the wild type *S. flexneri* serotype 3b

ansB and *ggt* knockout templates, carrying the kanamycin resistance gene (kan^R) flanked by 600–1000 bp regions homologous to each target gene were generated in plasmids, pNV1875 and pNV1876 (carrying *ansB* and *ggt* knockout templates, respectively) as described in Section 2.6.1. The *ansB* and *ggt* knockout templates were isolated from pNV1878 and pNV1879, respectively by PCR using the AnsBFP1–AnsBRP6 and GgtFP1–GgtRP6 primer pairs (Table 2.4), respectively.

Insertional inactivation of target genes in potential *ansB* (SFL2283) and *ggt* (SFL2285) mutants was confirmed by colony PCR using a forward primer, which binds to a region upstream of the knockout template and a reverse primer, which binds within each knockout template (Figure 3.1.A and B). The PCR product obtained from SFL2283 (~3.5 kb) using AnsB-KO2 and AnsB-RP6 (Table 2.4) primers was ~1 kb larger than that obtained from the parent strain (~2.5 kb), confirming the insertion of the kanamycin resistance (kan^R) gene into the *ansB* gene (Figure 3.1.A and C). The PCR product obtained from SFL2285 (~3.7 kb) using Ggt–KO2 and Ggt–RP6 primers, is similar in size to the PCR product obtained from the parent strain (~3.7 kb) as expected because the knockout template generated was designed to replace 1 kb of the coding region of *ggt* with the kan^R gene (~1 kb) (Figure 3.1.B and C). Insertional inactivation of the *ansB* and *ggt* genes in SFL2283 and SFL2285, respectively was confirmed by sequencing.

A

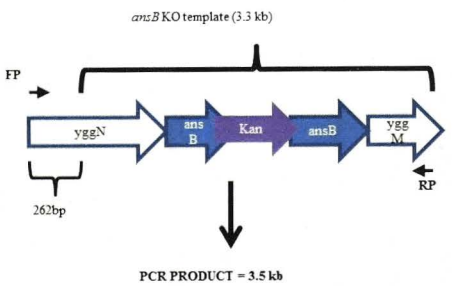
ansB KO template (3.3 kb)
FP
yggN
ans B
Kan
ansB
ygg M
RP
262bp
PCR PRODUCT = 3.5 kb

B

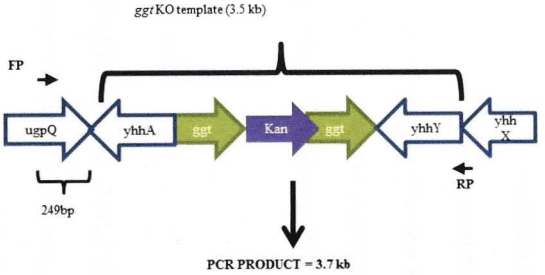
ggt KO template (3.5 kb)
FP
ugpQ
yhhA
ggt
Kan
ggt
yhhY
yhh X
RP
249bp
PCR PRODUCT = 3.7 kb

C

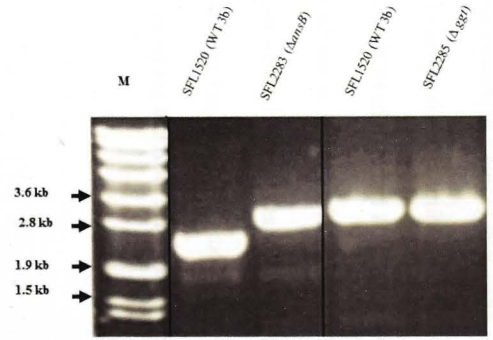
M
SFL1520 (WT 3b)
SFL2283 (ΔansB)
SFL1520 (WT 3b)
SFL2285 (Δggt)
3.6 kb
2.8 kb
1.9 kb
1.5 kb

D

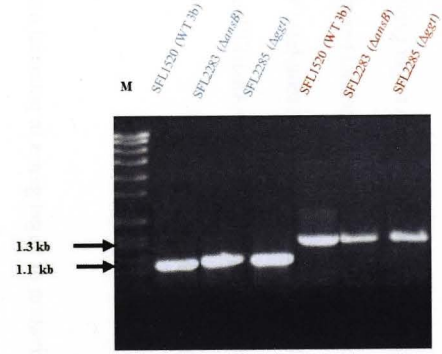
M
SFL1520 (WT 3b)
SFL2283 (ΔansB)
SFL2285 (Δggt)
SFL1520 (WT 3b)
SFL2283 (ΔansB)
SFL2285 (Δggt)
1.3 kb
1.1 kb

Figure 3.1: Confirming the insertional inactivation of the *ansB* and *ggt* genes in an *S. flexneri* serotype 3b (SFL1520). A and B: Schematic representations of the PCR-based screening approach used to confirm the insertional inactivation of *ansB* and *ggt* genes, respectively. All PCR reactions were set up using a forward primer (FP) which binds upstream of the knockout template within the bacterial chromosome and a reverse primer (RP) which binds to the 3` end of the inserted knockout template. **C:** Results of colony PCR-based screening of potential *ansB* (SFL2283) and *ggt* (SFL2285) mutants. **D:** Colony PCR to confirm the presence of the 220 kb virulence plasmid in SFL1520, SFL2283 and SFL2285. M: SPP-1 *EcoRI* marker, relevant marker sizes are indicated. *apy* (in blue) primers amplify the 1.16 kb, *apy* gene from the wild type 3b strain,SFL1520 as well as both mutant strains, SFL2283 and SFL2285. *virG* **(in red)** primers amplify the 1.39 kb *icsA/virG* gene from all strains tested.

Excessive handling and manipulation of *S. flexneri* strains often result in the loss of the virulence plasmid; therefore, the presence of the virulence plasmids in the wild type (SFL1520), *ansB* (SFL2283) and *ggt* (SFL2285) mutant strains was confirmed by PCR using *apyI* and *virG* specific primers before every assay performed in this study. These two genes were chosen as they lie on opposite sides of the 220 kb, virulence plasmid. Results of *apyI* and *virG* PCR reactions confirmed that both mutant strains carry intact virulence plasmids (Figure 3.1.D).

3.2.2 Assessing the expression and secretion of virulence-plasmid encoded Ipa proteins

The *S. flexneri* virulence plasmid-encoded invasion protein antigens (Ipa) are important components of the T3SS needle complex. Virulent strains of *S. flexneri* have well-established mechanisms that regulate the expression and secretion of these Ipa proteins. Western blotting was performed to compare the levels of IpaB and IpaD, two prominent type 3 effector proteins, in the wild type (SFL1520), *ΔansB* (SFL2283) and *Δggt* (SFL2285) strains to determine if the mutant strains efficiently express and secrete virulence-plasmid encoded proteins. Secretory proteins were isolated from SFL1520, SFL2283 and SFL2285 (Section 2.9.1.2) and the levels of IpaB and IpaD in secretory proteins was determined using anti-IpaB and ant-IpaD antibodies, respectively. A *S. flexneri* strain devoid of the virulence plasmid (SFL1223) was used as the negative control. No differences in the expression and secretion of IpaB and IpaD were detected in the *ΔansB* (SFL2283), *Δggt* (SFL2285) and the wild type 3b strain (SFL1520) (Figure 3.2). These results suggest that expression and secretion of key virulence plasmid-encoded proteins remain unaffected by *ansB* and *ggt* mutations

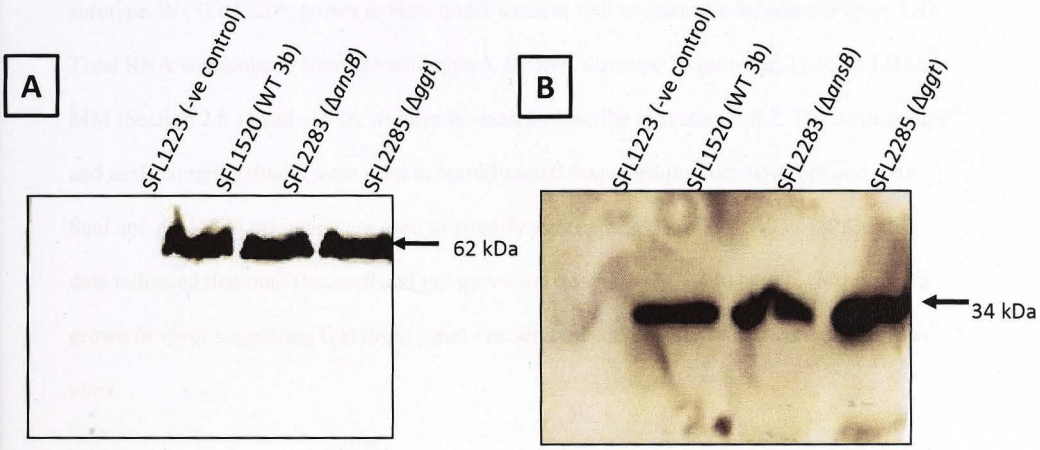

Figure 3.2: Western immunoblots of IpaB and IpaD levels in wild type *S. flexneri* serotype 3b and *ansB* and *ggt* mutant strains. 20 µg of secreted proteins preparations isolated from wild type (SFL1520) and Δ*ansB* (SFL2283) and Δ*ggt* (SFL2285) were separated using SDS-PAGE, following which they were electroblotted onto PVDF membranes and probed with anti-Ipa B (**A**) and anti-IpaD (**B**) primary antibodies. The levels of secreted IpaB (~62 kDa) and IpaD (~34 kDa) produced by all strains was visualized using a chemilumenescence reader. No differences were observed in the secretory levels of the invasion proteins between mutant and wild type strains.

3.2.3 Physiological characterization of *ansB* and *ggt* mutations in *S. flexneri*

3.2.3.1 Confirming the expression of *ansB* and *ggt* in SFL1520 cells grown *in vitro*

Before performing any physiological studies, reverse transcriptase polymerase chain reaction (RT-PCR) was used to confirm the expression of *ansB* and *ggt* in the wild type *S. flexneri* serotype 3b (SFL1520), grown *in vitro* under nutrient rich or starved conditions (Figure 3.3). Total RNA was isolated from the wild type *S. flexneri* serotype 3b grown at 37 °C in LB and MM (Section 2.8.1) and cDNA was synthesized as describe in section 2.8.2. The ansB.compF and ansB.compR primers were used to amplify *ansB* (expected product 1046 bp) and ggt–SacI and ggt–XbaI primers were used to amplify *ggt* (expected product 548 bp). RT-PCR data indicated that both the *ansB* and *ggt* genes were expressed in wild type *S. flexneri* cells grown *in vitro,* suggesting that these genes encode products required for bacterial growth *in vitro*

3.2.3.2 Measuring the effects of *ansB* and *ggt* mutations on cellular asparaginase and glutaminase activities

AnsB is an identified L-asparaginase in *E. coli* that catalyzes the conversion of L-asparagine to L-aspartate with the release of ammonia. Ammonia release assays were performed to determine if this function was conserved in *S. flexneri*. Bacterial cells expressing L-asparaginase, when treated with asparagine, would breakdown asparagine and release ammonia, thus increased ammonia levels correlate with increased breakdown of asparagine. SFL1520, SFL2283 and SFL2285 cells were treated with asparagine and the amount of released ammonia was measured as described in section 2.7.2. Results of ammonia assays show that the wild type *S. flexneri* serotype 3b (SFL1520) and Δ*ggt* (SFL2285) (carrying

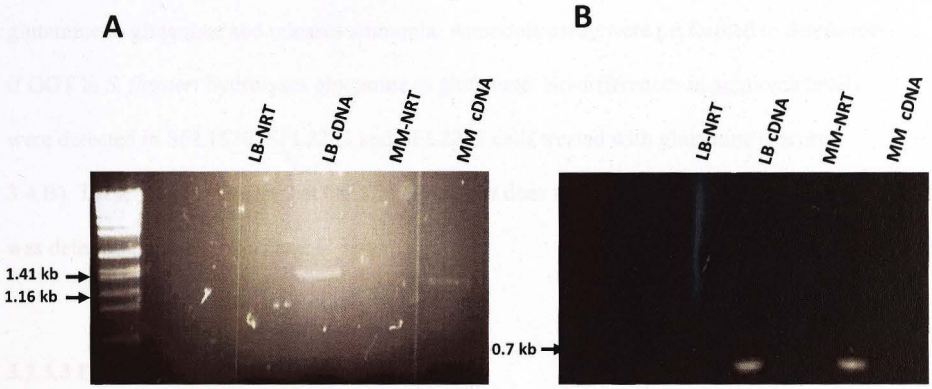

Figure 3.3: Reverse Transcriptase PCR (RT-PCR) to determine if the *ansB* and *ggt* genes are expressed in wild type *S. flexneir* serotype 3b (SFL1520) cells growth *in vitro*. **A:** expression of *ansB* in SFL1520 grown in nutrient rich Luria Bertani (LB) broth and minimal media (MM). **B:** expression of *ggt* in SFL1520 grown in LB broth and MM. Each set of RT-PCR results is accompanied by a no template control (NTC) and a no reverse transcriptase control (NRT) to check for contamination from the PCR reagent and chromosomal DNA, respectively.

intact *ansB*) released significantly more ammonia than the Δ*ansB* strain (SFL2283) (Figure 3.4.A). These results suggest that AnsB in *S. flexneri* functions as an L-asparaginase.

GGT in *H. pylori* and *C. jejuni* has been identified as a glutaminase that breaks down glutamine to glutamate and releases ammonia. Ammonia assay were performed to determine if GGT in *S. flexneri* hydrolyses glutamine to glutamate. No differences in ammonia levels were detected in SFL1520, SFL2283 and SFL2285 cells treated with glutamine (Figure 3.4.B). These results suggest that GGT in *S. flexneri* does not function as a glutaminase as was determined in *H. pylori* and *C. jejuni*.

3.2.3.3 Effects of mutations on bacterial growth

After establishing that both *ansB* and *ggt* genes were expressed in wild type *S. flexneri* cells grown *in vitro,* growth studies were performed in order to determine if the metabolic activities of AnsB and GGT were required for *in vitro* growth of *S. flexneri.* Liquid cultures of SFL1520, SFL2283 and SFL2285 cells were grown at 30 °C or 37 °C and the optical density of cultures was measured at 30 minute intervals. No mutation-related growth defects were detected when strains were grown under nutrient rich (LB media) conditions at both 37 °C and 30 °C (Figure 3.5 A and B). To determine if AnsB and GGT were active under stressed conditions, growth studies were performed under nutrient starved conditions using MM (Figure 3.5 C and D). No significant ($p > 0.05$, ANOVA) growth retardation was observed in Δ*ansB* or Δ*ggt* mutant strains, suggesting that AnsB and GGT are not essential for bacterial growth *in vitro*.

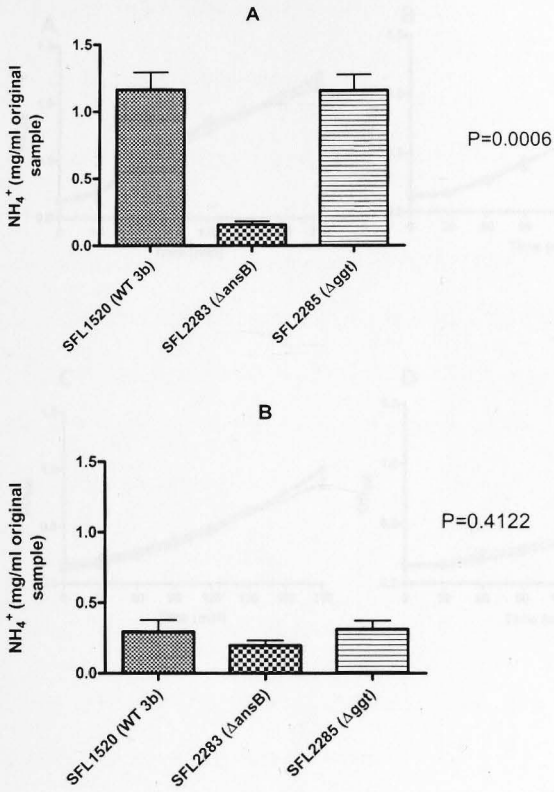

Figure 3.4: Ammonia assays used to determine the asparaginase and glutaminase activities of *ansB* and *ggt* mutants. *S. flexneri* parental strain SFL1520 or isogenic mutant Δ*ansB* (SFL2283) and Δ*ggt* (SFL2285) strains at 3 x 10^8 colony forming units (CFU) per ml, were incubated in phosphate buffered saline (PBS) with 5 mM asparagine **(A)** or glutamine **(B)**. Ammonia production was measured after 60 minutes **(A)** and 180 minutes **(B)** incubation at 37 °C. Hydrolysis of asparagine and glutamine was measured by quantifying ammonia production. Error bars represent the standard error obtained from three independent experimental measurements.

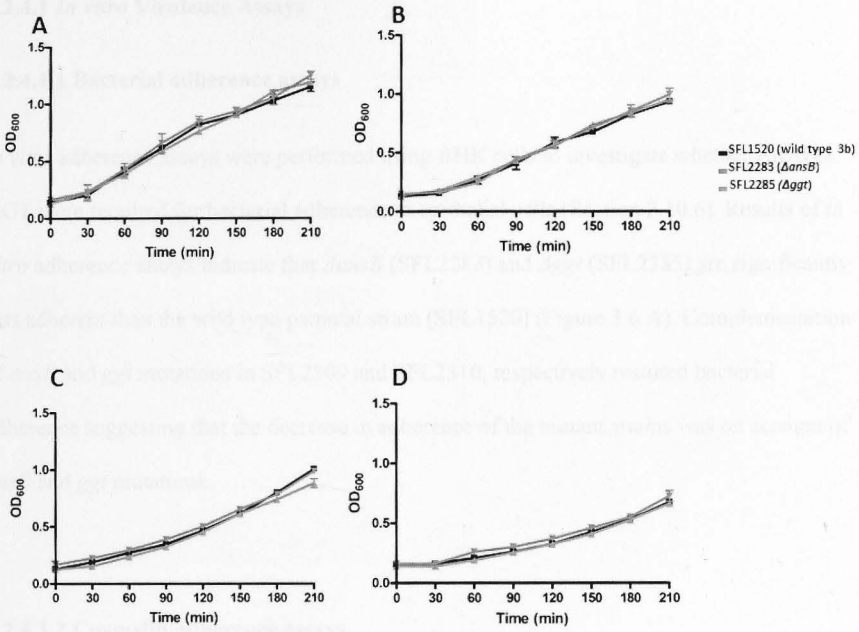

Figure 3.5: Growth studies to assess the effect of *ansB* and *ggt* mutations on bacterial growth. A-D represent growth curves of the wild-type *S. flexneri* serotype 3b strain (SFL1520-black), *ansB* (SFL2283-red) and *ggt* (SFL2285-blue) mutants, plotted as optical density readings at 600 nm (OD_{600}) (y-axis) versus time (x-axis). **A:** Growth in Luria-Bertani (LB) broth at 37 °C, **B:** Growth in minimal media (MM) at 37 °C. **C:** Growth in LB at 30 °C, **D:** Growth in MM at 30 °C. Statistical analysis using the Log Rank test revealed no significant difference in the growth patterns under all four conditions examined $p > 0.05$. Results represent the means of three experimental repeats with standard errors (error bars).

3.2.4 Virulence studies

3.2.4.1 *In vitro* Virulence Assays

3.2.4.1.1 Bacterial adherence assays

in vitro adherence assays were performed using BHK cells to investigate whether AnsB or GGT were required for bacterial adherence to epithelial cells (Section 2.10.6). Results of *in vitro* adherence assays indicate that *ΔansB* (SFL2283) and *Δggt* (SFL2285) are significantly less adherent than the wild type parental strain (SFL1520) (Figure 3.6.A). Complementation of *ansB* and *ggt* mutations in SFL2309 and SFL2310, respectively restored bacterial adherence suggesting that the decrease in adherence of the mutant strains was on account of *ansB* and *ggt* mutations.

3.2.4.1.2 Coverslip adherence assays

In order to visualize the differences in the adherence of the mutant and wild type strains, a coverslip adherence assay was performed (Section 2.10.7). Consistent with bacterial adherence assays, Giemsa staining of infected BHK monolayers showed a decrease in the number of adherent bacteria in monolayers infected with Δ*ansB* (SFL2283) and Δ*ggt* (SFL2285) strains (Figure 3.6.C and D) compared with wild type *S. flexneri* serotype 3b (SFL1520) (Figure 3.6.B) and complemented strains SFL2309 and SFL2310 (Figure 3.6.E and F). The number of adherent bacteria per BHK cell was determined in three independent blind experiments to validate the microscopic findings. Δ*ansB* (SFL2283) and Δ*ggt* (SFL2285) cells show a significant drop in the number of adherent bacterial cells when compared with SFL1520, SFL2309 and SFL2310 (Figure 3.6.G). Results of *in vitro*

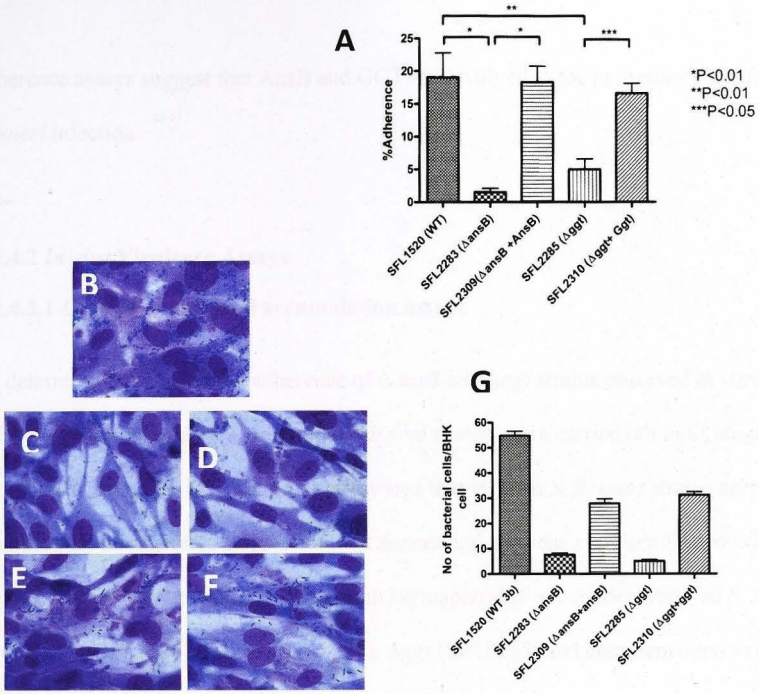

Figure 3.6*:* Results of *in vitro* adherence assays for wild type *S. flexneri* serotype 3b strain (SFL1520), Δ*ansB* (SFL2283), Δ*ggt* (SFL2285), SFL2309 (SFL2283 + a plasmid copy of *ansB*) or SFL2310 (SFL2285 + a plasmid copy of *ggt*). A: Bacterial adherence to baby hamster kidney cells plotted as percentage adherence, a ratio of the number of adherent and intracellular bacteria to the total number of bacterial cells in the infecting inoculum (y-axis). Results represent the means of three independent blind repeats with standard errors. **B-F:** Results of coverslip adherence assay performed to compare the adherence properties of SFL1520 (**B**), SFL2283 (**C**), SFL2285 (**D**), SFL2309 (**E**) and SFL2310 (**F**). Coverslips containing each bacterial strain were stained with Giemsa stain and examined using an oil immersion lense. **G:** A graph depicting the number of adherent bacteria counted per BHK cell under 1000 X magnification (y-axis). Results are the mean of 10 cells across 10 fields with standard errors, counted at random in a blind experiment.

adherence assays suggest that AnsB and GGT are involved in the preliminary stages of *S. flexneri* infection.

3.2.4.2 *In vivo* Virulence Assays

3.2.4.2.1 *C. elegans* bacterial accumulation assays

To determine if the defective adherence of Δ*ansB* and Δ*ggt* strains observed *in vitro* had an effect on bacterial virulence, preliminary *in vivo* studies were carried out in *C. elegans*. Burton and colleagues [283] have demonstrated that virulent *S. flexneri* strains accumulate in the intestinal lumina of *C. elegans* and kill nematodes, whereas avirulent *S. flexneri* strains are digested by the nematodes. Young adult hermaphrodite nematodes were fed *S. flexneri* serotype 3b (SFL1520), Δ*ansB* (SFL2283), Δ*ggt* (SFL2285) and complemented strains SFL2309 (SFL2283 + *ansB*) and SFL2310 (SFL2285 + *ggt*) for 24 hours and bacterial accumulation assays were carried out as described in section 2.13.5. *C. elegans* fed SFL1520 show accumulation of the virulent, wild type parental strain (SFL1520) in their intestinal lumina, whereas worms fed both Δ*ansB* (SFL2283) and Δ*ggt* strains (SFL2285) had significantly decreased intraluminal bacterial counts (Figure 3.7.A). Complementation of *ansB* and *ggt* mutations in SFL2309 and SFL2310, respectively, increased bacterial accumulation, suggesting that AnsB and GGT are required for *S. flexneri* virulence in *C. elegans*.

To confirm bacterial accumulation in the nematode intestinal lumina, nematodes were fed GFP^+ tagged *S. flexneri* strains and visualized by fluorescence microscopy (Section 2.13.10.1). Wild type *S. flexneri* accumulated in the nematode intestinal lumen (Figure 3.7.B). No fluorescence was detected in worms fed the Δ*ansB* and Δ*ggt* strains (Figure 3.7.C and D, respectively).

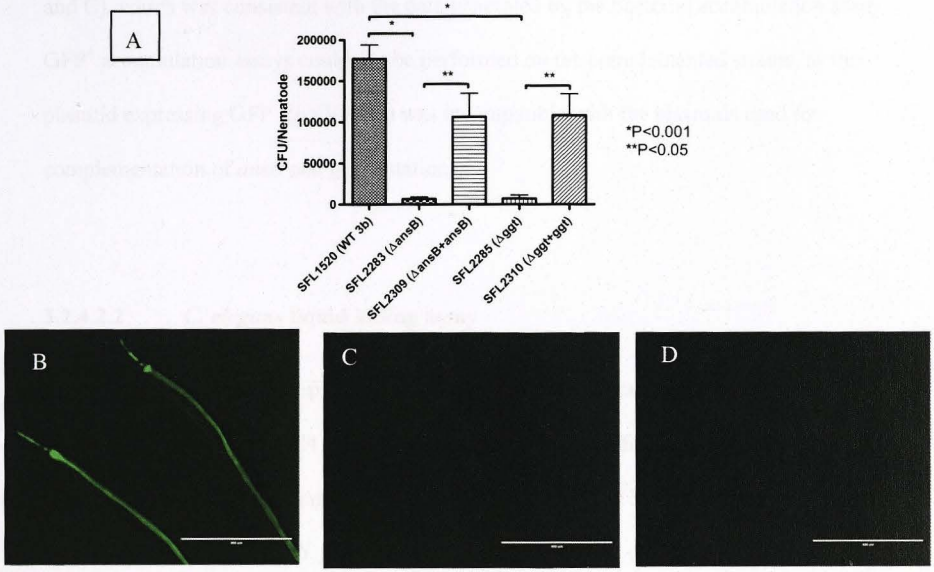

Figure 3.7: *in vivo* characterization of *ansB* and *ggt* mutations using *C. elegans* bacterial accumulation assays. A: Young adult hermaphrodite nematodes were fed *S. flexneri* 3b (SFL1520), Δ*ansB* (SFL2283), Δ*ggt* (SFL2285), SFL2309 (SFL2283 + plasmid copy of *ansB*) or SFL2310 (SFL2285 + plasmid copy of *ggt*) for 24 hours. 20 nematodes were picked and mechanically disrupted to release internalized bacteria. Diluted lysates were plated on LB agar plates carrying appropriate antibiotics, and colonies were scored in order to quantify *S. flexneri* cells associated with each nematode. Statistical analysis performed using One-way ANOVA show increased accumulation of SFL1520, SFL2309 and SFL2310 and digestion of SFL2283 and SFL2285 in the nematode gut. Results represent the means of three experimental repeats with standard error (error bars) **B:** Young adult hermaphrodite nematodes infected as above with GFP^+- tagged SFL1520 (**B**), SFL2283 (**C**) and SFL2285 (**D**). Wild type *S. flexneri* 3b accumulates in the nematode intestinal lumen while Δ*ansB* (SFL2283) and Δ*ggt* (SFL2285) strains fail to accumulate in the worm gut lumen. Scale bar = 400 μm.

and C), which was consistent with the data generated by the bacterial accumulation assay. GFP^+ accumulation assays could not be performed on the complemented strains, as the plasmid expressing GFP^+ (pNV1908) was incompatible with the plasmids used for complementation of *ansB* and *ggt* mutations.

3.2.4.2.2 *C. elegans* liquid killing assay

Kesika and colleagues have previously shown that virulent strains of *S. flexneri* kill *C. elegans* in liquid culture [284]. Liquid killing assays were performed to compare the killing rates of Δ*ansB* (SFL2283), Δ*ggt* (SFL2285) and the wild type 3b strain (Section 2.13.4). *C. elegans* fed with wild type *S. flexneri* serotype 3b (SFL1520), died much faster (TD_{50}= 42 h) than worms fed with Δ*ansB* (SFL2283) and Δ*ggt* (SFL2285) (less than 50% killing in 48 Hours; Figure 3.8). These findings along with the bacterial accumulation data, suggest that AnsB and GGT are required for the virulence of *S. flexneri* in *C. elegans.*

3.2.4.2.3 Murine pulmonary model of shigellosis

As preliminary *in vivo* studies in *C. elegans* indicated that the Δ*ansB* and Δ*ggt* strains showed reduced virulence, these strains were also tested using the well-established murine pulmonary model of shigellosis [83, 225, 318]. Six to eight week old female Balb/c mice (Animal Resource Centre,WA) were inoculated intranasally with a sub-lethal dose (2×10^7 CFU/ 10 µL) of the wild type pathogenic strain (SFL1520), Δ*ansB* (SFL2283) and Δ*ggt* (SFL2285). When inoculated intranasally, virulent strains of *S. flexneri* colonize the lungs of infected mice and cause pneumonia. The lung counts obtained from mice inoculated with the Δ*ansB* and Δ*ggt* strains 24 hours post infection were significantly lower than mice infected with the wild type strain (Figure 3.9.A).

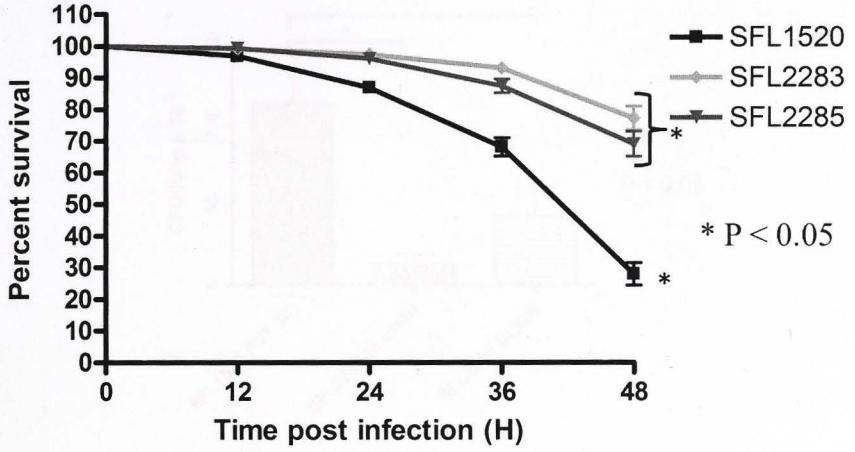

Figure 3.8: Results of *S. flexneri*-mediated killing assays in *C. elegans*. The above graph represents the results of *C. elegans* liquid killing assays. 20 synchronized adult nematodes were treated with log phase cultures of *S. flexneri* 3b (SFL1520), Δ*ansB* (SFL2283), or Δ*ggt* (SFL2285) strains grown at 37 °C to express virulence factors. Infected nematodes were monitored for 48 hours and survival was scored every 12 hours. Results represent the mean of three independent blind experimental repeats with standard errors (error bars). Worms treated with *ansB* and *ggt* mutant strains show a significant increase in the survival rates compared to nematodes infected with wild type *S. flexneri* 3b ($p < 0.05$, Log Rank test).

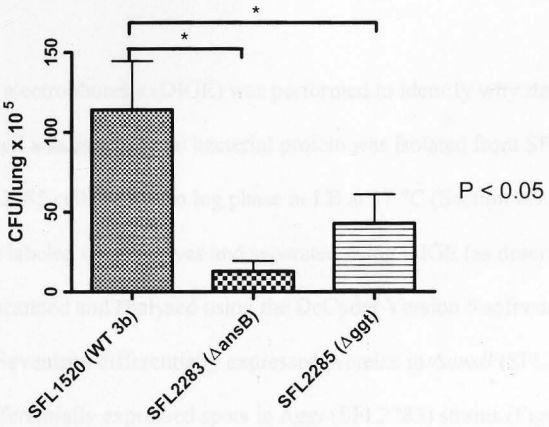

Figure 3.9: Lung counts of mice inoculated intranasally with a sub-lethal dose (2 x10^7 CFU) of *S. flexneri* 3b (SFL1520), Δ*ansB* (SFL2283) or Δ*ggt* (SFL2285). 20 mice per strain were euthanized 24 hours post-inoculation, and their lungs were isolated and homogenized. Dilutions of the homogenates were plated to determine the number of bacterial cells. Results represent the mean values of lung counts obtained from 20 mice infected with each strain in a blind experiment with standard errors (error bars). Statistical analysis performed using One way ANOVA, shows a significant decrease in the lung counts of mice infected with both the *ansB* and *ggt* mutant strains, 24 hours post infection.

The results of mouse studies further demonstrate that AnsB and GGT are required for the initial stages of infection.

3.2.5 Identification of changes in the *S. flexneri* proteome caused by *ansB* and *ggt* mutations

Differential in-gel electrophoresis (DIGE) was performed to identify why *ΔansB* and *Δggt* strains show reduced adherence. Total bacterial protein was isolated from SFL1520, SFL2283 and SFL2285 cells grown to log phase in LB at 37 °C (Section 2.9.2.1). Proteins were differentially labeled with Cy dyes and separated using DIGE (as described in Section 2.9.2). Gels were scanned and analysed using the DeCyder Version 5 software package (Section 2.9.2.3). Seventeen differentially expressed proteins in Δ*ansB* (SFL2283) (Figure 3.10.A) and 31 differentially expressed spots in Δ*ggt* (SFL2283) strains (Figure 3.11.A) were recognized and excised from the gels for identification by peptide sequencing as described in section 2.9.2.4 and submitted to the Mass Spectrometry Facility, ANU for LC-MS analysis. Proteins were identified using MASCOT (Matrix Science) database searches, as described in section 2.9.2.4. Six out of seventeen recognized *ansB* proteins, were identified (Figure 3.11.1-6 and Table 3.1) and seven out of thirty-one *ggt* proteins were identified (Figure 3.12.1-6 and Table 3.2).

The chaperone protein DnaK, was found to be up-regulated in both Δ*ansB* (SFL2283) and Δ*ggt* (SFL2283). In SFL2283, expression of all six identified proteins (RplL, Udp, Mdh, OmpA, GroEL and DnaK) was up-regulated. In SFL2285, expression of three (out of seven)

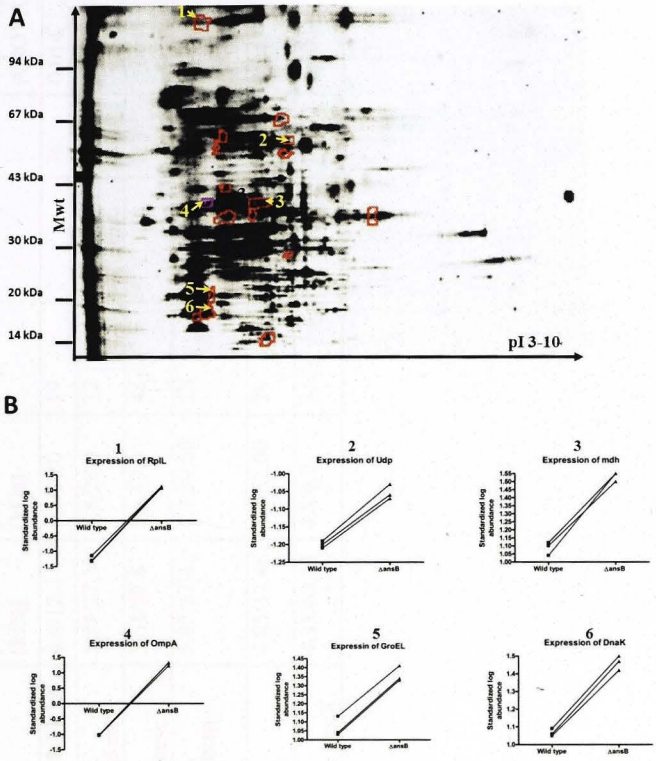

Figure 3.10: A: Differential in-gel electrophoresis analysis of the Δ*ansB* proteome. The above gel represents total proteins of wild type *S. flexneri* serotype 3b and Δ*ansB*, differentially labeled with Cy3 and Cy5. Highlighted regions represent differentially expressed proteins in the Δ*ansB* identified using the DeCyder version 5 software package. Arrows indicate proteins identified by peptide mass fingerprinting. **B:** Graphs 1-6 represent the differential expression of spots identified by peptide mass fingerprinting. All six proteins identified to be differentially expressed in the Δ*ansB* are up-regulated in the mutant strain.

Table 3.1: Differentially expressed spots in the *ansB* mutant

Sopt No.	Gene name	Differential expression in mutant	Accession number (UniProt)	Description	Predicted pI/Mwt (kDa)	Observed pI/Mwt (kDa)	Coverage (%)	n (peptides matched)	Score	*P* value One Way ANOVA
1	rplL	Up-regulated	Q0SY14	ribosomal protein L7/L12	4.6/12.3	4.7/10.0	19	2	36	0.014
2	udp	Up-regulated	F5MTS6	Uridine phosphorylase	5.81/27.3	5.8/28.0	32	4	41	2.7e-005
3	mdh	Up-regulated	F5NLQ6	Malate dehydrogenase	5.61/32.5	5.5/39.0	44	5	123	0.0041
4	ompA	Up-regulated	Q0T678	ompA Outer membrane protein 3a	5.87/37.4	4.7/39.00	23	7	43	0.02
5	groEL	Up-regulated	Q0SXD6	60 kDa chaperonin	4.85/47.46	4.8/67.00	29	11	130	0.047
6	dnaK	Up-regulated	I6CN04	Chaperone protein DnaK	4.83/69.13	4.8/6.9	31	13	175	0.00046

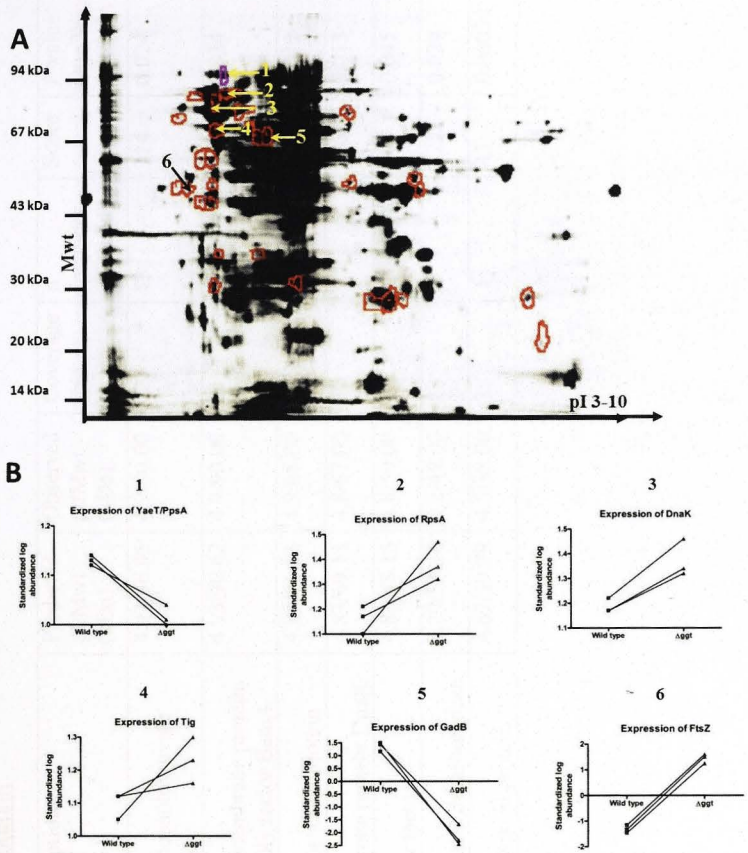

Figure 3.11: A: Differential in-gel electrophoresis analysis of the Δ*ggt* proteome. The above gel represents total proteins of wild type *S. flexneri* serotype 3b and Δ*ggt* differentially labeled with Cy3 and Cy5. Highlighted regions represent spots that are differentially expressed in the Δ*ggt* identified using the DeCyder version 5 software package. Arrows indicate spots identified by peptide mass fingerprinting. **B:** Graphs 1-6 represent the differential expression of spots identified by peptide mass fingerprinting in wild type and *ggt* mutant strains. **1:** YaeT and PpsA were identified from the same spot as these two proteins have very similar molecular weights and pI values. The expression of RpsA, DnaK, Tig and FtsZ is up-regulated in Δ*ggt,* while the YaeT, PpsA and GadB are down-regulated in Δ*ggt.*

Table 3.2: Differentially expressed spots in the *ggt* mutant

Sopt No.	Gene name	Differential expression in mutant	Accession number (UniProt	Description	Predicted pI/Mwt (kDa)	Observed pI/Mwt (kDa)	Coverage (%)	n (peptides matched)	Score	*P* value One Way ANOVA
1	ppsA	Down-regulated	F5MM47	Phosphoenolpyruvate synthase	4.93/86.95	4.9/90.00	22	13	114	0.024
2	yaeT	Down-regulated	I0V9F3	Outer membrane protein assembly factor BamA	4.93/90.62	4.9/90.00	11	8	43	0.024
3	rpsA	Up-regulated	P0AG70	30S ribosomal protein	4.89/61.23	4.9/68.00	36	14	208	0.012
4	dnaK	Up-regulated	I6CN04	Chaperone protein DnaK	4.83/69.13	4.8/67.00	57	9	1535	0.013
5	tig	Up-regulated	P0A852	Trigger factor	4.83/48.16	4.8/50.00	60	13	267	0.045
6	gadB	Down-regulated	P69912	Glutamate decarboxylase	5.29/53.16	5.2/49.00	28	7	125	0.029
7	ftsZ	Up-regulated	F5QTJ4	Cell division protein	4.67/39.79	4.3/38.00	7	1	43	0.00034

spots were down-regulated (PpsA, YaeT, and GadB) and four proteins (RspA, DnaK, FtsZ and Tig) were up-regulated. YaeT and PpsA were identified from the same spot, both these proteins have very similar molecular weights and pI values, hence it is not unusual that they appear in the same region on the gel and it is likely that, the excised spot contained peptides from both proteins. The DeCyder software package identifies differentially expressed spots, by comparing the fluorescence produced by differentially labeled, wild type and mutant proteins in a selected region. If several proteins are present in the region of interest, the software fails to identify individual proteins. Therefore the overall difference in fluorescence produced by the wild type and mutant proteins, in such regions is taken into account to determine if the spot is up-regulated or down-regulated. Because YaeT and PpsA were identified from the same region on the gel, we cannot conclude whether both proteins are down-regulated or if one protein is up-regulated while the other is down-regulated.

3.2.5.1 qRT-PCR to confirm DIGE analysis

Quantitative real-time reverse transcription polymerase chain reaction (qRT-PCR) was performed to confirm DIGE results (Figure 3.12). The transcript levels of identified proteins were analysed using qRT-PCR, in three independent biological replicates, using the bacterial *hisG* gene as a control gene to normalize the expression of all tested genes. Consistent with the DIGE analysis, the expression of *rplL, udp, ompA, groEL* and *dnaK* was up-regulated in Δ*ansB* (SFL2283), no significant differences were observed in the expression of *mdh* (Figure 3.12.A). qRT-PCR also confirmed that the expression of r*spA, dnaK, ftsZ* and *tig* (Figure 3.12.B) were up-regulated and *gadB* (Figure 3.12.C) was down-regulated in Δ*ggt* (SFL2285). Contrary to the DIGE analysis, the expression of *yaeT* and *ppsA* was found to be up-regulated at the transcript level in Δ*ggt* (SFL2285) (Figure 3.12. B). This result, coupled with the fact

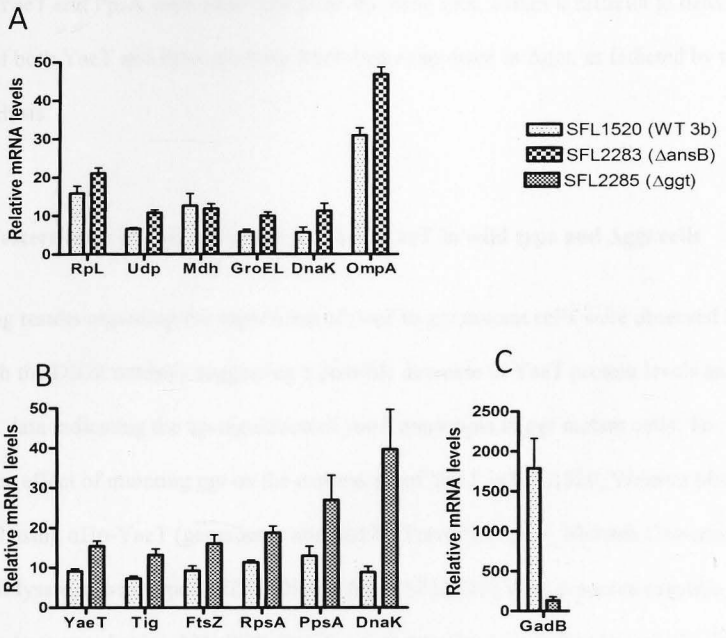

Figure 3.12: Reverse transcription quantitative PCR (qRT-PCR) to verify differential in-gel electrophoresis (DIGE) analysis. A: qRT-PCR analysis of differentially expressed spots identified in the Δ*ansB* (SFL2283). The levels of mRNA transcripts of *rplL, udp, groEL, dnaK* and *ompA,* in SFL2283 are significantly higher than SFL1520 ($p < 0.005$, unpaired, t-test), verifying the DIGE analysis. **B:** qRT-PCR analysis of differentially expressed spots in the Δ*ggt* (SFL2285). mRNA levels of *tig, ftsZ, rpsA,* and *dnaK* in SFL2285 are significantly higher that SFL1520 ($p < 0.005$, unpaired, t-test), verifying DIGE analysis. mRNA levels of *yaeT,* and *ppsA* contradict the DIGE analysis. **C:** qRT-PCR analysis of the expression levels of *gadB* in *S. flexneri* 3b (SFL1520) and the *ggt* mutant. A significant decrease in the mRNA levels of *gadB* in SFL2285 is consistent with the DIGE analysis. The expression of all genes was normalized to the housekeeping gene, *hisG.* The data presented are the means of three biological repeats, and error bars indicate the standard errors of the means.

that both YaeT and PpsA were identified from the same spot, makes it difficult to determine if levels of both YaeT and PpsA proteins were down-regulated in Δ*ggt*, as indicted by the DIGE analysis.

3.2.5.2 Western blots to determine the levels of YaeT in wild type and Δ*ggt* cells

Conflicting results regarding the expression of *yaeT* in *ggt* mutant cells were observed in this study, with the DIGE analysis suggesting a possible decrease in YaeT protein levels and qRT-PCR data indicating the up-regulation of *yaeT* transcripts in *ggt* mutant cells. To confirm the effect of mutating *ggt* on the expression of YaeT in SFL1520, Western blots were performed using αHp-YaeT (generously donated by Trevor Lithgow, Monash University). Whole cell lysate of wild type (SFL1520) and Δ*ggt* (SFL2285) were prepared (Section 2.9.1.1) and separated using 12% SDS-PAGE gel electrophoresis. Following which, the proteomes of SFL1520 and SFL2285 were probed with αHp-YaeT to compare the levels of YaeT in each of these strains. Results of western blots indicate that the expression of YeaT is down-regulated in Δ*ggt*, which is consistent with the DIGE analysis (Figure 3.13). These results along with the results of qRT-PCR data, suggest that two conflicting mechanisms potentially regulate the expression of YaeT in SFL2285 cells.

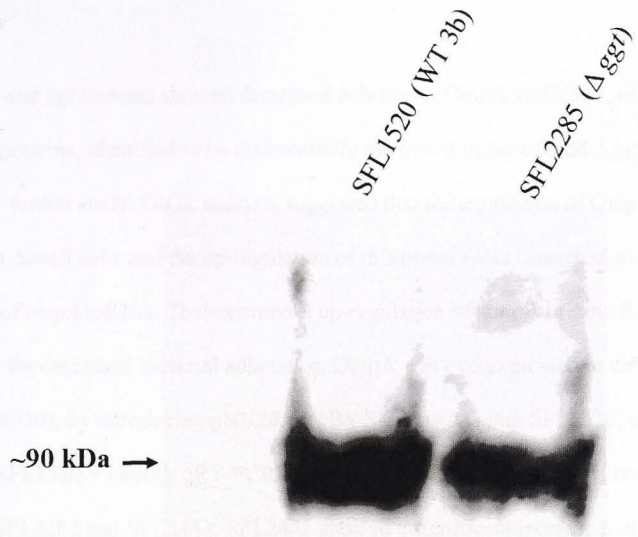

Figure 3.13: Western immunoblots of YaeT in wild type *S. flexneri* serotype 3b (SFL1520) and the *ggt* mutant strain (SFL2285). Total bacterial protein was isolated from cultures corresponding to 1 x 10^9 CFU from both SFL1520 and SFL2285. Proteins were separated using SDS-PAGE, following which they were electroblotted onto PVDF membranes and probed with anti-HpYaeT. Anti-Rabbit IgG (Sigma) was used as the secondary antibody and the levels of YaeT (~90 kDa) in each strain was visualized using a chemiluminescence reader. The expression of YaeT in SFL2285 is down-regulated when compared with SFL1520.

3.2.5.3 Overexpression of OmpA in SFL1520 and increased expression of YaeT in the *Δggt* strain

Since *ansB* and *ggt* mutants showed decreased adherence, OmpA and YaeT, two outer membrane proteins, identified to be differentially expressed in Δ*ansB* and Δ*ggt* strains were selected for further study. DIGE analysis suggested that the expression of OmpA was up-regulated in Δ*ansB* cells and the up-regulation of this protein was consistent with increased expression of *ompA* mRNA. To determine if up-regulation of OmpA in Δ*ansB* cells was responsible for decreased bacterial adherence, OmpA was overexpressed in the wild type strain (SFL1520), by introducing pNV2052 (pBS SK + *ompA*) into SFL1520, to generate SFL2443 (SFL1520 + *ompA*). qRT-PCR was performed to compare the levels of *ompA* in SFL1520, SFL2283 and SFL2443. SFL2443 showed a significant increase in the expression of *ompA* compared to the wild type strain. No significant differences were observed *ompA* transcripts in SFL2443 and SFL2283 (Figure 3.14.A).

To determine if the down-regulation of YaeT in SFL2285 (Δ*ggt*), was responsible for the decreased adherence of this strain, SFL2285 was transformed with pNV2053 (pBS SK + a plasmid copy of *yeaT*) to create SFL2444 (*Δggt* + *yaeT*). qRT-PCR was performed to compare the levels of *yaeT* in SFL1520, SFL2285, SFL2444 (Figure 3.14.B). The expression of *yaeT* transcripts in SFL2444 was significantly higher than wild type and Δ*ggt* mutant cells (Figure 3.14.B). Western blots using αHp-YaeT were also performed to compare the levels of YaeT in SFL1520, SFL2285 and SFL2444 (Figure 3.14.C). Western blots failed to show a significant increase in YaeT levels in SFL2444 when compared with SFL2285.

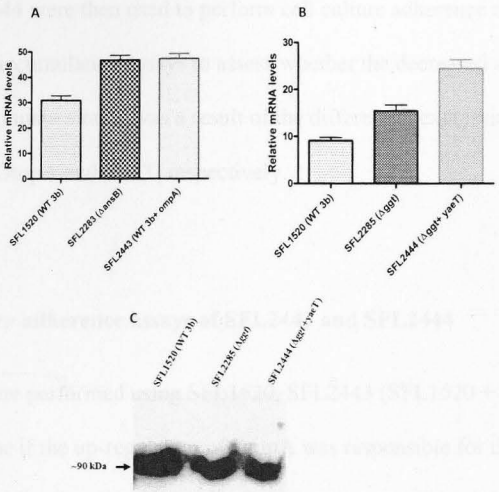

Figure 3.14: Comparing OmpA and YaeT levels in wild type *S. flexneri* and AnsB and Ggt mutant strains. A: Reverse transcription quantitative PCR (qRT-PCR) analysis to determine the transcript levels of *ompA* in SFL1520 (wild type *S. flexneri* serotype 3b), SFL2283 (Δ*ansB*) and SFL2443 (SFL1520 + pNV2053 carrying *ompA*). *ompA* levels in SFL2443 are significantly higher than SFL1520 ($p < 0.005$, unpaired, t-test) . **B:** qRT- PCR analysis to compare the transcript levels of *yaeT* in SFL1520, SFL2285 (Δ*ggt*) and SFL2444 (SFL2285 + pNV2054 carrying *yaeT*). *yaeT* expression in both SFL2285 and SFL2444 are higher than SFL1520 ($p < 0.005$, unpaired, t-test). Expression of all genes was normalized to the housekeeping gene *hisG.* The data presented are the means of three biological repeats, and error bars indicate the standard errors of the means. **C:** Western immunoblots using anti-HpYaet, to compare the levels of YaeT protein in SFL1520, SFL2285 and SFL2444. No observable differenced in the levels of YaeT in SFL2285 and 2444.

SFL2443 and SFL2444 were then used to perform cell culture adherence assays and *in vivo C. elegans* bacterial accumulation assays to assess whether the decreased adherence shown by the *ansB* and *ggt* mutant strains was a result of the differential expression of outer membrane proteins, OmpA and YaeT, respectively.

3.2.5.3.1 *In vitro* adherence assays of SFL2443 and SFL2444

Adherence assays were performed using SFL1520, SFL2443 (SFL1520 + pNV2052), SFL2283 to determine if the up-regulation of OmpA was responsible for the decreased adherence of Δ*ansB* cells. Results of *in vitro* adherence assays indicated that the overexpression of OmpA in the wild type strain significantly decreased bacterial adherence, as SFL2443 cells were less adherent than SFL1520 (Figure 3.15). *in vitro* adherence assays were also performed using SFL1520, SFL2285 and SFL2444 (SFL2285 + pNV2054) to determine if the down-regulation of YaeT was responsible for the decreased adherence of Δ*ggt* cells. SFL2444 was significantly more adherent than SFL2285 but less adherent than SFL1520, suggesting that the increased expression of YaeT in the *ggt* mutant strain increases the adherence of this mutant strain but fails to restore bacterial adherence to wild type levels (Figure 3.15).

3.2.5.3.2 *In vivo C. elegans* bacterial accumulation assays of SFL2443 and SFL2444

In vivo bacterial accumulation assays in *C. elegans* were performed to determine if the overexpression of *ompA* in wild type *S. flexneri* decreased bacterial virulence *in vivo*. Results of *in vivo C. elegans* bacterial accumulation assays using SFL1520, SFL2283 and SFL2443 were consistent with *in vitro* adherence assays and suggest that the overexpression of OmpA

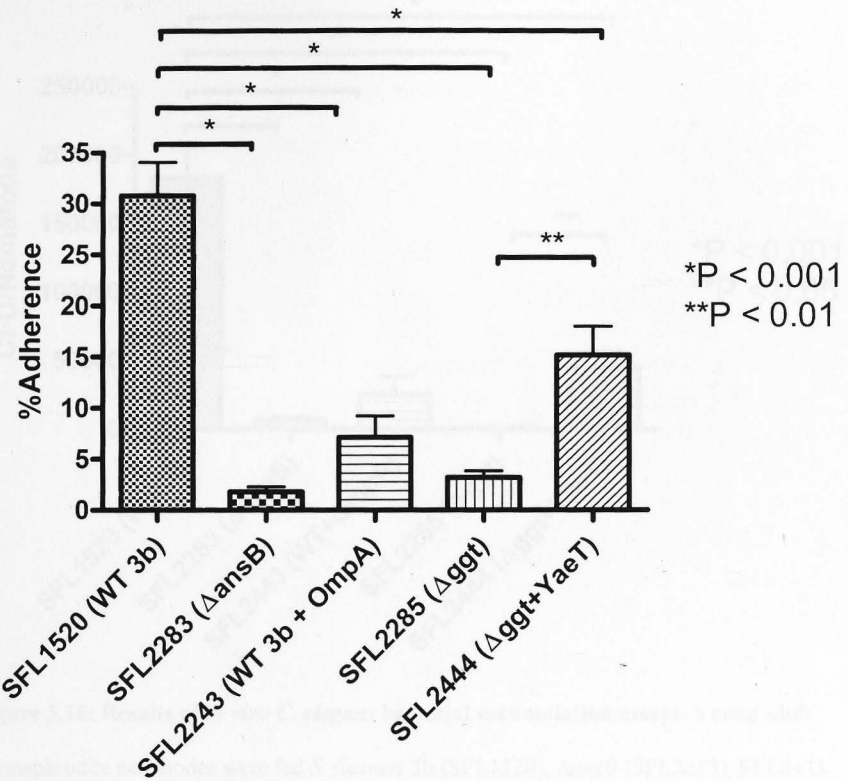

Figure 3.15: Results of *in vitro* adherence assays for SFL2443 (SFL1520 overexpressing *ompA*) and SFL2444 (SFL2285 + *yaeT*), wild type *S. flexneri* 3b (SFL1520), Δ*ansB* (SFL2283), *Δggt* (SFL2285) strains plotted as percentage adherence, a ratio of the number of adherent and intracellular bacteria to the total number of bacterial cells in the infecting inoculum (y-axis). There is a significant decrease in the adherence of SFL2443 (SFL1520 overexpressing *ompA*) compared to SFL1520. SFL2444 (SFL2285 with increased expression of *yaeT*) is significantly more adherent than SFL2285. Results are the means of three independent blind repeats with standard errors (error bars). Statistical significance was determined using one way ANOVA with post hoc Bonferroni's Multiple Comparison Test.

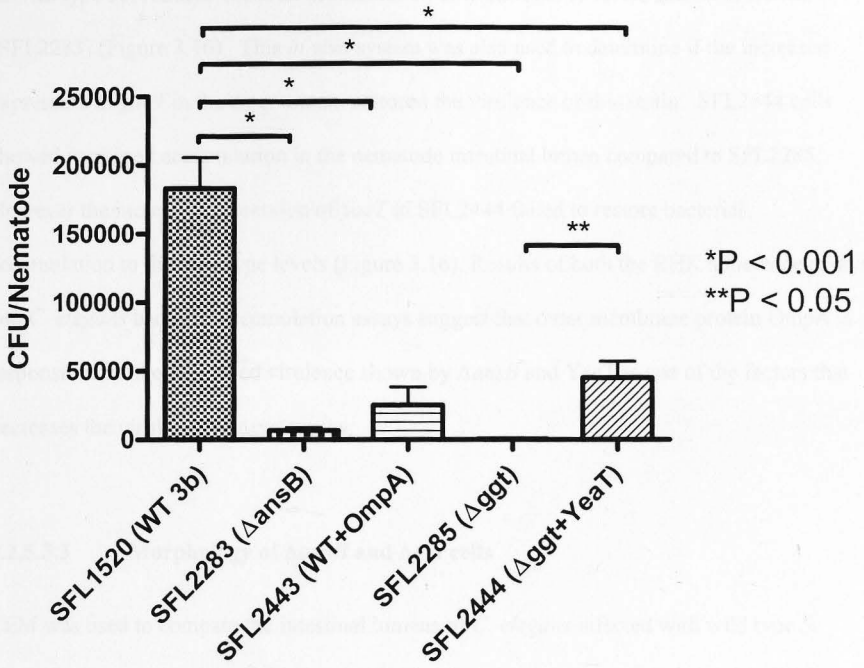

Figure 3.16: Results of *in vivo C. elegans* bacterial accumulation assays. Young adult hermaphrodite nematodes were fed *S. flexneri* 3b (SFL1520), Δ*ansB* (SFL2283), SFL2443 (SFL1520 overexpressing *ompA*), Δ*ggt* (SFL2285) or SFL2444 (SFL2285 + *yaeT*) for 24 hours. 20 nematodes were picked and mechanically disrupted to release internalized bacteria. Diluted lysates were plated on LB agar plates carrying appropriate antibiotics, and colonies were scored in order to quantify *S. flexneri* cells associated with each nematode. There is a significant decrease in the accumulation of SFL2443 (SFL1520 overexpressing *ompA*) compared to SFL1520. The accumulation of SFL2444 (SFL2285 with increased expression of *yaeT*) in the nematode intestinal lumen is significantly higher than SFL2285. Results are the means of three independent blind repeats with standard errors (error bars). Statistical significance was determined using one way ANOVA with post hoc Bonferroni's Multiple Comparison Test.

in wild type 3b, reduces bacterial accumulation in nematodes to levels similar to *ΔansB* (SFL2283) (Figure 3.16). This *in vivo* system was also used to determine if the increased expression of *yaeT* in the Δ*ggt* mutant restored the virulence of this strain. SFL2444 cells showed increased accumulation in the nematode intestinal lumen compared to SFL2285. However the increased expression of *yaeT* in SFL2444 failed to restore bacterial accumulation to the wild type levels (Figure 3.16). Results of both the BHK adherence assays and *C. elegans* bacterial accumulation assays suggest that outer membrane protein OmpA is responsible for the decreased virulence shown by Δ*ansB* and YaeT is one of the factors that decreases the virulence of Δ*ggt* strains.

3.2.5.3.3 Morphology of Δ*ansB* and Δ*ggt* cells

TEM was used to compare the intestinal lumens of *C. elegans* infected with wild type *S. flexneri* serotype 3b (SFL1520), Δ*ansB* (SFL2283) and Δ*ggt* (SFL2285) cells. Ultrathin sections of animals infected with each strain for 24 and 96 hours were examined. 24 hours post infection, worms infected with SFL1520 had intact bacterial cells within their intestinal lumens and consistent with bacterial accumulation and GFP^+ fluorescence assays, no intralumenal bacterial cells were observed in worms infected with SFL2283 and SFL2285. Ninety six hours post infection, intraluminal bacteria were observed in worms infected with SFL1520, SFL2283 and SFL2285 (Figure 3.17). Interestingly, intraluminal Δ*ansB* cells had irregular cell envelopes (Figure 3.17.B and E) while wild type *S. flexneri* cells had well defined cell boundaries (Figure 3.17.A and D). These findings indicate that the up-regulation of OmpA may disrupt the integrity of the bacterial cell envelope which would have a direct effect on bacterial adherence. Very few intraluminal Δ*ggt* cells were observed 96 hours post infection and no differences were observed in the cellular morphologies of wild type and Δ*ggt* cells.

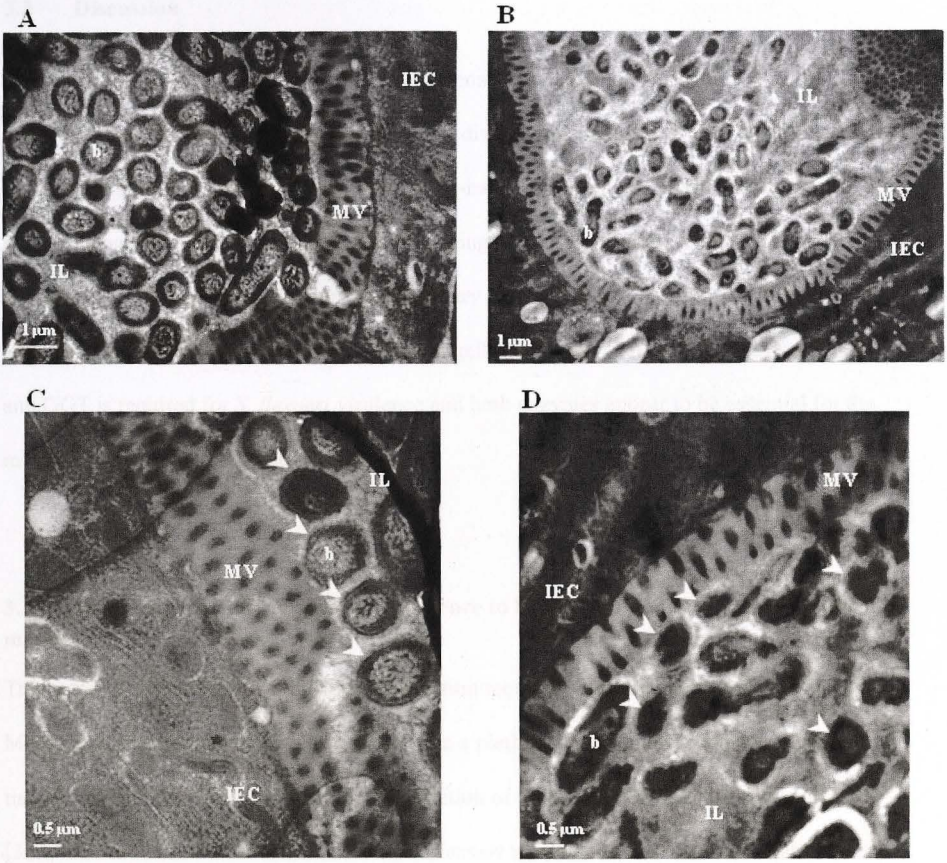

Figure 3.17: Morphology of wild type and *ansB* mutant cells in the intestinal lumina of *C. elegans*. Transmission electron micrographs of transverse mid body sections of *C. elegans* infected with wild type *S. flexneri* serotype 3b (SFL1520) (**A, C**), Δ*ansB* and (SFL2283) (**B, D**) for 96 hours. Δ*ansB* cells have irregular cell envelopes when compared with intraluminal SFL1520 cells (as indicated by white arrowheads). IEC-nematode intestinal epithelial cell; MV-microvilli; IL-nematode intestinal lumen; b-bacterial cells.

3.3 Discussion

This chapter characterizes the role of metabolic enzymes, AnsB and GGT in *S. flexneri* virulence. *ansB* and *ggt* genes were successfully disrupted in a highly virulent *S. flexneri* serotype 3b strain using the λ red-mediated PCR-based approach [317]. The effect of mutations on bacterial virulence was assessed using *in vitro* cell culture assays and two *in vivo* models, *C. elegans* and the murine pulmonary model. Results of *in vitro* bacterial adherence assays and both *in vivo* models of shigellosis suggest that the expression of AnsB and GGT is required for *S. flexneri* virulence and both enzymes appear to be essential for the initial stages of bacterial pathogenesis.

3.3.1 AnsB and GGT aid *S. flexneri* adherence to host cells, in an IpaB-independent manner

The successful establishment of bacterial infection requires adherence to host tissue. Members of the family *Enterobacteriaceae,* use a plethora of strategies to adhere to host tissues, ranging from the use of pili to the secretion of highly specialized adhesion molecules [319]. The molecular mechanisms used by *S. flexneri* to adhere to host cells are relatively unknown and understanding these mechanisms may allow us to target specific bacterial effectors molecules in novel therapeutic measures.

A recent study identified OspE1 and OspE2 mediated bacterial adherence following exposure to bile salts [320]. Type 1 fimbriae are the most common adhesins in Gram-negative bacteria. Fimbriae including the type 1 fimbria have been identified in *S. flexneri* [321, 322], and it has been hypothesized that these fimbriae aid bacterial adhesion. It has been long known that the entry of *S. flexneri* into host tissue depends on T3SS encoded factors. Previous studies have

shown that the bacterial T3SS Ipa proteins, especially IpaB facilitate adherence to mammalian tissue [25, 26, 323]. IpaB produced by *S. flexneri* during infection, interacts with the host hyaluronic receptor CD44 and mobilizes this host receptor in cholesterol-rich lipid rafts. This interaction facilitates bacterial adherence and entry into host cells through the recruitment of a cascade of signaling molecules [323].

The results of western immunoblots using anti-IpaB antibodies indicate that the IpaB levels are conserved between wild type and Δ*ansB* and Δ*ggt* strains (Figure 3.2). The impaired adherence shown by these mutant strains therefore suggests that there may be an IpaB-independent mechanism involved in *S. flexneri* adherence to host cells.

3.3.2 AnsB and *S. flexneri* adherence

3.3.2.1 Metabolic activity of AnsB and bacterial virulence

The L-asparaginase activity of AnsB has previously been shown to enhance bacterial colonization of mammalian cells by increased hydrolysis of asparagine, in the case of *H. pylori* [324, 325] and *C. jejuni* [314, 326, 327] however, the role of this enzyme in *S. flexneri* virulence has not yet been elucidated. The results of ammonia release assays (Figure 3.4.A) suggest that AnsB in *S. flexneri* functions as an L-asparaginase, as is the case in *E. coli* [315] and *S. enterica* [328]. This reaction features in several metabolic pathways including nitrogen, cyanoamino acid, alanine and aspartate metabolism [329].

The involvement of L-asparaginase in several metabolic pathways suggests that mutating *ansB* could lead to metabolic impairments, which in turn, could decrease overall bacterial fitness. However, no differences in the growth rates of *ansB* mutant and wild type strains were detected in this study, which suggests that although *ansB* is expressed and functional in wild type *S. flexneri* cells grown *in vitro,* the activity of this enzyme is not required for bacterial growth *in vitro* under nutrient rich and nutrient starved conditions (Figure 3.5). These findings suggest that the virulence phenotypes observed in this study are not likely to be a result of metabolic impairments leading to decreased bacterial fitness.

Bacterial adherence has been found to be favored by local environmental factors such as the alkaline milieu of the intestine, humidity and anaerobiosis [330]. Since the expression of AnsB has been known to be induced by anaerobiosis, it seems likely, that this enzyme could play a role in bacterial survival within the harsh environments of the gastrointestinal tract. The activity of AnsB could also be required for the expression and secretion of potential adhesins.

3.3.2.2 Up-regulation of OmpA in *ansB* mutants, and defective adherence

Comparative analysis of the proteomes of the *ans*B mutant and wild type *S. flexneri* strains indicated that this mutation results in the up-regulation of several *S. flexneri* proteins (Figure 3.10 and Table 3.1) including proteins involved in stress responses (DnaK and GroEL), protein translation (RplL), metabolism (Udp and Mdh) and an outer membrane protein (OmpA).

OmpA is a prominent outer membrane protein found in Gram-negative bacteria, whose role in pathogenesis has been extensively studied [331, 332]. Studies in *E. coli* [333] and EHEC [334, 335] have shown that OmpA, plays a key role in the initial stages of bacterial adherence and invasion. OmpA is involved in maintaining the structural integrity of cellular outer membranes [336, 337]. The up-regulation of OmpA in Δ*ansB* could therefore disrupt the integrity of the bacterial outer membrane, which could explain the decreased adherence of Δ*ansB* cells. To determine the effects of elevated OmpA levels on bacterial adherence, OmpA was overexpressed in the wild type strain. Overexpression of OmpA in wild type *S. flexneri* decreased bacterial adherence to BHK cells and accumulation in *C. elegans* (Figure 3.15 and 3.16). These results suggest that the decreased adherence of the *ansB* mutant strain may be attributed to the up-regulation of OmpA (identified using DIGE and confirmed using qRT-PCR).

It is generally believed that the overexpression of membrane proteins affects the integrity of cell membranes and cell viability [338]. Therefore the overexpression of OmpA would affect cellular protein homeostasis, which in turn could have an effect on the overall integrity of the cellular envelope. TEM micrographs of intraluminal *ΔansB* cells indicate that the integrity of the bacterial cell envelope is compromised on knocking out the *ansB* gene and this phenotype is most likely a result of the up-regulation of OmpA. These findings suggest that the defective adherence of *ansB* mutant cells could be due to OmpA-mediated disruption of the bacterial cell envelope integrity.

3.3.3 GGT and *S. flexneri* adherence

3.3.3.1 Metabolic activity of GGT and bacterial virulence

Studies in *H. pylori* [312, 339] have identified GGT as an important virulence factor, playing a role in bacterial colonization and pathogenesis [311, 340-342]. Similarly, studies in *C. jejuni* have also shown that *ggt* mutants show defective colonization of mice [343] and avian intestinal cells [344]. The glutaminase activity of GGT enables *H. pylori* and *C. jejuni* cells to use extracellular glutamine and glutathione as a source for glutamate, and it has been suggested that GGT-mediated hydrolysis of glutamine, is required for the virulence of these pathogens [311, 325, 345]. To determine if the glutaminase activity of GGT in *H. pylori* and *C. jejuni,* is conserved in *S. flexneri*, ammonia assays were performed. No differences were observed in the amount of ammonia produced by wild type and Δ*ggt* cells treated with glutamine, which suggests that GGT in *S. flexneri* fails to hydrolyse glutamine. This is not unusual as the protein sequence of GGT in *S. flexneri* only shares ~50% amino acid identity with GGT in both *H. pylori* and *C. jejuni.*

Previous studies in *E. coli* have indicated that GGT enables bacterial cells to utilize exogenous glutathione (GSH) as a source of cysteine and glycine, suggesting that the physiological role of GGT in *E. coli* could be catalysis of the initial step of cysteine/glycine salvage [346]. Since *S. flexneri* is a close relative of *E. coli,* and the protein sequence of GGT in *S. flexneri* shares 99% aa identity with its *E. coli* counterpart; it is likely that the primary function of GGT in *S. flexneri* is glutathione metabolism. The results of *in vitro* growth studies (Figure 3.5) indicate that the enzymatic activity of GGT is not required for bacterial growth under nutrient rich and starved conditions. It therefore seems likely that although not

essential, GGT may contribute to ability of *S. flexneri* to cope with growth limiting factors during infection.

3.3.3.3 Differential expression of YaeT (BamA) in *ggt* mutants and defective adherence

Previous studies in *S. flexneri* and enteropathogenic *E. coli* have indicated that the YaeT (BamA) in combination with BamD, constitutes the core component of the bacterial assembly machinery, which is essential for the proper folding, secretion and assembly of autotransporter proteins and adhesins [347-349]. The differential expression of this protein in the *ggt* mutant strains would therefore affect the folding and secretion of a plethora of autotransportes including IcsA and adhesion molecules.

Conflicting results regarding the expression of *yaeT* in *ggt* mutant cells were observed in this study, with the DIGE analysis and western immunoblots suggesting decreased levels of YaeT protein and qRT-PCR data indicating the up-regulation of *yaeT* transcripts in *ggt* mutant cells. These results suggest that two competing effects potentially control YaeT levels in *ggt* mutant cells, transcriptional up-regulation of *yaeT* and translational-down-regulation of YaeT protein.

Although several studies have characterized the structure and function of bacterial YaeT, little is known about the regulation of YaeT expression. Rhodius A. *et al.* identified *yaeT* as a core member of the σ^E-regulon, which is activated in response to envelope stress, thus suggesting that the expression of *yaeT* mRNA is increased on account of envelope stress. Another study in *S. typhimurium* reported that *Δhfq* strains show overexpression of YaeT

protein suggesting that protein levels are negatively regulated by Hfq or an siRNA-type mechanism [350]. In this chapter, DIGE analysis and western immunoblots suggest the down-regulation of YeaT while qRT-PCR results indicate an increase in *yaeT* transcripts in Δ*ggt*. These results could suggest that two competing effects potentially control YaeT levels in *ggt* mutant cells, transcriptional up-regulation of *yaeT* possibly due to increased activity of σ^E-mediated stress responses (discussed above) and translational down-regulation of YaeT possibly due to Hfq-mediated silencing [350].

The down-regulation of YaeT in the *ggt* mutant strain would, result in the faulty folding and secretion of autotransporters and other essential adhesion molecules which could explain the defective adherence observed in Δ*ggt* (SFL2285). In support of this hypothesis, increasing the expression of *yaeT* in *ggt* mutant cells (SFL2444) increased the adherence of this mutant strain, indicating that YaeT may play a role in *S. flexneri* adherence. However although increasing the expression of *yaeT* in *ggt* cells increased bacterial adherence, these cells were still significantly less adherent than the wild type strain, suggesting the virulence phenotype of the *ggt* mutants may be a result of the combined effect of multiple factors.

3.4 Conclusion

In this chapter, periplasmic enzymes, AnsB and GGT have been identified as novel virulence factors in *S. flexneri*. Results of *in vitro* adherence assays and *in vivo* virulence assays indicate that both enzymes are involved in the early stages of *S. flexneri* pathogenesis. Differential-in gel electrophoresis identified that *ansB* and *ggt* mutants exert pleotropic effects on the expression of a number of *S. flexneri* genes including two prominent bacterial outer membrane proteins, OmpA and YaeT that are known to be required for adherence to

host cells. Virulence assays performed using wild type cells overexpressing OmpA, suggest that the up-regulation of OmpA could be the leading cause for the defective adherence of *ansB* mutant cells. Data obtained from the DIGE analysis of *ggt* mutant cells, suggest that the mutation of this gene, activates a σ^E-mediated stress response as indicated by the differential expression of several members of the σ^E regulon (Discussed in Chapter 6). I propose that GGT modulates the virulence of *S. flexneri* by regulating extracellular glutathione levels, which is critical to maintaining the redox homeostasis of the periplasmic compartment, required for the folding and assembly of membrane proteins. The requirement of AnsB and GGT for the virulence of *S. flexneri* makes them attractive candidates for designing new vaccine strategies.

Chapter 4

Determining the complete genome sequence of *S. flexneri* bacteriophage, SfII and the identification and characterization of potential bacteriophage, SfV-encoded virulence factors

Chapter 4: Determining the complete genome sequence of *S. flexneri* bacteriophage, SfII and the identification and characterization of potential bacteriophage, SfV-encoded virulence factors

4.1 Introduction

S. flexneri strains are susceptible to infection by several temperate, lambdoid bacteriophages. The vast majority of the bacteriophage genome is of no benefit to the bacterial host as it orchestrates the redirection of bacterial resources towards the maintenance and production of its own viral particles. A subset of the bacteriophage genome has been found to encode virulence factors that play a role in bacterial pathogenesis and survival within mammalian hosts [351]. The list of bacteriophage-encoded virulence factors is growing and this field of research is of importance as bacteriophage-encoded products have been found to play a role in many aspects of bacterial pathogenesis (Table 1.4).

To date in *S. flexneri,* the O-antigen modifying genes - the glucosyltransferase (*gtr*) and the *O*-acteyltrensferase (*oac*) clusters are the only set of bacteriophage-encoded genes that have been linked to bacterial pathogenesis [5]. Previous studies in both Gram-positive and Gram-negative pathogens have identified bacteriophage genes that are involved in different stages of bacterial pathogenesis [351, 352] (Table 1.4); these findings warrant the need to study *S. flexneri* phages further.

Obtaining the complete genome sequence of an organism is one of the most efficient ways to gain insight into its complex biology. Five *S. flexneri* bacteriophages have been completely sequenced; SfV [158], SfI [155], SfIV [157], Sf6 [160] and SfX [12]. Here, bacteriophage SfII was isolated from a *S. flexneri* serotype 2a strain and completely sequenced. *S. flexneri* serotype 2a accounts for the majority of *S. flexneri* isolates in humans [16] hence it is important to understand why this strain is so prevalent. SfII is a serotype converting phage that carries the *gtrII* gene cluster, which convert serotype Y strains to serotype 2a strains. In addition to serotype conversion through O-antigen modification, bacteriophage SfII may contribute more to *Shigella* pathogenesis. In order to investigate this hypothesis, the complete SfII genome sequence was analysed and compared to the genomes of SfI, SfIV, SfV and Sf6 and other published lambdoid phage genomes.

While the SfII genome was being sequenced, virulence studies were performed to determine if bacteriophage SfV-encoded genes contribute to the virulence of *S. flexneri*. Preliminary virulence studies were performed to compare the virulence of a *S. flexneri* serotype Y (SFL1339) strain carrying no bacteriophage genes, and a SfV lysogen in the SFL1339 background (SFL1871). To stabilize SfV in this lysogenized strain for genetic manipulations, the integrase and excisionase (*int-xis*) genes of the phage were previously knocked out to prevent the excision of SfV from the host chromosome (Roberts, PhD thesis, ANU). *In vitro* cell culture assays and *C. elegans* bacterial accumulation and survival assays were used to compare the virulence of the 'phage-less' SFL1339 strain and the SfV lysogen (SFL1871). Results of these virulence assays indicate that the presence of bacteriophage SfV genes increased the virulence of SFL1339.

Previous studies have shown that the *gtr* cluster of *S. flexneri* is required for pathogenesis [353] and the lysogen used in this study carries the *gtrV* cassette. Therefore one can argue that the increased virulence of the lysogen could be due to the *gtrV*-mediated O-antigen modifications of SFL1339. To determine if SfV genes outside of the *gtr* cluster, also contribute to bacterial virulence, all the uncharacterized bacteriophage genes that lie upstream of the *gtrV* cluster in SfV (14 genes in total) and one gene encoding a DNA adenine methylase were selected for further virulence studies. These genes were selected based on prior knowledge of phage gene expression during its lifecycle. During the lysogenic cycle phage genes encoding structural elements, late regulatory and lytic proteins, are repressed. Therefore uncharacterized proteins lying in these regions were omitted in this study. Phage genes expressed in the lysogen included those involved in the maintenance of lysogeny, providing superinfection immunity and other genes that benefit the host strain. Reverse transcription polymerase chain reaction (RT-PCR) was used to determine if the 15 selected uncharacterized phage genes were expressed in the host when grown *in vitro* at 37 ºC. Using this approach, 13 out of 15, selected SfV genes were identified to be expressed in the lysogen. The expression of SfV genes in the lysogenized host suggests that these genes may provide some benefit to the host.

A cassette of five SfV genes (*orfs28-32*) identified to be expressed in the lysogen, with homologues in *S. flexneri* bacteriophage SfIV (*orfs* 30-34) and *E. coli* phage cdtI was selected for further study. This five gene cassette was deleted from the SfV lysogen using the λ red-mediated PCR-based approach [317]. *In vitro* cell culture assays and *in vivo C. elegans* virulence assays indicated that the expression of genes within the *orf28-32* cluster contribute to the virulence of the host strain.

4.2 Results

4.2.1 Complete Genome Sequence of SfII: a Serotype Converting bacteriophage of the highly prevalent, *Shigella flexneri* serotype 2a

4.2.1.1 Sequencing bacteriophage SfII

Elizabeth Tran, at the University of Adelaide, previously generated an SfII library, by dividing the SfII genome into 8 fragments, using *PstI* digests and cloning individual fragments into pBlueScript vectors [156]. We obtained this library and sequenced fragments 1, 2, 4, 6 and 7, in plasmids pNV1942, pNV1943, pNV1944, pNV1946, pNV1947 (Table 2.3), respectively, using Sanger sequencing. The M13 Forward and Reverse primers, complementary to the multiple cloning sites of pBlueScript vectors, were initially used to obtain phage sequences. Plasmids carrying fragments 3, 5 and 8 were not available therefore these fragments were isolated from the SfII lysogen (SFL2345) by PCR, using Fragment.3.F–Fragment.3.R and Fragment.8.F–Fragment.8.R primer pairs, respectively (Figure 4.1). Primer walking was used to fill in gaps and determine the arrangement of fragments. DNA sequences were assembled into contigs using Bioedit [302]. Putative ORF's were identified using the NCBI ORF Finder and CLC Main Workbench version 6.5.

4.2.1.2 Overview of the SfII genome

The complete genome of bacteriophage SfII has been deposited in GenBank under the accession no. KC736978. The genome of SfII is linear, double-stranded, of 41,475 bp with an average G+C content of 49.17%, corresponding to 58 coding sequences (CDSs). Most of the genome (71.57%) is predicted to be transcribed from the sense strand while 19.14% of the genome including the *gtr* cluster, is predicted to be transcribed by the antisense strand. Database searches of the 58 predicted CDSs using NCBI BlastX identified, 41 CDSs had

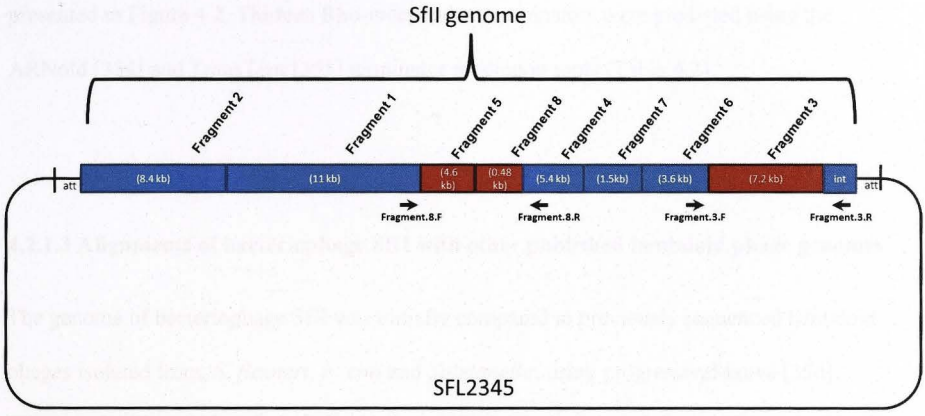

Figure 4.1: Sequencing strategy used to completely sequence bacteriophage SfII. The above figure is a diagrammatic representation of bacteriophage SfII in the lysogenic strain, SFL2345. The SfII genome can be divided into 8 fragments by *PstI* digests. Fragments 1, 2, 4, 6 and 7 (fragments highlighted in blue) were sequenced from plasmid clones donated by ElizabethTran, (University of Adelaide). Fragments 5, 8, and 3 (in red), were isolated from SFL2345 by colony PCR using region specific primers (arrows), following which they were sequenced.

assigned functions and 17 as hypothetical proteins. A complete list of the 58 predicted ORF's is presented in Table 4.1. A functional map of SfII based on the above predictions is presented in Figure 4.2. Thirteen Rho-independent terminators were predicted using the ARNold [354] and TransTem [355] terminator prediction tools (Table 4.2).

4.2.1.3 Alignments of bacteriophage SfII with other published lambdoid phage genomes

The genome of bacteriophage SfII was initially compared to previously sequenced lambdoid phages isolated from, *S. flexneri*, *E. coli* and *Salmonella*, using progressiveMauve [356] (Figure 4.3). The results of multiple alignments indicate that bacteriophage SfII shares high levels of DNA sequence similarity with *S. flexneri* phages, SfI (98% nucleotide identity and 51% coverage; BlastN), SfIV (97% nucleotide identity and 63% coverage; BlastN) and SfV (98% nucleotide identity and 59% coverage; BlastN). Considerable similarity was also observed with *E. coli* phages cdtI (97% nucleotide identity and 12% coverage; BlastN) and phiP27 (80% nucleotide identity and 12% coverage; BlastN) and *Salmonella* phage ST64B (84% nucleotide identity and 28% coverage; BlastN). SfII showed limited similarity to the other lambdoid phages included in this study (Figure 4.3).

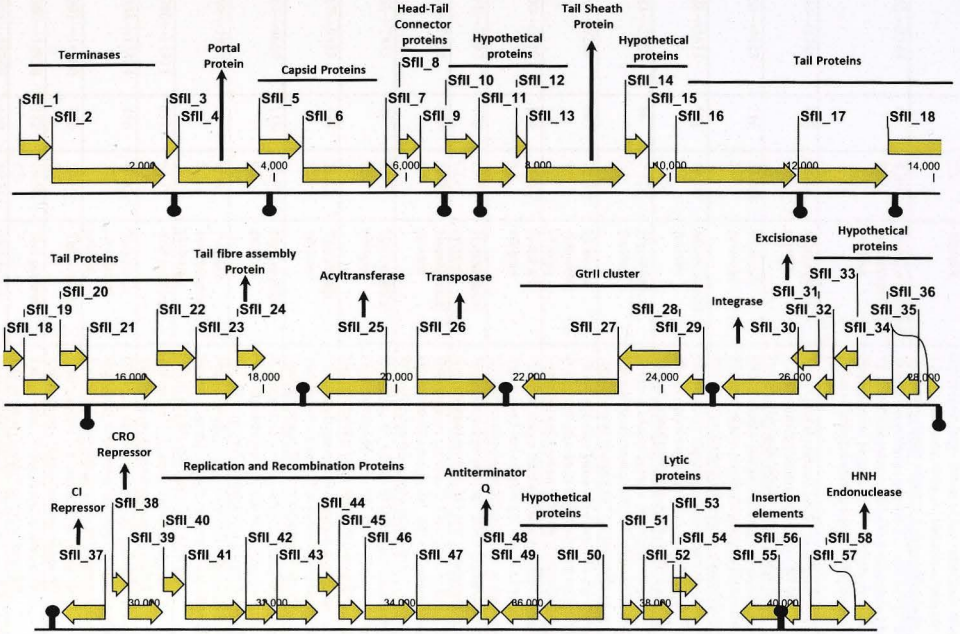

Figure 4.2: Complete genome of bacteriophage SfII. Schematic representation of the SfII genome, with its predicted coding regions and some functional assignments. The arrowheads indicate the direction of transcription. Predicted Rho-independent terminator structures are indicated as hairpin structures.

Table 4.1: Analysis of the predicted Orfs in the SfII genome

ORF	Gene co-ordinates and orientation	Size (aa)	Mol. mass (kDa)/ pI	Function	Related phage proteins	GenBank Accession no.	BlastX e value (%identity)
SfII_1	126→620	164	17.85/ 9.4	Small terminase subunit	Putative phage terminase, small subunit, P27 family protein Small terminase subunit [Enterobacteria phage SfV] Terminase small subunit [Enterobacteria phage SfI]	YP_002115130 NP_599033 AFR52509	5e-115(100) 4e-113(99) 4e-113(99)
SfII_2	617→2350	577	65.25/ 5.6	Large terminase subunit	Bacteriophage V large terminase subunit [Shigella sp. D9] Terminase large subunit [Enterobacteria phage SfI] Large terminase subunit [Enterobacteria phage SfV] Terminase large subunit [*Salmonella* phage ST64B]	WP_000088161 AFR52510 NP_599034 NP_700375	0.0(99) 0.0(99) 0.0(98) 0.0(91)
SfII_3	2362→2544	60	6.38/ 9.1	Putative integral membrane protein	Putative membrane protein [*E. coli* 2731150] Hypothetical protein 003 [Enterobacteria phage SfI] Hypothetical protein SFV_0236 [*S. flexneri* 5 str. 8401] Putative integral membrane protein [*Salmonella* phage ST64B]	WP_001297668 AFR52511 YP_687817 NP_700376	2e-15(100) 3e-14(97) 1e-13(94) 2e-14(94)
SfII_4	2544→3785	413	46.12/ 6.1	Phage portal protein	Phage portal protein, HK97 family [*E. coli* 2.4168] Portal protein [*Salmonella* phage ST64B] Portal protein [Enterobacteria phage SfI]	WP_001524100 NP_700377 AFR52512	0.0(99) 0.0(99) 0.0(99)
SfII_5	3763→4413	216	23.98/ 5.5	Prohead protease	HK97 family phage prohead protease [*E. coli* SMS-3-5] Putative phage pro-head protease [Enterobacteria phage SfI] Pro-head protease [*Salmonella* phage ST64B]	YP_001743250 AFR52513 NP_700378	6e-154(100) 7e-154(100) 5e-152(99)
SfII_6	4428→5633	401	44.26/ 5.3	Major capsid protein	Phage major capsid protein [Enterobacteria phage SfI] Phage major capsid protein, HK97 family [*E. coli* 2.4168] Major capsid protein precursor [*Salmonella* phage ST64B]	AFR52514 EII65486 NP_700379	0.0(99) 0.0(99) 0.0(96)
SfII_7	5683→5883	66	7.12/ 9.1	Hypothetical protein	Putative bacteriophage protein [*E. coli*] Hypothetical protein SfI_007 [Enterobacteria phage SfI] Hypothetical protein sb7 [*Salmonella* phage ST64B]	WP_001459469 AFR52515 NP_700380	2e-24(100) 2e-23(96) 6e-19(86)
SfII_8	5886→6209	107	12.56/ 4.6	Head-tail connector protein	Phage gp6-like head-tail connector protein [*E. coli* 3.2608] Phage gp6-like head-tail connector protein [*E. coli* 2731150] Hypothetical protein SfVp06 [Enterobacteria phage SfV]	EIH56530 EMW82796 NP_599038	1e-72(100) 4e-72(99) 8e-41(68)
SfII_9	6206→6616	136	15.62/ 8.9	Head tail adaptor	Putative phage head-tail adaptor [Enterobacteria phage SfI] Phage head-tail adaptor [*E. coli* KTE159] Hypothetical protein SfVp07 [Enterobacteria phage SfV]	AFR52516 EOW56935 NP_599039	1e-96(100) 4e-96(99) 2e-64(96)
SfII_10	6591→7097	168	19.78/ 12.1	Hypothetical protein	Hypothetical protein SfI_0010 [Enterobacteria phage SfI] Hypothetical protein SfVp08 [Enterobacteria phage SfV]	AFR52517 NP_599040	2e-75(100) 7e-74(98)
SfII_11	7094→7654	186	20.79/ 4.4	Hypothetical protein	Hypothetical protein ECDEC10F_6192 [*E. coli* DEC10F] Hypothetical protein SfI_0011 [Enterobacteria phage SfI] SfVp09 [Enterobacteria phage SfV]	EHW83610 AFR52518 NP_599041	8e-134(100) 2e-131(98) 4e-132(99)
SfII_12	7663→7833	56	6.39/ 9.3	Hypothetical protein	Hypothetical protein SfVp10 [Enterobacteria phage SfV] Hypothetical protein SfI_0012 [Enterobacteria phage SfI] Hypothetical protein sb12 [*Salmonella* phage ST64B]	NP_599042 AFR52518 NP_700385	2e-31(100) 2e-31(100) 2e-24(85)
SfII_13	7817→9313	498	53.23/ 5.5	Tail sheath protein	Tail sheath protein [Enterobacteria phage SfV] Tail sheath protein [Enterobacteria phage SfI] Bacteriophage Mu tail sheath protein (GpL) [*E. coli*]	NP_599043 AFR52519 WP_000155705	0.0(99) 0.0(98) 0.0(99)
SfII_14	9313→9669	118	12.92/ 4.8	Hypothetical protein	Hypothetical protein SfVp12 [Enterobacteria phage SfV] Hypothetical protein SfI_0014 [Enterobacteria phage SfI] Tail tube protein [*Salmonella* phage ST64B]	NP_599044 AFR52520 NP_700387	2e-82(100) 2e-82(100) 9e-65(83)
SfII_15	9669→9938	82	9.94/ 5.2	Putative bacteriophage protein	Phage protein [*E. coli* UMNK88]hypothetical protein Putative bacteriophage protein [Enterobacteria phage SfI] SfVp13 [Enterobacteria phage SfV]	YP_006132129 AFR52522 NP_599045	3e-58(100) 2e-54(99) 7e-57(98)
SfII_16	10080→11915	611	65.39/ 9.1	Tail protein	Tail protein [Enterobacteria phage SfV] Tail protein [Enterobacteria phage SfI]	NP_599046 AFR52523	0.0(99) 0.0(99)
SfII_17	11934→13304	456	49.43/ 5.6	Tail/DNA circulation protein	DNA circulation protein [*E. coli* MS 119-7] Hypothetical protein SfI_0017 [Enterobacteria phage SfI] Tail/DNA circulation protein [Enterobacteria phage SfV]	ZP_07105018 AFR52524 NP_599047	0.0(99) 0.0(98) 0.0(98)
SfII_18	13301→14380	359	39.19/ 5.1	Tail protein	MuP protein [Enterobacteria phage SfI] Tail protein [Enterobacteria phage SfV]	AFR52525 NP_599048	0.0(99) 0.0(99)
SfII_19	14380→14928	182	19.58/ 6.9	Tail protein	Tail protein [Enterobacteria phage SfV] Tail protein [Enterobacteria phage SfI]	NP_599049 AFR52526	2e-129(99) 2e-129(99)
SfII_20	14925→15353	142	16.36/ 5.8	Tail protein	Phage GP46 family protein [*E. coli* DEC14B] Tail protein [Enterobacteria phage SfV] Putative tail protein [Enterobacteria phage SfI]	EHX73482 NP_599050 AFR52527	2e-96(100) 1e-95(99) 1e-95(99)
SfII_21	15340→16398	352	38.18/ 5.0	Tail protein	Phage tail protein [*E. coli* KTE31] Tail protein [Enterobacteria phage SfV] Hypothetical protein SfI_0021 [Enterobacteria phage SfI]	EOU82947 NP_599051 AFR52528	0.0(100) 0.0(99) 0.0(98)
SfII_22	16389→16973	194	21.73/ 5.1	Tail protein	Tail protein [Enterobacteria phage SfI] Tail protein [Enterobacteria phage SfV] Tail protein [*E. coli* DEC7B]	AFR52529 NP_599052 EHW00738	8e-130(100) 2e-129(98) 6e-127(97)
SfII_23	16977→17627	216	22.64/ 7.7	Hypothetical protein	Unnamed protein product [*S. flexneri* 2a str. 301] Hypothetical protein SfVp21 [Enterobacteria phage SfV]	NP_706263 NP_599053	9e-147(100) 2e-134(95)

					Hypothetical protein Sfi_0023 [Enterobacteria phage SfI]	AFR52530	4e-134(95)
SfII_24	17599→18033	144	16.25/ 5.1	Tail fibre assembly protein	Phage tail fiber protein [*S. flexneri* 2a str. 301]	NP_706262	2e-102(100)
					Caudovirales tail fibre assembly family protein [*S.flexneri* VA-6]	EGK28007	2e-102 (100)
					Putative phage tail fiber protein [Enterobacteria phage SfI]	AFR52531	5e-91(92)
					Tail fibre assembly protein [Enterobacteria phage SfV]	NP_599054	4e-91(91)
SfII_25	18806←19855	349	40.12/ 9.2	Acyltransferase	Acyltransferase family protein [*S. flexneri* 2a str. 2457T]	EFS11261	0.0(100)
					Hypothetical protein SF0309 [*S. flexneri* 2a str. 301]	NP_706261	0.0(100)
					Acyltransferase family protein [*S. flexneri* K-304]	EGK31482	0.0(100)
					Acyltransferase [*S. flexneri*]	WP_000613535	5e-157(99)
SfII_26	20308→21498	396	45.46/ 10.5	Transposase	Transposase DDE domain protein [*S. flexneri* 2a str. 2457T]	EFS11262	0.0(99)
					Transposase ISSfl3 [*S. flexneri*]	WP_001111520	0.0(99)
					Transposase [*E. coli*]	WP_016159268	0.0(99)
SfII_27	21887←23348	486	55.78/ 9.1	Serotype-specific glucosyltransferase	Glucosyl tranferase II [*S. flexneri* phage SfII]	AAC39273	0.0(100)
					Glucosyl tranferase II [*S. flexneri* 2a str. 2457T]	NP_836041	0.0(99)
					gtrII gene product [*S. flexneri* 2a str. 301]	NP_706259	0.0(99)
SfII_28	23344←24274	309	34.85/ 6.9	Bactoprenol glucosyltransferase	Bactoprenol glucosyl transferase [*S. flexneri* 2a str. 301]	NP_706258	0.0(100)
					Bactoprenol glucosyl transferase [*Shigella* phage SfII]	AAC39272	0.0(100)
					Bactoprenol glucosyltransferase [Enterobacteria phage SfV]	NP_599056	0.0(98)
					Bactoprenol glucosyltransferase [Enterobacteria phage SfI]	AFR52533	0.0(98)
SfII_29	24270←24633	120	13.3/ 9.6	Putative flippase	Unknown protein [*Shigella* phage SfII]	AAC39271	2e-70(100)
					Putative flippase [Enterobacteria phage SfV]	NP_599057	2e-69(99)
					Flippase [Enterobacteria phage SfI]	AFR52534	2e-69(99)
					gtrAI gene product [*S. flexneri* 2a str. 301]	NP_706257	2e-68(98)
SfII_30	24894←26058	387	44.94/ 9.8	Integrase	Phage integrase family site-specific recombinase [Enterobacteria phage SfI]	AFR52475	0.0(99)
					Integrase [Enterobacteria phage SfV]	NP_599058	0.0(98)
					Phage integrase [*S. flexneri* 2a str. 2457T]	NP_836047	0.0(99)
SfII_31	25935←26351	138	15.56/ 9.7	Excisionase	Excisionase [Escherichia coli]	WP_001310200	2e-96(99)
					Excisionase [Enterobacteria phage SfV]	ZP_05937981	1e-94(96)
					Excisionase [Enterobacteria phage SfI]	AFR52476	1e-74(95)
					Excisionase [Shigella phage SfX]	AAD10294	6e-19(41)
SfII_32	26284←26590	101	12.12/ 4.8	Hypothetical protein	Hypothetical protein SfVp28 [Enterobacteria phage SfV]	NP_599060	2e-66(100)
					Conserved hypothetical protein [*S. flexneri* 2a str. 301]	AAN41957	2e-66(100)
					Conserved hypothetical protein; CPS-53 (KpLE1) prophage [*E. fergusonii* ATCC 35469]	CAQ88120	1e-65(99)
SfII_33	26589←26952	120	13.79/ 4.7	Hypothetical protein	Hypothetical protein SfVp29 [Enterobacteria phage SfV]	NP_599061	5e-82(99)
					Conserved hypothetical protein; CPS-53 (KpLE1) prophage [*E. fergusonii* ATCC 35469]	CAQ88121	5e-82(99)
					Hypothetical protein PcdtI_gp36 [Phage cdtI]	YP_001272549	4e-80(96)
						EHW00692	3e-76(99)
SfII_34	26943←27479	110	20.38/ 5.5	Hypothetical protein	Conserved hypothetical protein; CPS-53 (KpLE1) prophage [*E. fergusonii* ATCC 35469]	CAQ88122	1e-124(97)
					Hypothetical protein SfVp30 [Enterobacteria phage SfV]	NP_599062	4e-124(96)
					Hypothetical protein PcdtI_gp37 [Phage cdtI]	YP_001272550	3e-126(97)
SfII_35	27535←27873	112	12.58/ 10.6	Hypothetical protein	Hypothetical protein HMPREF9542_02137 [*E. coli* MS117-3]	EGB88400	3e-71(95)
					Conserved hypothetical protein [*E. fergusonii* ATCC 35469]	CAQ91833	2e-61(96)
					Hypothetical protein PcdtI_gp40 [Phage cdtI]	YP_001272553	4e-24(64)
SfII_36	27994→28185	63	7.23/ 4.9	Hypothetical protein	Hypothetical protein HMPREF9534_01518 [*E. coli* MS69-1]	EFJ82427	9e-37(100) 1e-35(98)
					Hypothetical protein EcE22_4050 [Escherichia coli E22]	EDV83662	
SfII_37	28703←29395	230	25.65/ 6.0	CI repressor	Putative cI regulatory protein [*E. coli* ETEC H10407]	YP_006113860	4e-167(100)
					Putative cI regulatory protein [*E. coli* O157:H43 str. T22]	ENO07177	7e-167(99)
					Regulatory protein [*Salmonella* phage ST64B]	NP_700411	3e-133(83)
SfII_38	29493→29753	86	9.76/ 9.5	Cro repressor	Antirepressor Cro [*E. coli* O103:H2 str. 12009]	YP_003220518	1e-54(100)
					Putative antirepressor protein Cro [*E. coli* O111:H- str. 11128]	YP_003237174	3e-52(94)
					Putative lambda repressor-like DNA-binding domain-containing protein [*E. coli* UMN026]	YP_002411623	6e-54(99)
SfII_39	29746→30297	183	20.01/ 4.8	Phage transcriptional regulator	Phage transcriptional regulator [*E. coli* KTE228]	ELD55966	9e-132(99)
					Phage regulatory protein CII [*E. coli* O103:H2 str. 12009]	YP_003220519	4e-121 (99)
					Hypothetical protein PcdtI_gp43 [Phage cdtI]	YP_001272556	6e-118(90)
SfII_40	30294→30632	112	12.2/ 9.1	Hypothetical protein	Hypothetical protein [*Escherichia* sp. TW09308]	WP_001087375	5e-54(99))
					e14 prophage protein [*E. coli* O55:H7 str. CB9615]	YP_003502582	1e-62(99)
					Conserved hypothetical protein; e14 prophage [*E. fergusonii* ATCC 35469]	CAQ88132	5e-62(96)
SfII_41	30642→31538	313	35/8.6	Replication	Replication protein [*E. coli*]	WP_000104970	0.0(99)
					Phage replication protein O [*E. coli* KTE68]	EOV65900	0.0(99)
					Phage O protein family protein [*S. flexneri* VA-6]	EGK28948	0.0(99)
SfII_42	31586→32071	167	18.51/ 9.9	PerC transcriptional activator family protein	PerC transcriptional activator family protein, CPS-53 (KpLE1) prophage; [*E. coli* str. K-12 substr. MG1655]	NP_416858	7e-111(99)
					PerC transcriptional activator family protein [*E. coli* MP021552]	EMU72183	1e-109(98)

					PerC transcriptional activator family protein [*E. coli* DH1] PerC transcriptional activator family protein [*Shigella* sp. D9]	YP_006091263 EGJ06486	1e-110(99) 6e-109(99)
SfII_43	32072→32725	217	24.50/ 5.8	DNA adenine methylase	DNA adenine methylase [Enterobacteria phage SfV] Putative DNA adenine methylase [Phage cdtI] Phage N-6-adenine-methyltransferase [*E. coli* DEC7B]	NP_599073 YP_001272560 EHW00771	2e-160(100) 4e-158(99) 4e-159(99)
SfII_44	32722→33048	108	12.03/ 9.3	LexA DNA-binding domain protein	LexA DNA-binding domain protein [*E. coli* 96.154] LexA family transcriptional regulator [*E. coli*] Hypothetical protein SfVp42 [Enterobacteria phage SfV]	EII00172 WP_000210154 NP_599074	2e-72(99) 5e-72(99) 3e-70(95)
SfII_45	33045→33434	129	14.17/ 9.3	RusA family protein	Endodeoxyribonuclease RusA family protein [*E. coli*] Crossover junction endodeoxyribonuclease [Enterobacteria phage SfV] Holliday junction resolvase [Phage cdtI]	WP_001501070 NP_599075 YP_001272562	2e-89(100) 2e-89(99) 8e-89(98)
SfII_46	33454→34251	265	29.77/ 9.2	KilA-N domain	KilA-N domain protein [*E. coli* DEC7B] KilA-N domain protein [*S. flexneri* VA-6] Hypothetical protein SfVp44 [Enterobacteria phage SfV]	EHW00778 EGK28953 NP_599076	0.0(99) 0.0(99) 2e-163(87)
SfII_47	34259→35248	329	37.13/ 7.71	Hypothetical protein	Hypothetical protein c3187 [*E. coli* CFT073] Hypothetical protein mEp460_049 [Enterobacteria phage mEp460] Hypothetical protein SD15574_5395 [*S. dysenteriae* 155-74]	NP_755069 AFM76086 EGI88864	0.0 (99) 0.0(99) 0.0(99)
SfII_48	35266→35577	103	11.7/ 9.3	Antiterminator protein Q	Phage antitermination Q family protein [*E. coli* Jurua 20/10] Phage antitermination protein Q [*E. coli* E1167] Antitermination protein Q homolog from lambdoid prophage DLP12 [*E. coli*]	EMX57588 EGC09492 WP_001205449	3e-64(89) 1e-63(88) 7e-54(72)
SfII_49	35581←36165	194	21.83/ 9.0	Hypothetical protein	Hypothetical protein [*E. coli*] Hypothetical protein ERBG_04465 [*E. coli* E1167] Putative membrane protein [*E. coli* Jurua 20/10]	WP_001122063 EGC09491 WP_004030018	1e-113(100) 3e-133(99) 2e-35(100)
SfII_50	36173←37195	340	38.45/ 8.9	Hypothetical protein	Hypothetical protein ECJURUA2010_0091 [*E. coli* Jurua 20/10] Hypothetical protein ERBG_04464 [*E. coli* E1167] Hypothetical protein EC2726800_0411 [*E. coli* 2726800]	EMX57590 EGC09490 EMX81086	0.0(100) 0.0(99) 0.0(99)
SfII_51	37481→37807	108	11.47/ 9.7	Holin	Phage holin, lambda family [*E. coli* Jurua 20/10] Lambda family protein phage holin [*E. coli* E1167] Holin [Enterobacteria phage SfV]	EMX57591 EGC09489 NP_599081	1e-55(100) 8e-55(99) 3e-53(97)
SfII_52	37811→38287	158	17.81/ 9.0	Lysin	Lysozyme [*E. coli* Jurua 20/10] Lysin [Enterobacteria phage SfV] Phage lysin [*E. coli* AA86]	EMX57592 NP_599082 EGH3717	6e-113(100) 2e-109(96) 4e-112(99)
SfII_53	38271→38663	130	14.58/ 9.4	RZ	Rz lytic protein from phage origin, coiled-coil [*E. coli*] Putative Rz lytic protein [*E. coli* E22] Putative Rz lytic protein [Enterobacteria phage SfV]	WP_001356120 EDV82641 NP_599083	6e-76(100) 2e-63(83) 2e-57(76)
SfII_54	38386→38820	144	16.37/ 9.8	RZ1	Hypothetical protein [*E. coli*] Putative Rz1 lytic protein [*E. coli* B str. REL606] Rz lytic protein from phage origin, coiled-coil [*E. coli*] Putative Rz1 lytic protein [Enterobacteria phage SfV]	WP_001181631 YP_003043948 WP_001356120 NP_599084	1e-73(100) 3e-46(76) 8e-43(100) 1e-42(73)
SfII_55	39323←39949	208	23.76/ 10.1	IS911 orfB	IS911 orfB [*S. flexneri* 2a str. 2457T] IS911 orfB [*S. flexneri* 2a str. 301] IS911 orfB [*S. flexneri* 5a str. M90T] Putative transposase OrfB [Enterobacteria phage Sf6]	NP_835950 NP_706457 NP_085444 NP_958229	2e-136(100) 2e-136(100) 8e-136(100) 1e-135(100)
SfII_56	39976←40278	100	11.54/ 9.9	IS911 orfA	IS911 orfA [*S. flexneri* 2a str. 2457T] S911 ORF1 [*S. flexneri* 2a str. 301] IS ORF1 [*S. flexneri* 5a str. M90T] Gene 56 protein [Enterobacteria phage Sf6]	NP_837023 NP_706169 NP_085444 NP_958230	4e-65(100) 7e-65(100) 2e-64(100) 4e-65(100)
SfII_57	40429→41049	206	22.81/ 5.4	Hypothetical protein	Hypothetical protein [*E. coli*] Hypothetical protein ECJURUA2010_0095 [*E. coli* Jurua 20/10]	WP_000634417 EMX57594	3e-147(100) 3e-147(100)
SfII_58	41125→41475	116	13.16/ 10.2	HNH endonuclease	HNH endonuclease family protein [*E. coli* Jurua 20/10] Hypothetical protein sb56 [*Salmonella* phage ST64B] HNH endonuclease family protein [*E. coli* DEC7B] Hypothetical protein SfVp53 [Enterobacteria phage SfV] HNH endonuclease family protein [Enterobacteria phage Sf1]	EMX57595 NP_700429 EHW00768 NP_599085 AFR52508	1e-78(100) 2e-74(93) 2e-74(95) 4e-74(93) 1e-73(94)

Table 4.2 : Putative Rho-independent terminators in the SfII genome

Position	Gene	Sequence	Strand	predicted free energy of terminator hairpin (Kcal/mol)
2380-2411	SfII_2	GCGCCTCTGGTGGGCGTGCTGGGGGCGCTTTT	Plus	-19.3
4066-4108	SfII_4	GCACACATGAAGGCCGGTTCGTTAACCGGCCTTTCTATTGGGT	Plus	-14.60
6859-6898	SfII_9	GAGAGGGAAACCGCCGTATCACCGGTGaTTTTTATCCGGC	Plus	-6.60
7457-7500	SfII_10	CTGAATCGTCATGAGCTGATTTATCAGTTCGaTTTTTCGGTCAT	Plus	-8.80
11928-11966	SfII_16	CTGTTAATGAGTCCCACTCCGGTGGGATTTTTTATGTAC	Plus	-9.80
13366--13405	SfII_17	CGGTGCCGGTGTTGAACGACTGGCGCGGGATTTCAGTGTG	Plus	-12.90
15468--15500	SfII_20	GTATGCGGCGGCGCTGCATACGGTTTACGGTTA	Plus	-15.0
18769-18810	SfII_25	AATGATAAAAAGGCGCAATTAATTGCGCCTTTTTATAGATAT	minus	-11.60
21423-21465	SfII_27	TACTTCGGTAAGTGCTGGCCAACCGGCACaaTATCTTTTCAGG	minus	-11.90
24704-24750	SfII_30	AAACATGTAAAGCCTTGCAAGCCATTGTGAGGCcTTATGTGTCTCAG	minus	-10.30
28211-28250	SfII_36	TGGGCTCGATGCCATGTGCGGTGAGCTCACTTTTCAAAAC	Plus	-17.8
28639-28677	SfII_37	CCCATCCATCGGCCACCGAAAGGTGGCTTTTTATTACCT	minus	-15.10
39842-39885	SfII_56	CAGCCCGTCTGCCGTCTGGTTTTTCAGGACGGTTTTTCCAGTAT	Plus	-7.6

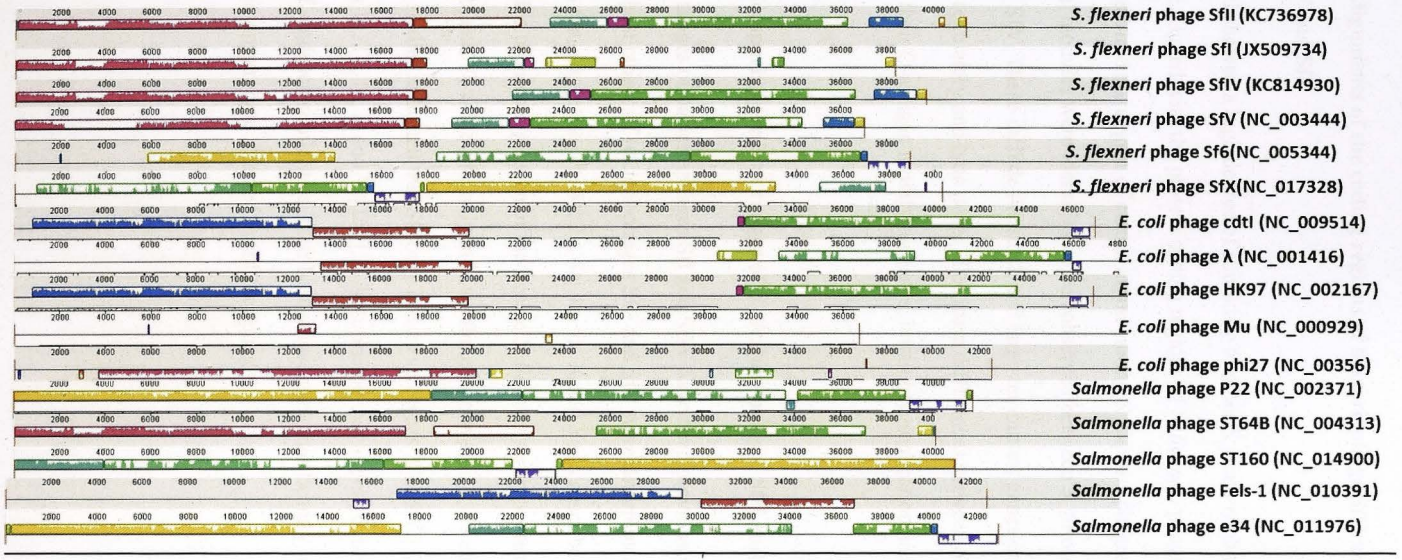

Figure 4.3: Alignment of bacteriophage SfII with its closest lambdoid phage homologues using progressiveMauve. The above figure represents the comparison of the SfII genome with its closest relatives. Colored outlined blocks surround regions of the genome sequence, that show homology to part of another genome. The colored bars inside the blocks are related to the level of sequence similarities.

4.2.1.4 Alignments of the coding regions of bacteriophage SfII and *S. flexneri* phages SfI, SfIV and SfV

Since SfII showed a high degree of similarity to other *S. flexneri* phage, the coding regions of SfII were aligned with the protein coding regions of *S. flexneri* phages SfI, SfIV and SfV, to gain insight into the degree of conservation among *S. flexneri* phages (Figure 4.4). Several functional modules were identified to be conserved between *S. flexneri* phages, SfII, SfI, SfIV and SfV. These include the small and large teminases, genes-encoding structural proteins, regulatory and lytic genes. The main differences between *S. flexneri* SfII, SfV and SfI lie in their O-antigen modifying genes, immunity, replication and Nin regions.

4.2.1.5 Comparing the host ranges of *S. flexneri* phages, SfII and SfV

The host ranges of bacteriophages SfI and SfIV have been previously determined [155, 157]. Here the host ranges of bacteriophages SfII and SfV were determined using twelve *S. flexneri* serotypes (1a, 1b, 1c, 2a, 2b, 3a, 3b, 4a, 4b, 5a, X and Y) as described in section 2.12.5. SfV was capable of infecting seven of the twelve *S. flexneri* serotypes tested (serotypes 1a, 1b, 2a, 2b, 3b, 4b, and Y) while SfII only infected three (serotypes 3b, 5a and Y) (Table 4.3). Previous studies indicated that SfI only infects serotypes X and Y [155] while SfIV infects serotypes 1a, 1b, 1c, X and Y [157]. It is surprising that although these phages have high degree of sequence similarities, their host ranges vary significantly with serotype Y being the only common serotype infected by all four phages.

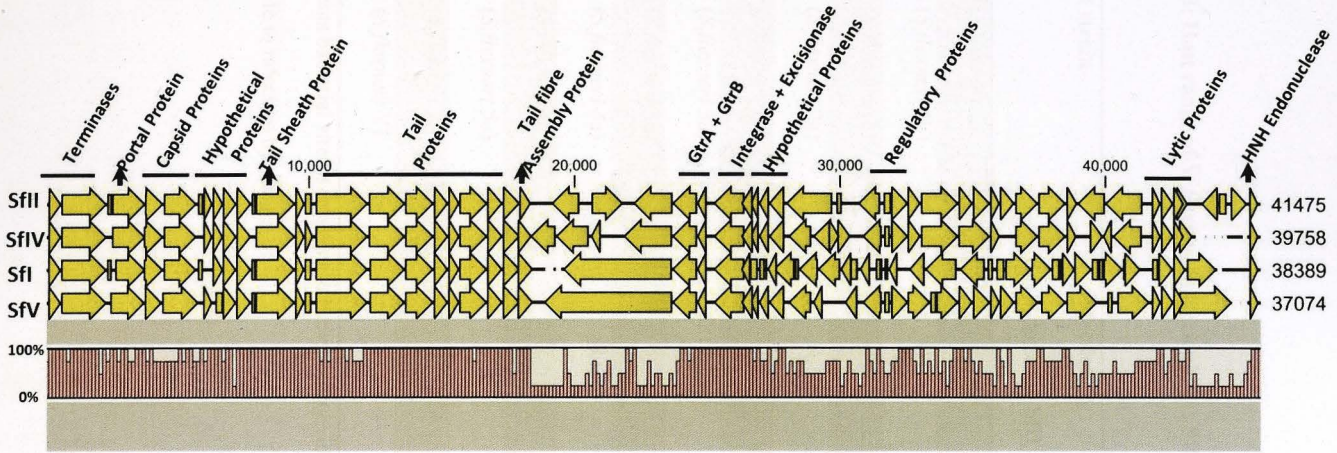

Figure 4.4: Comparison of the coding regions of SfII with other serotype converting phages of *S. flexneri*. Coding regions of SfII were aligned to annotated coding regions of SfI (JX509734), SfIV (KC814930) and SfV (NC_003444) using CLC Main Workbench version 6.5. Arrows represent coding regions and indicate the direction of transcription. Conserved functional modules between the phages have been indicated (solid lines). Bar graphs represent % conservation in the nucleotide sequence.

Table 4.3: Host range of *S. flexneri* bacteriophages SfII and SfV

Bacterial strain	Infection by Bacteriophage SfII	Infection by Bacteriophage SfV
SFL1499 (*S.flexneri* 1a)	R	S
SFL1496 (*S.flexneri* 1b)	R	S
SFL1500 (*S.flexneri* 1c)	R	R
SFL2345 (*S.flexneri* 2a)	R	S
SFL1510 (*S.flexneri* 2b)	R	S
SFL1516 (*S.flexneri* 3a)	R	R
SFL1520 (*S.flexneri* 3b)	S	S
SFL1253 (*S.flexneri* 4a)	R	R
SFL1350 (*S.flexneri* 4b)	R	S
SFL1871 (*S.flexneri* 5a)	S	R
SFL1537 (*S.flexneri* X)	R	R
SFL1353 (*S.flexneri* Y)	S	S

R represents bacterial strains resistant to bacteriophage infection while S represents strains susceptible to infection by phage.

Bacteriophage tail proteins identify bacterial receptors and initiate infection. Since large variations were observed in the host ranges of *S. flexneri* serotype converting phages, the amino acid sequences of the tail proteins of SfII, SfI, SfIV, and SfV were compared using BlastP, to identify differences in the tail proteins of these phages (Table 4.4). Most of the tail proteins of these four phages show over 98% aa identity. The main differences between the tail proteins of all four phages are as follows; (1) SfII_7 annotated as a hypothetical protein is unique to SfII and SfI with no homologues in SfIV and SfV. (2) SfII_12 has no homologue in SfIV, and shows < 95% identity with the corresponding protein in SfI and SfV. (3) SfII_15 and SfII_16 show < 50% identity with the SfIV homologues. (4) SfII_24, which encoded the tail fibre assembly protein shows < 92% identity with homologues in SfI, SfIV and SfV. These differences in the amino acid sequences of tail proteins could account for the varied host ranges of SfI, SfII, SfIV and SfV.

4.2.2 Identification and characterization of potential bacteriophage SfV-encoded virulence factors

While the genome of bacteriophage SfII was being sequenced, virulence studies were carried out using the completely sequenced *S. flexneri* bacteriophage, SfV. SfV is a serotype converting *S. flexneri* phage that encodes the O-antigen modifying *gtrV,* gene cluster. Lysogenization of SfV results in the conversion of serotype Y strains to serotype 5a strains [357, 358]. To determine if lysogenization of bacteriophage SfV improved the virulence of *S. flexneri* serotype Y (SFL1339), the virulence of SFL1339 was compared with a SfV lysogen previously created in this serotype Y background (SFL1871). The SfV integrase (*int*) and excisionase (*xis*) genes were previously knocked out of SFL1871, in order to stabilize the lysogen by inhibiting bacteriophage excision (Roberts, PhD thesis, ANU). *In vitro* adherence and invasion assays and *in vivo C. elegans* bacterial

Table 4.4: Comparison of amino acid sequences of predicted tail proteins of *S. flexneri* bacteriophages SfII, SfI, SfIV and SfV.

SfII CDS	% identity with SfI homologue	% identity with SfIV homologue	% identity with SfV homologue
SfII_7 (Hypothetical protein)	97	No homologue	No homologue
SfII_8 (Head-tail connector protein)	100	100	100
SfII_9 (Head-tail adaptor protein)	100	100	100
SfII_10 (Hypothetical protein)	100	100	98
SfII_11 (Hypothetical protein)	98	99	99
SfII_12 (Hypothetical protein)	94	No homologue	68
SfII_13 (Tail sheath protein)	100	100	100
SfII_14 (Hypothetical protein)	100	100	100
SfII_15 (Hypothetical protein)	99	46	98
SfII_16 (Tail protein)	99	24	99
SfII_17 (Tail/DNA circulation protein)	98	98	98
SfII_18 (Tail protein)	99	99	99
SfII_19 (Tail protein)	99	100	99
SfII_20 (Tail protein)	98	99	99
SfII_21 (Tail protein)	99	99	99
SfII_22 (Tail protein)	99	99	98
SfII_23 (Hypothetical protein)	95	95	95
SfII_24 (Tail fibre assembly protein)	92	92	91

accumulation and killing assays were performed to compare the virulence of *S. flexneri* serotype Y and the SfV lysogen.

4.2.2.1 Lysogenization of wild type *S. flexneri* serotype Y by bacteriophage SfV, increases bacterial virulence

4.2.2.1.1 SfV genes enhance the adherence and invasion of *S. flexneri* serotype Y *in vitro*

In vitro adherence and invasion assays were performed using BHK cells (as described in Section 2.10.5) to investigate whether the presence of the SfV genome enhanced the virulence of SFL1339 (serotype Y strain). Results of four independent *in vitro* assays indicated that lysogenization of *S. flexneri* serotype Y by SfV, significantly increased bacterial adherence and invasion (Figure 4.5.A and B). This phenotype was consistently observed across all four repeats however there were large variations in the numerical outputs between repeats. To account for numerical variations between experimental repeats, plate ID was set as the blocking factor and one way ANOVA was used to determine statistical significance. These findings suggest that there are genes within the SfV genome that contribute to bacterial virulence.

4.2.2.1.2 SfV genes increase the accumulation of *S. flexneri* serotype Y in the *C. elegans* intestinal lumina

To determine if the increased adherence and invasion of the SfV lysogen (SFL1871) observed *in vitro* had an effect on bacterial virulence; preliminary *in vivo* studies were carried out in *C. elegans*. Results of the *C. elegans* bacterial accumulation showed pronounced

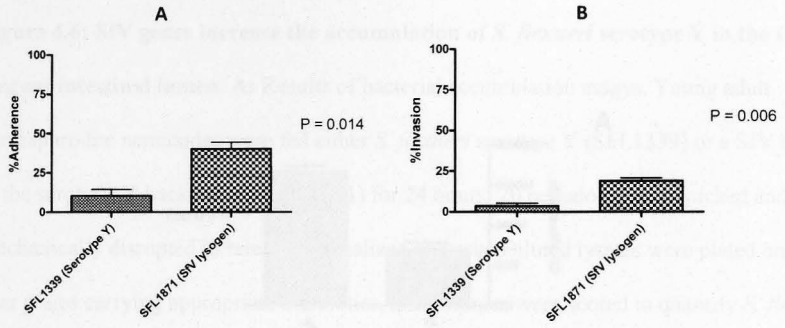

Figure 4.5: Bacteriophage SfV genes play a role in bacterial adherence and invasion *in vitro*. **A:** Adherence of *S. flexneri* serotype Y (SFL1339), compared to a SfV lysogen in SFL1339 (SFL1871), plotted as percentage adherence, a ratio of the number of adherent and intracellular bacteria to the total number of bacterial cells in the infecting inoculum (y-axis). **B:** Invasion of BHK monolayers by SFL1339 and SFL1871, plotted the percentage of the number of intracellular bacteria to the total number of adherent and intracellular bacteria. Lysogenization of *S. flexneri* serotype Y by SfV, results in a significant increase in the adherence and invasion of this strain ($p < 0.05$, one way ANOVA with plate ID set the blocking factor). Results are the means of four independent biological repeats with standard errors (error bars).

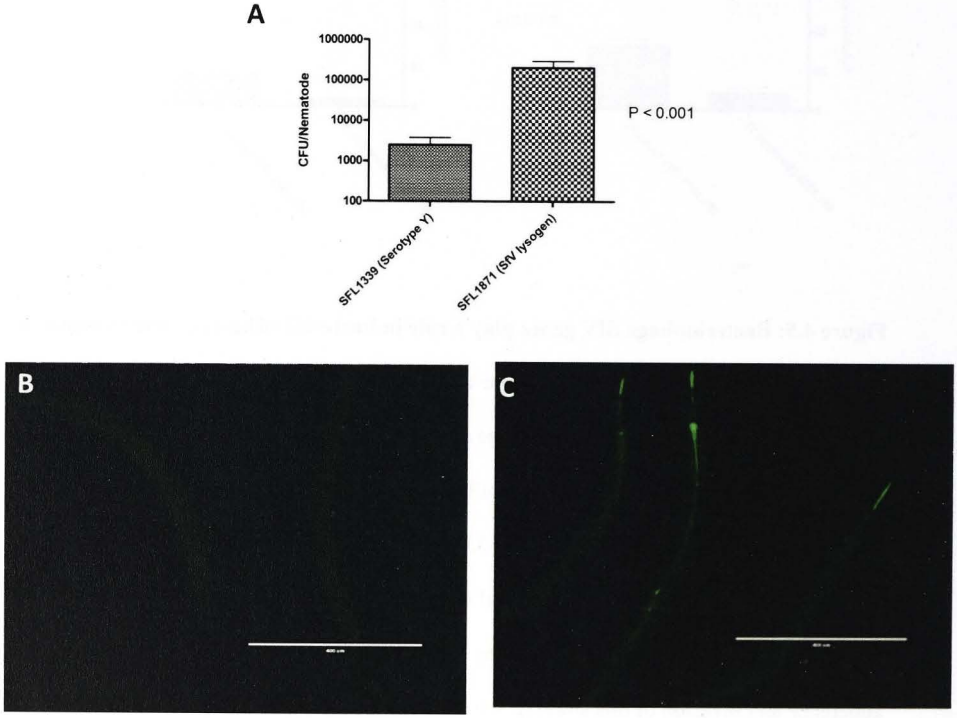
A
1000000
100000
10000
1000
100
CFU/Nematode
P < 0.001
SFL1339 (Serotype Y)
SFL1871 (SfV lysogen)
B
C

Figure 4.6: SfV genes increase the accumulation of *S. flexneri* serotype Y in the *C. elegans* intestinal lumen. A: Results of bacterial accumulation assays. Young adult hermaphrodite nematodes were fed either *S. flexneri* serotype Y (SFL1339) or a SfV lysogen in the serotype Y background (SFL1871) for 24 hours. 20 nematodes were picked and mechanically disrupted to release internalized bacteria. Diluted lysates were plated on LB agar plates carrying appropriate antibiotics, and colonies were scored to quantify *S. flexneri* cells associated with each nematode. Results represent the means of four independent biological repeats. Statistical analysis performed using one way ANOVA with the plate ID set as the blocking factor, shows a significant increase in the accumulation of SFL1871 when compared with SFL1339. **B and C:** Representative images of GFP^+ accumulation assays. Young adult hermaphrodite nematodes infected as above with SFL2503 (SFL1339 expressing GFP^+) and SFL2504 (SFL1871 expressing GFP^+) for 24 hours. Infected nematodes were visualized using the EVOS fluorescence microscope. Nematodes infected with SFL2504 show accumulation of the lysogenized bacterial cells within their intestinal lumina (**C**) while worms infected with SFL2503 have no bacterial cells within their lumina (**B**). Scale bar = 400 μm.

accumulation of the SfV lysogen (SFL1871) within the intestinal lumina of infected worms, compared with *S. flexneri* serotype Y (SFL1339), which was digested by the nematodes (Figure 4.6.A). In order to confirm bacterial accumulation, nematodes were fed GFP^+-tagged SFL1339 and SFL1871 (SFL2503 and SFL2504, respectively) and 20-30 animals were observed using fluorescence microscopy. Worms fed SFL2504 (GFP^+-tagged SFL1871) showed accumulation of GFP^+-tagged bacterial cells within their intestinal lumina (Figure 4.6.C), while no detectable fluorescence was observed in worms fed SFL2503 (GFP^+-tagged SFL1339) (Figure 4.6.B). These results suggest that the virulence of *S. flexneri* serotype Y increases on incorporating the SfV genome into the bacterial genome.

4.2.2.1.3 SfV genes increase *S. flexneri* serotype Y-mediated killing of *C. elegans*

C. elegans liquid killing assays were performed as described previously [284], to determine if the accumulation of SFL1871 in the intestinal lumina of nematodes resulted in increased killing of worms. Results of liquid killing assays indicate that *C. elegans* fed the SfV lysogen (SFL1871), died much faster than worms maintained on serotype Y (SFL1339) ($p < 0.001$, Logrank test) (Figure 4.7). These findings along with the bacterial accumulation suggest that bacteriophage SfV genes enhance the virulence of *S. flexneri* serotype Y in *C. elegans*.

4.2.2.2 Identification of potential SfV genes that contribute to the virulence of its host

Virulence studies indicated that lysogenization of *S. flexneri* serotype Y by SfV increases the virulence of this strain. In order to determine if uncharacterized SfV genes contribute to host virulence, comparative genomics was used to identify 15 uncharacterized, cryptic bacteriophage genes in SfV (Table 4.5 and Figure 4.8.A). Reverse transcription polymerase chain reaction (RT-PCR) was used to determine if the identified cryptic phage genes were

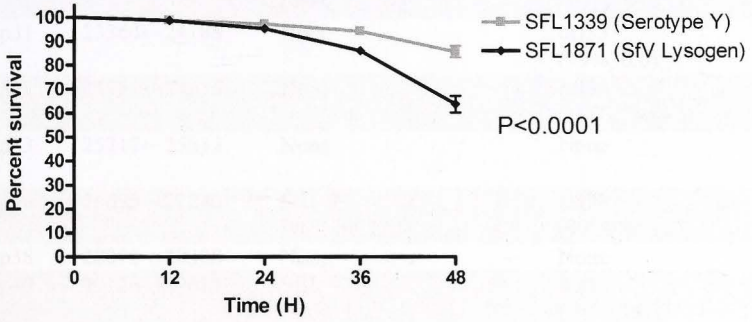

Figure 4.7: Bacteriophage SfV genes increase *S. flexneri* serotype Y-mediated killing of *C. elegans*. Synchronized young, adult, hermaphrodite nematodes were treated with log phase cultures of *S. flexneri* serotype Y (SFL1339) and a SfV lysogen (SFL1871), grown at 37 ºC to express virulence genes. Worms were scored for survival every 12 hours. Results represent data obtained from four independent blind biological repeats each with at least four technical repeats (each technical repeat with 20-50 nematodes) with standard error (error bars). Worms infected with SFL1871 show a significant decrease in survival rates when compared to worms fed SFL1339 ($p < 0.0001$, Logrank test).

Table 4.5: List of uncharacterized genes in bacteriophage SfV

SfV gene	Location	Homologue in SfII (%Identity, E value-BLASTP)	Homologue in SfIV (%Identity, E value-BLASTP)
SfVp28	22042←22347	SfII_32 (100%, 1e-74)	orf30 (100%, 1e-74)
SfVp29	22347←22709	SfII_33 (99%, 6e-90)	orf31 (100%, 6e-91)
SfVp30	22700←23236	SfII_34 (96%, 7e-132)	orf32 (99%, 5e-137)
SfVp31	23364←24188	None	orf33 (99%, 0.0)
SfVp32	24254←24616	None	orf34 (100%, 3e-86)
SfVp33	25217←25513	None	None
SfVp36	26695→27246	SfII_39 (90% 3e-120)	orf39 (90%, 8e-125)
SfVp38	28072→28308	None	None
SfVp40	29126→29614	SfII_42 (94%, 1e-113)	orf42 (94%, 1e-115)
SfVp41	29614→30267	SfII_43 (100%, 5e-168)	None
SfVp42	30264→30590	SfII_44 (95%, 3e-78)	orf43 (96%, 9e-79)
SfVp44	30996→31805	SfII_46 (87%, 7e-178)	orf44 (67%, 2e-126)
SfVp45	31885→32802	SfII_47 (99%, 0.0)	orf45 (99%,0.0)
SfVp47	33818→34012	None	None
SfVp48	34162→35214	None	None

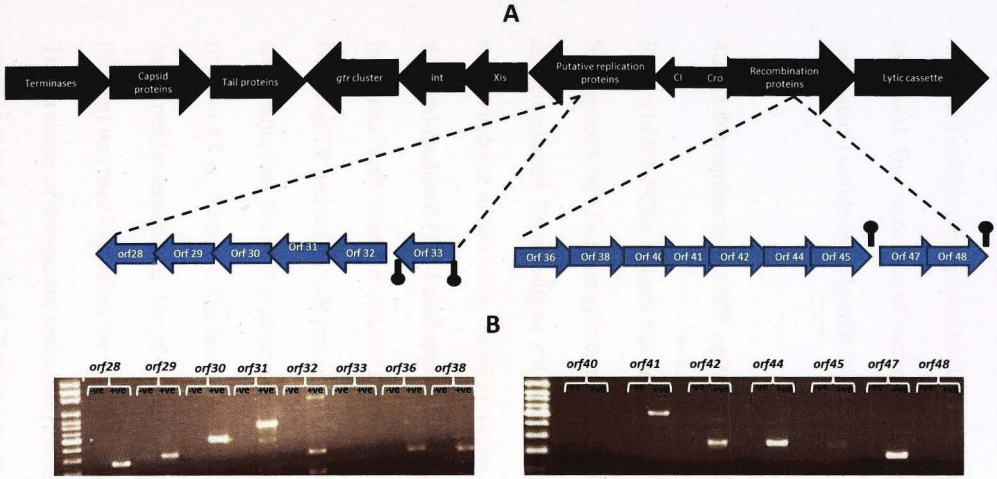

Figure 4.8: Detection of SfV gene expression in the lysogen, SFL1871 by reverse transcriptase PCR (RT-PCR). A: Schematic representation of the SfV genome (black arrows represent functional modules) with the cryptic SfV genes selected for expression study highlighted (blue arrows). Hairpin structures indicate Rho-independent terminators predicted previously [158]. **B:** Expression of cryptic SfV genes within the lysogen (SFL1871) was determined using RT-PCR. Randomly primed cDNA was produced from total RNA isolated from a mid-log phase culture of SFL1871. cDNA was used to set up PCRs with primers specific for SfV genes of interest (+ve). Each set of RT-PCR results was set up with a no reverse transcriptase control (-ve) to check for contamination from the chromosomal DNA. The names of the screened genes of interest appear above the gels. *orf28, orf29, orf30, orf31, orf32, orf36, orf38, orf41, orf42, orf44, orf45, orf47* and *orf48* (13 out of 15 genes screened) are expressed in the lysogen when grown *in vitro* at 37 °C. No PCR products seen in the *orf33* and *40* +ve lanes, suggesting that these two genes are not expressed in the SfV lysogen.

expressed in the host (SFL1871) when grown *in vitro* at 37 °C (*S. flexneri* virulence genes are expressed at this temperature). Results of RT-PCR suggest that 13 out of the 15 uncharacterized genes were expressed in the host grown *in vitro,* under the conditions used (Figure 4.8.B). SfV *orf28*, *orf29*, *orf30*, *orf31*, *orf32*, *orf36*, *orf38*, *orf41*, *orf42*, *orf44*, *orf45*, *orf47* and *orf48* were expressed in the lysogenic strain, while *orf33* and *orf40* were not expressed. The expression of bacteriophage genes in the lysogenized host, suggests that these genes may provide some benefit to the host.

4.2.2.3 Disruption of the SfV *orf28-32* gene cluster in SFL1871

Results of RT-PCRs indicate that *orf28*, *orf29*, *orf30*, *orf31* and *orf32* are all expressed in the SfV lysogen. *orfs28-32* lie upstream of the *gtrV* cluster and all 5 genes are transcribed by the antisense strand. To investigate if the expression of genes within this gene cluster contributed to the virulence of SFL1871, the *orf28-32* five gene cluster was disrupted in SFL1871 using the λ red-mediated PCR-based approach to generate SFL2500 (Δ*orf28-32*) [317]. The insertional inactivation of *orfs28-32* in SFL2500 was confirmed by colony PCR using the GtrB.BglII.R and orf28-32.R primers. The PCR product isolated from SFL2500 is ~ 4.1 kb and smaller than the PCR product isolated from the parent strain, SFL1871 as expected (Figures 4.9.A, B and C). The insertional inactivation of *orfs28-32* in SFL2500 was further confirmed by sequencing. The slide agglutination test using monovalent anti-TypeV antisera (Seiken) was used to confirm the expression of the *gtrV* cluster in Δ*orfs28-32* (SFL2500). The virulence of this mutant strain (Δ*orf 28-32*) was determined using the *in vitro* BHK invasion assays and *in vivo C. elegans* accumulation and killing assays. The presence of virulence plasmids in all strains was confirmed by PCR using *apyI* and *virG* specific primers before each assay performed in this study.

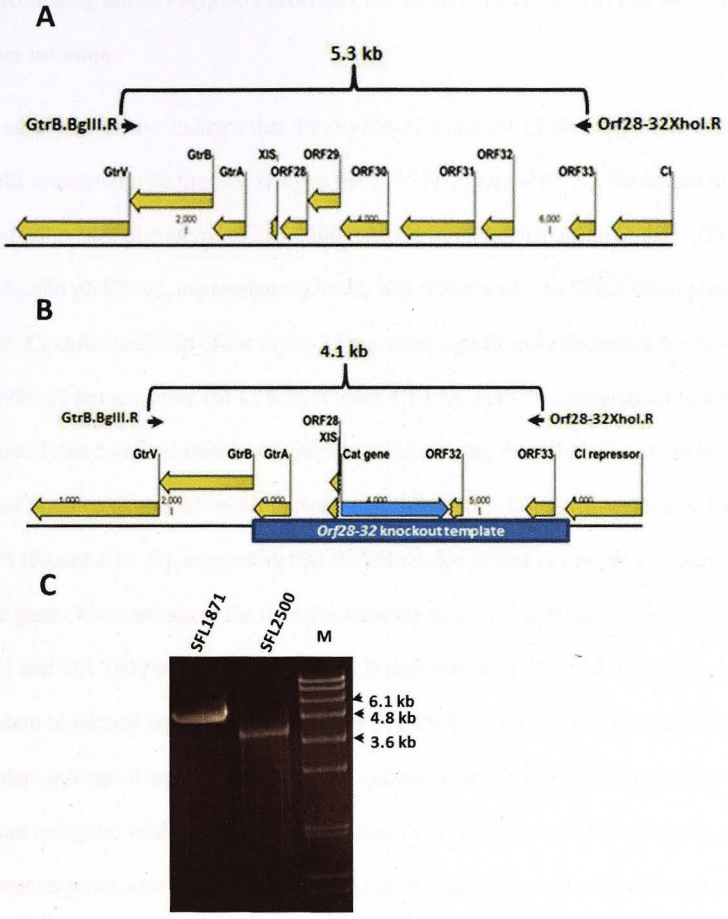

Figure 4.9: Confirming the insertional inactivation of SfV *orfs28-32* in SFL2500. A: A diagrammatic representation of the arrangement of the *orfs28-32* locus in SFL1871. **B:** Diagrammatic representation of the *orf28-32* locus in SFL2500 (Δ*orf28-32*). **C:** Colony PCR-based confirmation of the insertional inactivation of *orfs28-32* in SFL2500 using the GtrB.BglII.R and orf28-32.R primers (indicated by black arrowheads). A 4.1 kb PCR product was successfully isolated form SFL2500 suggesting the insertional inactivation of the *orf28-32* locus.

4.2.2.4 Knocking out SfV*orf28-32* increases the adherence of SFL1871 *in vitro* but decreases invasion

In vitro adherence assays indicate that the Δ*orf28-32* strain (SFL2500) was more adherent to BHK cells compared with the SfV lysogen (SFL1871) (Figure 4.10. A). To ensure that the increased-adherence phenotype of SFL2500 resulted from the disruption of the *orf28-32* genes, plasmid pNV2062, expressing *orf28-32,* was introduced into SFL2500 to generate SFL2506. Complementation of the *orf28-32* mutation significantly decreases the adherence of the *orf28-32* mutant strain (SFL2500) (Figure 4.10.A). These results suggest that the disruption of this 5 gene cluster is responsible for increasing the adherence of the host strain. Results of invasion assays however, indicate that SFL2500 is less invasive than SFL1871 and SFL2506 (Figure 4.10. B), suggesting that the expression of one or several genes in the SfV *orf28-32* gene cluster enhances the invasive capacity of the bacterial host. Results of SFL1871 and SFL2500 in Figures 4.10.A and B represent data obtained from nine independent biological repeats while results of SFL2506 represent data obtained from four independent biological repeats. SFL2506 was generated after five initial experiments were carried out using the wild type and mutant strains alone, therefore only four repeats of the complementation experiment could be carried out in conjunction with the wild type and mutant strain within the given time frame. To account for this unbalanced experimental set up, linear mixed models were generated using REML to compare the virulence of SFL1871, SFL2500 and SFL2506.

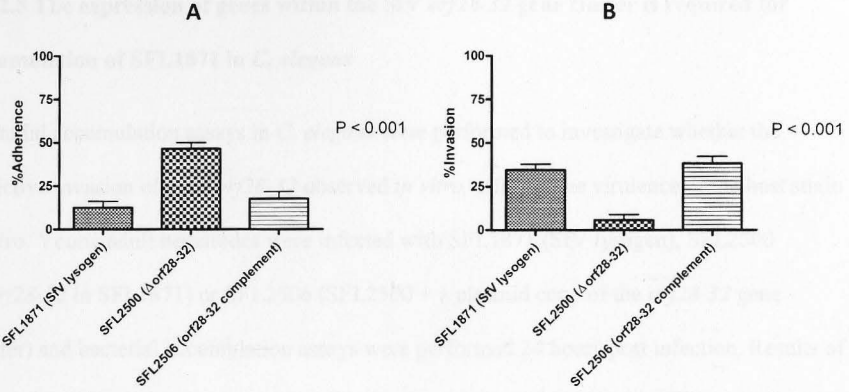

Figure 4.10: Results of *in vitro* assays for SFL1871 (SfV lysogen in serotype Y), SFL2500 (Δ*orf28-32* in SFL1871) and SFL2506 (SFL2500 + plasmid expressing *orf28-32*). A: Adherence of SFL1871, SFL2500 and SFL2506 plotted as percentage adherence, a ratio of the number of adherent and intracellular bacteria to the total number of bacterial cells in the infecting inoculum (y-axis). The adherence of SFL2500 is significantly increased when compared with SFL1871 and SFL2506 ($p < 0.001$, one way ANOVA, with post hoc LSD Test). **B:** Invasion of BHK monolayers by SFL1871, SFL2500 and SFL2506, plotted as a percentage of the number of intracellular bacteria to the total number of adherent and intracellular bacteria. SFL2500 is significantly less invasive than SFL1871 and SFL2506 ($p < 0.01$, One Way ANOVA, with post hoc LSD Test). Results are the means of at least three independent biological repeats with standard errors (error bars). Linear mixed models were generated using REML to compare the virulence of these strains as the number of experimental repeats per strain was unbalanced.

4.2.2.5 The expression of genes within the SfV *orf28-32* gene cluster is required for accumulation of SFL1871 in *C. elegans*

Bacterial accumulation assays in *C. elegans* were performed to investigate whether the defective invasion of the Δ*orf28-32* observed *in vitro,* affected the virulence of the host strain *in vivo.* Young adult nematodes were infected with SFL1871 (SfV lysogen), SFL2500 (Δ*orf28-32* in SFL1871) or SFL2506 (SFL2500 + a plasmid copy of the *orf28-32* gene cluster) and bacterial accumulation assays were performed 24 hours post infection. Results of bacterial accumulation assays suggest that the Δ*orf28-32* strain (SFL2500) is less virulent than the SfV lysogen (SFL1871) *in vivo,* as SFL2500 showed reduced accumulation when compared with SFL1871 (Figures 4.11.A). Bacterial accumulation was restored on complementation of Δ*orf28-32* in SFL2506 suggesting that the expression of one or several of these genes is essential for bacterial virulence. Results of SFL1871 and SFL2500 in Figures 4.11.A represent data obtained from seven independent biological repeats while results of SFL2506 represent data obtained from three independent biological repeats. To account for this unbalanced experimental set up, linear mixed models were generated using REML to compare the virulence of SFL1871, SFL2500 and SFL2506.

SLF2500 was tagged with GFP^+, in SFL2505 and worms infected with this strain were compared with nematodes infected with SFL2504 (GFP^+-tagged SFL1871) using fluorescence microscopy. SFL2505 cells appear to accumulate in the nematode pharynx but failed to accumulate in the nematode intestinal lumen (Figure 4.11.C) while SFL2504 cells accumulated in the intestinal lumina of infected worms (Figure 4.11.B). These results suggest that the expression of SfV genes within the *orf28-32* cluster enhances the virulence of its host strain. GFP^+ accumulation assays could not be carried out on the complemented strain as the plasmid used for complementation of the *orf28-32* mutation was not compatible with the plasmid expressing GFP^+.

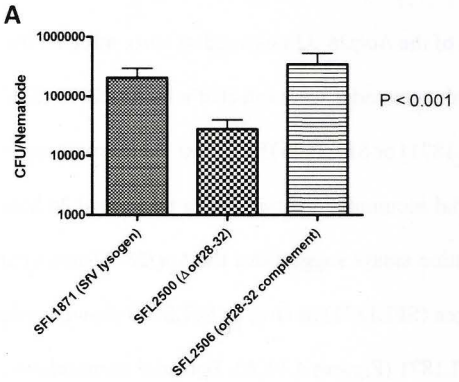
A
1000000
100000
10000
1000
CFU/Nematode
P < 0.001
SFL1871 (SfV lysogen)
SFL2500 (Δorf28-32)
SFL2506 (orf28-32 complement)

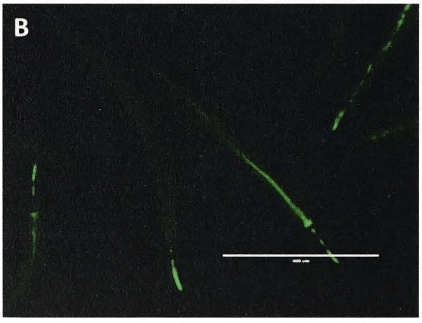
B

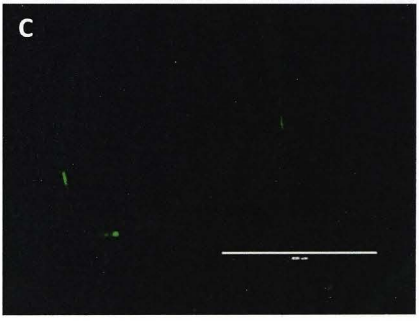
C

Figure 4.11: Expression of SfV *orfs*28-32 is required for accumulation of SFL1871 in the intestinal lumen of *C. elegans*. **A:** Results of bacterial accumulation assays. Young adult hermaphrodite nematodes were fed the SfV lysogen of serotype Y (SFL1871), Δ*orf 28-32* (SFL2500) or its complement, SFL2506 (SFL2500 + a plasmid copy of *orf28-32*) for 24 hours. 20 nematodes were picked and mechanically disrupted to release internalized bacteria. Diluted lysates were plated on LB agar plates carrying appropriate antibiotics, and colonies were scored in order to quantify *S. flexneri* cells associated with each nematode. There is a significant decrease in the accumulation SFL2500 compared with SFL1871 and SFL2506 ($p < 0.001$, one way ANOVA with post hoc LSD Test). Results are the means of at least three independent biological repeats with standard errors (error bars). Linear mixed models were generated using REML to compare the virulence of these strains as the number of experimental repeats per strain was unbalanced. **B and C:** Representative images of GFP^+ accumulation assays. Young adult hermaphrodite nematodes infected as above with SFL2504 (SFL1871 expressing GFP^+) and SFL2505 (SFL2500 expressing GFP^+) for 24 hours. Infected nematodes were visualized using the EVOS fluorescence microscope. Nematodes infected with SFL2504 show accumulation of the lysogenized bacterial cells within their intestinal lumina (**B**) while worms infected with SFL2505 have no bacterial cells within their lumina (**C**). Scale bar = 400 μm.

4.2.2.6 The expression of genes within the SfV *orf28-32* gene cluster is not required for the SFL1871-mediated killing of *C. elegans*

Liquid killing assays were performed (Section 2.13.4) to determine if the decreased accumulation of SFL2500 in the nematode intestinal lumina had an effect on nematode killing. Results of liquid killing assays suggest that genes within the *orf28-32* gene cluster are not essential for nematode killing, as nematodes fed SFL2500 showed similar survival rates as worms fed SFL1871 ($p = 0.0621$, Logrank test) (Figure 4.12). The results of *in vivo* bacterial accumulation assays are consistent with *in vitro* invasion data and suggest that the expression of SfV-encoded *orf28, orf29, orf30, orf31* and/or *orf32* enhances the virulence of the host strain at the onset of infection. Results of nematode killing assays however suggest that the expression of these genes has no effect on prolonged infection.

4.3 Discussion

4.3.1 Complete Genome Sequence of SfII

In this chapter, bacteriophage SfII, isolated from a virulent *S. flexneri* 2a serotype, strain NCTC4 [156], was completely sequenced. Previous electron microscopy data [156] shows that SfII morphologically resembles bacteriophages belonging to group A1, comprising the family *Myoviridae* and order *Caudovirales* [359]. SfII confers its host with the serotype-converting O-antigen modifying glucosyltransferase (*gtr*) genes. Not much is known about temperate bacteriophages of *S. flexneri* outside their role in serotype conversion. To further our understanding of *S. flexneri* phages, the genome of SfII was compared to the genomes of other lambdoid phages.

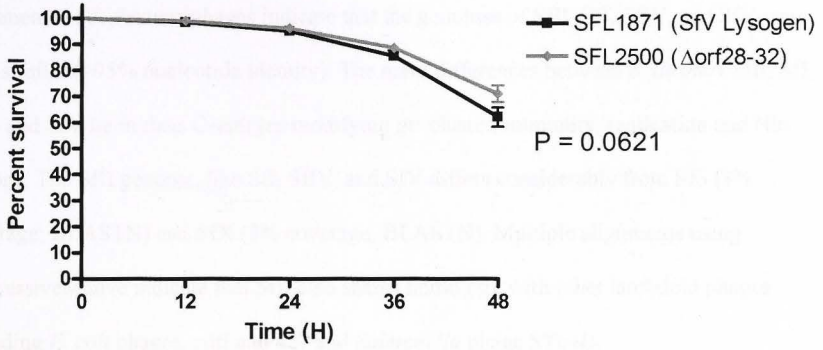

Figure 4.12: SfV *orfs28-32* are not required for *S. flexneri*-mediated killing of *C. elegans*. Synchronized young, adult, hermaphrodite nematodes were treated with log phase cultures of a SfV lysogen in a serotype Y background (SFL1871-in black) or Δ*orf28-32* in SFL1871 (SFL2500-in grey) grown at 37 ºC to express virulence genes. Worms were scored for survival every 12 hours. Results represent data obtained from three independent biological repeats each with at least four technical repeats (each technical repeat with 20-50 nematodes) with standard error (error bars). No significant differences in survival rates of worms infected with SFL2500 and SFL1871 ($p = 0.0621$, Logrank test) we observed.

Nucleotide and protein homology searches with other published *S. flexneri* phage genomes indicate that SfII, like SfV, SfI, SfIV, Sf6 and SfX, is a member of the temperate, lambdoid group of bacteriophages with conserved arrangements of early and late genes. Genome alignments of *S. flexneri* phages indicate that the genomes of SfII, SfI, SfIV, and SfV were very similar (>95% nucleotide identity). The main differences between *S. flexneri* SfII, SfI, SfIV and SfV lie in their O-antigen modifying *gtr* cluster, immunity, replication and Nin regions. The SfII genome, like SfI, SfIV, and SfV differs considerably from Sf6 (3% coverage; BLASTN) and SfX (5% coverage; BLASTN). Multiple alignments using progressiveMauve indicate that SfII also shares homology with other lambdoid phages including *E. coli* phages, cdtI and ϕ27 and *Salmonella* phage ST64B.

The entire SfII can be divided into 6 functional modules based on the predicted functions of coding regions. Each functional module of bacteriophage SfII is discussed in subsequent sections.

4.3.1.1 DNA packaging

Experiments in the 1970's suggest that during the assembly of phage particles, phage DNA is inserted into a preformed protein shell, known as the procapsid or prohead [360, 361]. Packaging of bacteriophage DNA into procapsids is driven by the hydrolysis of ATP which involves two bacteriophage proteins namely, the large and small terminases. These terminases recognize DNA for packaging, translocate the DNA to the proheads and transfer it into the porheads through a ring of portal proteins.

SfII_1 and SfII_2, encode phage small and large terminase subunits, respectively. The amino acid sequences of the small and large terminases of phages SfII, SfI, SfIV and SfV, are very similar (>98% amino acid identity), which suggests that these phages use the same packaging mechanisms. Analysis of the SfII nucleotide sequence show cohesive end (*cos*) sites spanning the 59 bp-125 bp region adjacent to the terminases. These findings provide strong evidence suggesting that SfII, like SfI, SfIV and SfV, uses the bacteriophage lambda-like packaging mechanism where, virion genomes are generated by *cos* site-specific DNA cleavage at the beginning and end of every packaging event.

4.3.1.2 Structural proteins

SfII_3 encodes a putative integral membrane protein which is also present in the SfI and *Salmonella* ST64B genomes. The function of this protein remains unknown but based on the location of this gene in the genome; it is possible that SfII_3 encodes a protein required for DNA packaging. SfII_4, SfII_5 and SfII_6, encoding phage portal protein, prohead protease and major capsid protein, respectively are conserved between SfI, SfIV, ST64B and *E. coli* phage, HK97. Little homology was found between the SfII_4, SfII_5 and SfII_6 and SfV *orf*s 3, 4 and 5. The SfII portal protein (SfII_4), proheads protease (SfII_5) and major capsid proteins (SfII_6) consist of 371, 228 and 401 amino acids, respectively, while their SFV counter parts consist of 424, 200 and 409 amino acids, respectively. Pairwise alignments of the SfII and SfV portal and capsid proteins show several amino acid changes between the two *S. flexneri* phages. These proteins are required for successful assembly of the capsid as well as the condensation of DNA within the capsid.

The size and sequence variations between the SfII and SfV portal, prohead protease and major capsid proteins suggest that the procapsid assembly mechanism used by these two *S.*

flexneri phages could vary. However, it should be noted that it is not uncommon for divergent homologues of the lambdoid phage family to vary significantly in their amino acid sequences yet maintain function. For instance, the crystal structures of several portal proteins from tailed bacteriophages showing little amino acid similarity, show similar polypeptide folds of their central domain which leads to the belief that they are highly divergent homologues [362]. Thus although the SfII and SfV portal and capsid proteins do not show sequence similarities, these proteins could be divergent homologues showing conserved structures and functions.

SfII_7-24, encoding proteins required for tail structure and assembly, have homologues in Sfl, SfIV, SFV, HK97, ST64B and ϕP27 phages (Figure 4.3). Host recognition by tailed phages occurs through interactions between attachment sites on tail proteins and host receptors molecules. The amino acid sequences of the tail proteins of SfII, Sfl, SfIV, and SfV were compared to identify differences in the tail proteins of these phages. Most of the tail proteins of *S. flexneri* infecting phages are over 95% identical at the amino acid level. This would suggest that these phages possibly infect the same bacterial host strains. Interestingly, the host range of all four phages vary considerably, with SfV showing the broadest host range (capable of infecting serotypes 1a, 1b, 2a, 2b, 3b, 4b, and Y), followed by SfIV (which infects serotypes 1a, 1b, 1c, X and Y), SfII (infects serotypes 3a, 5a and Y) and Sfl (infecting serotypes X and Y). SfII_24, which encoded the tail fibre assembly protein shows <91% identity with homologues in Sfl, SfIV and SfV. The phages tail fibre is an important phage protein that binds to bacterial receptors for adsorption [363-365]. A recent study in *P. aeruginosa* phages, PαP1 and JG004, reported that a single point mutation in the tail fibre assembly proteins of these phages, significantly alters their host ranges [366]. Therefore it is

likely that the varied host ranges of *S. flexneri* phages is due to amino acid changes in their tail fibre proteins.

4.3.1.3 O-antigen modification

SfII_27 encodes *gtrII*, the gene responsible for the type specific modification of the O-antigen in *S. flexneri* 2a strains. SfII_28, 29, 30 and 31 were identified as *gtrB*, *gtrA*, integrase and excisionase, respectively. Homologues of these genes were seen in other lamboid phages including SfI, SfIV, SfV, Sf6, SfX and *Salmonella* phages e34, ST64T and ST104. As expected no similarity was observed between *gtrII* and the type-specific O-antigen modifying gene of *S. flexneri* phages. *gtrA* and *gtrB* on the other hand appear to be highly conserved among several lambdoid phages.

4.3.1.4 Early Regulatory elements in SfII

SfII_37, 38 and 39 are homologous to phage regulatory proteins, cI, Cro and cII, respectively. This suggests that SfII like SfI, SfIV, SfV and most other lambdoid phages, uses the lambda-like repression model to regulate gene expression. In lambdoid phages, the *cI* and *cro* genes lie adjacent to each other and are transcribed in opposite directions, thereby regulating the expression of early and late phage genes, respectively [367]. This regulatory cascade, therefore determines whether the phage follows the lytic or lysogenic pathway. The binding of cI repressor molecules to operator sequences flanking the *cI* genes, promotes lysogeny and inhibits the transcription of late genes [367]. The Cro protein has higher affinity to the operator sequence flanking *cI*, thus it dislodges the cI repressor from this operator and prevents further expression of the cI repressor. This in turn, promotes the transcription of late genes which trigger the lytic pathway.

Homologues of cIII and N proteins, other lambda regulatory elements, although present in SfI, were not observed in SfII. The N protein is an important protein in the regulation of bacteriophage λ, as this protein allows RNA polymerase to transcribe several phage genes, including cII and cIII, genes required for DNA recombination and integration of the prophage [368, 369]. The presences of a Rho-independent terminator downstream of the *cI* gene (SfII_37), suggests that one of the hypothetical protein SfII_32-36, although not homologous to N, could potentially perform the function of the N protein in bacteriophage SfII.

4.3.1.5 DNA Replication

SfII_41-46, encompass the DNA replication module of bacteriophage SfII as these genes encode proteins homologous to known replication proteins (Table 4.1). Based on BlastX results the following putative functions were assigned; SfII_41 (phage-O protein family), SfII_42 (putative transcriptional activator), SfII_43 (DNA adenine methylase), SfII_44 (LexA like DNA-binding protein), SfII_45 (RusA-DNA recombination and holiday junction resolvase), SfII_46 (KilA-N domain protein-a DNA binding protein transcription activator). The arrangement of genes in the replication modules of SfII and SfI vary significantly (Figure 4.4). The arrangement of replication genes in SfII, SfIV and SfV are similar with the main differences being SfII_42, 43 and 45 homologues are not present in SfIV and SfII_41 has no homologue in SfV.

In bacteriophage λ, the origin of replication lies in the middle of the phage replicative O gene, similarly, in SfII, the nucleotide sequence of SfII_41 contains direct repeats (TTCTGACCCGTCAAAA; nt 30,935-30,949; 30,950-30,964 and 30,965-30,979) which are

characteristic features of an origin of replication. This suggests that SfII_41 is an initiator of bacteriophage DNA replication similar to the lambdoid O protein [370].

4.3.1.6 Late Regulatory elements in SfII

The late regulatory module of SfII has an organization similar to that of other lambdoid phages. SfII_48, encodes the phage antiterminator Q, a protein that regulates the expression of lytic proteins in lambdoid phage. SfII_51-54, encode the phage lytic genes; holin, lysin, RZ and RZ1, respectively. The SfII lytic cassette is highly similar to the lytic cassettes of SfIV, SfV, ST64B and bacteriophage λ.

SfII_58 encodes a HNH endonuclease domain protein which has homologues in SfI, SfIV and SfV. This gene is also present in lambdoid phages HK97, Mu, ϕP27, and *Salmonella* phage ST64B. The HNH domain has been identified in a range of DNA-binding proteins, performing DNA binding and cleavage functions [371, 372]. The precise function of this protein in lambdoid phages has not yet been elucidated but it has been proposed that this DNA-binding protein could play a role in controlling the timing of lysis [157].

4.3.1.7 Genes unique to SfII

Analysis of the SfII genome sequence identified several proteins which did not have homologues in other *S. flexneri* phages. The following genes are unique to SfII; SfII_25 (acyltransferase), SfII_27 (*gtrII*), SfII_26, SfII_55 and SfII_56 (insertion elements) and SfII_35, SfII_36, SfII_40, SfII_49, SfII_ 50 and SfII_57 (hypothetical proteins). It will be

interesting to study these hypothetical proteins in the context of bacteriophage evolution and *S. flexneri* serotype 2a pathogenesis.

4.3.2 Characterizing cryptic SfV genes and the identification of novel SfV-encoded virulence factors

4.3.2.1 Lysogenization of wild type *S. flexneri* serotype Y by bacteriophage SfV, increases the virulence of the host strain

To determine if the presence of bacteriophage SfV in a *S. flexneri* serotype Y strain (SFL1339) had an effect on the virulence of this strain, virulence assays were performed using the serotype Y strain and an SfV lysogen (SFL1871) created in the serotype Y background. Results of *in vitro* cell culture and *in vivo C. elegans* virulence assays indicate that lysogenization of SFL1339 by SfV significantly increases the virulence of this strain. These findings suggest that bacteriophage SfV genes contribute to the virulence of its host. The presence of the 220 kb virulence plasmid in both SFL1871 and SFL1339 was confirmed using PCR to amplify *apyI* and *virG* prior to each virulence study, to ensure that both strains carried intact virulent plasmids. However, the stability of the virulence plasmid in these strains was not tested over the course of each experiment; therefore although unlikely, we cannot rule out the possibility that SFL1339 harbors an unstable virulence plasmid. The loss of the virulence plasmid from SFL1339 would also result in the phenotypes observed in this study. However, based on prior knowledge of bacteriophage genes increasing the virulence of a plethora of bacterial hosts (Sections 1.7.3 and 1.7.4), it is likely that lysogenization of *S. flexneri* serotype Y with SfV increases the virulence of the host strain.

West and colleagues have previously shown that the phage-encoded glucosylation of *S. flexneri* O-antigen, shortens the LPS molecule which in turn enhances the T3SS function and promotes bacterial invasion [353]. The SfV lysogen used in this study (SFL1871) carries the *gtrV* cassette therefore it is possible that O-antigen modification of the lysogen would increase the virulence of this strain. The focus of this study, however, was to identify uncharacterized SfV genes and determine if any of these genes contribute to host virulence. Therefore we proceeded to identify uncharacterized SfV genes and determine if any of these genes were expressed in the lysogen.

4.3.2.2 Uncharacterized SfV genes expressed in the SfV lysogen, SFL1871

To determine if SfV genes outside of the *gtrV* cluster contribute to the pathogenesis of the lysogen (SFL1871), RT-PCR was performed to identify uncharacterized SfV genes that were expressed by the lysogenic strain grown at 37 °C (Figure 4.8.B). 15 uncharacterized genes (*orf28, orf29, orf30, orf31, orf32, orf33 orf36, orf38, orf40, orf41, orf42, orf44, orf45, orf47* and *orf48*) were selected for expression screening by RT-PCR based on prior knowledge of gene expression throughout the phage lifecycle (Figure 4.8.A).

orf28-32 which encompass a 5 gene cassette lying downstream of the O-antigen modifying cluster, was selected for expression screening as these genes encode hypothetical proteins of unknown functions with homologues in a number of prophage-related genes in *E. coli* and *Salmonella* spp. Furthermore, this gene cassette is also present in *S. flexneri* phage SfIV and the *E. coli* phage cdtI. This conservation across multiple prophage and phage genomes potentially suggest an essential function of these genes. RT-PCR-based expression screening

indicates that the *orf28-32* gene cassette is expressed in the SfV lysogen, suggesting that these genes maybe beneficial to the host.

orf33 and *orf47-48* were previously identified to form part of morons [158]. Morons are transcriptionally independent units that are believed to be expressed in prophages, and their expression has been proposed to confer a selective advantage on the host [373]. Therefore these genes were included in the expression screen. Results of RT-PCRs indicate that *orf33* is not expressed in the SfV lysogen while *orf47* is expressed and *orf48* is weakly expressed (Figure 4.8.B). *orf33* is unique to SfV and no homologues of this gene were seen in *S. flexneri* phages SfI, SfII and SfIV. Although BlastP analysis of the Orf33 amino acid sequence identified similar hypothetical proteins in *E. coli* and *Salmonella* prophages, analysis of the *orf33* sequence failed to identify a ribosome binding site (RBS) upstream of this Orf, which suggests that this Orf could have been previously mis-annotated [158]. Therefore the fact that *orf33* was not expressed in the lysogen could simply be because this region fails to encode a protein.

orf41 and *orf48* were selected as they encode proteins showing high identity to DNA adenine methyltransferases (Dam). Dams have been shown to play an important role in the virulence of a number of pathogens including *Salmonella*, *Haemophilus, Yersinia* and *Vibrio* species and in pathogenic *E. coli* [374, 375]. Both *orf41* and *orf48* were identified to be expressed in the SfV lysogen, suggesting that the bacteriophage SfV-encoded Dams may play an important role in the virulence of *S. flexneri* strains.

SfV *orf36, orf40, orf42, orf44* and *orf45* were selected for expression screening as these genes encode hypothetical proteins, many of which have DNA-binding sites. Furthermore, these genes are also present in SfII and SfIV suggesting an important role in *S. flexneri* phage biology. SfV *orf38* shares homology with a hypothetical protein with unknown function present in several *E. coli* and *Salmonella* prophages. This gene is unique to SfV therefore it was included in the expression screen. Results of RT-PCRs indicate that all the above genes except *orf40* are expressed in the SfV lysogen.

Homologues of *orf40* are also present in SfII (SfII_42) and SfIV (*orf42*). BlastP analysis of the amino acid sequence of Orf40 identified this protein as a member of the *perC* transcriptional activator family of proteins. The PerC protein of EPEC has been previously identified as an activator of the locus of enterocyte effacement (LEE) pathogenicity island [376], which encodes the T3SS required for the virulence of EPEC [377]. The chromosome of EPEC strains encodes several copies of PerC-like protein showing varying degree of similarities to PerC, all located within prophages or porphage-like regions scattered throughout the chromosome [376]. SfV Orf40 shows limited homology to EPEC PerC (32% identity) therefore it is possible that there are other copies of PerC-like proteins within the *S. flexneri* chromosome, that activate the expression of the T3SS. In this case, the SfV-encoded *perC* gene would be redundant and its expression would not benefit the host, this could explain why *orf40* is not expressed in the lysogen.

Attempts were made to generate knockout templates to disrupt all 13 genes identified as expressed in the SfV lysogen but only the *orf28-32* cassette could be successfully knocked out within the given time frame.

4.3.2.3 Construction of *orf28-32* knockout mutant, SFL2500

In the SfV genome, *orf28, orf29, orf30, orf31* and *orf32* are transcribed from the antisense strand. SfV sequence analysis by Aillison *et al* [158], identified no terminator sequences in the *orf28-32* region. This finding coupled with the expression of all five genes in the lysogen, suggests that these genes could form part of an operon. Since *orf28, orf29, orf30, orf31* and *orf32* were all identified to be expressed in SFL1871, we decided to knockout this 5 gene cassette as a preliminary step to identify if the expression of any of these genes contributed to the virulence of the host strain. The o*rf28-32* locus was successfully disrupted in SFL2500 using the λ red-mediated PCR-based approach [317]. Attempts were also made to knockout each of these genes individually. Although *orf29, orf30* and *orf32* were successfully disrupted in SFL1871, the virulence plasmids were lost from all of these mutant strains. Therefore they could not be used for further virulence studies.

4.3.2.4 Predicted role of SfV Orfs28-32 in bacterial hosts

Virulence assays performed in this study suggest that the expression of one or several genes in the *orf28-32* gene cluster is required for bacterial invasion *in vitro* and for accumulation in *C. elegans*. *In vitro* adherence assays however indicate that knocking out *orf28-32* increases the adherence of the SfV lysogen. The increased adherence of SFL2500 (Δ*orf28-32*), suggests that the expression of one or several of these genes could potentially repress the expression of bacterial adherence factors. BalstP and conserved domain (CDD) searches [378] were performed to identify the possible functions of Orf28, Orf29, Orf30, Orf31 and Orf32.

4.3.2.4.1 *orf28* encodes a putative DNA-binding protein that could negatively regulate the expression of host genes

BlastP analysis of Orf28 identified homologues of this protein, annotated as hypothetical and DNA-binding proteins in *E. coli* and *S. flexneri* prophages. CDD searches identified the presence of the N-terminal region of the Herpes-ICP4 protein in Orf28 (Figure 4.13.A). The ICP4 family of viral proteins is required for the transcription of early and late viral genes in the Herpes simplex virus (HSV) [379]. The N-terminal region of ICP4 contains sites for DNA-binding and the binding of ICP4 represses transcription from three Herpes genes (LAT, ICP4 and ORF-P). These genes have high affinity-ICP4 binding sites spanning their transcription initiation regions [380-382]. Faber and Wilcox identified the ICP4 binding sites upstream of the *icp4* mRNA start site using DNA-binding immunoassays [380]. They compared the sequence of ICP4 binding sites in different strains of HSV and proposed a consensus sequence; nnATCGTCnnYnCCGRCnnCRYCR where, n represents positions with no apparent consensus; R- represents purines at these positions; Y- represents pyrimidines at these positions. BlastN analysis failed to identify the above consensus sequence in published whole genome sequences of *S. flexneri* serotypes 2a and 5a.

The presence of an N-terminal ICP4 domain in Orf28 coupled with its homology to several bacterial DNA-binding proteins, suggests that this protein may be a transcriptional repressor of host gene expression. The expression of *orf28* in the SfV lysogen (SFL1871) could have a negative effect on the expression of bacterial proteins required for adherence. This hypothesis could explain why *orf28-32* mutant cells show increased bacterial adherence. Further studies to identify potential Orf28 binding sites in the host chromosome, would provide valuable

information regarding bacteriophage-mediated regulation of host virulence genes and the possible identification of novel *S. flexneri* adherence factors.

4.3.2.4.2 *orf29* encodes a hypothetical protein that may be involved in RNAi-based immunity

BlastP analysis indicated that Orf29 encodes a hypothetical protein present in numerous *E. coli* and *Salmonella* prophages. CDD searches identified a Cas10_III domain in the N-terminal region of Orf29 (Figure 4.13.B) and a DUF551 domain (domain of unknown function) in the C-terminal region of Orf29. Cas10_III is a member of the CRISPR (Clustered Regularly Interspaced Short Palindromic Repeats) and Cas (CRISPR associated proteins) protein system in prokaryotes. The CRISPR/Cas system (CASS) is a mechanism of defense against invading phages [383-385] and it has been hypothesized that this system functions like the eukaryotic RNAi systems [386]. It has also been proposed that the *cas* genes encode proteins required for the prokaryotic siRNA-like system [386]. Cas10 protein is the largest subunit of Type 3 CRISPR-Cas systems and is homologous to polymerases and cyclases but the actual biochemical activity of Cas10 remains unknown [387]. The presence of a Cas10 domain in SfV Orf29, could suggest that this protein is involved in the RNAi-based immunity of the lysogen, if this is the case, the expression of this gene in the lysogen would be to prevent infection by other phages.

It remains unclear at this stage whether the expression of *orf29* is responsible for the phenotypes observed in this study. However, the presence of a Cas10_III domain in Orf29 and the conservation of *orf29* across *S. flexneri* phages, SfII (*SfII_33*) and SfIV (*orf_31*) and

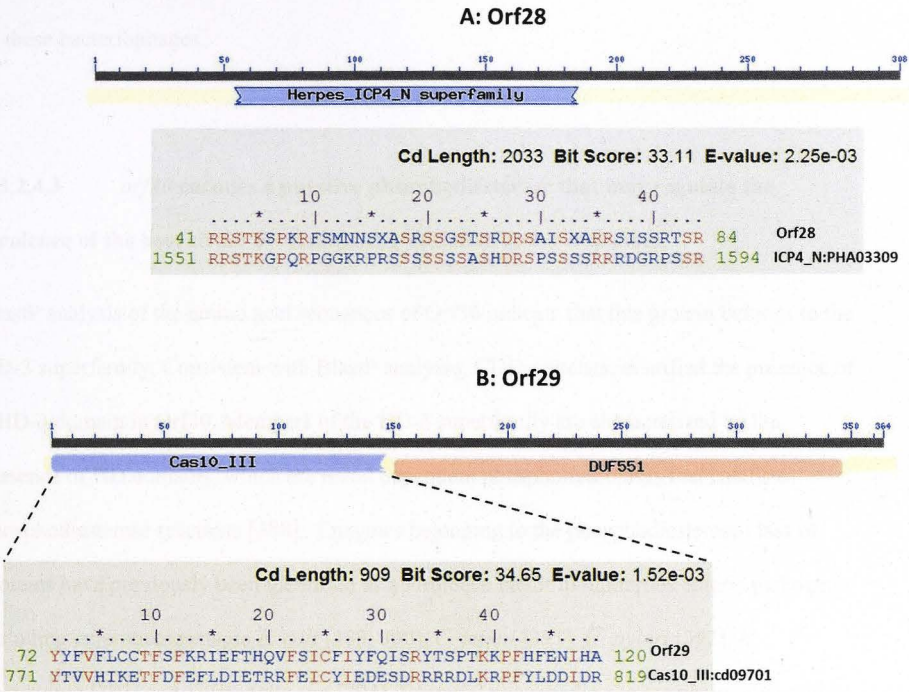

Figure 4.13: Results of conserved domain searches of SfV Orf28 (A) and Orf29 (B). Conserved domain searches were performed using the NCBI Conserved Domain Database (CDD), to identify the potential functions of SfV Orf28 and Orf29. **A:** CDD searches identified a Herpes ICP4 N-terminal domain in Orf28. **B:** A cas10_III domain was identified in SfV Orf29. Amino acid sequence alignments of identified conserved domains are presented below each gene with the conserved amino acids in red.

E. coli phages cdtI (*gp36*), could suggest a new conserved RNAi-based immunity mechanism in these bacteriophages.

4.3.2.4.3 *orf30* encodes a putative phosphodiesterase that may regulate the virulence of the host strain by modulating oxidative stress responses

BlastP analysis of the amino acid sequences of Orf30 indicate that this protein belongs to the HD-3 superfamily. Consistent with BlastP analyses, CDD searches identified the presence of a HD-3 domain in Orf30. Members of the HD-3 superfamily are characterized by the presence of HD domains, which are metal dependent phosphohydrolases that catalyze phosphodiesterase reactions [388]. Enzymes belonging to the phosphodiesterase class of proteins have previously been identified as a virulence factor in numerous enteric pathogens including enterohemorrhagic *E. coli* [389, 390], *C. jejuni* [391], *H. pylori* [392], *K. pneumonia* [393] and *Salmonella* spp [394]. Bacterial phosphodiesterases positively regulate the oxidative stress response by modulating cyclic di-GMP (c-di-GMP) levels [395, 396]. In bacteria, c-di-GMP is an important second messenger regulating the expression of genes involved in several essential functions including cell surface remodeling and adhesion [396], biofilm formation [397, 398], and the virulence of animal and plant pathogens [399, 400].

The predicted HD-3 domain in SfV Orf30 suggests that this protein may exhibit phophodiesterase activity which could influence the virulence of the host strain. If this were the case, the absence of Orf30 in SFL2500 would lead to decreased resistance to oxidative stress which in turn would decrease the virulence of this strain. Further virulence studies

using an *orf30* knockout mutant need to be conducted to determine if Orf30 modulates the virulence of the host.

4.3.2.4.4 *orf31* and *orf32* encode hypothetical protein with unknown functions

BlastP and CDD searches identify Orf31 as a member of the DUF2303 superfamily of proteins. Members of the DUF2303 family of proteins are hypothetical proteins with conserved domains. BlastP analysis identified homologues of Orf32 in several *E. coli* and *Salmonella* prophages annotated as hypothetical proteins. CDD analysis identified no conserved domains in Orf32. It remains unclear at this stage whether Orf31 or Orf32 are responsible for the virulence phenotypes observed in this study.

Although CDD searches provide some insight into the potential roles of these hypothetical proteins it should be noted that the observed e-values are not very small. Thus the above predicted functions of SfV *orf28, orf29, orf30, orf31* and *orf32* remain speculatitive at this stage and require further experimental verification.

4.4 Conclusion

In this chapter the complete genome sequence of *S. flexneri* bacteriophage, SfII was determined. Nucleotide and protein homology searches with other published *S. flexneri* phage genomes indicate that SfII, like SfI, SfIV, SfV, SfX and Sf6, is a member of the temperate, lambdoid group of bacteriophages with conserved arrangements of early and late genes. Although the SfII genome shares similarities with SfI, SfIV and SfV, the host ranges of all

four phages differ significantly, with SfV showing a much broader host range than the other three phages. The main differences between *S. flexneri* SfII, SfI, SfIV and SfV lie in their O-antigen modifying *gtr* cluster, immunity, replication and Nin regions.

While the SfII genome was being sequenced, virulence studies were carried out in the completely sequenced *S. flexneri* phage SfV. Preliminary virulence studies using a *S. flexneri* serotype Y and an SfV lysogen in the same background, indicated that genes within the SfV genome increase the virulence of the host strain. 15 uncharacterized SfV genes were selected as virulence candidate genes. RT-PCR analysis identified 13 out of the selected 15 candidate genes (*orf28-32, orf36, orf38, orf41-42, orf44, orf45, orf47* and *orf48*) as expressed in the lysogen. The *orf28-32* gene cassette was successfully disrupted in the SfV lysogen and virulence assays indicated that the expression of one or several genes within this gene cassette increase the virulence of the lysogen. Each of these genes now needs to be characterized individually to identify their specific contribution, if any, to the virulence of the host. Construction of further gene disruptions could not be accomplished within the given time frame. The results of this study suggest the bacteriophage genes outside of the O-antigen modifying gene cluster contribute to the virulence of *S. flexneri* strains.

Chapter 5

Characterizing a new animal model for shigellosis- *C. elegans*

Chapter 5: Characterizing a new animal model for shigellosis- *C. elegans*

5.1 Introduction

S. flexneri has a very narrow host range and only infects human and non-human primate hosts, as a result of which there is no simple intestinal small animal model available. The lack of a relevant *in vivo* model of shigellosis has been one of the major impediments to the development of preventive and therapeutic measures. A number of alternative animal models have been identified that use mucosal surfaces outside of the colon as sites of infection. The most commonly used *in vivo* models of shigellosis are the murine pulmonary model of shigellosis [83, 225, 318] and the guinea pig keratoconjunctivitis model [233]. However, both these *in vivo* models lack clinical relevance, as the site of *S. flexneri* infection and symptoms produced do not mirror *S. flexneri* infection in humans.

In recent years the soil-dwelling roundworm, *Caenorhabditis elegans,* has been used extensively to study host-pathogen interactions *in vivo,* uncovering a wealth of information about microbial virulence factors and host defense responses [401]. This *in vivo* model is particularly useful to study enteric pathogens, as the nematode intestinal cells share morphological similarities with human intestinal cells, including apical, finger-like microvilli anchored into a cytoskeletal terminal web composed of actin and intermediate filaments. In addition, the human innate immune system shares many characteristics with that of *C. elegans* (Section 1.9.3) and thus mechanisms of bacterial and host responses may be paralleled in mammalian cells [402].

A range of bacterial virulence factors have been shown to be required for both nematode and mammalian pathogenesis [288, 289, 294, 403-405], further validating the use of *C. elegans* as a relevant *in vivo* model to study host-pathogen interactions. On account of these characteristics, the list of bacterial pathogens that are known to infect *C. elegans* is growing and includes prominent human pathogens such as *S.enterica, P. aeruginosa,* EPEC and *S. marcescens* [227-229, 267].

In the past decade, two independent groups [283, 284] have found preliminary evidence suggesting *C. elegans* can potentially be used as an *in vivo* model for shigellosis. These studies demonstrate that *S. flexneri* kills *C. elegans* in an infection-like process that requires live bacterial cells harboring intact virulence plasmids. Both studies also report that *S. flexneri* accumulates in the *C. elegans* intestine and kills the nematodes on solid media [283] and in liquid culture [284]. However, *C. elegans* as a model for shigellosis has not been completely understood as the *S. flexneri*-mediated killing response and the nematode responses to *S. flexneri* infection remain unknown.

This study aims to further our understanding of the interactions between *S. flexneri* and *C. elegans* in order to establish this *in vivo* model as a viable alternative to study *S. flexneri* pathogenesis. Transmission electron microscopy was used to shed light on the cellular interactions between *S. flexneri* cells and the *C. elegans* intestinal cells. To gain insight into *S. flexneri*-induced host responses, the proteome of nematodes infected with *S. flexneri* was compared with control worms.

5.2 Results

5.2.1 Wild type *S. flexneri* serotype 3b kills *C. elegans* and killing requires the expression of bacterial virulence plasmid-encoded genes

Previous studies have reported that wild type *S. flexneri* serotypes 2a [283] and 2b [284] kill *C. elegans*. Here, the *S. flexneri* 3b strain (SFL1520), shown to be virulent in the murine pulmonary models of shigellosis, was chosen, to characterize the pathogenesis of this strain in *C. elegans*. Liquid infection assays [284] were performed to determine if SFL1520 kills nematodes. An avirulent *S. flexneri* (SFL1223) (which does not carry the virulence plasmid) and the *E. coli* OP50 strain (laboratory strain that nematodes are maintained on) were included as control strains in this study.

The results of liquid killing assays (Figure 5.1) indicate that SFL1520 kills nematodes, while nematodes maintained on the control strains show prolonged survival. Consistent with previous studies, the results of liquid mortality assays indicate that *S. flexneri* requires the virulence plasmid-encoded factors for *C. elegans* killing, as the survival of worms fed SFL1520 (carrying an intact virulence plasmid) is significantly reduced compared with worms fed SFL1223 (Figure 5.1). *S. flexneri* serotype 3b kills nematodes in liquid culture with a TD_{50}= 46 ± 1 h (Figure 5.1). The main drawback of using the liquid killing assay was that nematode survival rates could not be determined after 48 hours. This was due to the large number of L1/L2 progeny larvae, which masked the adults, making it difficult to score survival. However, since the liquid killing assay is reproducible and fast, this assay was employed as an *in vivo* virulence assay in this thesis.

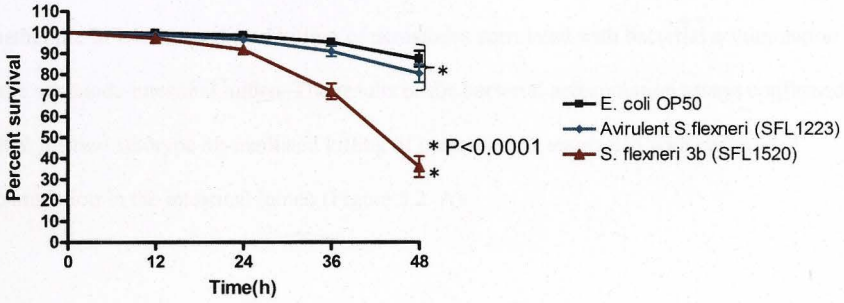

Figure 5.1: *S. flexneri* is pathogenic to *C. elegans*. Survival curves of wild-type N2 nematodes when fed *E. coli* OP50 (in black), an avirulent, virulence plasmid-cured *S. flexneri* (SFL1223) strain (in blue), or virulent *S. flexneri* serotype 3b strain (in red). Survival of nematodes in liquid culture. 20-50 synchronized adult nematodes were treated with log phase cultures of *E. coli* OP50, SFL1520 or SFL1223 strains grown at 37 °C. Infected nematodes were monitored for 48 hours and survival was scored every 12 hours. Survival curves represent data from three independent experiments, each using 20-50 nematodes. Nematodes fed SFL1520 show a significant decrease in survival rates in liquid cultures ($p < 0.0001$, Log rank test).

5.2.2 Wild type *S. flexneri* accumulates in the nematode intestinal lumen

Burton *et al,* [283] have previously shown that virulent *S. flexneri* serotype 2a kills *C. elegans* by accumulation in the intestinal lumen, while avirulent *S. flexneri* strains are digested by the nematodes. Bacterial accumulation assays using wild type *S. flexneri* serotype 3b (SFL1520), avirulent *S. flexneri* (SFL 1223), and *E. coli* OP50 (B2298) were performed to determine whether the SFL1520-mediated killing of nematodes correlated with bacterial accumulation in the nematode intestinal lumen. The results of the bacterial accumulation assays confirmed that *S. flexneri* serotype 3b-mediated killing of nematodes is associated with bacterial accumulation in the intestinal lumen (Figure 5.2. A).

To confirm the accumulation of SFL1520 in the intestinal lumina of nematodes, worms were fed GFP^+ -tagged *S. flexneri* serotype 3b (SFL2312), avirulent *S. flexneri* (SFL2311) and *E. coli* OP50 (B2515). The profile of GFP^+-tagged bacterial accumulation in the nematode gut was examined using fluorescence microscopy. Results of GFP^+ accumulation assays further confirmed that wild type *S. flexneri* serotype 3b (SFL1520) accumulates in the nematode intestinal lumen while the avirulent strain (SFL1223) and *E. coli* OP50 are digested (Figure 5.2. B).

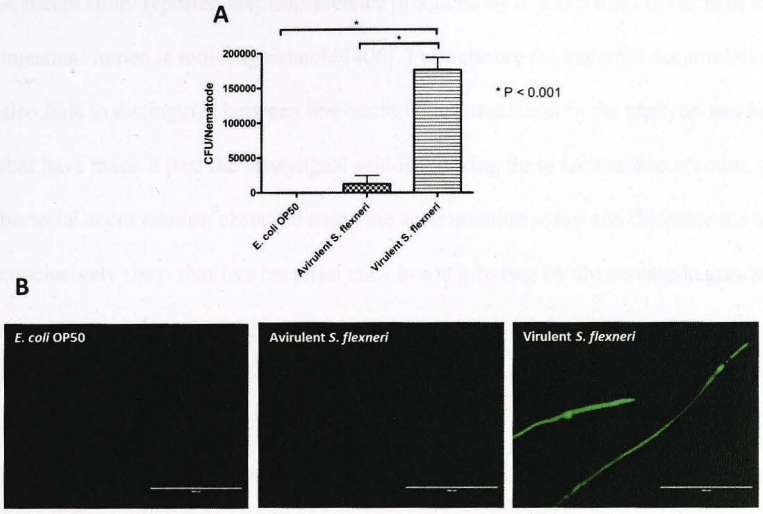

Figure 5.2: Virulent *S. flexneri* serotype 3b accumulates in *C. elegans* intestinal lumen 24 hours post infection. A: Young adult hermaphrodite N2 nematodes were fed either *E. coli* OP50 (B2298), avirulent *S. flexneri* (SFL1223) or virulent *S. flexneri* serotype 3b (SFL1520) for 24 hours at 22 °C. 20 worms were picked off each bacterial lawn, disrupted using glass beads and appropriate dilutions of each lysate were plated on LB agar to obtain bacterial counts. SFL1520 shows a significant increase in bacterial accumulation compared with SFL1223 and *E. coli* OP50 ($p < 0.001$, One Way ANOVA). Results represent the means of three independent experimental repeats with standard errors (error bars). **B:** Young adult hermaphrodite N2 nematodes were fed *E. coli* OP50, avirulent *S. flexneri* (SFL1223) or virulent *S. flexneri* 3b (SFL1520) tagged with GFP^+ for 24 h and fluorescence was observed using the EVOS digital inverted microscope (AMG). Scale bar = 400 μm.

A recent study reported that fluorescence produced by live and dead bacteria in the nematode intestinal lumen is indistinguishable [406]. Furthermore the bacterial accumulation assays also fails to distinguish between live bacterial accumulation in the pharynx and bacterial cells that have made it past the pharyngeal grinder. Taking these factors into account, the results of bacterial accumulation observed using the accumulation assay and fluorescence assays fail to conclusively show that live bacterial cells evade grinding by the nematode grinder and accumulate in the intestinal lumen.

To determine if live *S. flexneri* cells accumulate in the nematode intestinal lumina, transmission electron microscopy (TEM) was used to compare the intestinal lumina of nematodes fed avirulent *S. flexneri* SFL1223 and virulent *S. flexneri* serotype 3b (SFL1520) over three time points, 24, 96 and 144 hours post infection. TEM micrographs clearly indicate the presence of intact *S. flexneri* serotype 3b (SFL1520) cells in infected nematode intestinal lumina, with the bacterial load increasing over time (Figure 5.3). These observations provide strong evidence suggesting that virulent *S. flexneri* cells escape nematode grinder-mediated breakdown and accumulate in the *C. elegans* intestinal lumina.

5.2.3 Intraluminal *S. flexneri* cells produce outer membrane vesicles (OMVs) and invade the *C. elegans* intestinal epithelial cells

TEM micrographs revealed that *S. flexneri* serotype 3b cells within the nematode intestinal lumen produce putative outer membrane vesicles (OMVs) (Figure 5.4.A and B). OMVs are secreted elements produced by Gram negative bacteria as part of a bacterial stress response, induced during infection of host tissues [407].

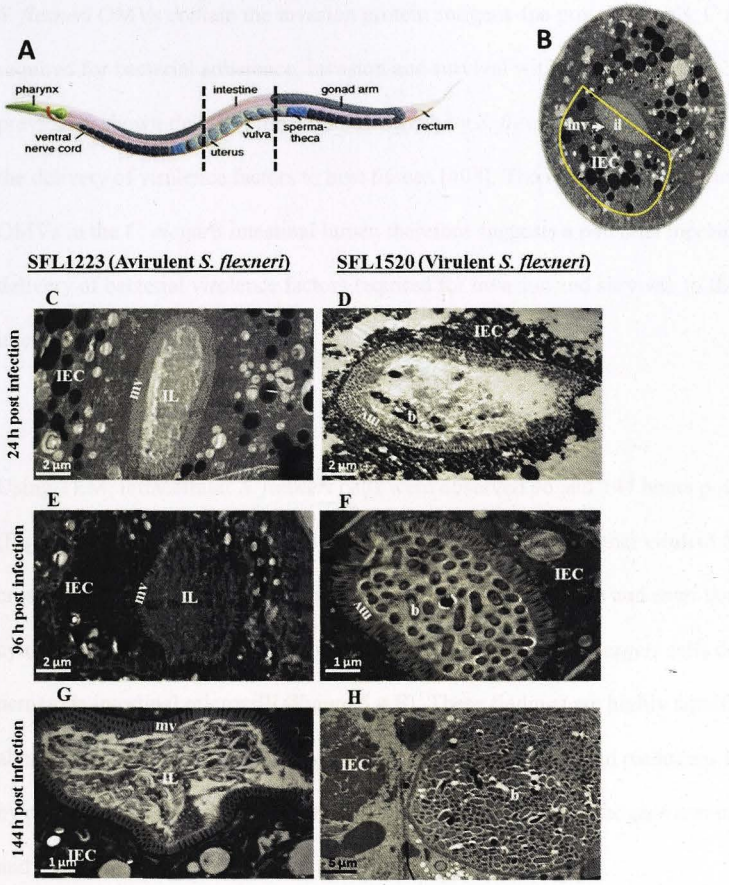

Figure 5.3: Virulent *S. flexneri* serotype 3b escape pharyngeal grinding and accumulate in the *C. elegans* intestinal lumen. A: Schematic representation of the *C. elegans* body plan with the plane of sections highlighted (artwork by Altun and Hall, © Wormatlas). **B:** Transverse section of the mid-body of a healthy nematode with the intestinal cell highlighted in yellow. **C-H:** Transmission electron micrographs of the transverse mid-body sections of animals feeding on plasmid-cured, avirulent *S. flexneri* (SFL1223) (**C, E, G**) and virulent *S. flexneri* serotype 3b (**D, F, H**) for 24 h (**C, D**), 96 h (**E, F**) and 144 h (**G, H**). IEC-intestinal epithelial cell; mv-microvilli; IL-intestinal lumen; b-intact *S. flexneri* cells.

S. flexneri OMVs contain the invasion protein antigens-Ipa proteins (IpaB, C & D) that are required for bacterial adherence, invasion and survival within infected tissues. It has been previously shown that the production of OMVs by *S. flexneri* cells provides a mechanism for the delivery of virulence factors to host tissues [408]. The identification of putative *S. flexneri* OMVs in the *C. elegans* intestinal lumen therefore suggests a potential mechanism for the delivery of bacterial virulence factors required for invasion and survival, to the nematode intestinal cells.

Using TEM, intracellular *S. flexneri* cells were observed 96 and 144 hours post infection (Figure 5.4.C and D, respectively). These observations indicate that virulent *S. flexneri* cells cross the protective, apical microvilli boundary of intestinal cells and enter the intestinal cell cytoplasm. TEM micrographs also suggest that intraluminal *S. flexneri* cells degrade the nematode intestinal microvilli (Figure 5.4.E). These findings are highly significant as, although several studies have shown that intracellular mammalian pathogens kill *C. elegans* by persistently colonizing the intestinal lumen, most of these pathogens remain extracellular and fail to invade the nematode intestinal cells [243].

5.2.4 Other phenotypes observed in the cytopathological examination of infected nematodes using transmission electron microscopy (TEM)

5.2.4.1 Worms infected with wild type *S. flexneri* for 24 hours display symptoms of fluid imbalance in the intestinal epithelial cells

24 hours post infection several nematodes infected with *S. flexneri* serotype 3b display signs of fluid imbalance (Figure 5.5). TEM micrographs of mid-body sections of animals infected

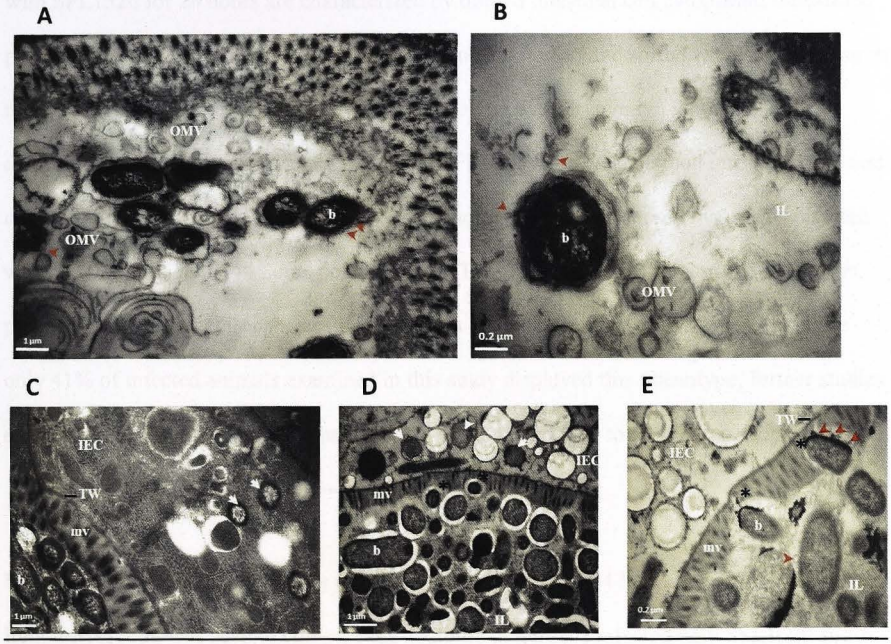

Figure 5.4: Intraluminal *S. flexneri* cells produce putative outer membrane vesicles (OMVs) and invade *C. elegans* intestinal epithelia. A-E: TEM micrographs of transverse mid-body sections of young adult nematodes infected with wild type *S. flexneri* serotype 3b (SFL1520) for 24 h (**A, B**), 96 h (**C**) and 144 h (**D, E**). **A, B:** Intraluminal bacterial cells produce putative outer membrane vesicles (OMVs); red arrowheads indicate OMV shedding from bacterial cells. **C, D:** White arrowheads indicate intracellular bacterial cells that have penetrated the ciliated epithelial barrier of the intestinal cell, 96 and 144 h post infection. **E:** Intraluminal *S. flexneri* cells degrading the apical microvilli boundary (asterisk) of the *C. elegans* intestinal cells. IEC- intestinal epithelial cells; mv-microvilli; IL-intestinal lumen; TW-terminal web; b-intraluminal bacterial cells; OMV-outer membrane vesicles.

with SFL1520 for 24 hours are characterized by diluted intestinal cell cytoplasm, fluid-filled pseudocoelom (the circulatory fluid-equivalent in nematodes) and shrunken tissues floating in the excess fluid (Figure 5.5.B and D). This phenotype was observed in 9 out of 22 (41%) animals observed. In comparison, animals fed SFL1223 have well-defined intestinal cells and organs (Figure 5.5.A and C). However, this phenotype was not observed in animals infected with SFL1520, 96 and 144 hours post infection. These observations suggest that *S. flexneri* potentially causes fluid imbalances in nematodes at the onset of infection. However, since only 41% of infected animals examined in this study displayed this phenotype, further studies need to be conducted to confirm that this observation is not due to fixation artifacts.

In order to determine if nematodes infected with SFL1520 for 24 hours accumulate fluid, light microscopy was used to compare the anatomy of animals infected with SFL1520 and *E. coli* OP50. Results of light microscopy failed to identify prominent changes indicating fluid retention, such as swelling and ill-defined cellular structures in the intestines of worms infected with *E. coli* OP50 and SFL1520 (Figure 5.6.A and B, respectively). The light microscopy images did, however, indicate that nematodes infected with SFL1520 showed a larger gap between the intestinal cell membranes and the nematode body walls when compared with control worms. This observation could suggest accumulation of fluid in these worms. Further experiments using markers to track fluid movements in infected worms would shed light on this phenotype. Light microscopy also indicated that nematodes infected with SFL1520 appear to retain embryos.

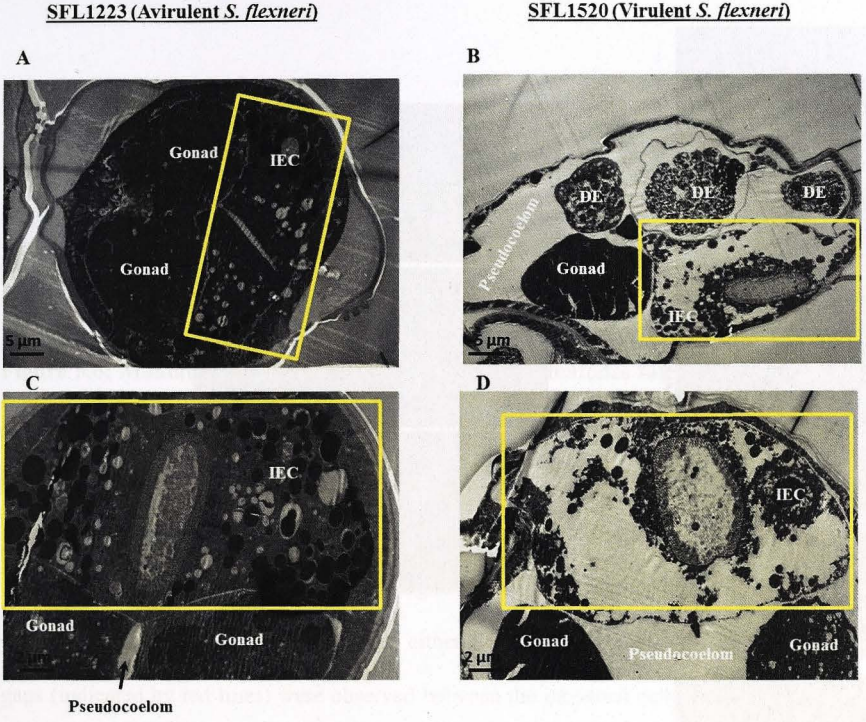

Figure 5.5: Worms infected with wild type *S. flexneri* for 24 hours display symptoms of fluid imbalance in the intestinal epithelial cells. This Figure shows transverse sections of *C. elegans* mid-bodies with intestinal cells highlighted (yellow boxes) 24 hours post infection with wild type *S. flexneri* serotype 3b, SFL1520 (**B and D**) and the avirulent *S. flexneri* strain, SFL1223 (**A and C**). Nematodes infected with SFL1520 show highly damaged intestinal cells, with the intestinal cytoplasm lacking ground substance. Nematodes infected with SFL1520 are also characterized by fluid-filled pseudocoelom, and shrunken tissues floating in the excess fluid (**B and D**). Nematodes infected with SFL1223 have well defined intestinal cell cytoplasms and the body of these animals is not filled with pseudocoelomic fluid (**A and C**).

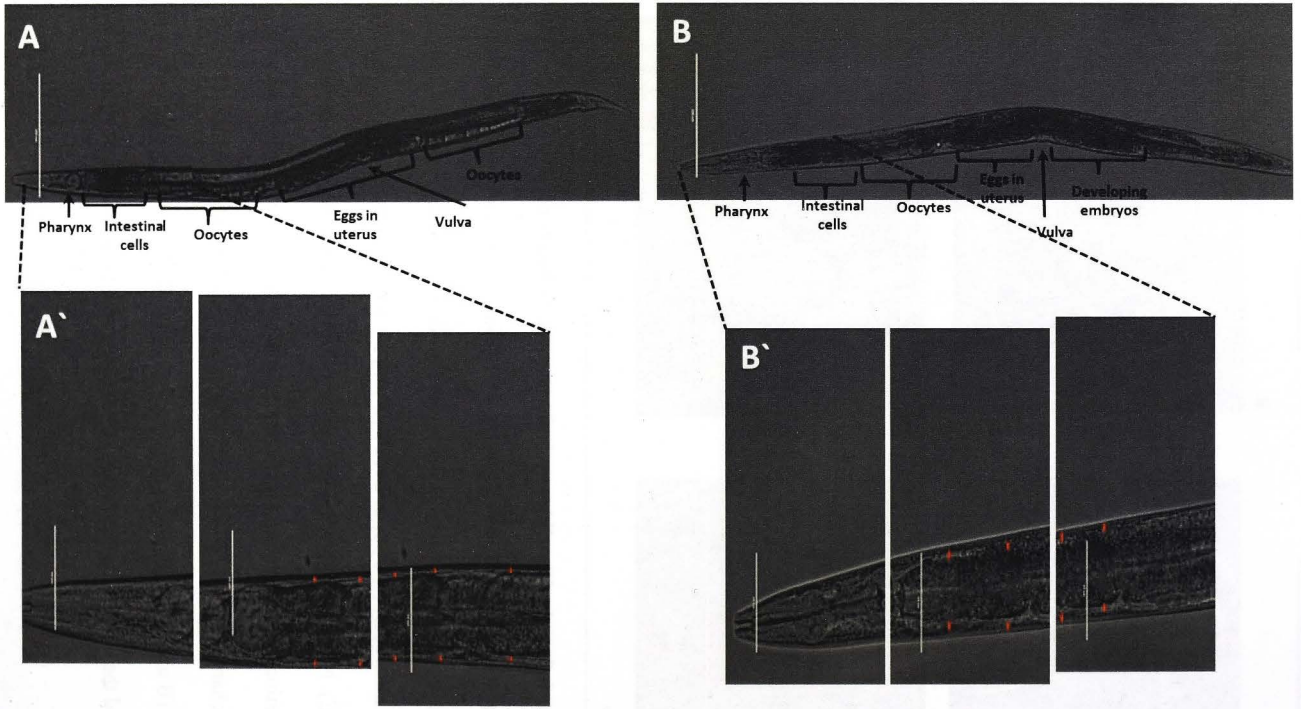
A
Oocytes
Pharynx
Intestinal cells
Oocytes
Eggs in uterus
Vulva
A`
B
Pharynx
Intestinal cells
Oocytes
Eggs in uterus
Vulva
Developing embryos
B`

Figure 5.6: Montage of light microscopy images of nematodes infected with virulent *S. flexneri* and *E. coli* OP50. Young adult hermaphrodite N2 nematodes were infected with either *S. flexneri* serotype 3b (SFL1520) or *E. coli* OP50 (B2298) for 24 hours at 22 °C. Light microscopy was used to compare the anatomy of worms infected with SFL1520 (**B and B`**) and B2298 (**A and A`**) using the EVOS digital inverted microscope (AMG). No prominent differences in the diameter of worms fed either SFL1520 or B2298 were observed. Larger gaps (indicated by red lines) were observed between the intestinal cells and the body wall in nematodes infected with SFL1520 when compared with worms fed B2298. Nematodes infected with SFL1520 appear to retain developing embryos (**B**); this phenotype is not seen in worms fed B2298 (**A**). Scale bar **A and B** = 200 μm and **A` and B`** = 50 μm

5.2.4.2 Infected worms retain embryos and show accumulation of cytoplasmic yolk granules

Consistent with light microscope images, TEM micrographs also indicate that worms infected with SFL1520 seemed to retain advance-stage embryos. In normal worms, the embryos stay within the mother up to the 64-cell stage. TEM analysis of worms infected with SFL1520 suggests that these worms retain advanced embryos, well beyond the 64-cell stage (Figure 5.7.A and B). Kesika and colleagues have previously reported that nematodes infected with virulent *S. flexneri* lay fewer eggs when compared with worms fed *E. coli* OP50 [284]. Embryo retention observed in worms infected with SFL1520 could explain the decreased egg laying reported by Kesika *et al.*

TEM analysis of infected worms also identified a significant accumulation of yolk granules in the intestinal cells of nematodes infected with SFL1520 when compared with animals infected with the avirulent strain (Figure 5.8.A and B). The accumulation of yolk granules in the intestinal cells could suggest defects in endocytosis, cell-cell signaling and trafficking. These defects could account for the fluid imbalance seen after 24 hour infection.

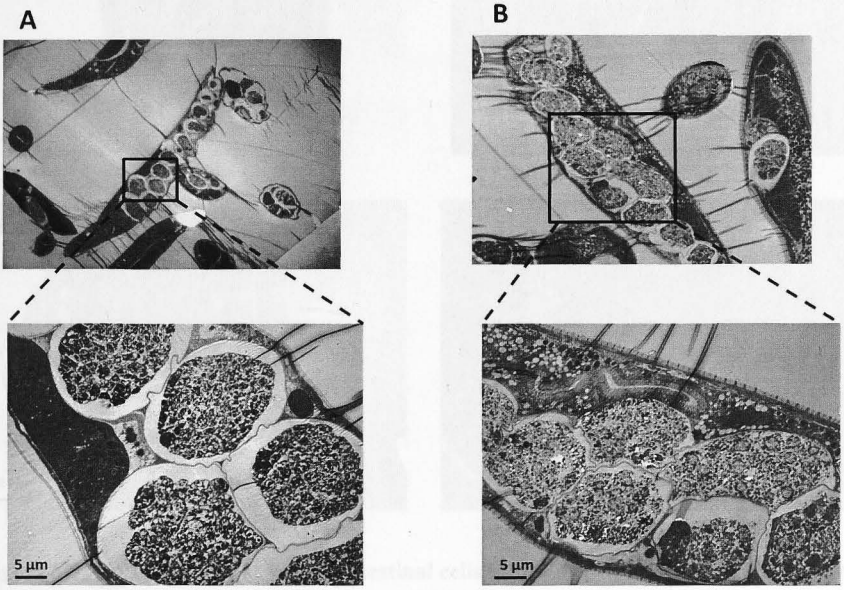

Figure 5.7: Nematodes infected with *S. flexneri* serotype 3b retain embryos. This figure shows longitudinal sections of *C. elegans* infected with wild type *S. flexneri* serotype 3b, SFL1520 for 24 h (**A**) and 96 h (**B**). Nematodes infected with SFL1520 retain developed embryos well beyond the 64-cell stage. Boxes highlight regions that have been magnified.

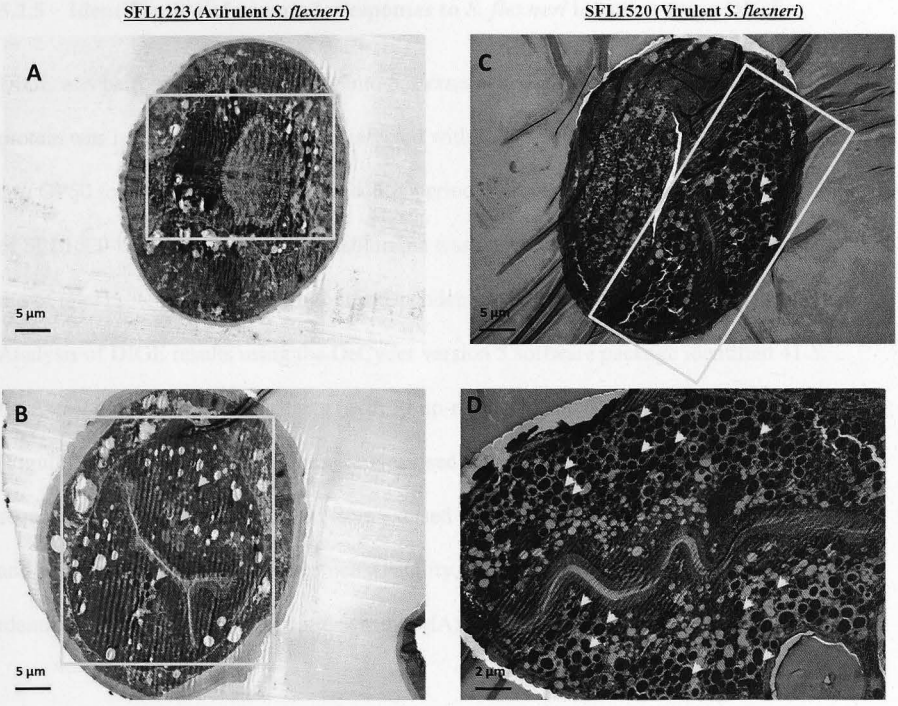

Figure 5.8: Accumulation of yolk in intestinal cells infected with wild type *S. flexneri* for 96 hours: Transverse mid-body sections of nematodes infected with avirulent *S. flexneri* showing very little yolk accumulation (**A and B**) and SFL1520 (virulent S. *flexneri)* showing accumulated yolk granules in the cytoplasm (**C and D**). Yellow boxes highlight the intestinal cells and arrows indicate a few of the yolk granules.

5.2.5 Identification of nematode responses to *S. flexneri* infection using DIGE

DIGE was performed to gain insight into *S. flexneri*-induced responses in *C. elegans*. Total protein was isolated from nematodes infected with *S. flexneri* serotype 3b (SFL1520) and *E. coli* OP50 for 24 hours. A 24 hour infection period was selected as significant accumulation of SFL1520 in the nematode intestinal lumina was observed at this time point (Figure 5.2). 2 mg of total protein, isolated from four independent experiments, was used to perform DIGE. Analysis of DIGE results using the DeCyder version 5 software package identified 41 *S. flexneri*-induced nematode proteins (with 37 up-regulated and 4 down-regulated proteins) (Figure 5.9). All 41 identified spots were excised from the gels for identification by peptide sequencing. Peptides were isolated from excised protein spots as described in section 2.9.2.4 and submitted to the Mass Spectrometry Facility, ANU, for LC-MS analysis. Proteins were identified through sequenced peptides using MASCOT (Matrix Science) database searches.

MASCOT searches using stringent search parameters (mass tolerance between 0.3 and 0.1 Da), only identified significant protein hits for 7 out of 41 spots (Table 5.1). Since the theoretical molecular weights (Mwt) and pI values of the 7 identified proteins, ACO-1, CCT-2, EEF-2, DAF-19, HSP-60, UNC-54 and UNC-41, were consistent with the Mwt and pI of spots predicted from the DIGE gels, it is likely that these proteins are *S. flexneri*-induced responses in *C. elegans*. Therefore these proteins were investigated further.

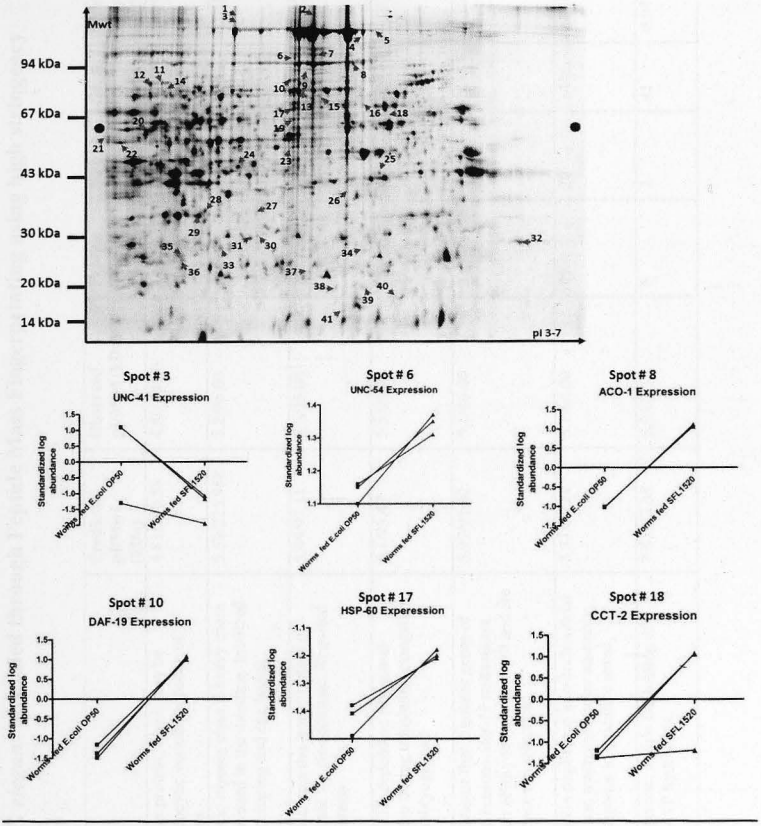

Figure 5.9:A: A representative 2 dimensional gel electrophoresis image of the *S. flexneri*-induced proteome of *C. elegans*. Red arrows indicate the protein spots identified AS differentially expressed in response to *S. flexneri* infection. All numbered spots were excised from the gel and submitted for LC-MS analysis. Proteins were identified through sequenced peptides using MASCOT (Matrix Science) (see Table 5.1). **B:** Differentially expressed spots identified using high stringency MASCOT search parameters. Graphs depicting the differences in standardized log abundance of identified spots in worms infected with virulent *S. flexneri* (SFL1520) and control worms maintained on *E. coli* OP50 across three biological replicates calculated using the DeCyder version 5 software package.

Table 5.1: Predicted *S. flexneri*-induced responses in *C. elegans* identified through Peptide Mass Fingerprinting using high stringency MASCOT search parameters

Identified protein	Gene name	*Shigella*-induced change in expression	Description	Predicted pI/Mwt (kDa)	Observed pI/Mwt (kDa)	Peptide Coverage (%)	No of peptides Matched	Score	P value (One Way ANOVA)
Putative stoned B-like protein	*unc-41*	Down-regulated	Potential adapter protein, which may be involved in endocytic vesicle recycling of synaptic vesicles	4.81/190.58	4.8/~94.00	3	7	27	0.029
Myosin-4	*unc-54*	Up-regulated	Encodes a muscle myosin class II heavy chain (MHC B). Expressed in the intestine. Involved in pharyngeal pumping and egg laying	5.59/225.958	5.2/96.00	8	5	134	0.038
Probable cytoplasmic aconitate hydratase	*aco-1*	Up-regulated	Enzyme that catalyzes the isomerization of citrate to isocitrate via cis-aconitate. Required for iron homeostasis	5.49/97.11	5.5/95.00	14	5	86	0.022
Elongation factor 2	*eef-2*	Up-regulated	Catalyzes the GTP-dependent ribosomal translocation step during translation elongation. Required for embryogenesis	6.1/95.47	5.5/95.00	18	8	72	0.022
RFX-like transcription factor	*daf-19*	Up-regulated	A transcription factor that regulates genes of ciliated sensory neurons. *daf-19* mutants are defective in their ability to taste or smell and are susceptible to bacterial infection!	5.97/91.42	5.1/86.00	2	3	24	0.040
Chaperonin homolog Hsp-60	*hsp-60*	Up-regulated	Heat shock protein implicated in mitochondrial protein import and macromolecular assembly. Required for response to oxidative stress	5.31/60.24	5.1/68.00	49	20	1446	0.040
T-complex protein 1 subunit beta	*cct-2*	Up-regulated	Molecular chaperone; assists the folding of proteins upon ATP hydrolysis.	5.65/53.38	5.6/67.5	6	2	41	0.047

5.2.5.1 Confirming the results of DIGE analysis using quantitative real-time reverse transcription PCR (qRT-PCR)

Quantitative real-time reverse transcription polymerase chain reaction (qRT-PCR) was used to compare mRNA levels of the seven identified nematode proteins, ACO-1, CCT-2, EEF-2, DAF-19, HSP-60, UNC-54 and UNC-41, in worms infected with *S. flexneri* serotype 3b (SFL1520) and control worms maintained on *E. coli* OP50 (Figure 5.10). Total RNA was isolated from nematodes fed SFL1520 and control worms, fed *E. coli* OP50 (Section 2.13.6). cDNA was synthesized and qRT-PCRs were performed (Section 2.13.7). The *C. elegans act-2* gene, which encodes actin, was used as a control gene to normalize all reactions, as the mRNA levels of *act*-2 are expected to remain constant in healthy and infected worms.

Consistent with the DIGE analysis, qRT-PCR indicated a significant increase in the transcript levels of *cct-2, daf-19, hsp-60* and *unc-54* and a decrease in the levels of *unc-41* transcripts in worms infected with SFL1520. No statistically significant differences were observed in the transcript levels of *aco-1* in infected and control worms ($p > 0.05$, unpaired t-test). *aco-1* encodes cytosolic aconitase, an enzyme whose expression is regulated post-translationally by iron levels. This would explain why although ACO-1 levels are elevated in response to *S. flexneri* infection, the mRNA levels in infected and control worms remain unchanged. Contrary to DIGE analysis, the expression of *eef-2* appears to be down-regulated at the transcriptional level, suggesting that the EEF-2 protein levels in infected worms are also potentially regulated post-transcriptionally.

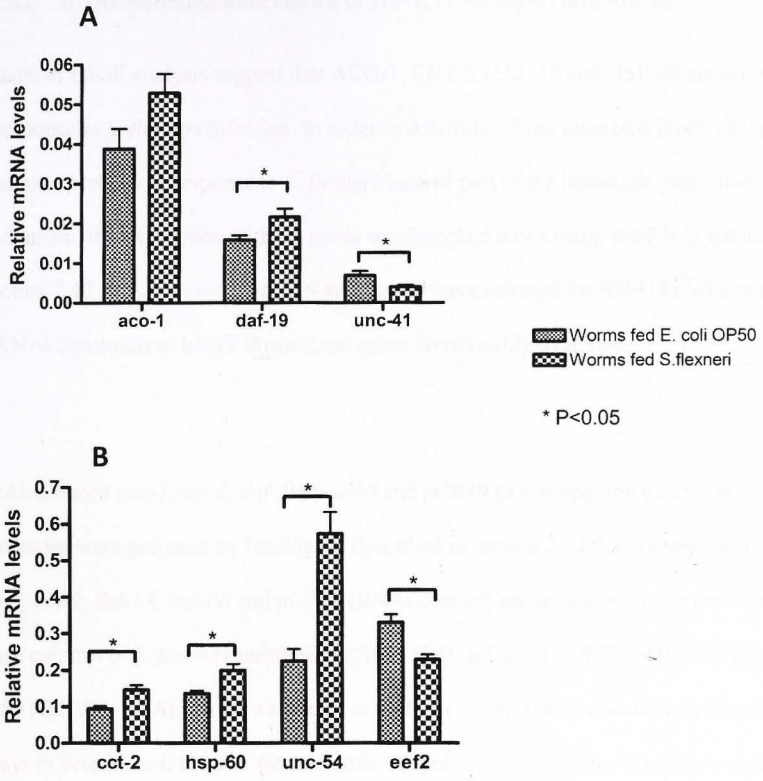

Figure 5.10: Reverse transcription quantitative PCR (qRT-PCR) analysis of *S. flexneri*-induced genes predicted by DIGE analysis. Transcript levels of *aco-1, daf-19* and *unc-41*(**A**), *cct-2, hsp-60, unc-54* and *eef-2* (**B**) were measured in synchronized young adult wild type animals feeding on *E. coli* OP50 or infected with *S. flexneri* serotype 3b for 24 h. Data represent the means of three biological replicates, each replicate measured in triplicate and normalized to the control gene, *act*-2, expressed as the ratio of the corresponding *S. flexneri*-induced levels and the basal *E. coli* OP50 levels. Asterisks indicate statistically significant differences identified using unpaired Student's *t*-tests and error bars represent standard error.

5.2.5.2 RNAi-mediated knockdown of *aco-1, cct-2, daf-19* and *hsp-60*

Results of DIGE analysis suggest that ACO-1, CCT-2 DAF-19 and HSP-60 are up-regulated in response to *S. flexneri* infection. In order to determine if the increased levels of these nematode proteins in response to *S. flexneri* formed part of the nematode protective mechanism, the expression of these genes was knocked down using the RNAi technology (Section 2.13.9). *aco-1, cct-2, daf-19* and *hsp-60* were selected for RNAi knockdown studies as RNAi constructs to knock down these genes were readily available.

RNAi-silenced *aco-1, cct-2, daf-19, hsp-60* and pCB19 (a non-specific dsRNA control) nematodes were prepared by feeding, as described in section 2.13.9.2. Young adult RNAi *aco-1, cct-2, daf-19, hsp-60* and pCB19 (RNAi control) nematodes were infected with log phase cultures of *S. flexneri* serotype 3b (SFL1520), avirulent *S. flexneri* (SFL1223) or *E. coli* OP50 (B2298). RNAi worms were used to perform bacterial accumulation and liquid killing assays to determine if these *S. flexneri*-induced genes play a role in protecting nematodes against *S. flexneri* infection.

5.2.5.3 The effect of silencing *S. flexneri*-induced host response genes on nematode survival

Survival was scored for 48 hours and killing curves were generated from the results of three independent, blind experimental repeats. *aco-1* RNAi worms fed *S. flexneri* serotype 3b showed a significant increase in survival rates compared with the RNAi control worms ($p < 0.0366$, Log rank test) (Figure 5.11.B). *cct*-2 RNAi nematodes appeared to be more susceptible to SFL1520 infection (TD_{50} 38 ± 2 h compared with TD_{50} = 46 ± 1 h of control

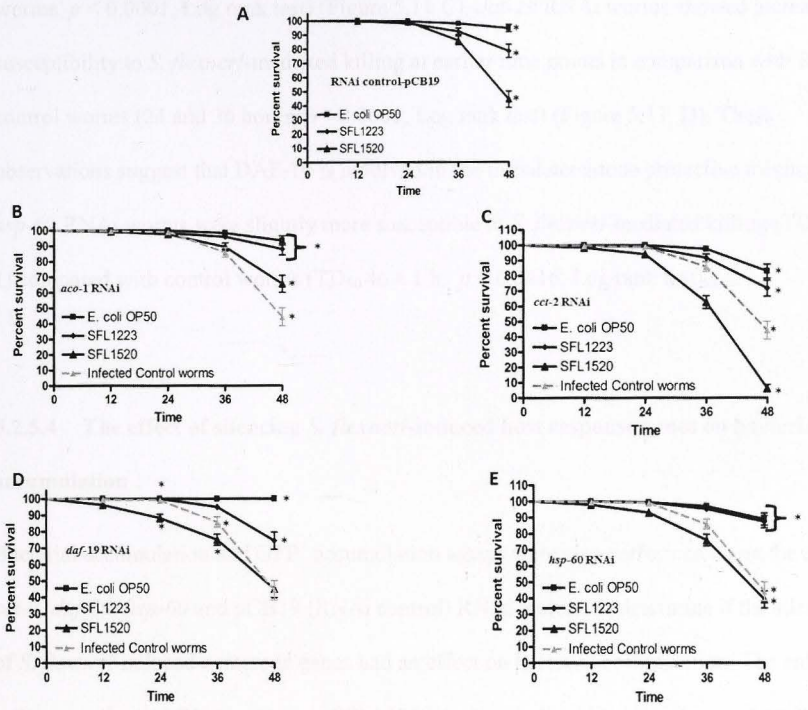

Figure 5.11: The effects of silencing *S. flexneri*-induced host response genes on nematode survival. After RNAi knockdown of *S. flexneri*-induced genes *aco-1* (**B**), *cct-2* (**C**), *daf-19* (**D**) and *hsp-60* (**E**), young adult hermaphrodites were treated with log phase cultures of either *E. coli* OP50, avirulent *S. flexneri* (SFL1223) or virulent *S. flexneri* serotype 3b (SFL1520) and scored at 12 hour intervals for survival. **A:** Nematodes treated with pCB19 (RNAi control vector) were used as a non-specific dsRNA control. Results represent data obtained from four independent biological repeats each with at least four technical repeats (each technical repeat with 20-50 nematodes) with standard error (error bars). The survival curves of RNAi worms infected with *S. flexneri* serotype 3b were compared with RNAi control-pCB19 worms infected with *S. flexneri* serotype 3b (grey, dashed curves); and asterisks indicate statistically significant differences in survival curves ($p < 0.05$), identified using Log rank tests.

worms, $p < 0.0001$, Log rank test) (Figure 5.11.C). *daf-19* RNAi worms showed increased susceptibility to *S. flexneri*-mediated killing at earlier time points in comparison with RNAi control worms (24 and 36 hours, $p < 0.0001$, Log rank test) (Figure 5.11. D). These observations suggest that DAF-19 is involved in the initial nematode protective mechanisms. *hsp*-60 RNAi worms were slightly more susceptible to *S. flexneri*-mediated killing (TD_{50} 45 ± 1) compared with control worms (TD_{50} 46 ± 1 h, $p < 0.0416$, Log rank test).

5.2.5.4 The effect of silencing *S. flexneri*-induced host response genes on bacterial accumulation

Bacterial accumulation and GFP^+ accumulation assays were also performed using the *aco-1, cct-2, daf-19, hsp-60* and pCB19 (RNAi control) RNAi worms, to determine if the silencing of *S. flexneri*-induced nematode genes had an effect on bacterial accumulation. The enhanced resistance of *aco-1* RNAi worms to SFL1520 infection in liquid culture (Figure 5.11.B) correlated with decreased bacterial accumulation (Figure 5.12.A and C). These observations suggest that Aco-1 acts as a negative regulator of host responses to *S. flexneri* infection.

The increased killing of *cct-2* RNAi worms (Figure 5.11.C) correlates with increased bacterial accumulation (Figure 5.12.A and D). These results suggest that CCT-2 induces or contributes to host protective mechanisms. Bacterial accumulation assays showed increased bacterial accumulation in *daf-19* RNAi worms (Figure 5.12.A and E) compared with the RNAi control worms. Increased bacterial accumulation in *daf-19* silenced worms suggests that the expression of this gene is required to control or eliminate intraluminal *S. flexneri.* No

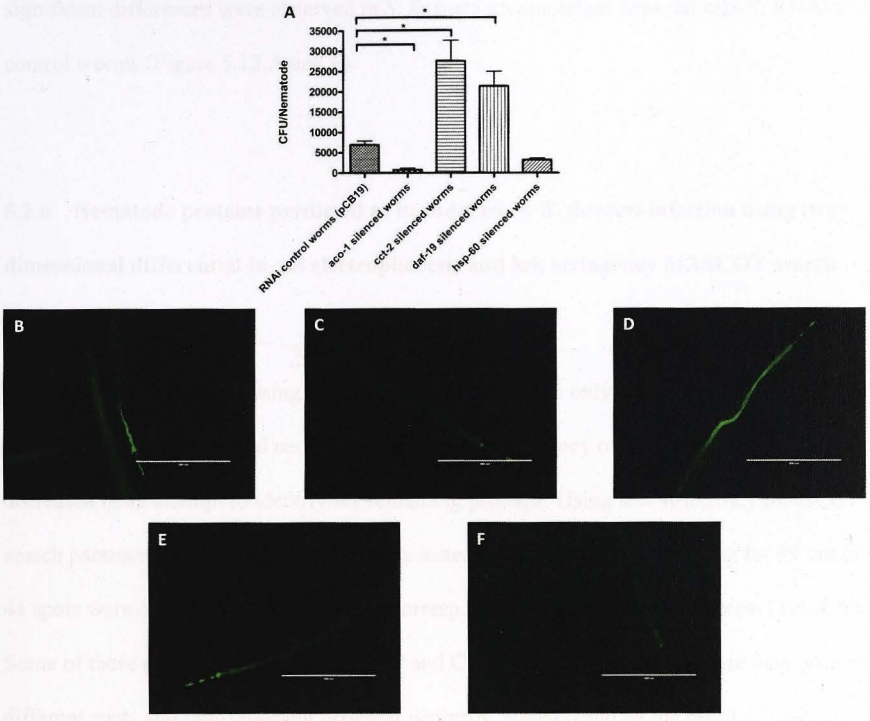

Figure 5.12: The effects of silencing *S. flexneri*-induced host response genes on accumulation of virulent *S. flexneri* in the nematode intestinal lumen. After RNAi knockdown of *S. flexneri*-induced genes *aco-1, daf-19, hsp-60* or pCB19 as an RNAi negative control, young adult hermaphrodites were transferred onto lawns of virulent *S. flexneri* (SFL1520) for 24 h. **A:** 20 worms were picked off bacterial lawns and disrupted, following which appropriate dilutions of each lysate were plated onto LB agar to obtain the intestinal bacterial counts. Results represent the means of three independent experimental repeats with standard error (error bars); asterisks indicate statistically significant differences ($p < 0.005$, unpaired *t*-tests). pCB19 (**B**), *aco-1* (**C**), *cct-2* (**D**), *daf-19* (**E**) and *hsp-60* (**F**) RNAi knockdown animals were transferred onto GFP^+-tagged SFL1520 for 24 h. Fluorescence was observed using the EVOS digital inverted microscope (AMG). Scale bar = 400 μm.

significant differences were observed in *S. flexneri* accumulation between *hsp-60* RNAi and control worms (Figure 5.12.A and F).

5.2.6 Nematode proteins predicted to be induced by *S. flexneri* infection using two-dimensional differential in-gel electrophoresis and low stringency MASCOT search parameters

Since MASCOT searches using stringent search parameters only identified seven out of 41 potential *S. flexneri*-induced nematode proteins, the stringency of the search parameters was decreased in an attempt to identify the remaining proteins. Using low stringency MASCOT search parameters (mass tolerance = 0.6 Da instead of 0.3 Da), significant hits for 39 out of 41 spots were obtained, with many spots corresponding to more than one protein (Table 5.2). Some of these proteins (UNC-22, NHR-77 and C10C6.6) were identified more than once in different spots and thus represent different isoforms, which could be the result of post-translational modifications or different splice variants of the same protein or protein degradation. Theoretical molecular weights (Mwt) and pI values of identified proteins were compared with the Mwt and pI of spots on the DIGE gels. Peptide coverage and distribution were also taken into account to eliminate false positive hits. Using these parameters, 46 potential nematode proteins induced in response to *S. flexneri* serotype 3b infection were identified (Table 5.2). Six out of the 39 spots corresponded to more than one positive identification (spot numbers 7, 8, 11, 25, 26 and 32) which could be due to false identification or the presence of several proteins with similar Mwt and/or pI values in these regions on the gels. The proteins identified using low stringency MASCOT search parameters were subdivided into different categories based on their biological functions. This subdivision of the identified proteins showed that most of the nematode proteins induced by *S. flexneri*

Table 5.2: Predicted *S. flexneri*-induced responses in *C. elegans* identified through Peptide Mass Fingerprinting using low stringency MASCOT search parameters

Spot No.	Pathogen-induced change in expression	Identified protein	UniProt Id	Gene Name	Biological function/relevant RNAi phenotypes	MASCOT Score	Theoretical Mwt (Da)/pI	Observed Mwt (Da)/pI	Sequence coverage	No of peptides matched
1	Down-regulated	Vacuolar protein sorting-associated protein 26	VPS26_CAEEL	*vps-26*	Protein transport/ Premature death	25	40926/5.81	>94000/4.8	4%	2
2	Down-regulated	Uncharacterized NTE family protein	YOL_CAEEL	ZK370.4	Predicted to be involved in phosphatidylcholine metabolic process/ No RNAi phenotypes specified	27	153212/6.53	>94000/5.2	2%	4
3	Down-regulated	Putative stoned B-like protein	STNB_CAEEL	*unc-41*	Locomotion and endocytosis/ defective movement, nervous system morphology variant	27	190581/4.81	>94000/4.8	3%	7
4	Up-regulated	UPF0533 protein	TPC13_CAEEL	C56C10.7	Probable trafficking protein/ No RNAi phenotypes specified	29	45329/5.48	>94000/5.6	3%	2
5	Up-regulated	Probable cation-transporting ATPase	YE56_CAEEL	C10C6.6	ATP catabolic process/ Sparse or enlarged yolk granules	31	133598/7.25	>94000/5.8	2%	5
6	Up-regulated	Myosin-4	MYO4_CAEEL	*unc-54*	Locomotion, pharyngeal pumping/ bag of worms, egg laying defect, sluggish, premature death	134	225958/5.59	~96000/5.2	8%	14
7	Up-regulated	Sterile alpha and TIR motif-containing protein	SARM1_CAEEL	*tir-1*	Innate immunity, neurogeneration, differentiation/ hypersensitivity to infection, reduced gene expression	30	113781/6.9	~97000/5.3	1%	3
		RING finger protein5	RNF5_CAEEL	*rnf-5*	E3 ubiquitin ligase/ extended lifespan	30	25298/6.22	~97000/5.3	9%	1
8	Up-regulated	Probable cytoplasmic aconitate hydratase	ACOC_CAEEL	*aco-1*	Cellular Iron homeostasis, TCA/ No RNAi phenotypes specified	86	97113/5.49	~95000/5.5	14%	8
		Elongation factor2	EF2_CAEEL	*eef-2*	Protein biosynthesis/ apoptosis reduced, extended lifespan	72	95477/6.1	~95000/5.5	18%	9
9	Up-regulated	DNA topoisomerase1	TOP1_CAEEL	*top-1*	DNA replication/ shortened lifespan, defective locomotion	29	94428/9.04	~93000/5.2	2%	4
10	Up-regulated	RFX-like transcription factor	DAF19_CAEEL	*daf-19*	Transcription factor/ cilia absent	24	91421/5.97	~86000/5.1	2%	3
11	Up-regulated	Uncharacterized protein	YAO6_CAEEL	F54D1.6	Unknown/ animals produce no or few embryos	25	164864/6.15	~90000/4.5	3%	7
		Nipped-B-like protein pqn-85	NPBL_CAEEL	*pqn-85*	Cell cycle/ defective locomotion	24	253743/5.79	~90000/4.5	4%	8
12	Up-regulated	DCT-5	DCT5_CAEEL	*dct-5*	Acts downstream of Daf16/FOXO/ induced dauer formation	26	24045/8.06	~90000/4.3	9%	2
13	Up-regulated	Uncoordinated protein79	UNC79_CAEEL	*unc-79*	Locomotion/ sluggish, odour chemocensory response variant	31	98899/6.07	~85000/5.2	6%	5
14	Up-regulated	Probable FAD synthase	FLAD1_CAEEL	R53.1	FAD biosysnthesis/ slow growth	28	59440/6.49	~85000/4.45	5%	4
15	Up-regulated	Uncharacterized protein	YKK6_CAEEL	C02F5.6	HEN1 (RNA 3'end methyltransferase) of Nematode/ No RNAi phenotypes specified	29	51993/5.23	~78000/4.4	1%	1
16	Up-regulated	Calcium-activated potassium channel	SLO1_CAEEL	*slo-1*	Potassium transport/ irregular pharyngeal pumping, desensitization to chemo attractants	25	131043/5.8	~72000/5.6	2%	4

17	Up-regulated	Chaperonin homolog	CH60_CAEEL	*hsp-60*	Protein refolding, embryo larva development/ maternal sterile	1446	60235/5.3	~68000/5.1	49%	7
18	Up-regulated	T-complex protein 1 subunit beta	TCPB_CAEEL	*cct-2*	Protein folding/ apoptosis reduced, maternal sterile, oocytes lack nuclei, resistant to oxidative stress-animals fail to respond to oxidative stress, endocytosis defective	41	57338/5.65	~67500/5.6	6%	2
19	Up-regulated	E3 ubiquitin-protein ligase	RPM1_CAEEL	*rpm-1*	Ubiquitin protein ligase that negatively regulates the p38 MAPK pathway expressed in pharynx / apoptosis reduced	28	425202/6.29	~67900/5.1	1%	6
20	Up-regulated	Muscle M-line assembly protein	UNC89_CAEEL	*unc-89*	Structural component of muscle M-line/ egg laying defective, locomotion defective, pharyngeal pumping reduced	24	8990003/5.42	~60000/4.3	2%	25
21	Up-regulated	Mediator of RNA polymerase II transcription subunit1.1	MED1_CAEEL	*sop-3*	Transcription regulation/slow growth, reduced brood size	28	165015/8.86	~57000/4.0	2%	3
22	Up-regulated	Heat shock 70 kDa protein F	HSP7F_CAEEL	*hsp-6*	Stress response/ reduced ATP, reduced pharyngeal pumping, shortened lifespan, reduced brood size	24	71086/5.89	~55000/4.1	3%	3
23	Up-regulated	Twitchin	UNC22_CAEEL	*unc-22*	Regulates muscle contraction and relaxation, expressed in the body wall, vulva, pharynx/ defective movement	49	792459/5.79	~50000/5.1	1%	12
24	Up-regulated	Ribosome biogenesis regulatory protein homolog	RRS1_CAEEL	*rrbs-1*	Ribosome biogenesis/maternal sterile, reduced oocytes,	24	37962/9.97	~44000/4.9	6%	3
25	Up-regulated	Uncharacterized protein	YMF7_CAEEL	F55H2.7	Unknown	29	44124/10.08	~42000/5.4	6%	3
		Nuclear hormone receptor family member-77	NHR77_CAEEL	*nhr-77*	Transcription regulation/ No RNAi phenotypes specified	25	42688/9.12	~42000/5.4	11%	3
26	Up-regulated	Copine family protein 2	CPNA2_CAEEL	*cpna-2*	Belongs to the copine family and is expressed in the body wall muscles/ No RNAi phenotypes specified	25	862013/5.21	~40000/5.5	1%	17
		Regulator of nonsense transcripts1	RENT1_CAEEL	*smg-2*	RNA dependent helicase, RNA interference, embryo genital morphogenesis/ defective mRNA surveillance, reduced susceptibility to RNAi	25	121142/6.46	~40000/5.5	2%	3
		Germline survival defective-1	GLS1_CAEEL	*gls-1*	Meiosis/ defective oogenesis	18	116684/8.44	~40000/5.5	7%	5
27	Up-regulated	N-terminal acetyltransferase B complex subunit NAA25 homolog	NAA25_CAEEL	*cra-1*	Catalyses acetylation of proteins/reduced number of oocytes and brood size	27	110296/6.41	~32000/4.9	2%	4
28	Up-regulated	No significant hits								
29	Up-regulated	No significant hits								
30	Up-regulated	Protein arginine N-methyltransferase 5	ANM5_CAEEL	*prmt-5*	Transcription regulation/ Increased spontaneous mutation	34	83582/5.86	~29000/4.9	2%	3
31	Up-regulated	Nuclear hormone receptor family member-19	NHR19_CAEEL	*nhr-19*	Transcription regulation/ No RNAi phenotypes specified	33	541000/9.06	~28500/4.87	5%	3

32	Down-regulated	Single-stranded DNA-binding protein, mitochondrial	MTSS1_CAEEL	*mtss-1*	DNA replication/ reduced hypoxia response	27	19227/9.77	~28000/6.7	8%	1
		Histone H3-like centromeric protein	CPAR1_CAEEL	*cpar-1*	Nucleosome assembly/ reduced brood size	24	29125/7.94	~28000/6.7	6%	2
33	Up-regulated	Twitchin	UNC22_CAEEL	*unc-22*	Regulates muscle contraction and relaxation, expressed in the body wall, vulva, pharynx/ defective movement	29	792459/5.79	~25000/4.7	1%	19
	Up-regulated	Homeobox protein	HM31_CAEEL	*ceh-31*	Multicellular organism development/ intestinal cell proliferation variant	28	28834/7.82	~25000/4.7	5%	2
34	Up-regulated	Origin recognition complex subunit 2	ORC2_CAEEL	*orc-2*	DNA replication/ sluggish	25	49460/6.03	~26000/5.6	5%	3
35	Up-regulated	UPF0046 protein	YW12_CAEEL	T07D4.2	Hydrolase activity/ No RNAi phenotypes specified	26	45353/9.17	~24000/4.6	9%	3
36	Up-regulated	Nuclear hormone receptor family member-77	NHR77_CAEEL	*nhr-77*	Transcription regulation/ No RNAi phenotypes specified	29	42688/9.12	~23000/4.6	4%	3
37	Up-regulated	26S proteasome non-ATPase regulatory subunit 6	PSMD6_CAEEL	*rpn-7*	ATP-dependent degradation of ubiquitinated proteins/ Increased apoptosis	31	47838/6.36	~21000/5.2	1%	1
38	Up-regulated	Mediator of RNA polymerase II transcription subunit 17	MED17_CAEEL	*mtd-17*	Transcription regulation/ defective egg laying, locomotion, endocytosis	27	77767/5.74	~20000/5.5	2%	3
39	Up-regulated	Probable cation-transporting ATPase	YE56_CAEEL	C10C6.6	ATP catabolic process/ Sparse or enlarged yolk granules	33	133598/7.25	~20000/5.6	2%	4
40	Up-regulated	26S proteasome non-ATPase regulatory subunit 3	PSMD3_CAEEL	*rpn-3*	Regulation of protein catabolic process/ increased apoptosis	24	57813/7.14	~18000/5.8	5%	3
41	Up-regulated	Cytoplasmic polyadenylation element-binding protein 1	CPB1_CAEEL	*cpb-1*	Differentiation, spermatogenesis/ Reduced brood size	30	63949/8.65	~13000/5.5	1%	1

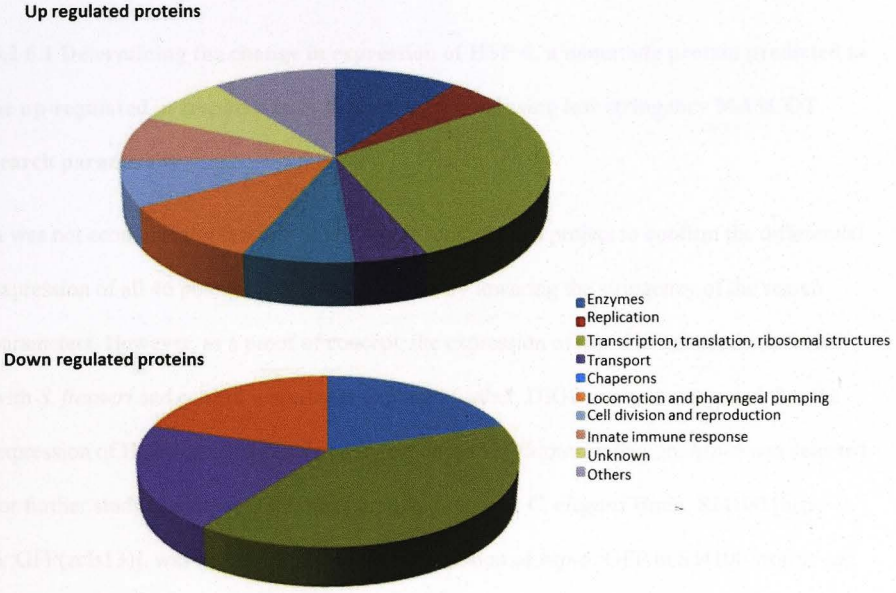

Figure 5.13: Graphical representation of the predicted biological functions of the up- and down-regulated *C. elegans* proteins identified in response to *S. flexneri* infection.

infection are involved in transcription and translation, followed closely by proteins required for movement and pharyngeal pumping (Figure 5.13).

5.2.6.1 Determining the change in expression of HSP-6, a nematode protein predicted to be up-regulated in response to *S. flexneri* infection, using low stringency MASCOT search parameters

It was not economically feasible or within the scope of this project to confirm the differential expression of all 46 potential proteins identified by lowering the stringency of the search parameters. However, as a proof of concept, the expression of *hsp-6* in nematodes infected with *S. flexneri* and control worms was explored further. DIGE analysis suggested that the expression of HSP-6 was up-regulated in response to *S. flexneri* infection. *hsp-6* was selected for further study as a *hsp-6*::GFP transcriptional reporter *C. elegans* strain, SJ4100 [hsp-6::GFP(zcIs13)], was readily available. The expression of *hsp-6*::GFP in SJ4100 worms can be easily observed using fluorescence microscopy to visualize the expression of GFP driven by the *hsp-6* promoter. Young adult SJ4100 nematodes were fed *E. coli* OP50 or *S. flexneri* serotype 3b (SFL1520) for 24 hours, following which the expression of *hsp-6*::GFP in the mitochondria throughout the nematode body was visualized using fluorescence microscopy. The result showed that nematodes infected with SFL1520 exhibited increased expression of GFP throughout their bodies (Figure 5.14.B) compared with control worms maintained on OP50 (Figure 5.14.A).

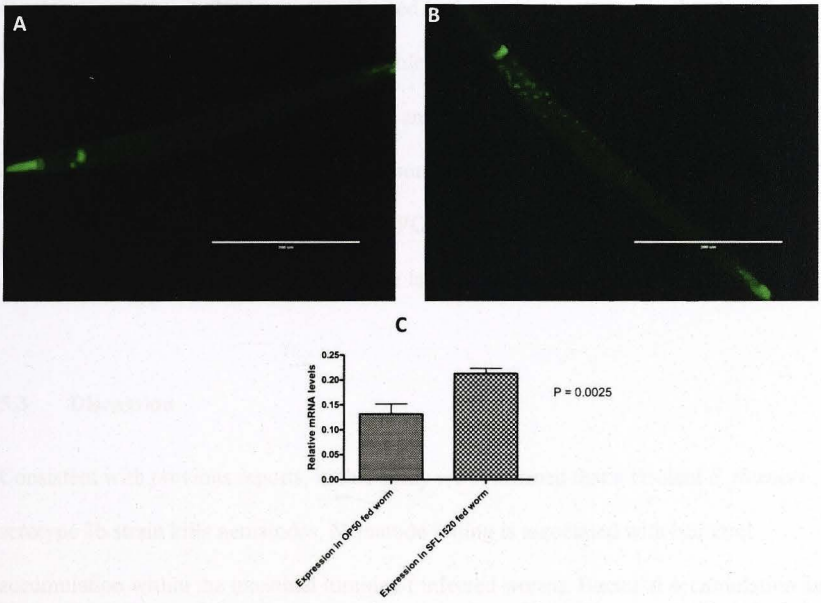

Figure 5.14: Determining the change in expression of *hsp-6* in nematodes infected with *S. flexneri.* Young adult, *hsp-6*::GFP *C. elegans* worms (SJ4100), were fed *E. coli* OP50 (**A**) or *S. flexneri* serotype 3b, SFL1520 (**B**) for 24 hours at 22 °C. Fluorescence microscopy was used to visualize the expression of GFP driven by the *hsp-6* promoter. Nematodes infected with SFL1520 show increased GFP expression in the mitochondria throughout their bodies (**B**) compared with control worms maintained on *E. coli* OP50 (**A and B**). Scale bar = 200 μm. **C:** Results of quantitative real time PCR to determine the expression of *hsp-6* in nematodes infected with *S. flexneri.* Transcript levels of *hsp-6* were measured in synchronized young adult N2 animals feeding on *E. coli* OP50 or infected with *S. flexneri* serotype 3b for 24 h. A significant increase in *hsp-6* mRNA was observed in response to *S. flexneri* infection ($p = 0.0025$, unpaired *t*-test). Data represent the means of three biological replicates, each replicate measured in triplicate and normalized to the control gene, *act*-2, expressed as the ratio of the corresponding *S. flexneri*-induced levels and the basal *E. coli* OP50 levels.

Quantitative real time PCRs were performed to determine the transcript levels of *hsp-6* in wild type, N2 nematodes infected with virulent *S. flexneri* and control worms maintained on *E. coli* OP50. The results of the qRT-PCR analysis show a significant increase in *hsp-6* expression in response to *S. flexneri* infection (Figure 5.14.C). The results of *hsp*-6::GPF reporter gene expression studies and qRT-PCR analysis are both consistent with the DIGE analysis and thus validate the results of the low stringency MASCOT search results.

5.3 Discussion

Consistent with previous reports, in this study we confirmed that a virulent *S. flexneri* serotype 3b strain kills nematodes. Nematode killing is associated with bacterial accumulation within the intestinal lumina of infected worms. Bacterial accumulation and *S. flexneri*-mediated killing of worms requires the expression of virulence plasmid-encoded genes as a virulence plasmid-cured *S. flexneri* strain failed to accumulate in nematode guts and also failed to kill worms. These results show that bacterial accumulation assays and nematode killing assays can efficiently distinguish between virulent and avirulent strains of *S. flexneri.*

Unlike the other animal models of shigellosis, virulence assays in *C. elegans* are cost-effective, reproducible and less labor intensive. Furthermore, *C. elegans* liquid killing assays have the additional advantage of being a high-throughput method to screen the virulence of numerous *S. flexneri* strains, as multiple replicates can be set up within each biological repeat. Despite the advantages of virulence assays in *C. elegans,* the mechanism of *S. flexneri* infection in nematodes and the nematode responses to infection remain unknown at present, limiting the use of this *in vivo* model of shigellosis.

The main aim of this study was to further our understanding of *S. flexneri* infection in *C. elegans* and to assess the suitability of *C. elegans* as a novel animal model to study *S. flexneri* pathogenesis. Transmission electron microscopy was used to study the cytopathology of infected nematodes and to track the *S. flexneri* infection process in nematodes. This is the first report of the cytopathology of *S. flexneri* infected worms. A proteomic approach was also used to identify *S. flexneri*-induced nematode responses.

5.3.1 Virulent *S. flexneri* cells ingested by *C. elegans* evade pharyngeal grinding, accumulate in the nematode intestinal lumen and invade the intestinal cells

Although bacterial accumulation assays and GFP^+ accumulation assays suggested that virulent strains of *S. flexneri* accumulate in the nematode gut, they do not prove this conclusively. The TEM micrographs obtained in this study, however clearly show intact *S. flexneri* cells within the intestinal lumina of infected worms, with the bacterial load increasing over time (Figure 5.3). This implies that some *S. flexneri* cells evade or escape pharyngeal grinding. The *C. elegans* grinder crushes ingested bacterial cells and is therefore the worm's primary defense against invading pathogens. The presence of increasing numbers of intact *S. flexneri* cells within the nematode intestinal lumen during the course of infection, clearly suggests that *S. flexneri* cells overcome or by pass this nematode defense mechanism.

A recent study proposed that the presence of O-antigen on bacterial surfaces protects bacterial cells from the macerating effects of the nematode grinder [255]. To test this hypothesis, the researchers treated an O-antigen expressing *E. coli* strain and an O-antigen

deficient control strain with glass beads and found that the presence of the O-antigen enhanced bacterial resistance to maceration. Both virulent and plasmid-cured *S. flexneri* strains used in our study express O-antigens on their surface, therefore it seems unlikely that the presence of O-antigen molecules alone protect bacterial cells against maceration in the nematode grinder.

Worms infected with virulent *S. flexneri* are sluggish, show impaired grinding of ingested food and fail to lay eggs as efficiently as control worms. All these symptoms correlate with an overall loss of energy and deficient neuromuscular functions. Furthermore, DIGE analysis identified several nematode proteins involved in locomotion (UNC-22, UNC-41, UNC-54, UNC-79 and UNC-89) and pharyngeal pumping (UNC-54, SLO-1 and HSP-6) as differentially expressed in response to *S. flexneri* infection. The differential expression of *unc-41, unc-54* and *hsp-6* was confirmed by qRT-PCR. Up-regulation of *hsp-6* promoter-driven GFP expression in nematodes infected with SFL1520 was also observed. These observations suggest that *S. flexneri* infection potentially induces overall systemic neuromuscular and mitochondrial defects in infected nematodes.

The TEM analysis also showed that *S. flexneri* cells cross the protective apical, microvilli brush border lining and invade the nematode intestinal cells. This observation is highly significant, as the ability of *S. flexneri* cells to invade human intestinal epithelial cells, is a critical step in bacterial pathogenesis. During human infection, *S. flexneri* cells exploit the transcytotic properties of specialized M cells to gain assess into the sub-epithelial space and invade the colonic and rectal epithelial cells via their less-protected basolateral surfaces (Section 1.3.1). *C. elegans* lacks specialized M cells and the results of TEM analysis in this

study suggest that *S. flexneri* invades the nematode intestinal cells through the apical side by degrading the protective microvilli (Figure 5.4.E). It is also possible that *S. flexneri* cells enter the intestinal cells through tight junctions between intestinal cells, however no evidence supporting this hypothesis was obtained in this study. The ability of *S. flexneri* to invade the *C. elegans* intestinal cells makes the use of this animal model a promising alternative to study shigellosis. Outside of Macaque monkeys none of the current animal models of shigellosis, show bacterial invasion of intestinal cells following oral infection.

The TEM micrographs also indicate that live *S. flexneri* cells within the nematode intestinal lumen produce structures that have the appearance of outer membrane vesicles (OMVs) (Figure 5.4.A and B). OMV production by gram negative bacteria in response to stress is a common phenomenon. Bacterial OMVs contain biologically active proteins, including virulence factors and active proteases that can degrade host cells [409-411]. *S. flexneri* OMVs contain the invasion protein antigens-Ipa proteins (IpaB, C and D) that are required for bacterial adherence, invasion and survival within infected tissues [408]. It has been previously shown that the production of OMVs by pathogenic bacteria provides a mechanism for the delivery of virulence factors to host tissues [412-416]. The identification of apparent *S. flexneri* OMVs in the *C. elegans* intestinal lumen therefore suggests a potential mechanism for the delivery of *S. flexneri* virulence factors to the nematode intestinal cells. However the identification of structures that resemble OMVs using EM is very preliminary and need further confirmation by additional experiments such as using immune-EM to identify *S. flexneri*-specific proteins in the putative OMVs.

5.3.2 *S. flexneri* infection potentially causes osmotic imbalance in nematode intestinal cells

In this study, the cytopathology of several nematodes infected with *S. flexneri* indicated that there appears to be an imbalance in intestinal osmoregulation in infected worms at the onset of infection (Figure 5.5). Forty one percent of animals observed in this study displayed this phenotype. In healthy animals, excess internal fluid is driven out of the intestinal cells into the pseudocoelom, following which it is transferred into the excretory cell to be expelled out of the animal as urine, thereby relieving the excess [417]. The above phenotype observed in 41% of infected animals suggests that the normal excretory mechanism is overwhelmed by a high rate of fluid leakage across the luminal villi into the intestinal cell cytoplasm.

Many animals and plants respond to the need to modify their internal ion balance by regulating the trafficking of certain ion transporters, channels, and exchangers. Vesicle trafficking and osmoregulation therefore appear to be interwoven. It is possible that virulence factors produced by *S. flexneri* at the onset of infection could inactivate or down-regulate the nematode ion transporters, endocytosis, and intracellular trafficking systems. TEM micrographs obtained in this study provide evidence that the intestinal cells of nematodes infected with virulent *S. flexneri* accumulate yolk granules. Yolk uptake is driven by receptor-mediated endocytosis. A group at Columbia University found that defects in the yolk receptor; *rme*-2 (LDL receptor superfamily), results in accumulation of yolk in the intestine [418]. Yolk accumulation in *S. flexneri* infected worms could be due to defects in endocytosis, cell-cell signaling or trafficking. These defects could also account for the fluid imbalance seen after 24 hour infection. Further experiments designed to investigate the distribution of the RME-2 and ion transporters in the intestinal cells of infected worms would

shed light on this hypothesis. Another possibility for defective osmoregulation in *S. flexneri* infected worms could be that the initial innate immune response mounted by the worms in response to *S. flexneri* infection, has downstream effects on osmoregulation.

During human infection, virulent *S. flexneri* invade the lining of the small intestine, damage cells, causing tiny sores (ulcerations) that bleed, and allow a considerable leakage of fluid containing proteins, electrolytes, and water. The fluid imbalance observed in response to the onset of *S. flexneri* infection in worms could have some correlation with the watery diarrhoea symptom seen in humans. However, since this phenotype was only observed in 41% of animals examined in this study, further experimental validation is needed to confirm this hypothesis.

5.3.3 *S. flexneri* infection in *C. elegans* causes embryo retention and/or defective egg laying

The cytopathology of infected nematode tissues showed that worms infected with virulent *S. flexneri* retained well advanced embryos (Figures 5.6 and 5.7). Infected worms appeared to be fertilizing eggs and the embryos seemed to develop normally. However, the uterus of infected worms was very swollen, with well-developed advanced embryos. Normal adult worms lay eggs every 30 s to 1 minute. Egg laying involves several neurons, working in synergy with the muscles of the uterus and vulva. Embryo retention could be due to improper neuromuscular functions. UNC-54, UNC-89 and MTD-17, identified as *S. flexneri*-induced responses in nematodes in the DIGE analysis (Tables 5.1 and 5.2), are proteins required for efficient egg-laying. Previously, Kesika and colleagues reported that worms infected with *S. flexneri* lay fewer eggs (26 ± 6 eggs per worm compared with 275 ± 15 eggs per worm in OP50 controls). They hypothesized that was due to a defect in gametogenesis.

TEM images obtained in this study did not provide any evidence of a defect in gametogenesis, but showed retention of fertilized, developing eggs, probably due to an egg-laying defect. Embryo retention could lead to internal hatching, which could be one of the factors responsible for nematode death.

5.3.4 Limitations of TEM analysis

TEM analysis of nematodes infected with *S. flexneri* was carried out in collaboration with Professor David Hall (Albert Einstein College of Medicine, New York). Nematodes have a thick, impermeable external cuticle which makes fixing and staining of worms very challenging. The microwave-assisted fixing and straining protocol developed by David Hall [308] was used in this study. Optimizing the microwave-assisted fixing and staining protocol proved challenging; samples fixed in Australia were sectioned and examined at the Albert Einstein College of Medicine, NYC. The time available to me to complete the microscopy was limited, just one month. It is highly likely that further analysis of infected nematode tissue would uncover other phenotypes.

5.3.5 First study to scan the proteome of *S. flexneri* infected worms

DIGE was performed in this study to identify *S. flexneri*-induced nematode responses. This is the first report to scan the proteome of *S. flexneri* infected worms. Although DIGE analysis identified 41 potential *S. flexneri*-induced proteins in *C. elegans,* only seven of these proteins were successfully identified using MASCOT searches. DIGE analysis showed that ACO-1, CCT-2, DAF-19, EEF-2, HSP-60 and UNC-54 were up-regulated and UNC-41 was down-regulated in nematodes infected with *S. flexneri* (Table 5.1). qRT-PCRs confirmed the differential expression of *cct-2, daf-19, hsp-60, unc-54* and *unc-41* predicted by DIGE

analysis. Results of qRT-PCR found no differences in *aco-1* levels in infected worms, and the expression of *eef-2* appeared to be down-regulated at the transcription level. These observations suggest that the expression of ACO-1 and EEF-2 is post-transcriptionally regulated in *S. flexneri* infected worms.

On lowering the stringency of the MASCOT search parameters, significant protein hits were identified for 39 out of 41 spots. Although these proteins provide some insight into *S. flexneri*-induced responses in nematodes, these results need further experimental verification. To verify whether increased expression of the proteins predicted using these parameters was, in fact, induced in response to *S. flexneri* infection, the expression of *hsp-6*, the gene coding one of the proteins identified using the low stringency search parameters, was investigated further in this study. Results of *hsp-6* transcriptional reporter gene experiments and qRT-PCR were consistent with the DIGE analysis and indicated that HSP-6 expression is up-regulated in response to *S. flexneri* infection. These observations suggest that those proteins predicted using the low stringency MASCOT search parameters could be a true *S. flexneri*-induced response.

5.3.6 *S. flexneri* disrupts iron homeostasis in the nematode intestinal cells by altering ACO-1 levels, potentially inducing a hypoxic response resulting in death

ACO-1 was shown to be up-regulated in response to *S. flexneri* infection. RNAi-mediated silencing of *aco-1* led to enhanced resistance to *S. flexneri* infection. These results suggest that the up-regulation of ACO-1 in response to *S. flexneri* infection contributes to nematode death. *aco-1* encodes cytoplasmic aconitase, an enzyme whose expression is negatively

regulated post-translationally by iron levels [419]. In *C. elegans, aco-1* is expressed in the cytosol of cells of the hypodermis and intestine [420]. Its mammalian homologue, iron regulatory protein 1 (IRP-1), expressed in the brain and intestinal cells, plays a central role in iron homeostasis. The up-regulation of ACO-1 in response to *S. flexneri* infection therefore suggests that *S. flexneri* potentially disrupts iron homeostasis in *C. elegans.*

A recent study showed that *P. aeruginosa* infection disrupts iron homeostasis in *C. elegans,* causing a *hif-1*-mediated hypoxic response leading to nematode death [421]. Similarly, *S. flexneri* could potentially kill nematodes by disrupting iron homeostasis, leading to the up-regulation of ACO-1 and the induction of a hypoxic response. Results of our DIGE analysis also identified the nematode MTSS-1 protein as down-regulated in response to *S. flexneri* infection. MTSS-1 is a mitochondrial single stranded DNA binding protein that is essential for mitochondrial DNA replication [422]. RNAi knock down of *mtss-1* in worms, results in transcriptional alterations leading to the induction of hypoxia responses [422]. The up-regulation of ACO-1 and down-regulation of MTSS-1 in response to *S. flexneri* suggests that *S. flexneri*-disrupts nematode iron homeostasis which potentially induces a hypoxic response culminating in death.

5.3.7 Innate immune responses triggered by CCT-2 and DAF-19

RNAi experiments indicated that *cct-2* and *daf-19* knock down worms showed enhanced susceptibility to *S. flexneri* infection (Figures 8.C, D and 9.A, D and E), suggesting that these responses form part of the nematode protective mechanism. CCT-2 has been predicted to interact with DAF-16, which forms part of the nematode DAF-2/DAF-16 insulin signaling

pathway [423]. A previous study reported that RNAi knock down of the chaperonin *cct-2*, inhibits the nuclear localization of DAF-16 in intestinal cells [423], suggesting that CCT-2 is required for the nuclear translocation of DAF-16. DAF-16 is a transcription factor that has been associated with the expression of several antimicrobial genes [271]. The increased susceptibility of *cct-2* RNAi worms to *S. flexneri* infection could therefore be due to the decreased expression of antimicrobial peptides as a result of defective nuclear translocation of DAF-16. The up-regulation of CCT-2 in response to *S. flexneri* coupled with the increased susceptibility of *cct-2* RNAi worms suggests that *S. flexneri* infection activates the DAF-2/DAF-16 insulin signaling pathway.

The transcription factor DAF-19 has recently been shown to play a role in the MAPK pathway in *C. elegans* [424]. DAF-19 mutant worms display enhanced susceptibility to killing by *P. aeruginosa* [424]. DAF-19 is an ortholog of the regulatory factor X (RFX), a transcription factor that is required for human adaptive immunity [425]. The up-regulation of DAF-19 in *S. flexneri* infected worms could therefore be part of the nematode innate immune response at the early stages of *S. flexneri* infection. Furthermore, TIR-1 was also shown to be up-regulated in response to *S. flexneri* infection using the low stringency MASCOT searches (Table 5.2). TIR-1 is the toll interleukin 1 receptor domain adaptor protein in *C. elegans* that activates the p38 MAPK innate immune response. During human infection, the multiplication of *S. flexneri* cells within infected intestinal cells activates the MAPK-mediated signaling pathway, thus leading to the production of inflammatory chemokines and cytokines and antimicrobial peptides [65, 426]. The up-regulation of both DAF-19 and TIR-1 in infected worms and the increased susceptibility of *daf*-19 RNAi worms suggests that the p38 MAPK pathway is potentially induced by *C. elegans* in response to *S. flexneri* infection.

5.3.8 Up-regulation of HSP-60 and HSP-6 in response to *S. flexneri* infection, indicates the activation of the mitochondrial unfolded protein stress response

Low stringency MASCOT searches identified HSP-6 as a protein that was up-regulated in response to *S. flexneri* infection. HSP-6 is a mitochondrial associated chaperone protein whose expression is known to be up-regulated in response to the mitochondria-specific unfolded protein response (UPR^{mt})[427]. UPR^{mt} is activated by the accumulation of misfolded mitochondrial proteins [428]. Mitochondrial functionality is essential for cellular function, not only as a source of energy but also as a source of reactive oxygen species (ROS), thought to be causative agents of aging and disease [429]. Mitochondrial dysfunction can therefore lead to accelerated aging, oxidative stress and apoptotic cell death; therefore maintenance of the balance of mitochondrial folding capacity is of vital importance to the health of an organism [430].

It has been previously shown that increase in HSP-6 expression correlates with inhibition of mitochondrial respiration [431]. The chaperone HSP-60 is another prominent UPR^{mt} marker. The up-regulation of both HSP-6 and HSP-60 in response to *S. flexneri* infection suggests the activation of UPR^{mt} and the potential inhibition of mitochondrial respiration in infected worms. Inhibition of respiration would result in lower energy levels which could account for a systemic neuromuscular defect in infected worms.

Previous studies have shown that *S. flexneri* infection of mammalian cells induced mitochondrial dysfunction, resulting in capsase-mediated necrotic cell death [432-434]. These studies suggest that the oxidative stress and innate signaling pathways triggered by

intracellular *S. flexneri* are tightly linked and these pathways converge at the mitochondria to control cell necrosis [432]. I therefore hypothesize that the UPR^{mt} response detected in *S. flexneri*-infected nematodes provides evidence that, as in mammalian infection, *S. flexneri* potentially induces mitochondrial dysfunction, which could lead to necrotic cell death.

5.4 Conclusion

Unlike humans and non-human primates, the small animal models of shigellosis fail to develop intestinal disease upon ingestion of *S. flexneri.* Here we have shown that virulent strains of *S. flexneri* are ingested by the nematode, *C. elegans,* and that *S. flexneri* cells invade the nematode intestinal cells. This is the first report to investigate the cytopathology and nematode responses to *S. flexneri* infection. DIGE analysis of the nematode proteome induced by *S. flexneri* suggests that both the DAF-2/DAF-16 insulin signaling pathway and the p38 MAPK pathway are potentially induced in response to bacterial infection. Our findings also suggest that *S. flexneri* disrupts iron homeostasis in nematodes and potentially induces a hypoxic response which could lead to death. The results of this study further our understanding of *S. flexneri* infection in *C. elegans,* opening up a new, convenient, economical alternative for screening *Shigella* mutant strains to identify attenuated strains for testing live vaccine strains and for the identification of novel virulence factors.

Chapter 6
General discussion

Chapter 6: General Discussion

Diarrhoeal disease is a major public health concern and *Shigella* strains account for 5-15% of the global burden of diarrhoeal disease [435]. Over 50 years of research has led to an increased understanding of *Shigella* pathogenesis, and the identification of numerous *Shigella* vaccine candidate antigens. However, the search for a commercially viable vaccine is ongoing. A thorough understanding of bacterial pathogenesis is paramount for the development of an effective vaccine. This thesis aimed to characterize the novel bacterial chromosomal virulence factors, AnsB and GGT, and identify bacteriophage-encoded virulence factors that contribute to host virulence. The identification of virulence factors expressed across multiple serotypes of *S. flexneri* would be immensely valuable to the development of vaccines that offer heterologous protection against multiple serotypes.

One of the major limitations of *Shigella* vaccine development has been the absence of a relevant animal model to study shigellosis. Most of the information regarding the pathogenesis of *Shigella* and identification of vaccine candidate antigens gathered over the years, has come from *in vitro* cell culture studies, the *in vivo* murine pulmonary model and the guinea pig keratoconjunctivitis model of shigellosis. Although these models have been used extensively to uncover a wealth of information, their major limitation lies in the fact that both animal models lack clinical relevance in terms of the site of infection and the symptoms produced. To this end, this thesis aimed to assess the suitability of using the nematode *C. elegans* as a novel small animal model of shigellosis.

6.1 AnsB and GGT novel *Shigella* virulence factors

To further our understanding of *S. flexneri* pathogenesis the role of *L-asparaginase* (AnsB) and γ-glutamyltranspeptidase (GGT), in bacterial pathogenesis was studied. These proteins were selected as both proteins are immunogenic in *S. flexneri* and have not been previously characterized in *S. flexneri.* The results of this thesis indicate that *ansB* and *ggt* mutations decrease the virulence of *S. flexneri* as indicated in *in vitro* and *in vivo* virulence studies. The results of *in vitro* cell culture assays show that *ansB* and *ggt* mutations decrease bacterial adherence to host cells. This is the first study to identify AnsB and GGT as potential virulence factor of *S. flexneri.* Taking all the data obtained from the virulence studies and DIGE analysis into account, the following models have been proposed to explain the role of AnsB and GGT in the virulence of *S. flexneri.*

6.1.1 AnsB up-regulates OmpA expression

The results of DIGE analysis and qRT-PCR (Figures 3.10 and 3.12.A), showed the up-regulation of OmpA in *ansB* mutant cells. These observations suggest that the expression of OmpA is negatively regulated by AnsB in *S. flexneri.* The expression of OmpA has been known to be environmentally responsive [332]. One of the environmental factors that regulate the expression of OmpA is the availability of nitrogen [436]. In *E. coli,* OmpA levels are elevated in response to nitrogen shortage [436], to facilitate an increased uptake of peptides to alleviate the nitrogen shortage. One of the identified functions of AnsB is to provide nitrogen and carbon sources from the hydrolysis of exogenous asparagine [437] (Figure 6.1.A). Nitrogen depletion increases the expression of *ansB* in yeast [438, 439], further suggesting that AnsB plays a role in nitrogen metabolism. *ansB* mutant cells would thus have lower nitrogen levels compared with wild type cells; therefore I propose that the

expression of OmpA in these mutant cells may be increased to alleviate this nitrogen shortage (Figure 6.1.C).

The structure of bacterial cell envelopes is strictly regulated, and appropriate levels of envelope proteins are constantly monitored and controlled. Under normal circumstances, OmpA levels in cells are negatively regulated by the sRNA MicA, induced as part of the σ^E-mediated envelope stress response (Figure 6.1.B). Extracytoplasmic stress such as the overproduction of outer membrane proteins, are known to activate σ^E expression, through a proteolytic signal transduction cascade, which ultimately leads to the cytoplasmic release of σ^E [440]. The transcription of *micA* is increased in response to cytoplasmic σ^E [441]. *micA* along with the RNA chaperone Hfq, then base pairs with and destabilizes *ompA* transcripts [442] (Figure 6.1.B).

A study by Wagner and colleagues [443], reported that the overexpression of membrane proteins in *E. coli* reduced cell viability. This was primarily as a result of the overexpressed proteins saturating the membrane translocation machinery, particularly the Sec translocon thereby limiting the capacity this translocon. This group reported that saturation of the Sec translocon by the overexpressed membrane protein had a severe impact on the cell envelope and cytoplasmic proteomes [443]. In *E. coli,* pro-OmpA molecules synthesized in the cell cytoplasm are translocated into the periplasmic space through the Sec translocon [444]. As proposed by Wagner *et al* [443], the up-regulation of OmpA in Δ*ansB* cell could limit the capacity of the Sec translocon, as a result of which the proteolytic signal transduction machinery of the envelope stress response could be compromised in Δ*ansB* cells (Figure 6.1C). If this is the case, the σ^E-mediated stress response is not activated, which leads to the

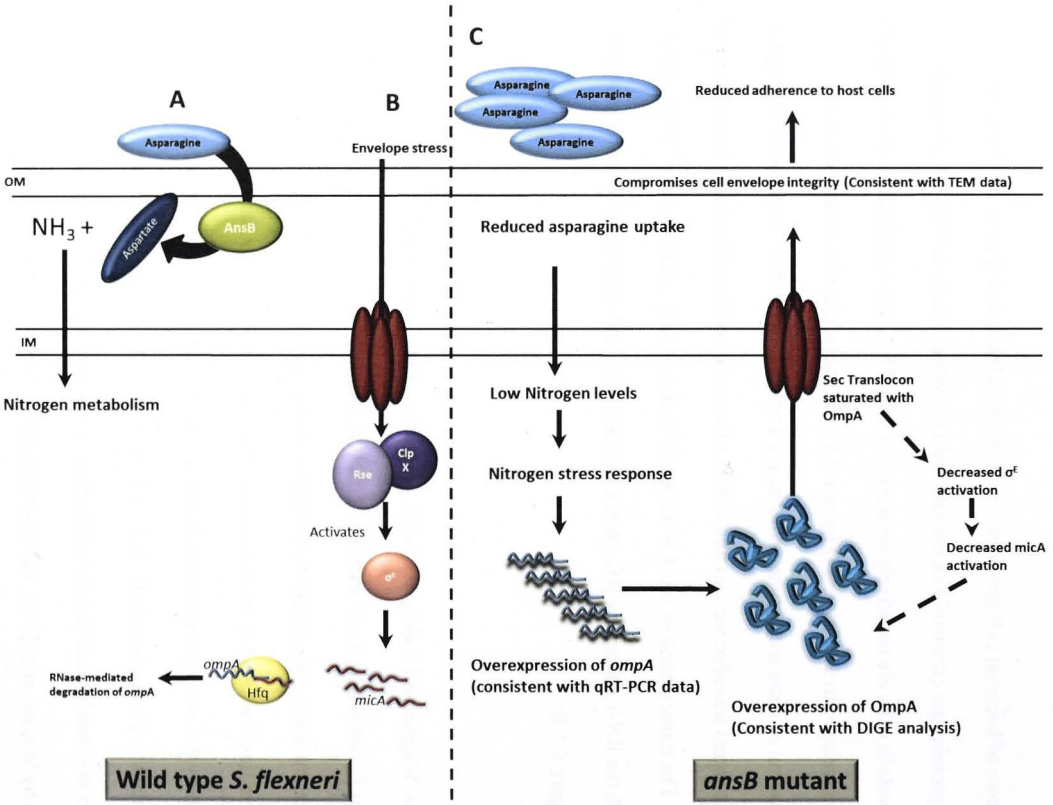
A
B
C
Asparagine
AnsB
Aspartate
NH_3 +
Nitrogen metabolism
OM
IM
Envelope stress
Rse
Clp X
Activates
σ^E
ompA
Hfq
RNase-mediated degradation of ompA
micA
Wild type S. flexneri
Asparagine
Asparagine
Asparagine
Asparagine
Reduced adherence to host cells
Compromises cell envelope integrity (Consistent with TEM data)
Reduced asparagine uptake
Low Nitrogen levels
Nitrogen stress response
Overexpression of ompA
(consistent with qRT-PCR data)
Sec Translocon saturated with OmpA
Decreased σ^E activation
Decreased micA activation
Overexpression of OmpA
(Consistent with DIGE analysis)
ansB mutant

Figure 6.1: Proposed model for how AnsB regulates the adherence of *S. flexneri.* A: Hydrolysis of asparagine by periplasmic AnsB in wild type cells produces aspartate and ammonia (NH_3), which then promotes cellular nitrogen metabolism. **B:** Sigma E (σ^E)-mediated activation of *micA,* negatively regulates *ompA* levels in wild type cells by interacting with the RNA chaperone, Hfq. **C:** Δ*ansB* cells fail to produce L-asparaginases (AnsB), which would lead to decreased nitrogen metabolism and therefore decreased intracellular nitrogen levels. Low cellular nitrogen levels activate the nitrogen stress response which results in the overexpression of outer membrane protein A (OmpA) to increase peptide uptake. Overexpression of OmpA, could saturate the Sec translocon and limit its capacity, which would compromise the signal transduction machinery involved in activating the σ^E-mediated envelope stress response. Decreased activation of σ^E would mean decreased transcription of *micA* and thus cellular regulation of OmpA is inhibited. The uncontrolled overexpression of OmpA would disrupt the integrity of the cell envelope as a result of which, Δ*asnB* strains show decreased bacterial adherence to host tissues.

unregulated expression of OmpA (Figure 6.1.C). This hypothesis is supported by the fact that we did not detect markers for envelope stress, such as the Skp or DegP chaperones, in the proteome of *ansB* mutant cells.

6.1.2 GGT modulates extracellular glutathione levels and therefore maintains the redox potential of the extracellular and periplasmic compartments

GGT in *E. coli* is involved in glutathione (GSH) metabolism, as it hydrolyses the transfer of the γ-glutamyl group from GSH to amino acids and peptides [316]. GSH is one of the most abundant nonprotein, thiols present in proteobacteria [445-447]. This molecule, plays a critical role in protecting cells against environmental stresses such as acidity, oxidative stresses and osmotic shock by maintaining the proper oxidation state of proteins [448]. GSH exists in either a reduced (GSH) or an oxidized (glutathione disulfide, GSSG) form, and participates in redox reactions through the reversible oxidation of its active thiol [449]. Maintenance and adjustment of the ratio of [GSH] to [GSSG], allows individual subcellular compartments to have different, appropriate redox balances. Pittman and colleagues have reported that GSH plays a key role in maintaining periplasmic redox homeostasis in *E. coli* [450].

The γ-linkage of GSH maintains its stability and GGT is the only enzyme known to degrade GSH in both prokaryotic and eukaryotic organisms. Mammalian GGTs have been extensively studied [316, 451], however not much is known about bacterial GGT. In *E. coli,* GGT is involved in maintaining exogenous GSH levels and *ggt* mutants have been previously reported to accumulate GSH in culture media [452]. Since *S. flexneri* is a close relative of *E.*

coli, it is likely, that GGT modulates exogenous GSH levels in *S. flexneri* as well. If this were the case, *Δggt* cells would have elevated extracellular GSH. Suzuki and colleagues have previously identified a GSH importer in *E. coli,* YliABCD, that transports extracellular GSH into the bacterial periplasmic space [453]. They also indicate that although *ggt* mutants in *E. coli* have elevated extracellular GSH levels, the concentration of extracellular GSH decreases gradually over prolonged incubation, which suggests, that extracellular GSH is imported into cells where it is broken down, to provide cysteine and glycine sources [454] (Figure 6.2). Previous studies in *E. coli* and *S. typhimurium* have also reported that cytoplasmic GSH is transported into the periplasmic space where it is hydrolyzed by GGT to liberate glutamic acid and cystenylglycine [452, 455] (Figure 6.2). Pittman and colleagues have identified a GSH transporter in *E. coli* that facilitates the transport of this molecule from the cytoplasm into the periplasmic space [450].

S. flexneri carry homologues of the ABC transporter, YilABCD, annotated as GsiABCD. Therefore it is likely that *S. flexneri* cells, like *E. coli* import extracellular GSH into their periplasmic space. Accumulation of extracellular GSH and its translocation into the periplasmic space of Δ*ggt* cells would create a reducing environment in the periplasmic compartment of these cells. The periplasmic space of bacterial cells is normally an oxidative compartment, that provides conditions favorable to the formation of protein disulfide bonds, to achieve proper tertiary structures [449].

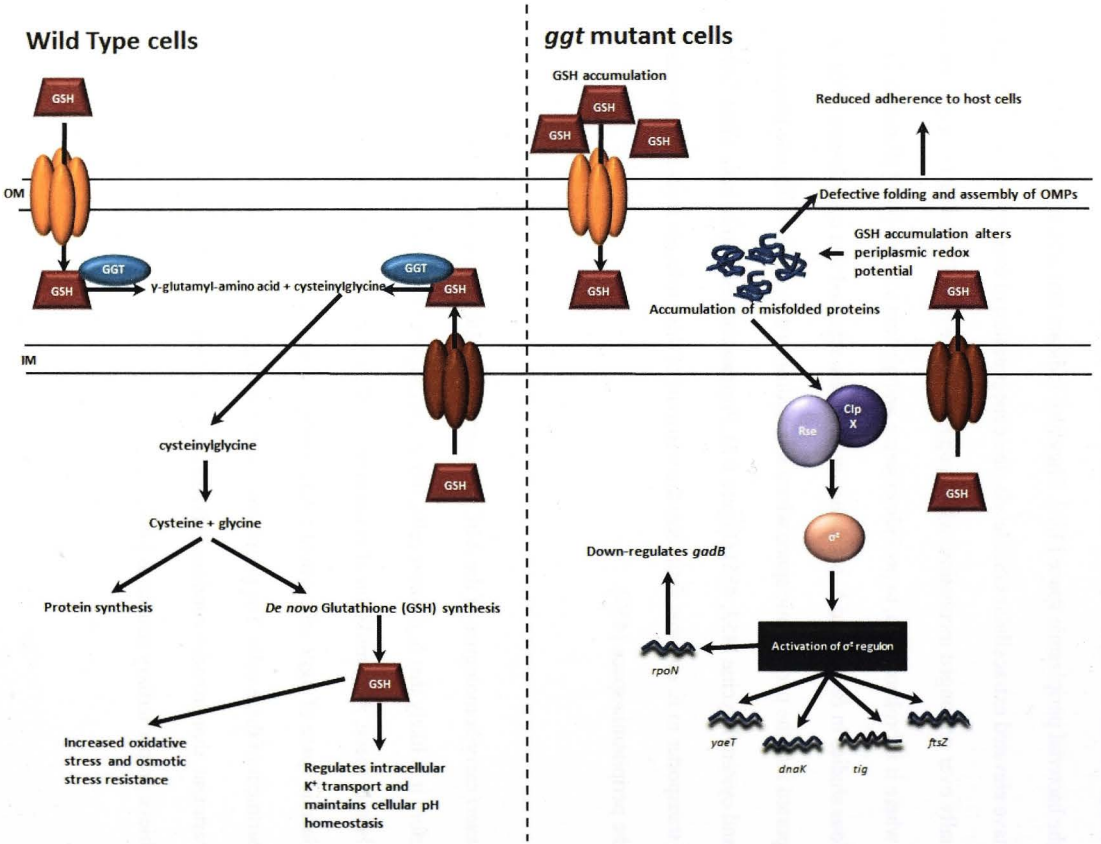
Wild Type cells
ggt mutant cells
GSH accumulation
Reduced adherence to host cells
OM
Defective folding and assembly of OMPs
GSH accumulation alters periplasmic redox potential
GGT
γ-glutamyl-amino acid + cysteinylglycine
Accumulation of misfolded proteins
IM
Rse
Clp X
cysteinylglycine
Cysteine + glycine
Down-regulates gadB
Protein synthesis
De novo Glutathione (GSH) synthesis
Activation of σ^E regulon
rpoN
yaeT
dnaK
tig
ftsZ
Increased oxidative stress and osmotic stress resistance
Regulates intracellular K$^+$ transport and maintains cellular pH homeostasis

Figure 6.2: Proposed model for how GGT regulates the adherence of *S. flexneri.* GGT encodes γ-glutamyltranspeptidase, an enzyme required for the hydrolysis of extracellular glutathione (GSH). In wild type cells GSH is transported into the periplasmic space through ABC transporters, where it is hydrolyzed by GGT to produce γ-glutamyl-amino acids and cysteinylglycine. Cysteinylglycine enters the cytosol where it is broken down into cysteine and glycine. Δ*ggt* cells fail to express GGT, as a result of which there is a buildup of extracellular GSH. GSH is a small molecule capable of entering the bacterial periplasmic space through the ABC transporter, GsiABCD (orange). The accumulation of GSH in the periplasmic space would alter the redox potential of this space and create a reducing environment, which is not conducive to protein folding and assembly, therefore leading to the accumulation of mis-folded proteins, which in turn would trigger the σ^E-mediated stress response. *yaeT, dnaK, tig* and *ftsz* are members of the σ^E-regulon, identified as up-regulated in Δ*ggt* cells. Activation of the σ^E-regulon also activates *rpoN*, which is a known inhibitor of *gadB* expression. The up-regulation of *yaeT, dnaK, tig, ftsz* and down-regulation of *gadB* in Δ*ggt,* identified in this study, therefore suggest the activation of the σ^E-mediated stress response in these cells, which suggests the accumulation of mis-folded proteins in these cells most likely due to GSH accumulation.

I hypothesize that GSH accumulation and translocation into the periplasmic compartments of Δ*ggt* cells, creates a reducing environment in this compartment that is not conducive to the proper folding and assembly of periplasmic proteins. Defective folding and assembly of periplasmic proteins would have a direct consequence on the assembly of outer membrane proteins, including adhesions. Defective assembly of surface molecule in *ggt* mutant cells could therefore explain the decreased adherence of these mutant cells (Figure 6.2).

DIGE analysis indicated that the *ggt* mutation exert pleiotropic effects on the expression of several other *S. flexneri* proteins (Figure 3.11 and Table 3.2) including proteins involved in translation (RpsA), cell division (FtsZ), acid resistance (GadB), carbohydrate metabolism (PpsA), protein folding and transport (DnaK and Tig), and an outer membrane protein (YaeT). qRT-PCR analysis identified *yaeT, dnaK, tig* and *ftsz* as up-regulated in Δ*ggt* cells (Figure 3.12.B), these genes have previously been identified as members of the σ^E regulon, and their expression is known to be up-regulated on σ^E activation [440, 456]. Both DIGE analysis and qRT-PCR data indicate a significant decrease in GadB levels in Δ*ggt* cells (Figures 3.11 and 3.12.C). GadB is part of the well characterized glutamate-dependent acid resistance (GDAR) pathway used by *E. coli* [457] and *S. flexneri* [458]. A recent study identified RpoN as a negative regulator of the GDAR pathway [459], which suggests, that the down-regulation of *gadB* could be due to the activation of RpoN. *rpoN* is another member of the σ^E regulon whose expression is up-regulated up on σ^E activation [440]. The increased expression of *yaeT, dnaK, tig* and *ftsz* and down-regulation of *gadB* transcripts in Δ*ggt* cells, therefore suggests the activation of a σ^E-mediated envelop stress response in *ggt* mutant cells (Figure 6.2).

σ^E activity is specifically activated by events or mutations that lead to envelope stress caused by the accumulation of unfolded or mis-folded proteins [460]. Activation of σ^E, up-regulates the transcription of a set of genes that form part of the σ^E regulon [461, 462]. Rhodius and colleagues have previously reported that the σ^E regulon in bacterial cells is composed of 89 predicted transcriptional units with a core set of genes conserved in most organisms [440]. These core genes coordinate the assembly and maintenance of bacterial LPS and outer membrane proteins in response to the accumulation of mis-folded proteins. *yaeT* and *ftsZ* were identified as members of the core regulon. The up-regulation of *yaeT* and *ftsZ* transcripts in Δ*ggt* cells, therefore suggests the activation of this pathway in response to the accumulation of improperly folded proteins in the periplasmic space.

DIGE and qRT-PCR data indicate that the expression of *tig* and *dnaK* was up-regulated in *ggt* mutant cells. Previous studies in *E. coli* have indicated that Tig interacts with DnaK to facilitate protein folding [463, 464]. The up-regulation of DnaK and Tig in Δ*ggt* cells provides further evidence suggesting the accumulation of mis-folded proteins in these mutants.

6.1.3 Future work

- The results of this thesis led to the hypothesis that the periplasmic enzyme, AnsB, of *S. flexneri* modulates bacterial adherence to host epithelial cells by regulating the expression of OmpA through the regulation of nitrogen metabolism. In order to determine whether low nitrogen levels do in fact increase the expression of OmpA in *S. flexneri* cells, wild type *S. flexneri* cells can be grown under low nitrogen conditions and the corresponding

ompA transcript and protein levels can be measured using qRT-PCR and western blotting, respectively.

- Transmission electron microscopy and immunohistochemistry using anti-OmpA antibodies can be used to compare the integrity of cell envelopes and the distribution of OmpA in wild type and Δ*ansB* cells. The LIVE/DEAD BacLight kit (Molecular Probes, Invitrogen) which is used to differentiate between bacterial cells with intact and damaged membranes can be used to compare the membrane integrity of wild type and Δ*ansB* cells. This kit has a mixture of the red- and green-fluorescent nucleic acid stains dyes propidium iodide (PI) and SYTO9, respectively. SYTO9 can penetrate all cells while PI only enters bacterial cells with altered membrane permeability. Therefore when the two dyes are used in combination, the presence of bacteria presenting defects in membrane integrity causes a reduction in the green fluorescence emission [465].

- Extracellular glutathione levels can be measured with glutathione reductase as described by Fahey *et al* [466]. To detect the accumulation of mis-folded proteins in *ggt* mutant cells protein aggregates from wild type and *ggt* mutant cells could be isolated and compared using SDS PAGE as described by Tomoyasu *et al* [467]. These experiments would shed light on the hypothesis GGT regulates the virulence of *S. flexneri* by modulating glutathione levels which in turn maintains the redox potential of cellular compartments required for proper protein folding.

- This study identified AnsB and GGT as novel virulence factors of *S. flexneri* making them significant candidates for the attenuation of live vaccines. Genes encoding AnsB

and GGT are present in all *S. flexneri* strains and therefore offer great promise for live vaccine strategies that provide heterologous protection against multiple serotypes. *ansB* and *ggt* can also be targeted as secondary mutations in existing live attenuated *Shigella* vaccines to achieve the desirable balance between reactogenicity and immunogenicity. *ansB* and *ggt* mutant strains generated in this study can be tested as live vaccine candidates in the murine pulmonary model of shigellosis, where mice treated with sub-lethal doses of both mutant strains cans be challenged by heterologous serotypes of wild type *S. flexneri* strains to determine if these vaccine candidates offer heterologous protection against multiple serotypes. It would also be interesting to generate *ansB* and *ggt* double mutant and test this strain as a potential live vaccine candidate.

6.2 Bacteriophage-encoded genes in host pathogenesis

The complete genome sequence of bacteriophage SfII was determined as one of the aims of this study. This was done to broaden our understanding of *S. flexneri* phage biology as not much is known about temperate bacteriophages of *S. flexneri* outside their role in serotype conversion. Sequence analysis showed that SfII contains features of lambdoid phages and shares a high degree of sequence similarity with *S. flexneri* serotype converting phages, SfI, SfII, SfIV and SfV. Interestingly, although these *S. flexneri* phages show a high degree of sequence conservation, their host ranges vary significantly. Analysis of the SfII genome sequence identified seven uncharacterized genes unique to SfII.

In vitro and *in vivo* virulence studies showed that lysogenization of a *S. flexneri* serotype Y strain with bacteriophage SfV, increased the virulence of the host strain. These results

suggest that the temperate bacteriophage, SfV, encodes virulence factors. This finding was not surprising as several bacteriophage-encoded virulence factors have been identified in a range of bacterial hosts (Table 1.4). However, outside of the O-antigen modifying gene cluster, no *S. flexneri* phage-encoded virulence factors have been identified thus far. To identify potential SfV-encoded virulence factors outside of the O-antigen modifying genes, RT-PCR was used to determine if 15 uncharacterized SfV genes were expressed in the lysogenized host.

RT-PCR analysis identified SfV *orf28, orf29, orf30, orf31, orf32, orf36, orf38, orf41, orf42, orf44, orf45, orf47* and *orf48* as expressed within the lysogen. This observation suggests that the expression of these genes may be advantageous to the host. Several attempts were made to knock out all 13 genes individually and as clusters, however only the SfV *orf28-32* five gene cassette could be successfully knocked out within the scope of this project. To determine whether genes within the SfV *orf28-32* cassette encode proteins that play a role in the pathogenesis of *S. flexneri,* a SfV *orf28-32* knockout mutant strain, SFL2500, was constructed. Interestingly the results of *in vitro* cell culture assays suggest that the deletion of this five gene cassette from the lysogen increased the adherence of the lysogen however SFL2500 was less invasive than its parent. These observations suggest that genes within this five gene cassette potentially contribute to different aspects of *S. flexneri* pathogenesis. With one or several genes acting as potential regulators of host gene expression (with *orf28* being the leading contender based on conserved domain searches, as discussed Section 4.3.2.4.1) and other genes encoding proteins that enhance the invasive capacity of the host strain (with *orf30* encoding a potential virulence factor, as discussed in Section 4.3.2.4.3). *In vivo* virulence studies in *C. elegans,* suggest that on knocking out the *orf28-32* cassette, the SfV lysogen shows reduced accumulation in the nematode intestinal lumen which suggest that one

or several of these genes encode virulence factors. However, mutating these genes had no effect on nematode killing which suggest that proteins encoded by the *orf28-32* cassette may be required at the onset of infection however these proteins are not required for prolonged infection. Future studies should determine bacterial accumulation over extended time periods to determine if the decreased accumulation observed in this study is in fact only seen at the onset of infection.

The results of virulence studies obtained with the *orf28-32* mutant open up several possibilities and a clear picture of the exact roles played by *orf28-32* in the pathogenesis of *S. flexneri* remains elusive. These results do however suggest that bacteriophage genes outside of the O-antigen modifying genes may play a role in the pathogenesis of *S. flexneri* strains.

6.2.1 Future work

- Sequence analysis identified SfII *orf35, orf36, orf40, orf41, orf49, orf50* and *orf57,* encoding hypothetical proteins to be unique to SfII. These genes are potential candidates for virulence studies. RT-PCR analysis to identify which of these genes is expressed in a SfII lysogen would help narrow down this list and identify potential SfII genes that encode protein that benefit the bacterial host.

- Further virulence studies using individual knockout mutants of *orfs28, 29, 30, 31* and *32* will help us pin down the phage genes directly responsible for the phenotypes observed in this study. Alternatively, the *orf28-32* mutant strain can be complemented with each individual gene to identify which of the five genes increases bacterial adherence and

decreases invasion. *orf28, orf29, orf30, orf31* and *orf32* also present in SfIV and therefore individual knockout mutants of these genes in the SfV lysogen could be complemented with genes isolated from SfIV. *orf28, orf29,* and *orf30* are also present in *S. flexneri* phage SfII and homologues of these genes are also present in the *S. flexneri* serotype 2a genome (AE0056741), therefore it will be interesting to see if knocking out *orf28, orf29* or *orf30* in this *S. flexneri* 2a strain affects its virulence.

- Knockout mutants should be constructed for the remaining eight genes identified to be expressed within the lysogen, *orf36, orf38, orf41, orf42, orf45, orf47* and *orf48* to determine if any of these genes contribute to the virulence or fitness of the host strain.

- To determine why the SfV iorf28-32 mutant showed increased adherence a 2-D proteomic screen can be used to compare the proteomes of the mutant and lysogen.

6.3 *C. elegans* as a model for shigellosis

The results obtained from examining the cytopathology of nematodes infected with a virulent strain of *S. flexneri* and scanning the proteome of *S. flexneri*-infected worms suggest that several parallels exist between *S. flexneri* infection in humans and nematodes. These results are highly significant, as they validate the use of *C. elegans* as a relevant small-intestinal animal model of shigellosis. Some of the similarities between *S. flexneri* infection in humans and *C. elegans* have been elucidated below;

6.3.1 Nematodes ingest *S. flexneri* and bacterial cells invade the intestinal epithelial cells

During human infection, *S. flexneri* cells ingested via the fecal-oral route, traverse the gastrointestinal tract and invade the intestinal epithelial cells. Similarly, the cytopathology of infected nematode tissue indicates that *S. flexneri* is ingested by the nematodes, bacterial cells accumulate in the intestinal lumen (Figure 5.2), following which they invade the intestinal epithelial cells (Figure 5.3). TEM micrographs obtained in this study suggest that *S. flexneri* invades the nematode intestinal cells through their apical surfaces by putatively degrading the apical brush border (Figure 5.4). It is also possible that *S. flexneri* cells gain access to the epithelial cells through the tight junctions between the nematode epithelial cells, and that bacterial cells induce their uptake by the epithelial cell by delivering T3SS effectors that trigger epithelial membrane ruffling and induce the formation of mactropinocytes as seen in human epithelial cell invasion [468]. However, no evidence to support this hypothesis was obtained in this study. Further TEM analysis of dead or dying worms may enable us to capture the precise invasion mechanism.

6.3.2 *S. flexneri* virulence factors required for infection of mammalian tissue are also required for virulence in *C. elegans*

Results of virulence assays performed in this study and a previous study by Burton and collegues [283], show that the expression of the *S. flexneri* virulence plasmid genes is essential for bacterial accumulation and killing of *C. elegans*. Bacterial strains devoid of the virulence plasmid are digested by the nematodes in a manner similar to *E. coli* OP50. Furthermore, potential *S. flexneri* virulence factors identified using *in vitro* cell culture assays and the murine pulmonary model of shigellosis in this study (AnsB, GGT and SfV Orfs28-32) were also found to be required for virulence in *C. elegans*. These results suggest that the

S. flexneri virulence factors required for mammalian infection are also essential for infection in *C. elegans,* thereby validating the use of *C. elegans* as an appropriate *in vivo* model to identify novel *S. flexneri* virulence factors.

6.3.3 *S. flexneri* infection induces the MAPK signaling pathway in mammalian cells and *C. elegans*

A proteomic screen of nematodes infected with *S. flexneri* identified DAF-19 as up-regulated in response to *S. flexneri* infection (Figure 5.9). RNAi experiments suggest that the *S. flexneri*-induced up-regulation of DAF-19 forms part of the nematode protective response mechanism against *S. flexneri* infection (Figure 5.11.D and 5.12), as knocking down DAF-19 increased the susceptibility of nematodes to *S. flexneri* infection. DAF-19 has recently been identified as a key regulator of the p38 MAPK cascade, which implies that the p38 MAPK signaling cascade is a potential innate response mounted by nematodes to *S. flexneri.* Furthermore, TIR-1 was also identified to be up-regulated in response to *S. flexneri* infection. TIR-1 is the toll interleukin 1 receptor domain adaptor protein in *C. elegans,* which activates the p38 MAPK innate immune response. These findings suggest that nematodes trigger the p38 MAPK pathway to control *S. flexneri* infection. Previous studies have reported that *S. flexneri* infection in mammals also triggers the p38 MAPK pathway [469, 470] and that this signaling cascade is induced by bacterial LPS. Our identification of elements of the p38 MAPK cascade up-regulated in *C. elegans* at the onset of infection, suggests that the innate responses to *S. flexneri* infection are similar in mammals and nematodes.

6.3.4 *S. flexneri* causes mitochondrial dysfunction in humans and nematodes, which potentially leads to necrotic cell death

DIGE analysis identified the nematode HSP-6 and HSP-60 proteins as *S. flexneri*-induced responses in worms. Both these proteins are well characterized markers of the mitochondrial unfolded protein response. These results imply that *S. flexneri* infection triggers mitochondrial stress responses in nematodes. As a consequence of mitochondrial dysfunction infected cells would have reduced energy levels this in turn could result in reduced pharyngeal pumping and egg laying phenotypes seen in nematode infected with virulent strains of *S. flexneri*. Similarly, *S. flexneri* infection in mammalian cells has also been associated with mitochondrial dysfunction [432]. Mitochondria dysfunction in infected epithelial cells has been proposed to cause necrotic cell death through the increased production of reactive oxygen species [432]. A similar mechanism leading to necrotic cell death could occur in infected nematode intestinal cells as suggested by the up-regulation of HSP-6 and HSP-60.

6.3.5 *S. flexneri* infection triggers an inflammatory response in humans and nematodes that causes tissue damage and osmotic imbalance

Previous studies in mammalian systems have shown that *S. flexneri*-encoded virulence factors, such as *sigA, shet1* and *shet2,* cause fluid accumulation in infected tissues [95, 98, 471]. Therefore it is possible that the apparent osmoregulatory defect observed in 41% of nematodes infected with *S. flexneri* for 24 hours (Figure 5.5), could be induced by bacterial virulence factors produced at the onset of infection. It is also possible that the initial nematode innate immune responses to *S. flexneri* infection could lead to defective osmoregulation.

A previous study reported that the hyperactivity of DAF-16-mediated immunity in nematodes is associated with increased expression of cellular water channels, which in turn disrupts cellular water homeostasis and increases nematode susceptibility to pathogens [472]. DAF-16 is closely related to the mammalian transcription factor FOXO3a, which has been linked to inflammation in response to infection [473, 474]. The up-regulation of CCT-2 in response to *S. flexneri* infection and the increased susceptibility of *cct-2* RNAi worms suggests that the DAF-2/DAF-16 insulin signaling pathway is induced in response to infection (Figure 5.11.C and 5.12). These results suggest that *S. flexneri* infection potentially induces an inflammatory response in nematodes and the fluid imbalance observed in response to the onset of *S. flexneri* infection in worms could correlate with the watery diarrhoea symptom seen in humans. However, since this phenotype was only observed in 41% of animals examined in this study, further experimental validation is needed to confirm this hypothesis.

6.3.6 Future work

This is a preliminary study which opens up a number of avenues that required further study to explore the molecular details of *S. flexneri* infection in *C. elegans*. Here I highlight some of these expreiments.

- The results of the cytopathology of *S. flexneri*-infected worms and DIGE analysis to identify *S. flexneri*-induced nematode responses open up several possibilities of *S. flexneri* pathogenesis in nematodes. In order to get a clearly picture of the infection process it would be a good idea to examine the cytopathology of dead and dying worms at later time points.

- The results of our virulence studies clearly suggest that the *S. flexneri* virulence plasmid is required for virulence in *C. elegans*. It will be interesting to identify the specific factors-encoded by the bacterial virulence plasmid that are required for virulence in *C. elegans*. As a preliminary step, *S. flexneri ipa* and *mxi-spa* mutants can be tested for virulence in *C. elegans*, to determine if the effector proteins encoded by these loci, known to be essential for mammalian infection are also critical for *S. flexneri* infection of worms. Following this a library of virulence plasmid mutant strains can be generated and the effect of each mutation on *C. elegans* infection can be determined to identify the specific *S. flexneri* effector molecules required for virulence in nematodes.

- The results of this thesis suggest that *S. flexneri* infection potentially activated the MAPK pathway in worms. In order to confirm this hypothesis prominent members of this signaling pathway such as TIR-1, NSY-1, SEK-1 and PMK-1 should be knocked down (using RNAi) or knocked out following which the effect of these mutations on nematode resistance to *S. flexneri* infection should be assessed.

- Our findings also suggest that *S. flexneri* activates the DAF-2-DAF-16 insulin signaling pathway. Reverse genetic studies involving the disruption of key members of this pathway such as DAF-2, DAF-16, AGE-1 and PDK-1 (Figure 1.6) and assessing their effect on *S. flexneri* infection would help confirm that this pathway is activated in response to *S. flexneri* infection.

- The results of this thesis also led to the hypothesis that *S. flexneri* utilizes host iron for infection which in turn disrupts iron homeostasis in infected tissues. To determine if iron molecules serve an important role in *S. flexneri* infection of *C. elegans,* killing assays using iron-chelating agents such as ciclopirox olamine (CPX) can be set up as described by Kirienko *et al* [421].

- Using RNAi technology the expression of *aco-1* was knocked down in this study and knocking down the expression of this gene increased nematode resistance to *S. flexneri* infection. In order to confirm whether the up-regulation of ACO-1 in response to *S. flexneri* infection results in nematode death, the effect of overexpressing ACO-1 on nematode survival can be assessed. The expression of genes induced as part of the hypoxic response in *S. flexneri* infected worms such as the hypoxia-inducing factor, *hif-1,* can be measured using qRT-PCR to confirm this hypothesis.

- The proteomic approach used in this study to identify *S. flexneri*-induced nematode responses only identified 7 differentially expressed nematode proteins. One of the major limitations of this approach is that a large amount of starting material is required for the successful identification of protein spots. Furthermore, proteins with extreme pIs or molecular weights, hydrophobic proteins and low-abundance proteins are poorly represented on 2-D gels. To set up the DIGE experiment in this study, 2mg of total protein was isolated from ~500 000 synchronized young adult worms per experimental repeat. These experiments were highly time consuming and labor intensive therefore proteins were isolated from only one time point of infection (24 h). Further high-throughput approaches such as whole genome transcription profiling (Microarrays) and

whole genome shotgun sequencing (RNAseq) [475] can be employed to observe *S. flexneri*-induced alterations in nematode cellular pathways in time-course experiments [239]. The results of such studies will present a clear picture of the specific pathways that are activated in response to *S. flexneri* infection over the course of infection.

Appendix A

Buffers, solutions and media

Bacterial culture

LB Broth

1.0 % w/v tryptone

0.5 % w/v yeast extract

0.5% w/v NaCl

-Adjust pH to 7.0. Autoclave

LB Broth Agar

1.5 % Bacto-agar to LB broth

-Adjust pH to 7.0. Autoclave

Minimal essential salts media

20% 5 X M9 salts stock solution

0.1% 1 M $MgSO_4$

0.01% 1 M $CaCl_2$

0.4 % w/v glucose

-Adjust pH to 7.0. Autoclave

5 X M9 Salts

In 1 L

64 g $Na_2HPO_4.7H_2O$

15 g K_2HPO_4

2.5 g NaCl

5 g NH_4Cl

-Adjust pH to 7.0. Autoclave

SOB Medium

2.0 % w/v tryptone

0.5 % w/v yeast extract

0.5% w/w NaCl

10 mM $MgCl_2$

10 mM $MgSO_4$

-Adjust pH to 7.0. Autoclave

SOC Medium

20 mM glucose added to a final concentration to autoclaved SOB medium

Congo red TSB agar plates

3 % w/v tryptic soy broth

0.15 % 4 M NaOH

1.5 % w/v agar

- Autoclave and add 1% filter sterilized 1 % w/v Congo red solution

Ampicillin

100 mg/mL stock

-1g of ampicillin powder added to 10 mL Milli-Q water. Filter sterilize.

-Store aliquots at -20°C

Chloramphenicol

25 mg/mL stock

-250 mg of chloramphinicol powder added to 10 mL ethanol.

-Protect from light

-Store at -20°C

30 mg/mL stock

-300 mg of chloramphinicol powder added to 10 mL ethanol.

-Protect from light

-Store at -20°C

Kanamycin

50 mg/mL stock

-500 mg of ampicillin powder added to 10 mL Milli-Q water. Filter sterilize.

-Store aliquots at -20°C

Plasmid Miniprep

Solution I

50 mM glucose

25 mM tris.Cl (pH 8.0)

10 mM EDTA (pH 8.0)

-Autoclave, Store at 4°C

Solution II

0.2 M NaOH

1.0 % w/v SDS

- Make fresh

Solution III

3 M CH_3COOK

2 M glacial acetic acid

-Autoclave, store at 4°C.

Agarose Gel electrophoresis

0.5 X TBE

45 mM Tris. HCl

45 mM boric acid

1 mM Na_2EDTA

Blue Loading Dye

1 mg/mL bromophenol blue

20 % (v/v) glycerol

1D SDS-PAGE gels

2 X Loading buffer

100 mM Tris.HCl (pH 6.8)

4 % w/v SDS

20 % Glycerol

2.5 % β-mercaptoethanol

0.2% bromophenol blue

-Store at -20°C

10 X Running buffer

1.92 M glycine

0.24 M Tris base

0.1 % w/v SDS

Coomassie Brilliant Blue Stain

0.5 % (w/v) Coomassie blue G250

50 % methanol

10 % acetic acid

Destain Solution

10 % acetic acid

40 % methanol

10 x PBS

8 % w/v NaCl

0.2 % w/v KCl

1.44 % w/v Na_2HPO_4

0.24 % w/v KH_2PO_4

- pH to 7.4, autoclave

2D SDS-PAGE

Solubilisation buffer

7 M urea,

4% (w/v) CHAPS,

1% (w/v) DTT,

1% (v/v) Ampholytes,

35 mM tris base

Cell wash solution

10 mM Tris pH 8.0

5 mM magnesium acetate

Cell lysis buffer

7 M Urea

2 M Thiourea

30mM Tris-base

4% (w/v) CHAPS

Complete protease inhibitor (Roche)

Rehydration solution

8 M urea

0.5% (w/v) CHAPS

0.2% (w/v) DTT

0.52% (w/v) bio-ampholytes

0.6% (w/v) bromophenol blue

Bacteriophage methods

NZCYM Medium

0.1% w/v casamino acids

0.066% w/v $MgSO_4.7H_2O$

0.167% w/v Yeast extract

0.167% w/v NaCl

0.5% soft agar

1% w/v Tryptone

0.5% w/v Yeast extract

0.5% w/v NaCl

0.5% w/v agar

SM Buffer

100 mM NaCl

25 mM Tris-HCL pH 7.5

8 mM $MgSO_4$

0.002% (w/v) gelatin

Gelatin-free SM buffer

100 mM NaCl

25 mM Tris-HCL pH 7.5

8 mM $MgSO_4$

TE Buffer

10 mM Tris.HCl, pH 7.5

1 mM EDTA, pH 8.0

C. elegans methods

Modified nematode growth media (NGM)

50 mM NaCl

0.35% (w/v) peptone

2% (w/v) agar

-Autoclave, cool to 55 °C

1 mM $CaCl_2$

1 mM $MgSO_4$

5 µ/mL cholesterol

25 mM Potassium phosphate

S-basal

0.1 M NaCl

0.05 M potassium phosphate pH 6.0

1 mL cholesterol (5 mg/mL in ethanol)

1 M potassium phosphate pH 6.0

0.132 M K_2HPO_4

0.868 M KH_2PO_4

Alkaline hypochlorite solution

4 M NaOH- 200 µL

Bleach (low strength White King)- 300 µL

Fixing solution 1

25 mM NaCl

1 mM $CaCl_2$

3.5% (v/v) glutaraldehyde

1.5% (v/v) paraformaldehyde

0.12 M cacodylate buffer pH 7.2

Fixing solution 2

2% (w/v) OsO_4

0.5% (w/v) $KFe(CN)_6$

1 mM $CaCl_2$

0.15 M cacodylate buffer pH 7.2

Wash solution

25 mM NaCl

1 mM $CaCl_2$

0.15 M cacodylate buffer pH 7.2

References

1. Jennison, A.V. and N.K. Verma, *Shigella flexneri infection: pathogenesis and vaccine development.* Fems Microbiology Reviews, 2004. **28**(1): p. 43-58.
2. Yang, J., et al., *Revisiting the molecular evolutionary history of Shigella spp.* J Mol Evol, 2007. **64**(1): p. 71-9.
3. Strockbine, N.A., Maurelli, A. T., *In Bergey's Manual of Systematic Bacteriology*. 2 ed. Genus Shigella, ed. D.J. Brenner, Krieg, N.R., Staley, J.T., . Vol. 2B. 2005, New York: Springer.
4. Hale, T.L., *Genetic basis of virulence in Shigella species.* Microbiol Rev, 1991. **55**(2): p. 206-24.
5. Allison, G.E. and N.K. Verma, *Serotype-converting bacteriophages and O-antigen modification in Shigella flexneri.* Trends in Microbiology, 2000. **8**(1): p. 17-23.
6. Perepelov, A.V., et al., *A new ethanolamine phosphate-containing variant of the O-antigen of Shigella flexneri type 4a.* Carbohydr Res, 2009. **344**(12): p. 1588-91.
7. Sun, Q., et al., *A novel plasmid-encoded serotype conversion mechanism through addition of phosphoethanolamine to the O-antigen of Shigella flexneri.* Plos One, 2012. **7**(9): p. e46095.
8. Simmons, D.A. and E. Romanowska, *Structure and biology of Shigella flexneri O antigens.* Journal of Medical Microbiology, 1987. **23**(4): p. 289-302.
9. Foster, R.A., et al., *Structural elucidation of the O-antigen of the Shigella flexneri provisional serotype 88-893: structural and serological similarities with S. flexneri provisional serotype Y394 (1c).* Carbohydr Res, 2011. **346**(6): p. 872-6.
10. Stagg, R.M., et al., *A novel glucosyltransferase involved in O-antigen modification of Shigella flexneri serotype 1c.* Journal of Bacteriology, 2009. **191**(21): p. 6612-7.
11. Sun, Q., et al., *Genesis of a novel Shigella flexneri serotype by sequential infection of serotype-converting bacteriophages SfX and Sfl.* Bmc Microbiology, 2011. **11**: p. 269.
12. Ye, C., et al., *Emergence of a new multidrug-resistant serotype X variant in an epidemic clone of Shigella flexneri.* Journal of Clinical Microbiology, 2010. **48**(2): p. 419-26.
13. Knirel, Y.A., et al., *O-antigen structure of Shigella flexneri serotype Yv and effect of the lpt-O gene variation on phosphoethanolamine modification of S. flexneri O-antigens.* Glycobiology, 2013. **23**(4): p. 475-85.
14. Perepelov, A.V., et al., *Shigella flexneri O-antigens revisited: final elucidation of the O-acetylation profiles and a survey of the O-antigen structure diversity.* FEMS Immunol Med Microbiol, 2012. **66**(2): p. 201-10.
15. Kotloff, K.L., et al., *Global burden of Shigella infections: implications for vaccine development and implementation of control strategies.* Bull World Health Organ, 1999. **77**(8): p. 651-66.
16. Levine, M.M., et al., *Clinical trials of Shigella vaccines: two steps forward and one step back on a long, hard road.* Nature Reviews Microbiology, 2007. **5**(7): p. 540-53.
17. DuPont, H.L., et al., *Inoculum size in shigellosis and implications for expected mode of transmission.* Journal of Infectious Diseases, 1989. **159**(6): p. 1126-8.
18. Wassef, J.S., D.F. Keren, and J.L. Mailloux, *Role of M cells in initial antigen uptake and in ulcer formation in the rabbit intestinal loop model of shigellosis.* Infection and Immunity, 1989. **57**(3): p. 858-63.
19. Neutra, M.R., E. Pringault, and J.P. Kraehenbuhl, *Antigen sampling across epithelial barriers and induction of mucosal immune responses.* Annu Rev Immunol, 1996. **14**: p. 275-300.

20. Sansonetti, P.J. and A. Phalipon, *M cells as ports of entry for enteroinvasive pathogens: mechanisms of interaction, consequences for the disease process.* Semin Immunol, 1999. **11**(3): p. 193-203.
21. Sakaguchi, T., et al., *Shigella flexneri regulates tight junction-associated proteins in human intestinal epithelial cells.* Cellular Microbiology, 2002. **4**(6): p. 367-81.
22. Zychlinsky, A., et al., *IpaB mediates macrophage apoptosis induced by Shigella flexneri.* Molecular Microbiology, 1994. **11**(4): p. 619-27.
23. Perdomo, J.J., P. Gounon, and P.J. Sansonetti, *Polymorphonuclear leukocyte transmigration promotes invasion of colonic epithelial monolayer by Shigella flexneri.* J Clin Invest, 1994. **93**(2): p. 633-43.
24. Perdomo, O.J., et al., *Acute inflammation causes epithelial invasion and mucosal destruction in experimental shigellosis.* Journal of Experimental Medicine, 1994. **180**(4): p. 1307-19.
25. Watarai, M., S. Funato, and C. Sasakawa, *Interaction of Ipa proteins of Shigella flexneri with alpha5beta1 integrin promotes entry of the bacteria into mammalian cells.* Journal of Experimental Medicine, 1996. **183**(3): p. 991-9.
26. Skoudy, A., et al., *CD44 binds to the Shigella IpaB protein and participates in bacterial invasion of epithelial cells.* Cellular Microbiology, 2000. **2**(1): p. 19-33.
27. Cossart, P. and P.J. Sansonetti, *Bacterial invasion: the paradigms of enteroinvasive pathogens.* Science, 2004. **304**(5668): p. 242-8.
28. Skoudy, A., et al., *A functional role for ezrin during Shigella flexneri entry into epithelial cells.* J Cell Sci, 1999. **112 (Pt 13)**: p. 2059-68.
29. Bernardini, M.L., et al., *Identification of icsA, a plasmid locus of Shigella flexneri that governs bacterial intra- and intercellular spread through interaction with F-actin.* Proc Natl Acad Sci U S A, 1989. **86**(10): p. 3867-71.
30. Iwai, H., et al., *A bacterial effector targets Mad2L2, an APC inhibitor, to modulate host cell cycling.* Cell, 2007. **130**(4): p. 611-23.
31. Salzman, N.H., M.A. Underwood, and C.L. Bevins, *Paneth cells, defensins, and the commensal microbiota: a hypothesis on intimate interplay at the intestinal mucosa.* Semin Immunol, 2007. **19**(2): p. 70-83.
32. Selsted, M.E. and A.J. Ouellette, *Mammalian defensins in the antimicrobial immune response.* Nat Immunol, 2005. **6**(6): p. 551-7.
33. Bevins, C.L., E. Martin-Porter, and T. Ganz, *Defensins and innate host defence of the gastrointestinal tract.* Gut, 1999. **45**(6): p. 911-5.
34. Islam, D., et al., *Downregulation of bactericidal peptides in enteric infections: a novel immune escape mechanism with bacterial DNA as a potential regulator.* Nat Med, 2001. 7(2): p. 180-5.
35. Franchi, L., et al., *Function of Nod-like receptors in microbial recognition and host defense.* Immunol Rev, 2009. **227**(1): p. 106-28.
36. Takeuchi, O. and S. Akira, *Pattern recognition receptors and inflammation.* Cell, 2010. **140**(6): p. 805-20.
37. Ting, J.P., J.A. Duncan, and Y. Lei, *How the noninflammasome NLRs function in the innate immune system.* Science, 2010. **327**(5963): p. 286-90.
38. Wang, Y., et al., *PYNOD, a novel Apaf-1/CED4-like protein is an inhibitor of ASC and caspase-1.* Int Immunol, 2004. **16**(6): p. 777-86.
39. Kinoshita, T., et al., *PYPAF3, a PYRIN-containing APAF-1-like protein, is a feedback regulator of caspase-1-dependent interleukin-1beta secretion.* J Biol Chem, 2005. **280**(23): p. 21720-5.
40. Imamura, R., et al., *Anti-inflammatory activity of PYNOD and its mechanism in humans and mice.* J Immunol, 2010. **184**(10): p. 5874-84.

41. Lautz, K., et al., *NLRP10 enhances Shigella-induced pro-inflammatory responses.* Cell Microbiol, 2012. **14**(10): p. 1568-83.
42. Phalipon, A. and P.J. Sansonetti, *Shigella's ways of manipulating the host intestinal innate and adaptive immune system: a tool box for survival?* Immunol Cell Biol, 2007. **85**(2): p. 119-29.
43. Inohara, N., et al., *Nod1, an Apaf-1-like activator of caspase-9 and nuclear factor-kappaB.* J Biol Chem, 1999. **274**(21): p. 14560-7.
44. Girardin, S.E., et al., *CARD4/Nod1 mediates NF-kappaB and JNK activation by invasive Shigella flexneri.* EMBO Rep, 2001. **2**(8): p. 736-42.
45. Inohara, N. and G. Nunez, *NODs: intracellular proteins involved in inflammation and apoptosis.* Nat Rev Immunol, 2003. **3**(5): p. 371-82.
46. Raqib, R., et al., *Cytokine secretion in acute shigellosis is correlated to disease activity and directed more to stool than to plasma.* Journal of Infectious Diseases, 1995. **171**(2): p. 376-84.
47. Schnupf, P. and P.J. Sansonetti, *Quantitative RT-PCR profiling of the rabbit immune response: assessment of acute Shigella flexneri infection.* PLoS One, 2012. **7**(6): p. e36446.
48. Way, S.S., et al., *An essential role for gamma interferon in innate resistance to Shigella flexneri infection.* Infection and Immunity, 1998. **66**(4): p. 1342-8.
49. Le-Barillec, K., et al., *Roles for T and NK cells in the innate immune response to Shigella flexneri.* Journal of Immunology, 2005. **175**(3): p. 1735-40.
50. Kim, D.W., et al., *The Shigella flexneri effector OspG interferes with innate immune responses by targeting ubiquitin-conjugating enzymes.* Proc Natl Acad Sci U S A, 2005. **102**(39): p. 14046-51.
51. Arbibe, L., et al., *An injected bacterial effector targets chromatin access for transcription factor NF-kappaB to alter transcription of host genes involved in immune responses.* Nat Immunol, 2007. **8**(1): p. 47-56.
52. Wang, F., et al., *Shigella flexneri T3SS effector IpaH4.5 modulates the host inflammatory response via interaction with NF-kappaB p65 protein.* Cell Microbiol, 2013. **15**(3): p. 474-85.
53. Reiterer, V., et al., *Shigella flexneri type III secreted effector OspF reveals new crosstalks of proinflammatory signaling pathways during bacterial infection.* Cell Signal, 2011. **23**(7): p. 1188-96.
54. Oberhelman, R.A., et al., *Prospective study of systemic and mucosal immune responses in dysenteric patients to specific Shigella invasion plasmid antigens and lipopolysaccharides.* Infection and Immunity, 1991. **59**(7): p. 2341-50.
55. Cohen, D., et al., *Immunoglobulin M, A, and G antibody response to lipopolysaccharide O antigen in symptomatic and asymptomatic Shigella infections.* Journal of Clinical Microbiology, 1989. **27**(1): p. 162-7.
56. Islam, D., et al., *Quantitative assessment of IgG and IgA subclass producing cells in rectal mucosa during shigellosis.* J Clin Pathol, 1997. **50**(6): p. 513-20.
57. DuPont, H.L., et al., *Immunity in shigellosis. II. Protection induced by oral live vaccine or primary infection.* Journal of Infectious Diseases, 1972. **125**(1): p. 12-6.
58. Formal, S.B., et al., *Effect of prior infection with virulent Shigella flexneri 2a on the resistance of monkeys to subsequent infection with Shigella sonnei.* Journal of Infectious Diseases, 1991. **164**(3): p. 533-7.
59. Rasolofo-Razanamparany, V., et al., *Predominance of serotype-specific mucosal antibody response in Shigella flexneri-infected humans living in an area of endemicity.* Infect Immun, 2001. **69**(9): p. 5230-4.

60. Li, A., et al., *Serum IgG antibody responses to Shigella invasion plasmid-coded antigens detected by immunoblot.* Scand J Infect Dis, 1994. **26**(4): p. 435-45.
61. Oaks, E.V., W.D. Picking, and W.L. Picking, *Antibody response of monkeys to invasion plasmid antigen D after infection with Shigella spp.* Clin Diagn Lab Immunol, 1996. **3**(2): p. 242-5.
62. Sayem, M.A., et al., *Differential host immune responses to epidemic and endemic strains of Shigella dysenteriae type I.* J Health Popul Nutr, 2011. **29**(5): p. 429-37.
63. Lowell, G.H., et al., *Antibody-dependent cell-mediated antibacterial activity: K lymphocytes, monocytes, and granulocytes are effective against shigella.* J Immunol, 1980. **125**(6): p. 2778-84.
64. Boullier, S., et al., *Secretory IgA-mediated neutralization of Shigella flexneri prevents intestinal tissue destruction by down-regulating inflammatory circuits.* J Immunol, 2009. **183**(9): p. 5879-85.
65. Ashida, H., et al., *Shigella infection of intestinal epithelium and circumvention of the host innate defense system.* Curr Top Microbiol Immunol, 2009. **337**: p. 231-55.
66. Ferreccio, C., et al., *Epidemiologic patterns of acute diarrhea and endemic Shigella infections in children in a poor periurban setting in Santiago, Chile.* Am J Epidemiol, 1991. **134**(6): p. 614-27.
67. Cohen, D., et al., *Prospective study of the association between serum antibodies to lipopolysaccharide O antigen and the attack rate of shigellosis.* Journal of Clinical Microbiology, 1991. **29**(2): p. 386-9.
68. Herrington, D.A., et al., *Studies in volunteers to evaluate candidate Shigella vaccines: further experience with a bivalent Salmonella typhi-Shigella sonnei vaccine and protection conferred by previous Shigella sonnei disease.* Vaccine, 1990. **8**(4): p. 353-7.
69. Coster, T.S., et al., *Vaccination against shigellosis with attenuated Shigella flexneri 2a strain SC602.* Infection and Immunity, 1999. **67**(7): p. 3437-43.
70. Islam, D., et al., *Immunoglobulin subclass distribution and dynamics of Shigella-specific antibody responses in serum and stool samples in shigellosis.* Infection and Immunity, 1995. **63**(5): p. 2054-61.
71. Azim, T., et al., *Lipopolysaccharide-specific antibodies in plasma and stools of children with Shigella-associated leukemoid reaction and hemolytic-uremic syndrome.* Clin Diagn Lab Immunol, 1996. **3**(6): p. 701-5.
72. Orr, N., et al., *Presence of specific immunoglobulin A-secreting cells in peripheral blood after natural infection with Shigella sonnei.* Journal of Clinical Microbiology, 1992. **30**(8): p. 2165-8.
73. Cohen, D., et al., *Detection of antibodies to Shigella lipopolysaccharide in urine after natural Shigella infection or vaccination.* Clin Diagn Lab Immunol, 1996. **3**(4): p. 451-5.
74. Kotloff, K.L., et al., *Safety, immunogenicity, and efficacy in monkeys and humans of invasive Escherichia coli K-12 hybrid vaccine candidates expressing Shigella flexneri 2a somatic antigen.* Infection and Immunity, 1992. **60**(6): p. 2218-24.
75. Kotloff, K.L., et al., *Evaluation of the safety, immunogenicity, and efficacy in healthy adults of four doses of live oral hybrid Escherichia coli-Shigella flexneri 2a vaccine strain EcSf2a-2.* Vaccine, 1995. **13**(5): p. 495-502.
76. Robin, G., et al., *Characterization and quantitative analysis of serum IgG class and subclass response to Shigella sonnei and Shigella flexneri 2a lipopolysaccharide following natural Shigella infection.* Journal of Infectious Diseases, 1997. **175**(5): p. 1128-33.

77. Klimpel, G.R., D.W. Niesel, and K.D. Klimpel, *Natural cytotoxic effector cell activity against Shigella flexneri-infected HeLa cells.* Journal of Immunology, 1986. **136**(3): p. 1081-6.
78. Sinha, A.K., M.K. Chakraborti, and S. Chakraborti, *Gut mucosal lymphocyte subpopulations in the host-defence of Shigella infected guinea-pigs.* Immunology Letters, 1992. **32**(1): p. 65-8.
79. Zwillich, S.H., A.D. Duby, and P.E. Lipsky, *T-lymphocyte clones responsive to Shigella flexneri.* Journal of Clinical Microbiology, 1989. **27**(3): p. 417-21.
80. Islam, D., et al., *Shigella infection induces cellular activation of T and B cells and distinct species-related changes in peripheral blood lymphocyte subsets during the course of the disease.* Infection and Immunity, 1995. **63**(8): p. 2941-9.
81. Sellge, G., et al., *Th17 cells are the dominant T cell subtype primed by Shigella flexneri mediating protective immunity.* J Immunol, 2010. **184**(4): p. 2076-85.
82. Nakanishi, K., et al., *Interleukin-18 regulates both Th1 and Th2 responses.* Annual review of immunology, 2001. **19**(1): p. 423-474.
83. van de Verg, L.L., et al., *Antibody and cytokine responses in a mouse pulmonary model of Shigella flexneri serotype 2a infection.* Infection and Immunity, 1995. **63**(5): p. 1947-54.
84. Nelson, M.R., et al., *Salmonella, Campylobacter and Shigella in HIV-seropositive patients.* AIDS, 1992. **6**(12): p. 1495-8.
85. Sanchez, T.H., et al., *Bacterial diarrhea in persons with HIV infection, United States, 1992-2002.* Clinical Infectious Diseases, 2005. **41**(11): p. 1621-7.
86. Angulo, F.J. and D.L. Swerdlow, *Bacterial enteric infections in persons infected with human immunodeficiency virus.* Clinical Infectious Diseases, 1995. **21 Suppl 1**: p. S84-93.
87. Lan, R. and P.R. Reeves, *Escherichia coli in disguise: molecular origins of Shigella.* Microbes Infect, 2002. **4**(11): p. 1125-32.
88. Maurelli, A.T., B. Blackmon, and R. Curtiss, 3rd, *Loss of pigmentation in Shigella flexneri 2a is correlated with loss of virulence and virulence-associated plasmid.* Infection and Immunity, 1984. **43**(1): p. 397-401.
89. Schroeder, G.N. and H. Hilbi, *Molecular pathogenesis of Shigella spp.: controlling host cell signaling, invasion, and death by type III secretion.* Clinical Microbiology Reviews, 2008. **21**(1): p. 134-56.
90. Nakayama, S. and H. Watanabe, *Involvement of cpxA, a sensor of a two-component regulatory system, in the pH-dependent regulation of expression of Shigella sonnei virF gene.* J Bacteriol, 1995. **177**(17): p. 5062-9.
91. Payne, S.M., et al., *Iron and pathogenesis of Shigella: iron acquisition in the intracellular environment.* Biometals, 2006. **19**(2): p. 173-80.
92. Porter, M.E. and C.J. Dorman, *A role for H-NS in the thermo-osmotic regulation of virulence gene expression in Shigella flexneri.* J Bacteriol, 1994. **176**(13): p. 4187-91.
93. Daskaleros, P.A. and S.M. Payne, *Cloning the gene for Congo red binding in Shigella flexneri.* Infect Immun, 1985. **48**(1): p. 165-8.
94. Thong, K.L., et al., *Detection of virulence genes in Malaysian Shigella species by multiplex PCR assay.* BMC Infect Dis, 2005. **5**: p. 8.
95. Al-Hasani, K., et al., *The sigA gene which is borne on the she pathogenicity island of Shigella flexneri 2a encodes an exported cytopathic protease involved in intestinal fluid accumulation.* Infection and Immunity, 2000. **68**(5): p. 2457-63.
96. Boisen, N., et al., *Short report: high prevalence of serine protease autotransporter cytotoxins among strains of enteroaggregative Escherichia coli.* Am J Trop Med Hyg, 2009. **80**(2): p. 294-301.

97. Henderson, I.R., et al., *Characterization of pic, a secreted protease of Shigella flexneri and enteroaggregative Escherichia coli.* Infect Immun, 1999. **67**(11): p. 5587-96.
98. Fasano, A., et al., *Effect of shigella enterotoxin 1 (ShET1) on rabbit intestine in vitro and in vivo.* Gut, 1997. **40**(4): p. 505-11.
99. Fasano, A., et al., *Shigella enterotoxin 1: an enterotoxin of Shigella flexneri 2a active in rabbit small intestine in vivo and in vitro.* J Clin Invest, 1995. **95**(6): p. 2853-61.
100. Moss, J.E., et al., *The selC-associated SHI-2 pathogenicity island of Shigella flexneri.* Mol Microbiol, 1999. **33**(1): p. 74-83.
101. Nassif, X., et al., *Evaluation with an iuc::Tn10 mutant of the role of aerobactin production in the virulence of Shigella flexneri.* Infect Immun, 1987. **55**(9): p. 1963-9.
102. Vokes, S.A., et al., *The aerobactin iron transport system genes in Shigella flexneri are present within a pathogenicity island.* Mol Microbiol, 1999. **33**(1): p. 63-73.
103. Luck, S.N., et al., *Ferric dicitrate transport system (Fec) of Shigella flexneri 2a YSH6000 is encoded on a novel pathogenicity island carrying multiple antibiotic resistance genes.* Infect Immun, 2001. **69**(10): p. 6012-21.
104. Turner, S.A., et al., *Nested deletions of the SRL pathogenicity island of Shigella flexneri 2a.* J Bacteriol, 2001. **183**(19): p. 5535-43.
105. Yoshida, S., et al., *Microtubule-severing activity of Shigella is pivotal for intercellular spreading.* Science, 2006. **314**(5801): p. 985-9.
106. Yoshida, S., et al., *Shigella deliver an effector protein to trigger host microtubule destabilization, which promotes Rac1 activity and efficient bacterial internalization.* EMBO J, 2002. **21**(12): p. 2923-35.
107. Tobe, T., et al., *Transcriptional control of the invasion regulatory gene virB of Shigella flexneri: activation by virF and repression by H-NS.* Journal of Bacteriology, 1993. **175**(19): p. 6142-9.
108. Sakai, T., C. Sasakawa, and M. Yoshikawa, *Expression of four virulence antigens of Shigella flexneri is positively regulated at the transcriptional level by the 30 kiloDalton virF protein.* Molecular Microbiology, 1988. **2**(5): p. 589-97.
109. Beloin, C., S. McKenna, and C.J. Dorman, *Molecular dissection of VirB, a key regulator of the virulence cascade of Shigella flexneri.* Journal of Biological Chemistry, 2002. **277**(18): p. 15333-44.
110. Ogawa, M., et al., *IcsB, secreted via the type III secretion system, is chaperoned by IpgA and required at the post-invasion stage of Shigella pathogenicity.* Mol Microbiol, 2003. **48**(4): p. 913-31.
111. Ogawa, M., et al., *Escape of intracellular Shigella from autophagy.* Science, 2005. **307**(5710): p. 727-31.
112. Allaoui, A., et al., *icsB: a Shigella flexneri virulence gene necessary for the lysis of protrusions during intercellular spread.* Mol Microbiol, 1992. **6**(12): p. 1605-16.
113. Egile, C., et al., *SopA, the outer membrane protease responsible for polar localization of IcsA in Shigella flexneri.* Mol Microbiol, 1997. **23**(5): p. 1063-73.
114. Shere, K.D., et al., *Disruption of IcsP, the major Shigella protease that cleaves IcsA, accelerates actin-based motility.* Mol Microbiol, 1997. **25**(3): p. 451-62.
115. Sansonetti, P.J., *Molecular basis of invasion of eucaryotic cells by Shigella.* Antonie Van Leeuwenhoek, 1988. **54**(5): p. 389-93.
116. Hamiaux, C., et al., *Structural mimicry for vinculin activation by IpaA, a virulence factor of Shigella flexneri.* EMBO Rep, 2006. **7**(8): p. 794-9.
117. Guichon, A., et al., *Structure-function analysis of the Shigella virulence factor IpaB.* Journal of Bacteriology, 2001. **183**(4): p. 1269-76.

118. Marquart, M.E., W.L. Picking, and W.D. Picking, *Soluble invasion plasmid antigen C (IpaC) from Shigella flexneri elicits epithelial cell responses related to pathogen invasion.* Infection and Immunity, 1996. **64**(10): p. 4182-7.
119. Picking, W.L., et al., *IpaD of Shigella flexneri is independently required for regulation of Ipa protein secretion and efficient insertion of IpaB and IpaC into host membranes.* Infection and Immunity, 2005. **73**(3): p. 1432-40.
120. Fernandez-Prada, C.M., et al., *Shigella flexneri IpaH(7.8) facilitates escape of virulent bacteria from the endocytic vacuoles of mouse and human macrophages.* Infection and Immunity, 2000. **68**(6): p. 3608-19.
121. Bodhidatta, L., et al., *Establishment of a Shigella sonnei human challenge model in Thailand.* Vaccine, 2012. **30**(49): p. 7040-5.
122. Wu, T., et al., *Live attenuated Shigella dysenteriae type 1 vaccine strains overexpressing shiga toxin B subunit.* Infect Immun, 2011. **79**(12): p. 4912-22.
123. Collins, T.A., et al., *Safety and colonization of two novel VirG(IcsA)-based live Shigella sonnei vaccine strains in rhesus macaques (Macaca mulatta).* Comp Med, 2008. **58**(1): p. 88-94.
124. Bedford, L., et al., *Further characterization of Shigella sonnei live vaccine candidates WRSs2 and WRSs3-plasmid composition, invasion assays and Sereny reactions.* Gut Microbes, 2011. **2**(4): p. 244-51.
125. Barnoy, S., et al., *Shigella sonnei vaccine candidates WRSs2 and WRSs3 are as immunogenic as WRSS1, a clinically tested vaccine candidate, in a primate model of infection.* Vaccine, 2011. **29**(37): p. 6371-8.
126. Rahman, K.M., et al., *Safety, dose, immunogenicity, and transmissibility of an oral live attenuated Shigella flexneri 2a vaccine candidate (SC602) among healthy adults and school children in Matlab, Bangladesh.* Vaccine, 2011. **29**(6): p. 1347-54.
127. Ranallo, R.T., et al., *Two live attenuated Shigella flexneri 2a strains WRSf2G12 and WRSf2G15: a new combination of gene deletions for 2nd generation live attenuated vaccine candidates.* Vaccine, 2012. **30**(34): p. 5159-71.
128. Ranallo, R.T., et al., *Virulence, inflammatory potential, and adaptive immunity induced by Shigella flexneri msbB mutants.* Infect Immun, 2010. **78**(1): p. 400-12.
129. McKenzie, R., et al., *Safety and immunogenicity of WRSd1, a live attenuated Shigella dysenteriae type 1 vaccine candidate.* Vaccine, 2008. **26**(26): p. 3291-6.
130. Dharmasena, M.N., et al., *Stable expression of Shigella sonnei form I O-polysaccharide genes recombineered into the chromosome of live Salmonella oral vaccine vector Ty21a.* Int J Med Microbiol, 2013. **303**(3): p. 105-13.
131. Dro, P.a.S., M. , *GlycoVaxyn Phase I clinical study shows positive data with Shigella dysenteriae vaccine candidate [online]* in *http://www.glycovaxyn.com/content/news/releases/10%2010%2008.pdf* 2010.
132. Theillet, F.X., et al., *Effects of backbone substitutions on the conformational behavior of Shigella flexneri O-antigens: implications for vaccine strategy.* Glycobiology, 2011. **21**(1): p. 109-21.
133. Phalipon, A., et al., *A synthetic carbohydrate-protein conjugate vaccine candidate against Shigella flexneri 2a infection.* J Immunol, 2009. **182**(4): p. 2241-7.
134. Martinez-Becerra, F.J., et al., *Broadly protective Shigella vaccine based on type III secretion apparatus proteins.* Infect Immun, 2012. **80**(3): p. 1222-31.
135. Heine, S.J., et al., *Evaluation of immunogenicity and protective efficacy of orally delivered Shigella type III secretion system proteins IpaB and IpaD.* Vaccine, 2013. **31**(28): p. 2919-29.
136. Berlanda Scorza, F., et al., *High yield production process for Shigella outer membrane particles.* PLoS One, 2012. **7**(6): p. e35616.

137. Czerkinsky, C.a.K., D. W. , *Novel Shigella protein antigens and methods* 2010: US.
138. Riddle, M.S., et al., *Safety and immunogenicity of an intranasal Shigella flexneri 2a Invaplex 50 vaccine.* Vaccine, 2011. **29**(40): p. 7009-19.
139. Tribble, D., et al., *Safety and immunogenicity of a Shigella flexneri 2a Invaplex 50 intranasal vaccine in adult volunteers.* Vaccine, 2010. **28**(37): p. 6076-85.
140. Camacho, A.I., et al., *Nanoparticle-based vaccine for mucosal protection against Shigella flexneri in mice.* Vaccine, 2013. **31**(32): p. 3288-94.
141. Mitra, S., M.K. Chakrabarti, and H. Koley, *Multi-serotype outer membrane vesicles of Shigellae confer passive protection to the neonatal mice against shigellosis.* Vaccine, 2013. **31**(31): p. 3163-73.
142. Camacho, A.I., et al., *Towards a non-living vaccine against Shigella flexneri: from the inactivation procedure to protection studies.* Methods, 2013. **60**(3): p. 264-8.
143. Pore, D. and M.K. Chakrabarti, *Outer membrane protein A (OmpA) from Shigella flexneri 2a: a promising subunit vaccine candidate.* Vaccine, 2013. **31**(36): p. 3644-50.
144. Bergh, O., et al., *High abundance of viruses found in aquatic environments.* Nature, 1989. **340**(6233): p. 467-8.
145. Chibani-Chennoufi, S., et al., *Phage-host interaction: an ecological perspective.* Journal of Bacteriology, 2004. **186**(12): p. 3677-86.
146. Wommack, K.E. and R.R. Colwell, *Virioplankton: viruses in aquatic ecosystems.* Microbiol Mol Biol Rev, 2000. **64**(1): p. 69-114.
147. Brussow, H. and R.W. Hendrix, *Phage genomics: small is beautiful.* Cell, 2002. **108**(1): p. 13-6.
148. Canchaya, C., et al., *Phage as agents of lateral gene transfer.* Current Opinion in Microbiology, 2003. **6**(4): p. 417-24.
149. Ochman, H., J.G. Lawrence, and E.A. Groisman, *Lateral gene transfer and the nature of bacterial innovation.* Nature, 2000. **405**(6784): p. 299-304.
150. Rodriguez-Valera, F., et al., *Explaining microbial population genomics through phage predation.* Nature Reviews Microbiology, 2009. **7**(11): p. 828-36.
151. Banks, D.J., S.B. Beres, and J.M. Musser, *The fundamental contribution of phages to GAS evolution, genome diversification and strain emergence.* Trends in Microbiology, 2002. **10**(11): p. 515-21.
152. Ohnishi, M., K. Kurokawa, and T. Hayashi, *Diversification of Escherichia coli genomes: are bacteriophages the major contributors?* Trends in Microbiology, 2001. **9**(10): p. 481-5.
153. Ackermann, H.W., *Frequency of morphological phage descriptions.* Archives of Virology, 1992. **124**(3-4): p. 201-9.
154. Campbell, A., S.J. Schneider, and B. Song, *Lambdoid phages as elements of bacterial genomes (integrase/phage21/Escherichia coli K-12/icd gene).* Genetica, 1992. **86**(1-3): p. 259-67.
155. Sun, Q., et al., *Isolation and genomic characterization of SfI, a serotype-converting bacteriophage of Shigella flexneri.* Bmc Microbiology, 2013. **13**(1): p. 39.
156. Mavris, M., P.A. Manning, and R. Morona, *Mechanism of bacteriophage SfII-mediated serotype conversion in Shigella flexneri.* Molecular Microbiology, 1997. **26**(5): p. 939-50.
157. Jakhetia, R., K.A. Talukder, and N.K. Verma, *Isolation, characterization and comparative genomics of bacteriophage SfIV: a novel serotype converting phage from Shigella flexneri.* Bmc Genomics, 2013. **14**(1): p. 677.

158. Allison, G.E., et al., *Complete genomic sequence of SfV, a serotype-converting temperate bacteriophage of Shigella flexneri.* Journal of Bacteriology, 2002. **184**(7): p. 1974-87.
159. Guan, S., D.A. Bastin, and N.K. Verma, *Functional analysis of the O antigen glucosylation gene cluster of Shigella flexneri bacteriophage SfX.* Microbiology, 1999. **145 (Pt 5)**: p. 1263-73.
160. Casjens, S., et al., *The chromosome of Shigella flexneri bacteriophage Sf6: Complete nucleotide sequence, genetic mosaicism, and DNA packaging.* Journal of Molecular Biology, 2004. **339**(2): p. 379-394.
161. Frobisher, M.a.J.B., *Transmissible toxicogenicity of streptococci.* Bull. Johns Hopkins Hospital, 1927. **41**: p. 167–173.
162. Casjens, S., *Prophages and bacterial genomics: what have we learned so far?* Molecular Microbiology, 2003. **49**(2): p. 277-300.
163. Finkelstein, R.A., *Cholera enterotoxin (choleragen): a historical perspective,*

, D.B.a.W.B.G.I. (ed.), Editor. 1992, Plenum Press: New York, N.Y. p. p. 155–187.
164. Mintz, E.D., T. Popovic, and P. A. Blake. , *Transmission of Vibrio cholerae O1, In I. K. Wachsmuth, P. A. Blake, and O. Olsvik*

(ed.), Vibrio cholerae and cholera: molecular to global perspectives. . 1994, Washington, D.C.: American Society for Microbiology. 345–356.
165. Waldor, M.K. and J.J. Mekalanos, *Lysogenic conversion by a filamentous phage encoding cholera toxin.* Science, 1996. **272**(5270): p. 1910-1914.
166. Fujii, N., et al., *Characterization of bacteriophage nucleic acids obtained from Clostridium botulinum types C and D.* Appl Environ Microbiol, 1988. **54**(1): p. 69-73.
167. Holmes, R.K. and L. Barksdale, *Genetic analysis of tox+ and tox- bacteriophages of Corynebacterium diphtheriae.* Journal of Virology, 1969. **3**(6): p. 586-98.
168. Uchida, T., D.M. Gill, and A.M. Pappenheimer, Jr., *Mutation in the structural gene for diphtheria toxin carried by temperate phage.* Nat New Biol, 1971. **233**(35): p. 8-11.
169. Huang, A., et al., *Cloning and expression of the genes specifying Shiga-like toxin production in Escherichia coli H19.* Journal of Bacteriology, 1986. **166**(2): p. 375-9.
170. Newland, J.W., et al., *Cloning of Shiga-Like Toxin Structural Genes from a Toxin Converting Phage of Escherichia-Coli.* Science, 1985. **230**(4722): p. 179-181.
171. Asakura, M., et al., *An inducible lambdoid prophage encoding cytolethal distending toxin (Cdt-I) and a type III effector protein in enteropathogenic Escherichia coli.* Proc Natl Acad Sci U S A, 2007. **104**(36): p. 14483-8.
172. Hayashi, T., et al., *Phage-conversion of cytotoxin production in Pseudomonas aeruginosa.* Molecular Microbiology, 1990. **4**(10): p. 1703-9.
173. McDonough, M.A. and J.R. Butterton, *Spontaneous tandem amplification and deletion of the shiga toxin operon in Shigella dysenteriae 1.* Molecular Microbiology, 1999. **34**(5): p. 1058-69.
174. Betley, M.J. and J.J. Mekalanos, *Staphylococcal enterotoxin A is encoded by phage.* Science, 1985. **229**(4709): p. 185-7.
175. Casman, E.P., *Staphylococcal enterotoxin.* Ann N Y Acad Sci, 1965. **128**(1): p. 124-31.
176. Coleman, D.C., et al., *Staphylococcus aureus bacteriophages mediating the simultaneous lysogenic conversion of beta-lysin, staphylokinase and enterotoxin A: molecular mechanism of triple conversion.* J Gen Microbiol, 1989. **135**(6): p. 1679-97.

177. Goshorn, S.C. and P.M. Schlievert, *Bacteriophage association of streptococcal pyrogenic exotoxin type C.* Journal of Bacteriology, 1989. **171**(6): p. 3068-73.
178. Johnson, L.P. and P.M. Schlievert, *Group A streptococcal phage T12 carries the structural gene for pyrogenic exotoxin type A.* Molecular & General Genetics, 1984. **194**(1-2): p. 52-6.
179. Weeks, C.R. and J.J. Ferretti, *The gene for type A streptococcal exotoxin (erythrogenic toxin) is located in bacteriophage T12.* Infection and Immunity, 1984. **46**(2): p. 531-6.
180. Waldor, M.K. and J.J. Mekalanos, *Lysogenic conversion by a filamentous phage encoding cholera toxin.* Science, 1996. **272**(5270): p. 1910-4.
181. Barondess, J.J. and J. Beckwith, *A bacterial virulence determinant encoded by lysogenic coliphage lambda.* Nature, 1990. **346**(6287): p. 871-4.
182. Vica Pacheco, S., O. Garcia Gonzalez, and G.L. Paniagua Contreras, *The lom gene of bacteriophage lambda is involved in Escherichia coli K12 adhesion to human buccal epithelial cells.* Fems Microbiology Letters, 1997. **156**(1): p. 129-32.
183. Reeve, J.N. and J.E. Shaw, *Lambda encodes an outer membrane protein: the lom gene.* Molecular & General Genetics, 1979. **172**(3): p. 243-8.
184. Vaca, S., et al., *Partial genetic characterization of FIZ15 bacteriophage of Pseudomonas aeruginosa.* Rev Latinoam Microbiol, 1993. **35**(3): p. 251-7.
185. Bensing, B.A., C.E. Rubens, and P.M. Sullam, *Genetic loci of Streptococcus mitis that mediate binding to human platelets.* Infection and Immunity, 2001. **69**(3): p. 1373-80.
186. Bensing, B.A., I.R. Siboo, and P.M. Sullam, *Proteins PblA and PblB of Streptococcus mitis, which promote binding to human platelets, are encoded within a lysogenic bacteriophage.* Infection and Immunity, 2001. **69**(10): p. 6186-6192.
187. Karaolis, D.K. and J.B. Kaper, *Vibrio cholerae TCP: a trifunctional virulence factor?: Response.* Trends Microbiol, 1999. **7**(10): p. 393.
188. Perna, N.T., et al., *Genome sequence of enterohaemorrhagic Escherichia coli O157:H7.* Nature, 2001. **409**(6819): p. 529-33.
189. Creuzburg, K., et al., *The Shiga toxin 1-converting bacteriophage BP-4795 encodes an NleA-like type III effector protein.* J Bacteriol, 2005. **187**(24): p. 8494-8.
190. Hemrajani, C., et al., *Role of NleH, a type III secreted effector from attaching and effacing pathogens, in colonization of the bovine, ovine, and murine gut.* Infect Immun, 2008. **76**(11): p. 4804-13.
191. Miyahara, A., et al., *Enterohemorrhagic Escherichia coli effector EspL2 induces actin microfilament aggregation through annexin 2 activation.* Cell Microbiol, 2009. **11**(2): p. 337-50.
192. Loukiadis, E., et al., *Distribution, functional expression, and genetic organization of Cif, a phage-encoded type III-secreted effector from enteropathogenic and enterohemorrhagic Escherichia coli.* J Bacteriol, 2008. **190**(1): p. 275-85.
193. Mirold, S., et al., *Isolation of a temperate bacteriophage encoding the type III effector protein SopE from an epidemic Salmonella typhimurium strain.* Proc Natl Acad Sci U S A, 1999. **96**(17): p. 9845-50.
194. Hardt, W.D., H. Urlaub, and J.E. Galan, *A substrate of the centisome 63 type III protein secretion system of Salmonella typhimurium is encoded by a cryptic bacteriophage.* Proc Natl Acad Sci U S A, 1998. **95**(5): p. 2574-9.
195. Stanley, T.L., C.D. Ellermeier, and J.M. Slauch, *Tissue-specific gene expression identifies a gene in the lysogenic phage Gifsy-1 that affects Salmonella enterica serovar typhimurium survival in Peyer's patches.* Journal of Bacteriology, 2000. **182**(16): p. 4406-13.

196. Brown, N.F., et al., *Salmonella phage ST64B encodes a member of the SseK/NleB effector family.* PLoS One, 2011. **6**(3): p. e17824.
197. Hynes, W.L. and J.J. Ferretti, *Sequence analysis and expression in Escherichia coli of the hyaluronidase gene of Streptococcus pyogenes bacteriophage H4489A.* Infection and Immunity, 1989. **57**(2): p. 533-9.
198. Sako, T., et al., *Cloning and expression of the staphylokinase gene of Staphylococcus aureus in Escherichia coli.* Molecular & General Genetics, 1983. **190**(2): p. 271-7.
199. Barondess, J.J. and J. Beckwith, *A Bacterial Virulence Determinant Encoded by Lysogenic Coliphage-Lambda.* Nature, 1990. **346**(6287): p. 871-874.
200. Figueroa-Bossi, N. and L. Bossi, *Inducible prophages contribute to Salmonella virulence in mice.* Molecular Microbiology, 1999. **33**(1): p. 167-76.
201. Kirn, T.J., et al., *Delineation of pilin domains required for bacterial association into microcolonies and intestinal colonization by Vibrio cholerae.* Mol Microbiol, 2000. **35**(4): p. 896-910.
202. Figueroa-Bossi, N., et al., *Variable assortment of prophages provides a transferable repertoire of pathogenic determinants in Salmonella.* Molecular Microbiology, 2001. **39**(2): p. 260-71.
203. Spanier, J.G. and P.P. Cleary, *Bacteriophage control of antiphagocytic determinants in group A streptococci.* Journal of Experimental Medicine, 1980. **152**(5): p. 1393-406.
204. Holloway, B.W. and G.N. Cooper, *Lysogenic conversion in Pseudomonas aeruginosa.* Journal of Bacteriology, 1962. **84**: p. 1321-4.
205. Robbins, P.W. and T. Uchida, *Studies on the chemical basis of the phage conversion of O-antigens in the E-group Salmonellae.* Biochemistry, 1962. **1**: p. 323-35.
206. Wright, A., *Mechanism of conversion of the salmonella O antigen by bacteriophageepsilon 34.* Journal of Bacteriology, 1971. **105**(3): p. 927-36.
207. Herrington, D.A., et al., *Toxin, toxin-coregulated pili, and the toxR regulon are essential for Vibrio cholerae pathogenesis in humans.* J Exp Med, 1988. **168**(4): p. 1487-92.
208. Taylor, R.K., et al., *Use of phoA gene fusions to identify a pilus colonization factor coordinately regulated with cholera toxin.* Proc Natl Acad Sci U S A, 1987. **84**(9): p. 2833-7.
209. Rui, H., et al., *Reactogenicity of live-attenuated Vibrio cholerae vaccines is dependent on flagellins.* Proc Natl Acad Sci U S A, 2010. **107**(9): p. 4359-64.
210. Karaolis, D.K., et al., *A bacteriophage encoding a pathogenicity island, a type-IV pilus and a phage receptor in cholera bacteria.* Nature, 1999. **399**(6734): p. 375-9.
211. Kaper, J.B., *Pathogenic Escherichia coli.* Int J Med Microbiol, 2005. **295**(6-7): p. 355-6.
212. Newland, J.W., et al., *Cloning of Shiga-like toxin structural genes from a toxin converting phage of Escherichia coli.* Science, 1985. **230**(4722): p. 179-81.
213. Boyd, E.F. and H. Brussow, *Common themes among bacteriophage-encoded virulence factors and diversity among the bacteriophages involved.* Trends in Microbiology, 2002. **10**(11): p. 521-9.
214. Hueck, C.J., *Type III protein secretion systems in bacterial pathogens of animals and plants.* Microbiol Mol Biol Rev, 1998. **62**(2): p. 379-433.
215. Wood, M.W., et al., *SopE, a secreted protein of Salmonella dublin, is translocated into the target eukaryotic cell via a sip-dependent mechanism and promotes bacterial entry.* Mol Microbiol, 1996. **22**(2): p. 327-38.
216. Uzzau, S., et al., *Epitope tagging of chromosomal genes in Salmonella.* Proc Natl Acad Sci U S A, 2001. **98**(26): p. 15264-9.

217. Figueroa-Bossi, N. and L. Bossi, *Inducible prophages contribute to Salmonella virulence in mice.* Molecular Microbiology, 1999. **33**(1): p. 167-176.
218. Mirold, S., et al., *Isolation of a temperate bacteriophage encoding the type III effector protein SopE from an epidemic Salmonella typhimurium strain.* Proceedings of the National Academy of Sciences of the United States of America, 1999. **96**(17): p. 9845-9850.
219. Robbins, P.W. and T. Uchida, *Determinants of specificity in Salmonella: changes in antigenic structure mediated by bacteriophage.* Fed Proc, 1962. **21**: p. 702-10.
220. De Groote, M.A., et al., *Periplasmic superoxide dismutase protects Salmonella from products of phagocyte NADPH-oxidase and nitric oxide synthase.* Proc Natl Acad Sci U S A, 1997. **94**(25): p. 13997-4001.
221. Farrant, J.L., et al., *Bacterial copper- and zinc-cofactored superoxide dismutase contributes to the pathogenesis of systemic salmonellosis.* Mol Microbiol, 1997. **25**(4): p. 785-96.
222. Philpott, D.J., J.D. Edgeworth, and P.J. Sansonetti, *The pathogenesis of Shigella flexneri infection: lessons from in vitro and in vivo studies.* Philos Trans R Soc Lond B Biol Sci, 2000. **355**(1397): p. 575-86.
223. Formal, S.B., et al., *Protection of Monkeys Against Experimental Shigellosis with Attenuated Vaccines.* J Bacteriol, 1965. **90**(1): p. 63-8.
224. Shipley, S.T., et al., *A challenge model for Shigella dysenteriae 1 in cynomolgus monkeys (Macaca fascicularis).* Comp Med, 2010. **60**(1): p. 54-61.
225. Voino-Yasenetsky, M.V. and M.K. Voino-Yasenetskaya, *Experimental pneumonia caused by bacteria of the Shigella group.* Acta Morphol Acad Sci Hung, 1962. **11**: p. 439-54.
226. Brenner, S., *The genetics of Caenorhabditis elegans.* Genetics, 1974. **77**(1): p. 71-94.
227. Darby, C., *Interactions with microbial pathogens.* WormBook (Ed) "The C. elegans Research Community", 2005. **(http://www.wormbook.org)**: p. 1-15.
228. Sifri, C.D., J. Begun, and F.M. Ausubel, *The worm has turned-microbial virulence modeled in Caenorhabditis elegans.* Trends in Microbiology, 2005. **13**(3): p. 119-27.
229. Powell, J.R. and F.M. Ausubel, *Models of Caenorhabditis elegans infection by bacterial and fungal pathogens.* Methods Mol Biol, 2008. **415**: p. 403-27.
230. Rout, W.R., et al., *Pathophysiology of Shigella diarrhea in the rhesus monkey: intestinal transport, morphological, and bacteriological studies.* Gastroenterology, 1975. **68**(2): p. 270-8.
231. Voinoyasenetsky, M.V. and M.V. Voinoyasenetsky, *Experimental Pneumonia Caused by Bacteria of Shigella Group.* Acta Morphologica Academiae Scientiarum Hungaricae, 1962. **11**(4): p. 439-&.
232. Fernandez, M.I., et al., *A newborn mouse model for the study of intestinal pathogenesis of shigellosis.* Cell Microbiol, 2003. **5**(7): p. 481-91.
233. Sereny, B., *Experimental shigella keratoconjunctivitis; a preliminary report.* Acta Microbiol Acad Sci Hung, 1955. **2**(3): p. 293-6.
234. Arm, H.G., et al., *Use of Ligated Segments of Rabbit Small Intestine in Experimental Shigellosis.* Journal of Bacteriology, 1965. **89**: p. 803-9.
235. Klass, M.R., *Aging in the nematode Caenorhabditis elegans: major biological and environmental factors influencing life span.* Mech Ageing Dev, 1977. **6**(6): p. 413-29.
236. Altun, Z.F., and Hall, D. H., , *Handbook of C. elegans anatomy*, in *WormAtlas*. 2005, http://www.wormatlas.org/handbook/contents.htm

237. White, J.G., *The Anatomy. In The nematode C. elegans* ed. W.B. Wood. Vol. Chapter 4. 1988, New York: Cold Spring Harbor Laboratory Press.
238. Avery, L., and Thomas, J.H. , *Feeding and Defecation, In C. elegans II,*, ed. T.B. D.L. Riddle, B.J. Meyer, and J.R. Priess 1997, New York: Cold Spring Harbor Laboratory Press
239. Irazoqui, J.E., et al., *Distinct pathogenesis and host responses during infection of C. elegans by P. aeruginosa and S. aureus.* Plos Pathogens, 2010. **6**: p. e1000982.
240. Gobel, V., et al., *Lumen morphogenesis in C. elegans requires the membrane-cytoskeleton linker erm-1.* Dev Cell, 2004. **6**(6): p. 865-73.
241. Segbert, C., et al., *Molecular and functional analysis of apical junction formation in the gut epithelium of Caenorhabditis elegans.* Dev Biol, 2004. **266**(1): p. 17-26.
242. Irazoqui, J.E., J.M. Urbach, and F.M. Ausubel, *Evolution of host innate defence: insights from Caenorhabditis elegans and primitive invertebrates.* Nat Rev Immunol, 2010. **10**(1): p. 47-58.
243. Balla, K.M. and E.R. Troemel, *Caenorhabditis elegans as a model for intracellular pathogen infection.* Cellular Microbiology, 2013. **15**(8): p. 1313-22.
244. Zhang, Y., H. Lu, and C.I. Bargmann, *Pathogenic bacteria induce aversive olfactory learning in Caenorhabditis elegans.* Nature, 2005. **438**(7065): p. 179-84.
245. Lee, K.Z., et al., *The fatty acid synthase fasn-1 acts upstream of WNK and Ste20/GCK-VI kinases to modulate antimicrobial peptide expression in C. elegans epidermis.* Virulence, 2010. **1**(3): p. 113-22.
246. Pujol, N., et al., *Distinct innate immune responses to infection and wounding in the C. elegans epidermis.* Curr Biol, 2008. **18**(7): p. 481-9.
247. Garcia-Garcia, E., J. Galindo-Villegas, and V. Mulero, *Mucosal immunity in the gut: the non-vertebrate perspective.* Dev Comp Immunol, 2013. **40**(3-4): p. 278-88.
248. Kumar, H., T. Kawai, and S. Akira, *Pathogen recognition in the innate immune response.* Biochem J, 2009. **420**(1): p. 1-16.
249. Akira, S., *Pathogen recognition by innate immunity and its signaling.* Proc Jpn Acad Ser B Phys Biol Sci, 2009. **85**(4): p. 143-56.
250. Rock, F.L., et al., *A family of human receptors structurally related to Drosophila Toll.* Proc Natl Acad Sci U S A, 1998. **95**(2): p. 588-93.
251. Medzhitov, R., P. Preston-Hurlburt, and C.A. Janeway, Jr., *A human homologue of the Drosophila Toll protein signals activation of adaptive immunity.* Nature, 1997. **388**(6640): p. 394-7.
252. Pukkila-Worley, R. and F.M. Ausubel, *Immune defense mechanisms in the Caenorhabditis elegans intestinal epithelium.* Curr Opin Immunol, 2012. **24**(1): p. 3-9.
253. Troemel, E.R., et al., *p38 MAPK regulates expression of immune response genes and contributes to longevity in C. elegans.* PLoS Genet, 2006. **2**(11): p. e183.
254. Kim, D.H., et al., *A conserved p38 MAP kinase pathway in Caenorhabditis elegans innate immunity.* Science, 2002. **297**(5581): p. 623-6.
255. Aballay, A., et al., *Caenorhabditis elegans innate immune response triggered by Salmonella enterica requires intact LPS and is mediated by a MAPK signaling pathway.* Curr Biol, 2003. **13**(1): p. 47-52.
256. Bolz, D.D., J.L. Tenor, and A. Aballay, *A conserved PMK-1/p38 MAPK is required in caenorhabditis elegans tissue-specific immune response to Yersinia pestis infection.* J Biol Chem, 2010. **285**(14): p. 10832-40.
257. Shivers, R.P., et al., *Phosphorylation of the conserved transcription factor ATF-7 by PMK-1 p38 MAPK regulates innate immunity in Caenorhabditis elegans.* PLoS Genet, 2010. **6**(4): p. e1000892.

258. Sifri, C.D., et al., *Caenorhabditis elegans as a model host for Staphylococcus aureus pathogenesis.* Infect Immun, 2003. **71**(4): p. 2208-17.
259. Takeda, K., et al., *Apoptosis signal-regulating kinase 1 in stress and immune response.* Annu Rev Pharmacol Toxicol, 2008. **48**: p. 199-225.
260. Lu, H.T., et al., *Defective IL-12 production in mitogen-activated protein (MAP) kinase kinase 3 (Mkk3)-deficient mice.* EMBO J, 1999. **18**(7): p. 1845-57.
261. Zhong, J., et al., *GCK is essential to systemic inflammation and pattern recognition receptor signaling to JNK and p38.* Proc Natl Acad Sci U S A, 2009. **106**(11): p. 4372-7.
262. Dong, C., R.J. Davis, and R.A. Flavell, *MAP kinases in the immune response.* Annu Rev Immunol, 2002. **20**: p. 55-72.
263. Tobiume, K., et al., *ASK1 is required for sustained activations of JNK/p38 MAP kinases and apoptosis.* EMBO Rep, 2001. **2**(3): p. 222-8.
264. Wolkow, C.A., et al., *Regulation of C. elegans life-span by insulinlike signaling in the nervous system.* Science, 2000. **290**(5489): p. 147-50.
265. Garsin, D.A., et al., *Long-lived C. elegans daf-2 mutants are resistant to bacterial pathogens.* Science, 2003. **300**(5627): p. 1921.
266. Evans, E.A., T. Kawli, and M.W. Tan, *Pseudomonas aeruginosa suppresses host immunity by activating the DAF-2 insulin-like signaling pathway in Caenorhabditis elegans.* PLoS Pathog, 2008. **4**(10): p. e1000175.
267. Anyanful, A., et al., *Conditioning protects C. elegans from lethal effects of enteropathogenic E. coli by activating genes that regulate lifespan and innate immunity.* Cell Host Microbe, 2009. **5**(5): p. 450-62.
268. Kawli, T. and M.W. Tan, *Neuroendocrine signals modulate the innate immunity of Caenorhabditis elegans through insulin signaling.* Nat Immunol, 2008. **9**(12): p. 1415-24.
269. Lin, K., et al., *Regulation of the Caenorhabditis elegans longevity protein DAF-16 by insulin/IGF-1 and germline signaling.* Nat Genet, 2001. **28**(2): p. 139-45.
270. Lee, S.S., et al., *DAF-16 target genes that control C. elegans life-span and metabolism.* Science, 2003. **300**(5619): p. 644-7.
271. Murphy, C.T., et al., *Genes that act downstream of DAF-16 to influence the lifespan of Caenorhabditis elegans.* Nature, 2003. **424**(6946): p. 277-83.
272. Miyata, S., et al., *DAF-16-dependent suppression of immunity during reproduction in Caenorhabditis elegans.* Genetics, 2008. **178**(2): p. 903-18.
273. Troemel, E.R., et al., *Microsporidia are natural intracellular parasites of the nematode Caenorhabditis elegans.* PLoS Biol, 2008. **6**(12): p. 2736-52.
274. Irazoqui, J.E., et al., *Role for beta-catenin and HOX transcription factors in Caenorhabditis elegans and mammalian host epithelial-pathogen interactions.* Proc Natl Acad Sci U S A, 2008. **105**(45): p. 17469-74.
275. Fire, A., et al., *Potent and specific genetic interference by double-stranded RNA in Caenorhabditis elegans.* Nature, 1998. **391**(6669): p. 806-11.
276. Tabara, H., A. Grishok, and C.C. Mello, *RNAi in C. elegans: soaking in the genome sequence.* Science, 1998. **282**(5388): p. 430-1.
277. Timmons, L. and A. Fire, *Specific interference by ingested dsRNA.* Nature, 1998. **395**(6705): p. 854.
278. Timmons, L., et al., *Inducible systemic RNA silencing in Caenorhabditis elegans.* Mol Biol Cell, 2003. **14**(7): p. 2972-83.
279. Knight, S.W. and B.L. Bass, *A role for the RNase III enzyme DCR-1 in RNA interference and germ line development in Caenorhabditis elegans.* Science, 2001. **293**(5538): p. 2269-71.

280. Tabara, H., et al., *The dsRNA binding protein RDE-4 interacts with RDE-1, DCR-1, and a DExH-box helicase to direct RNAi in C. elegans.* Cell, 2002. **109**(7): p. 861-71.
281. Tops, B.B., et al., *RDE-2 interacts with MUT-7 to mediate RNA interference in Caenorhabditis elegans.* Nucleic Acids Research, 2005. **33**(1): p. 347-55.
282. Kennedy, S., D. Wang, and G. Ruvkun, *A conserved siRNA-degrading RNase negatively regulates RNA interference in C. elegans.* Nature, 2004. **427**(6975): p. 645-9.
283. Burton, E.A., Pendergast, A. M., Aballay, M., *The Caenorhabditis elegans ABL-1 Tyrosine Kinase Is Required for Shigella flexneri Pathogenesis.* Appl Environ Microbiol. , 2006. **72**(7): p. 5043-5051.
284. Kesika, P., S. Karutha Pandian, and K. Balamurugan, *Analysis of Shigella flexneri-mediated infections in model organism Caenorhabditis elegans.* Scand J Infect Dis, 2011. **43**(4): p. 286-95.
285. Darby, C., et al., *Lethal paralysis of Caenorhabditis elegans by Pseudomonas aeruginosa.* Proc Natl Acad Sci U S A, 1999. **96**(26): p. 15202-7.
286. Gallagher, L.A. and C. Manoil, *Pseudomonas aeruginosa PAO1 kills Caenorhabditis elegans by cyanide poisoning.* Journal of Bacteriology, 2001. **183**(21): p. 6207-14.
287. Mahajan-Miklos, S., et al., *Molecular mechanisms of bacterial virulence elucidated using a Pseudomonas aeruginosa-Caenorhabditis elegans pathogenesis model.* Cell, 1999. **96**(1): p. 47-56.
288. Tan, M.W., S. Mahajan-Miklos, and F.M. Ausubel, *Killing of Caenorhabditis elegans by Pseudomonas aeruginosa used to model mammalian bacterial pathogenesis.* Proc Natl Acad Sci U S A, 1999. **96**(2): p. 715-20.
289. Tan, M.W., et al., *Pseudomonas aeruginosa killing of Caenorhabditis elegans used to identify P. aeruginosa virulence factors.* Proc Natl Acad Sci U S A, 1999. **96**(5): p. 2408-13.
290. Wareham, D.W., A. Papakonstantinopoulou, and M.A. Curtis, *The Pseudomonas aeruginosa PA14 type III secretion system is expressed but not essential to virulence in the Caenorhabditis elegans-P. aeruginosa pathogenicity model.* Fems Microbiology Letters, 2005. **242**(2): p. 209-16.
291. Mellies, J.L., et al., *The global regulator Ler is necessary for enteropathogenic Escherichia coli colonization of Caenorhabditis elegans.* Infect Immun, 2006. **74**(1): p. 64-72.
292. Anyanful, A., et al., *Paralysis and killing of Caenorhabditis elegans by enteropathogenic Escherichia coli requires the bacterial tryptophanase gene.* Mol Microbiol, 2005. **57**(4): p. 988-1007.
293. Aballay, A. and F.M. Ausubel, *Programmed cell death mediated by ced-3 and ced-4 protects Caenorhabditis elegans from Salmonella typhimurium-mediated killing.* Proc Natl Acad Sci U S A, 2001. **98**(5): p. 2735-9.
294. Labrousse, A., et al., *Caenorhabditis elegans is a model host for Salmonella typhimurium.* Curr Biol, 2000. **10**(23): p. 1543-5.
295. Tenor, J.L., et al., *Caenorhabditis elegans-based screen identifies Salmonella virulence factors required for conserved host-pathogen interactions.* Curr Biol, 2004. **14**(11): p. 1018-24.
296. Kurz, C.L., et al., *Virulence factors of the human opportunistic pathogen Serratia marcescens identified by in vivo screening.* EMBO J, 2003. **22**(7): p. 1451-60.
297. Mallo, G.V., et al., *Inducible antibacterial defense system in C. elegans.* Curr Biol, 2002. **12**(14): p. 1209-14.
298. Michael F.W. Festing, V.B., Robert D. Combes, Marlies Halder, Coenraad F.M. Hendriksen, Bryan R. Howard, David P. Lovell, Graham J. Moore, Philip Overend

and Marie S. Wilson, *Reducing the Use of Laboratory Animals in Biomedical Research: Problems and Possible Solutions*, in *The Report and Recommendations of ECVAM Workshop 29*. 1998, ALTA. p. 283-301.
299. Yanisch-Perron, C., J. Vieira, and J. Messing, *Improved M13 phage cloning vectors and host strains: nucleotide sequences of the M13mp18 and pUC19 vectors.* Gene, 1985. **33**(1): p. 103-19.
300. Brenner, S., *Genetics of Caenorhabditis-Elegans.* Genetics, 1974. **77**(1): p. 71-94.
301. Sambrook, J., Fritsch, E.F., Maniatis, T. , *Molecular cloning : a laboratory manual.* 2nd ed. 1989: Cold Spring Harbor, N.Y. : Cold Spring Harbor Laboratory Press, .
302. Hall, T.A., *BioEdit: a user-friendly biological sequence alignment editor and analysis program for Windows 95/98/NT.* Nucleic Acids Symposium Series, 1999.

41: p. 95-98.
303. Bradford, M.M., *A rapid and sensitive method for the quantitation of microgram quantities of protein utilizing the principle of protein-dye binding.* Anal Biochem, 1976. **72**: p. 248-54.
304. Mathesius, U., *Flavonoids induced in cells undergoing nodule organogenesis in white clover are regulators of auxin breakdown by peroxidase.* Journal of Experimental Botany, 2001. **52**: p. 419-426.
305. Cravioto, A., et al., *Adhesive Factor Found in Strains of Escherichia-Coli Belonging to the Traditional Infantile Enteropathogenic Serotypes.* Current Microbiology, 1979. **3**(2): p. 95-99.
306. Lindberg, G.K., et al., *Purification and characterization of bacteriophage N4-induced DNA polymerase.* Journal of Biological Chemistry, 1988. **263**(23): p. 11319-26.
307. Sulston, J., and Hodgkin, J., *Methods: The nematode Caenorhabditis elegans*, ed. W.B. Wood. 1988, Cold Spring Harbor, New York: Cold Spring Harbor Laboratory Press.
308. Hall, D.H., E. Hartwieg, and K.C.Q. Nguyen, *Chapter 4 - Modern Electron Microscopy Methods for C. elegans*, in *Methods in Cell Biology*, H.R. Joel and S. Andrew, Editors. 2012, Academic Press. p. 93-149.
309. Jennison, A.V., R. Raqib, and N.K. Verma, *Immunoproteome analysis of soluble and membrane proteins of Shigella flexneri 2457T.* World J Gastroenterol, 2006. **12**(41): p. 6683-8.
310. Cheung, N.K.V., I.Y. Chau, and P.F. Coccia, *Antibody-Response to Escherichia-Coli L-Asparaginase - Prognostic-Significance and Clinical Utility of Antibody Measurement.* American Journal of Pediatric Hematology Oncology, 1986. **8**(2): p. 99-104.
311. Schmees, C., et al., *Inhibition of T-cell proliferation by Helicobacter pylori gamma-glutamyl transpeptidase.* Gastroenterology, 2007. **132**(5): p. 1820-1833.
312. McGovern, K.J., et al., *gamma-glutamyltransferase is a Helicobacter pylori virulence factor but is not essential for colonization.* Infection and Immunity, 2001. **69**(6): p. 4168-4173.
313. Kullas, A.L., et al., *L-asparaginase II produced by Salmonella typhimurium inhibits T cell responses and mediates virulence.* Cell Host Microbe, 2012. **12**(6): p. 791-8.
314. Zautner, A.E., et al., *Epidemiological association of Campylobacter jejuni groups with pathogenicity-associated genetic markers.* Bmc Microbiology, 2012. **12**: p. 171.
315. Jennings, M.P. and I.R. Beacham, *Analysis of the Escherichia-Coli Gene Encoding L-Asparaginase-Ii, Ansb, and Its Regulation by Cyclic-Amp Receptor and Fnr Proteins.* Journal of Bacteriology, 1990. **172**(3): p. 1491-1498.

316. Tate, S.S. and A. Meister, *gamma-Glutamyl transpeptidase: catalytic, structural and functional aspects.* Mol Cell Biochem, 1981. **39**: p. 357-68.
317. Datsenko, K.A. and B.L. Wanner, *One-step inactivation of chromosomal genes in Escherichia coli K-12 using PCR products.* Proceedings of the National Academy of Sciences of the United States of America, 2000. **97**(12): p. 6640-6645.
318. Mallett, C.P., et al., *Evaluation of Shigella vaccine safety and efficacy in an intranasally challenged mouse model.* Vaccine, 1993. **11**(2): p. 190-6.
319. Pizarro-Cerda, J. and P. Cossart, *Bacterial adhesion and entry into host cells.* Cell, 2006. **124**(4): p. 715-27.
320. Faherty, C.S., et al., *Shigella flexneri effectors OspE1 and OspE2 mediate induced adherence to the colonic epithelium following bile salts exposure.* Molecular Microbiology, 2012. **85**(1): p. 107-21.
321. Utsunomiya, A., et al., *Studies on novel pili from Shigella flexneri. I. Detection of pili and hemagglutination activity.* Microbiology and Immunology, 1992. **36**(8): p. 803-13.
322. Snellings, N.J., B.D. Tall, and M.M. Venkatesan, *Characterization of Shigella type 1 fimbriae: expression, FimA sequence, and phase variation.* Infection and Immunity, 1997. **65**(6): p. 2462-7.
323. Lafont, F., et al., *Initial steps of Shigella infection depend on the cholesterol/sphingolipid raft-mediated CD44-IpaB interaction.* EMBO J, 2002. **21**(17): p. 4449-57.
324. Shibayama, K., et al., *Biochemical and pathophysiological characterization of Helicobacter pylori asparaginase.* Microbiology and Immunology, 2011. **55**(6): p. 408-417.
325. Leduc, D., et al., *Coupled Amino Acid Deamidase-Transport Systems Essential for Helicobacter pylori Colonization.* Infection and Immunity, 2010. **78**(6): p. 2782-2792.
326. de Haan, C.P., et al., *Association of Campylobacter jejuni metabolic traits with multilocus sequence types.* Appl Environ Microbiol, 2012. **78**(16): p. 5550-4.
327. Thompson, S.A. and E.C. Gaynor, *Campylobacter jejuni Host Tissue Tropism: A Consequence of Its Low-Carb Lifestyle?* Cell Host & Microbe, 2008. **4**(5): p. 409-410.
328. Jennings, M.P., S.P. Scott, and I.R. Beacham, *Regulation of the ansB gene of Salmonella enterica.* Molecular Microbiology, 1993. **9**(1): p. 165-72.
329. Yang, J., et al., *ShiBASE: an integrated database for comparative genomics of Shigella.* Nucleic Acids Research, 2006. **34**(Database issue): p. D398-401.
330. Reis, R.S. and F. Horn, *Enteropathogenic Escherichia coli, Samonella, Shigella and Yersinia: cellular aspects of host-bacteria interactions in enteric diseases.* Gut Pathog, 2010. **2**(1): p. 8.
331. Krishnan, S. and N.V. Prasadarao, *Outer membrane protein A and OprF: versatile roles in Gram-negative bacterial infections.* Febs Journal, 2012. **279**(6): p. 919-31.
332. Smith, S.G., et al., *A molecular Swiss army knife: OmpA structure, function and expression.* Fems Microbiology Letters, 2007. **273**(1): p. 1-11.
333. Shin, S., et al., *Escherichia coli outer membrane protein A adheres to human brain microvascular endothelial cells.* Biochem Biophys Res Commun, 2005. **330**(4): p. 1199-204.
334. Torres, A.G. and J.B. Kaper, *Multiple elements controlling adherence of enterohemorrhagic Escherichia coli O157:H7 to HeLa cells.* Infection and Immunity, 2003. **71**(9): p. 4985-95.
335. Torres, A.G., et al., *Outer membrane protein A of Escherichia coli O157:H7 stimulates dendritic cell activation.* Infection and Immunity, 2006. **74**(5): p. 2676-85.

336. Rasmussen, A.A., et al., *Regulation of ompA mRNA stability: the role of a small regulatory RNA in growth phase-dependent control.* Molecular Microbiology, 2005. **58**(5): p. 1421-9.
337. Johansen, J., et al., *Down-regulation of outer membrane proteins by noncoding RNAs: unraveling the cAMP-CRP- and sigmaE-dependent CyaR-ompX regulatory case.* Journal of Molecular Biology, 2008. **383**(1): p. 1-9.
338. Wagner, S., et al., *Rationalizing membrane protein overexpression.* Trends in Biotechnology, 2006. **24**(8): p. 364-71.
339. Chevalier, C., et al., *Essential role of Helicobacter pylori gamma-glutamyltranspeptidase for the colonization of the gastric mucosa of mice.* Mol Microbiol, 1999. **31**(5): p. 1359-72.
340. Busiello, I., et al., *Helicobacter pylori gamma-glutamyltranspeptidase upregulates COX-2 and EGF-related peptide expression in human gastric cells.* Cellular Microbiology, 2004. **6**(3): p. 255-267.
341. Gong, M., et al., *Helicobacter pylori gamma-glutamyl transpeptidase is a pathogenic factor in the development of peptic ulcer disease.* Gastroenterology, 2010. **139**(2): p. 564-73.
342. Shibayama, K., et al., *A novel apoptosis-inducing protein from Helicobacter pylori.* Mol Microbiol, 2003. **47**(2): p. 443-51.
343. Hofreuter, D., et al., *Unique features of a highly pathogenic Campylobacter jejuni strain.* Infection and Immunity, 2006. **74**(8): p. 4694-4707.
344. Barnes, H.A., et al., *gamma-Glutamyl transpeptidase has a role in the persistent colonization of the avian gut by Campylobacter jejuni.* Microbial Pathogenesis, 2007. **43**(5-6): p. 198-207.
345. Shibayama, K., et al., *Metabolism of glutamine and glutathione via gamma-glutamyltranspeptidase and glutamate transport in Helicobacter pylori: possible significance in the pathophysiology of the organism.* Molecular Microbiology, 2007. **64**(2): p. 396-406.
346. Suzuki, H., W. Hashimoto, and H. Kumagai, *Escherichia-Coli K-12 Can Utilize an Exogenous Gamma-Glutamyl Peptide as an Amino-Acid Source, for Which Gamma-Glutamyl-Transpeptidase Is Essential.* Journal of Bacteriology, 1993. **175**(18): p. 6038-6040.
347. Jain, S. and M.B. Goldberg, *Requirement for YaeT in the outer membrane assembly of autotransporter proteins.* Journal of Bacteriology, 2007. **189**(14): p. 5393-8.
348. Bodelon, G., E. Marin, and L.A. Fernandez, *Role of periplasmic chaperones and BamA (YaeT/Omp85) in folding and secretion of intimin from enteropathogenic Escherichia coli strains.* Journal of Bacteriology, 2009. **191**(16): p. 5169-79.
349. Wagner, J.K., et al., *Contribution of the periplasmic chaperone Skp to efficient presentation of the autotransporter IcsA on the surface of Shigella flexneri.* Journal of Bacteriology, 2009. **191**(3): p. 815-21.
350. Sittka, A., et al., *The RNA chaperone Hfq is essential for the virulence of Salmonella typhimurium.* Molecular Microbiology, 2007. **63**(1): p. 193-217.
351. Wagner, P.L. and M.K. Waldor, *Bacteriophage control of bacterial virulence.* Infection and Immunity, 2002. **70**(8): p. 3985-3993.
352. Boyd, E.F. and H. Brussow, *Common themes among bacteriophage-encoded virulence factors and diversity among the bacteriophages involved.* Trends Microbiol, 2002. **10**(11): p. 521-9.
353. West, N.P., et al., *Optimization of virulence functions through glucosylation of Shigella LPS.* Science, 2005. **307**(5713): p. 1313-7.

354. Gautheret D, L.A., *Direct RNA Motif Definition and Identification from Multiple Sequence Alignments using Secondary Structure Profiles.* . J Mol Biol, 2001 **313**: p. 1003–11.
355. Kingsford, C.L., K. Ayanbule, and S.L. Salzberg, *Rapid, accurate, computational discovery of Rho-independent transcription terminators illuminates their relationship to DNA uptake.* Genome Biol, 2007. **8**(2): p. R22.
356. Darling, A.E., B. Mau, and N.T. Perna, *progressiveMauve: Multiple Genome Alignment with Gene Gain, Loss and Rearrangement.* Plos One, 2010. **5**(6).
357. Huan, P.T., et al., *Molecular characterization of the genes involved in O-antigen modification, attachment, integration and excision in Shigella flexneri bacteriophage SfV.* Gene, 1997. **195**(2): p. 217-27.
358. Huan, P.T., et al., *Shigella flexneri type-specific antigen V: cloning, sequencing and characterization of the glucosyl transferase gene of temperate bacteriophage SfV.* Gene, 1997. **195**(2): p. 207-16.
359. Ackermann, H.W., *Tailed bacteriophages: the order caudovirales.* Advances in Virus Research, Vol 83: Bacteriophages, Pt B, 1998. **51**: p. 135-201.
360. Luftig, R.B. and C. Ganz, *Bacteriophage T4 head morphogenesis. IV. Comparison of gene 16-, 17-, and 49-defective head structures.* Journal of Virology, 1972. **10**(3): p. 545-54.
361. Kaiser, D., M. Syvanen, and T. Masuda, *DNA Packaging Steps in Bacteriophage-Lambda Head Assembly.* Journal of Molecular Biology, 1975. **91**(2): p. 175-&.
362. Casjens, S.R., *The DNA-packaging nanomotor of tailed bacteriophages.* Nat Rev Micro, 2011. **9**(9): p. 647-657.
363. Tetart, F., et al., *Bacteriophage T4 host range is expanded by duplications of a small domain of the tail fiber adhesin.* J Mol Biol, 1996. **258**(5): p. 726-31.
364. Mahichi, F., et al., *Site-specific recombination of T2 phage using IP008 long tail fiber genes provides a targeted method for expanding host range while retaining lytic activity.* Fems Microbiology Letters, 2009. **295**(2): p. 211-217.
365. Wang, J., M. Hofnung, and A. Charbit, *The C-terminal portion of the tail fiber protein of bacteriophage lambda is responsible for binding to LamB, its receptor at the surface of Escherichia coli K-12.* J Bacteriol, 2000. **182**(2): p. 508-12.
366. Le, S., et al., *Mapping the tail fiber as the receptor binding protein responsible for differential host specificity of Pseudomonas aeruginosa bacteriophages PaP1 and JG004.* PLoS One, 2013. **8**(7): p. e68562.
367. Campbell, A., *Comparative molecular biology of lambdoid phages.* Annu Rev Microbiol, 1994. **48**: p. 193-222.
368. Greenblatt, J., J.R. Nodwell, and S.W. Mason, *Transcriptional antitermination.* Nature, 1993. **364**(6436): p. 401-6.
369. Das, A., *Control of transcription termination by RNA-binding proteins.* Annu Rev Biochem, 1993. **62**: p. 893-930.
370. Weigel, C. and H. Seitz, *Bacteriophage replication modules.* Fems Microbiology Reviews, 2006. **30**(3): p. 321-381.
371. Gorbalenya, A.E., *Self-splicing group I and group II introns encode homologous (putative) DNA endonucleases of a new family.* Protein Sci, 1994. **3**(7): p. 1117-20.
372. Shub, D.A., H. Goodrichblair, and S.R. Eddy, *AMINO-ACID-SEQUENCE MOTIF OF GROUP-I INTRON ENDONUCLEASES IS CONSERVED IN OPEN READING FRAMES OF GROUP-II INTRONS.* Trends in Biochemical Sciences, 1994. **19**(10): p. 402-404.
373. Hendrix, R.W., et al., *The origins and ongoing evolution of viruses.* Trends Microbiol, 2000. **8**(11): p. 504-8.

374. Low, D.A., N.J. Weyand, and M.J. Mahan, *Roles of DNA adenine methylation in regulating bacterial gene expression and virulence.* Infect Immun, 2001. **69**(12): p. 7197-204.
375. Wion, D. and J. Casadesus, *N6-methyl-adenine: an epigenetic signal for DNA-protein interactions.* Nat Rev Microbiol, 2006. **4**(3): p. 183-92.
376. Porter, M.E., et al., *The LEE1 promoters from both enteropathogenic and enterohemorrhagic Escherichia coli can be activated by PerC-like proteins from either organism.* J Bacteriol, 2005. **187**(2): p. 458-72.
377. Mellies, J.L., et al., *The Per regulon of enteropathogenic Escherichia coli : identification of a regulatory cascade and a novel transcriptional activator, the locus of enterocyte effacement (LEE)-encoded regulator (Ler).* Mol Microbiol, 1999. **33**(2): p. 296-306.
378. Altschul, S.F., et al., *Gapped BLAST and PSI-BLAST: a new generation of protein database search programs.* Nucleic Acids Res, 1997. **25**(17): p. 3389-402.
379. Wagner, E.K., J.F. Guzowski, and J. Singh, *Transcription of the herpes simplex virus genome during productive and latent infection.* Prog Nucleic Acid Res Mol Biol, 1995. **51**: p. 123-65.
380. Faber, S.W. and K.W. Wilcox, *Association of herpes simplex virus regulatory protein ICP4 with sequences spanning the ICP4 gene transcription initiation site.* Nucleic Acids Res, 1988. **16**(2): p. 555-70.
381. Gu, B., R. Kuddus, and N.A. DeLuca, *Repression of activator-mediated transcription by herpes simplex virus ICP4 via a mechanism involving interactions with the basal transcription factors TATA-binding protein and TFIIB.* Mol Cell Biol, 1995. **15**(7): p. 3618-26.
382. Leopardi, R., N. Michael, and B. Roizman, *Repression of the herpes simplex virus 1 alpha 4 gene by its gene product (ICP4) within the context of the viral genome is conditioned by the distance and stereoaxial alignment of the ICP4 DNA binding site relative to the TATA box.* J Virol, 1995. **69**(5): p. 3042-8.
383. Barrangou, R., et al., *CRISPR provides acquired resistance against viruses in prokaryotes.* Science, 2007. **315**(5819): p. 1709-12.
384. Cady, K.C., et al., *The CRISPR/Cas adaptive immune system of Pseudomonas aeruginosa mediates resistance to naturally occurring and engineered phages.* J Bacteriol, 2012. **194**(21): p. 5728-38.
385. Levin, B.R., et al., *The population and evolutionary dynamics of phage and bacteria with CRISPR-mediated immunity.* PLoS Genet, 2013. **9**(3): p. e1003312.
386. Makarova, K.S., et al., *A putative RNA-interference-based immune system in prokaryotes: computational analysis of the predicted enzymatic machinery, functional analogies with eukaryotic RNAi, and hypothetical mechanisms of action.* Biol Direct, 2006. **1**: p. 7.
387. Makarova, K.S., Y.I. Wolf, and E.V. Koonin, *Comparative genomics of defense systems in archaea and bacteria.* Nucleic Acids Res, 2013. **41**(8): p. 4360-77.
388. Aravind, L. and E.V. Koonin, *The HD domain defines a new superfamily of metal-dependent phosphohydrolases.* Trends Biochem Sci, 1998. **23**(12): p. 469-72.
389. Janka, A., et al., *Cytolethal distending toxin gene cluster in enterohemorrhagic Escherichia coli O157:H- and O157:H7: characterization and evolutionary considerations.* Infect Immun, 2003. **71**(6): p. 3634-8.
390. Johnson, W.M. and H. Lior, *A new heat-labile cytolethal distending toxin (CLDT) produced by Escherichia coli isolates from clinical material.* Microb Pathog, 1988. **4**(2): p. 103-13.

391. Hassane, D.C., R.B. Lee, and C.L. Pickett, *Campylobacter jejuni cytolethal distending toxin promotes DNA repair responses in normal human cells.* Infect Immun, 2003. **71**(1): p. 541-5.
392. Chien, C.C., et al., *Identification of cdtB homologues and cytolethal distending toxin activity in enterohepatic Helicobacter spp.* J Med Microbiol, 2000. **49**(6): p. 525-34.
393. Huang, C.J., et al., *YjcC, a c-di-GMP phosphodiesterase protein, regulates the oxidative stress response and virulence of Klebsiella pneumoniae CG43.* PLoS One, 2013. **8**(7): p. e66740.
394. Hisert, K.B., et al., *A glutamate-alanine-leucine (EAL) domain protein of Salmonella controls bacterial survival in mice, antioxidant defence and killing of macrophages: role of cyclic diGMP.* Mol Microbiol, 2005. **56**(5): p. 1234-45.
395. Ryan, R.P., et al., *Cyclic di-GMP signaling in bacteria: recent advances and new puzzles.* J Bacteriol, 2006. **188**(24): p. 8327-34.
396. Lacey, M.M., J.D. Partridge, and J. Green, *Escherichia coli K-12 YfgF is an anaerobic cyclic di-GMP phosphodiesterase with roles in cell surface remodelling and the oxidative stress response.* Microbiology, 2010. **156**(Pt 9): p. 2873-86.
397. Wilksch, J.J., et al., *MrkH, a novel c-di-GMP-dependent transcriptional activator, controls Klebsiella pneumoniae biofilm formation by regulating type 3 fimbriae expression.* PLoS Pathog, 2011. **7**(8): p. e1002204.
398. Krasteva, P.V., et al., *Vibrio cholerae VpsT regulates matrix production and motility by directly sensing cyclic di-GMP.* Science, 2010. **327**(5967): p. 866-8.
399. Hengge, R., *Principles of c-di-GMP signalling in bacteria.* Nat Rev Microbiol, 2009. **7**(4): p. 263-73.
400. Kulasakara, H., et al., *Analysis of Pseudomonas aeruginosa diguanylate cyclases and phosphodiesterases reveals a role for bis-(3'-5')-cyclic-GMP in virulence.* Proc Natl Acad Sci U S A, 2006. **103**(8): p. 2839-44.
401. Kurz, C.L. and J.J. Ewbank, *Infection in a dish: high-throughput analyses of bacterial pathogenesis.* Current Opinion in Microbiology, 2007. **10**(1): p. 10-6.
402. Joshua, G.W., et al., *A Caenorhabditis elegans model of Yersinia infection: biofilm formation on a biotic surface.* Microbiology, 2003. **149**(Pt 11): p. 3221-9.
403. Aballay, A., P. Yorgey, and F.M. Ausubel, *Salmonella typhimurium proliferates and establishes a persistent infection in the intestine of Caenorhabditis elegans.* Curr Biol, 2000. **10**(23): p. 1539-42.
404. Kurz, C.L. and J.J. Ewbank, *Caenorhabditis elegans for the study of host-pathogen interactions.* Trends in Microbiology, 2000. **8**(3): p. 142-4.
405. Alegado, R.A., et al., *Characterization of mediators of microbial virulence and innate immunity using the Caenorhabditis elegans host-pathogen model.* Cellular Microbiology, 2003. **5**(7): p. 435-44.
406. Hsiao, J.Y., et al., *Live and dead GFP-tagged bacteria showed indistinguishable fluorescence in Caenorhabditis elegans gut.* Journal of Microbiology, 2013. **51**(3): p. 367-72.
407. McBroom, A.J., and M. J. Kuehn., *Release of outer membrane vesicles by Gram-negative bacteria is a novel envelope stress response.* Mol.

Microbiol. , 2007. **63**: p. 545–558.
408. Kadurugamuwa, J.L. and T.J. Beveridge, *Membrane vesicles derived from Pseudomonas aeruginosa and Shigella flexneri can be integrated into the surfaces of other gram-negative bacteria.* Microbiology, 1999. **145 (Pt 8)**: p. 2051-60.

409. Negrete-Abascal, E., et al., *Membrane vesicles released by Actinobacillus pleuropneumoniae contain proteases and Apx toxins.* FEMS Microbiol Lett, 2000. **191**(1): p. 109-13.
410. Grenier, D., *Inactivation of human serum bactericidal activity by a trypsinlike protease isolated from Porphyromonas gingivalis.* Infect Immun, 1992. **60**(5): p. 1854-7.
411. Rosen, G., et al., *Proteases of Treponema denticola outer sheath and extracellular vesicles.* Infect Immun, 1995. **63**(10): p. 3973-9.
412. Furuta, N., H. Takeuchi, and A. Amano, *Entry of Porphyromonas gingivalis outer membrane vesicles into epithelial cells causes cellular functional impairment.* Infect Immun, 2009. **77**(11): p. 4761-70.
413. Amano, A., H. Takeuchi, and N. Furuta, *Outer membrane vesicles function as offensive weapons in host-parasite interactions.* Microbes Infect, 2010. **12**(11): p. 791-8.
414. Kuehn, M.J. and N.C. Kesty, *Bacterial outer membrane vesicles and the host-pathogen interaction.* Genes Dev, 2005. **19**(22): p. 2645-55.
415. Bomberger, J.M., et al., *Long-distance delivery of bacterial virulence factors by Pseudomonas aeruginosa outer membrane vesicles.* PLoS Pathog, 2009. **5**(4): p. e1000382.
416. Schertzer, J.W. and M. Whiteley, *Bacterial outer membrane vesicles in trafficking, communication and the host-pathogen interaction.* J Mol Microbiol Biotechnol, 2013. **23**(1-2): p. 118-30.
417. Nelson, F.K. and D.L. Riddle, *Functional study of the Caenorhabditis elegans secretory-excretory system using laser microsurgery.* J Exp Zool, 1984. **231**(1): p. 45-56.
418. Grant, B. and D. Hirsh, *Receptor-mediated endocytosis in the Caenorhabditis elegans oocyte.* Molecular Biology of the Cell, 1999. **10**(12): p. 4311-4326.
419. Kim, Y.I., et al., *Transcriptional regulation and life-span modulation of cytosolic aconitase and ferritin genes in C.elegans.* Journal of Molecular Biology, 2004. **342**(2): p. 421-33.
420. Gourley, B.L., et al., *Cytosolic aconitase and ferritin are regulated by iron in Caenorhabditis elegans.* Journal of Biological Chemistry, 2003. **278**(5): p. 3227-34.
421. Kirienko, N.V., et al., *Pseudomonas aeruginosa disrupts Caenorhabditis elegans iron homeostasis, causing a hypoxic response and death.* Cell Host Microbe, 2013. **13**(4): p. 406-16.
422. Sugimoto, T., et al., *Caenorhabditis elegans par2.1/mtssb-1 is essential for mitochondrial DNA replication and its defect causes comprehensive transcriptional alterations including a hypoxia response.* Exp Cell Res, 2008. **314**(1): p. 103-14.
423. Wang, J., et al., *RNAi screening implicates a SKN-1-dependent transcriptional response in stress resistance and longevity deriving from translation inhibition.* PLoS Genet, 2010. **6**(8).
424. Xie, Y., et al., *RFX transcription factor DAF-19 regulates 5-HT and innate immune responses to pathogenic bacteria in Caenorhabditis elegans.* PLoS Genet, 2013. **9**(3): p. e1003324.
425. Reith, W. and B. Mach, *The bare lymphocyte syndrome and the regulation of MHC expression.* Annu Rev Immunol, 2001. **19**: p. 331-73.
426. Ogawa, M., et al., *The versatility of Shigella effectors.* Nat Rev Microbiol, 2008. **6**(1): p. 11-6.

427. Benedetti, C., et al., *Ubiquitin-like protein 5 positively regulates chaperone gene expression in the mitochondrial unfolded protein response.* Genetics, 2006. **174**(1): p. 229-39.
428. Yoneda, T., et al., *Compartment-specific perturbation of protein handling activates genes encoding mitochondrial chaperones.* J Cell Sci, 2004. **117**(Pt 18): p. 4055-66.
429. Raha, S. and B.H. Robinson, *Mitochondria, oxygen free radicals, disease and ageing.* Trends Biochem Sci, 2000. **25**(10): p. 502-8.
430. Kirstein-Miles, J. and R.I. Morimoto, *Caenorhabditis elegans as a model system to study intercompartmental proteostasis: Interrelation of mitochondrial function, longevity, and neurodegenerative diseases.* Dev Dyn, 2010. **239**(5): p. 1529-38.
431. Yang, W. and S. Hekimi, *Two modes of mitochondrial dysfunction lead independently to lifespan extension in Caenorhabditis elegans.* Aging Cell, 2010. **9**(3): p. 433-47.
432. Carneiro, L.A., et al., *Shigella induces mitochondrial dysfunction and cell death in nonmyleoid cells.* Cell Host Microbe, 2009. **5**(2): p. 123-36.
433. Lembo-Fazio, L., et al., *Gadd45alpha activity is the principal effector of Shigella mitochondria-dependent epithelial cell death in vitro and ex vivo.* Cell Death Dis, 2011. **2**: p. e122.
434. Galluzzi, L. and G. Kroemer, *Shigella targets the mitochondrial checkpoint of programmed necrosis.* Cell Host Microbe, 2009. **5**(2): p. 107-9.
435. Camacho, A.I., J.M. Irache, and C. Gamazo, *Recent progress towards development of a Shigella vaccine.* Expert Rev Vaccines, 2013. **12**(1): p. 43-55.
436. Baev, M.V., et al., *Growth of Escherichia coli MG1655 on LB medium: determining metabolic strategy with transcriptional microarrays.* Appl Microbiol Biotechnol, 2006. **71**(3): p. 323-8.
437. Jennings, M.P. and I.R. Beacham, *Co-dependent positive regulation of the ansB promoter of Escherichia coli by CRP and the FNR protein: a molecular analysis.* Molecular Microbiology, 1993. **9**(1): p. 155-64.
438. Dunlop, P.C. and R.J. Roon, *L-Asparaginase of Saccharomyces cerevisiae: an extracellular Enzyme.* Journal of Bacteriology, 1975. **122**(3): p. 1017-24.
439. Pauling, K.D. and G.E. Jones, *Asparaginase II of Saccharomyces cerevisiae: inactivation during the transition to stationary phase.* Biochim Biophys Acta, 1980. **616**(2): p. 271-82.
440. Rhodius, V.A., et al., *Conserved and variable functions of the sigmaE stress response in related genomes.* PLoS Biol, 2006. **4**(1): p. e2.
441. Udekwu, K.I. and E.G. Wagner, *Sigma E controls biogenesis of the antisense RNA MicA.* Nucleic Acids Research, 2007. **35**(4): p. 1279-88.
442. Johansen, J., et al., *Conserved small non-coding RNAs that belong to the sigmaE regulon: role in down-regulation of outer membrane proteins.* Journal of Molecular Biology, 2006. **364**(1): p. 1-8.
443. Wagner, S., et al., *Consequences of membrane protein overexpression in Escherichia coli.* Mol Cell Proteomics, 2007. **6**(9): p. 1527-50.
444. Baars, L., et al., *Defining the role of the Escherichia coli chaperone SecB using comparative proteomics.* J Biol Chem, 2006. **281**(15): p. 10024-34.
445. Fahey, R.C., et al., *Occurrence of glutathione in bacteria.* Journal of Bacteriology, 1978. **133**(3): p. 1126-9.
446. Fahey, R.C. and A.R. Sundquist, *Evolution of glutathione metabolism.* Adv Enzymol Relat Areas Mol Biol, 1991. **64**: p. 1-53.
447. Penninckx, M.J. and M.T. Elskens, *Metabolism and functions of glutathione in micro-organisms.* Adv Microb Physiol, 1993. **34**: p. 239-301.

448. Masip, L., K. Veeravalli, and G. Georgiou, *The many faces of glutathione in bacteria.* Antioxid Redox Signal, 2006. **8**(5-6): p. 753-62.
449. Smirnova, G.V. and O.N. Oktyabrsky, *Glutathione in bacteria.* Biochemistry (Mosc), 2005. **70**(11): p. 1199-211.
450. Pittman, M.S., H.C. Robinson, and R.K. Poole, *A bacterial glutathione transporter (Escherichia coli CydDC) exports reductant to the periplasm.* J Biol Chem, 2005. **280**(37): p. 32254-61.
451. Chikhi, N., et al., *Gamma-glutamyl transpeptidase gene organization and expression: a comparative analysis in rat, mouse, pig and human species.* Comp Biochem Physiol B Biochem Mol Biol, 1999. **122**(4): p. 367-80.
452. Suzuki, H., H. Kumagai, and T. Tochikura, *Isolation, genetic mapping, and characterization of Escherichia coli K-12 mutants lacking gamma-glutamyltranspeptidase.* Journal of Bacteriology, 1987. **169**(9): p. 3926-31.
453. Suzuki, H., et al., *The yliA, -B, -C, and -D genes of Escherichia coli K-12 encode a novel glutathione importer with an ATP-binding cassette.* J Bacteriol, 2005. **187**(17): p. 5861-7.
454. Suzuki, H., W. Hashimoto, and H. Kumagai, *Escherichia coli K-12 can utilize an exogenous gamma-glutamyl peptide as an amino acid source, for which gamma-glutamyltranspeptidase is essential.* Journal of Bacteriology, 1993. **175**(18): p. 6038-40.
455. Owens, R.A. and P.E. Hartman, *Export of glutathione by some widely used Salmonella typhimurium and Escherichia coli strains.* Journal of Bacteriology, 1986. **168**(1): p. 109-14.
456. Dartigalongue, C., D. Missiakas, and S. Raina, *Characterization of the Escherichia coli sigma E regulon.* J Biol Chem, 2001. **276**(24): p. 20866-75.
457. Lin, J., et al., *Comparative analysis of extreme acid survival in Salmonella typhimurium, Shigella flexneri, and Escherichia coli.* Journal of Bacteriology, 1995. **177**(14): p. 4097-104.
458. Waterman, S.R. and P.L. Small, *Identification of sigma S-dependent genes associated with the stationary-phase acid-resistance phenotype of Shigella flexneri.* Mol Microbiol, 1996. **21**(5): p. 925-40.
459. Riordan, J.T., et al., *Inactivation of alternative sigma factor 54 (RpoN) leads to increased acid resistance, and alters locus of enterocyte effacement (LEE) expression in Escherichia coli O157 : H7.* Microbiology, 2010. **156**(Pt 3): p. 719-30.
460. Mecsas, J., et al., *The activity of sigma E, an Escherichia coli heat-inducible sigma-factor, is modulated by expression of outer membrane proteins.* Genes Dev, 1993. **7**(12B): p. 2618-28.
461. Raivio, T.L. and T.J. Silhavy, *Periplasmic stress and ECF sigma factors.* Annu Rev Microbiol, 2001. **55**: p. 591-624.
462. Alba, B.M. and C.A. Gross, *Regulation of the Escherichia coli sigma-dependent envelope stress response.* Molecular Microbiology, 2004. **52**(3): p. 613-9.
463. Deuerling, E., et al., *Trigger factor and DnaK cooperate in folding of newly synthesized proteins.* Nature, 1999. **400**(6745): p. 693-6.
464. Teter, S.A., et al., *Polypeptide flux through bacterial Hsp70: DnaK cooperates with trigger factor in chaperoning nascent chains.* Cell, 1999. **97**(6): p. 755-65.
465. R.P., H., *Handbook of fluorescent probes and research chemicals.*

. 6th ed,, ed. O. Eugene. 1996, Molecular Probes Inc.

466. Fahey, R.C., S. Brody, and S.D. Mikolajczyk, *Changes in the glutathione thiol-disulfide status of Neurospora crassa conidia during germination and aging.* J Bacteriol, 1975. **121**(1): p. 144-51.
467. Tomoyasu, T., et al., *Genetic dissection of the roles of chaperones and proteases in protein folding and degradation in the Escherichia coli cytosol.* Mol Microbiol, 2001. **40**(2): p. 397-413.
468. Menard, R., C. Dehio, and P.J. Sansonetti, *Bacterial entry into epithelial cells: the paradigm of Shigella.* Trends Microbiol, 1996. **4**(6): p. 220-6.
469. Kohler, H., S.P. Rodrigues, and B.A. McCormick, *Shigella flexneri Interactions with the Basolateral Membrane Domain of Polarized Model Intestinal Epithelium: Role of Lipopolysaccharide in Cell Invasion and in Activation of the Mitogen-Activated Protein Kinase ERK.* Infect Immun, 2002. **70**(3): p. 1150-8.
470. Kasper, C.A., et al., *Cell-cell propagation of NF-kappaB transcription factor and MAP kinase activation amplifies innate immunity against bacterial infection.* Immunity, 2010. **33**(5): p. 804-16.
471. Nataro, J.P., et al., *Identification and cloning of a novel plasmid-encoded enterotoxin of enteroinvasive Escherichia coli and Shigella strains.* Infect Immun, 1995. **63**(12): p. 4721-8.
472. Singh, V. and A. Aballay, *Regulation of DAF-16-mediated Innate Immunity in Caenorhabditis elegans.* J Biol Chem, 2009. **284**(51): p. 35580-7.
473. Lin, L., J.D. Hron, and S.L. Peng, *Regulation of NF-kappaB, Th activation, and autoinflammation by the forkhead transcription factor Foxo3a.* Immunity, 2004. **21**(2): p. 203-13.
474. Snoeks, L., et al., *Tumor suppressor Foxo3a is involved in the regulation of lipopolysaccharide-induced interleukin-8 in intestinal HT-29 cells.* Infect Immun, 2008. **76**(10): p. 4677-85.
475. Qian, F., et al., *Identification of genes critical for resistance to infection by West Nile virus using RNA-Seq analysis.* Viruses, 2013. **5**(7): p. 1664-81.